1-1-2014

Molecular-Genetic Mechanisms of Memory Formation in Mouse Models of Neurodevelopmental and Neuropsychiatric Disorders

Hannah Schoch
University of Pennsylvania, hanm@mail.med.upenn.edu

Molecular-Genetic Mechanisms of Memory Formation in Mouse Models of Neurodevelopmental and Neuropsychiatric Disorders

Abstract
Neurodevelopmental and neuropsychiatric disorders are a significant and expanding global health crisis. Many individuals affected by these disorders have social and cognitive symptoms represent significant sources of ongoing disability that are refractory to available treatment options. The search for cures and therapies for disorders fundamentally requires an understanding of the core neuropathology and insight into the underlying molecular mechanisms at work. In this dissertation, I describe experiments that we performed to explore molecular and genetic mechanisms underlying memory impairment and enhancement in mice. Synaptic structural proteins form a critical and adjustable framework that supports recruitment of neurotransmitter receptors and facilitates signal transduction. In Chapter 2, we explored a role for the autism-related gene Protocadherin 10 (Pcdh10) as a key regulator of dendritic spine morphology and synapse elimination. We found that mice with reduced PCDH10 have deficits in amygdala function, including impairments in conditioned fear, social interactions and gamma synchrony, as well as increased density of immature filopodia-type spines. In the second part of this dissertation, we showed that the co-repressor SIN3A is a negative regulator of memory formation. In Chapter 3, we demonstrated that reducing levels of SIN3A enhances in long-term memory and hippocampal synaptic plasticity, and increases expression of Homer1, a gene encoding a post-synaptic density protein that regulates signaling through metabotropic glutamate receptors. In Chapter 4, we identified contextual fear deficits in transgenic mice expressing Cre recombinase in forebrain neurons. These results expand our understanding of molecular mechanisms of memory formation, and identify new therapeutic targets for improving cognitive function.

Degree Type
Dissertation

Degree Name
Doctor of Philosophy (PhD)

Graduate Group
Cell & Molecular Biology

First Advisor
Ted Abel

Keywords
epigenetics, Homer1, memory formation, mouse models, Pcdh10, Sin3a

Subject Categories
Neuroscience and Neurobiology

MOLECULAR-GENETIC MECHANISMS OF MEMORY FORMATION IN MOUSE MODELS OF NEURODEVELOPMENTAL AND NEUROPSYCHIATRIC DISORDERS

Hannah Schoch

A DISSERTATION

in

Cell and Molecular Biology

Presented to the Faculties of the University of Pennsylvania

in

Partial Fulfillment of the Requirements for the

Degree of Doctor of Philosophy

2014

Supervisor of Dissertation

_____

Ted Abel, Ph.D. Brush Family Professor of Biology

Graduate Group Chairperson

_____

Dan Kessler, Ph.D. Associate Professor of Cell and Developmental Biology

Dissertation Committee

Marisa Bartolomei, Ph.D. Professor of Cell and Developmental Biology

Teresa Reyes, Ph.D. Assistant Professor of Pharmacology

Peter Klein, MD, Ph.D. Professor of Medicine

Tracy Bale, Ph.D. Professor of Neuroscience in Psychiatry

ACKNOWLEDGMENT

This journey entailed many thousand miles, yet it did not start with one particular step. It was only through the careful guidance of many that I found myself on this path, and only through the patient support of a hundred more was able to reach this point in my journey. Truly, this is not the end of the journey, but only a pause at the top of a hill to look back and appreciate the magnificence of the forest that I may have missed in my scramble to reach the next tree.

Much of my success I owe to the support and guidance of Ted Abel. He stuck with me through my early years when I broke everything that I touched (RIP Gs alpha mice) and opened new doors for me to follow my obsession with developmental disorders. Ted taught me so many important life lessons- how to stop doing experiments and THINK, how to peel back the fancy tools to expose the soft center of what is actually being measured, and how to stand tall and be confident in my understanding and interpretation of my results. I will go on to my next adventure well prepared for the challenges ahead. T-6 years to the RO1.

I also want to express my sincere appreciation for all the help and guidance I received from my thesis committee members, Marisa, Teresa, Peter and Tracy. Through the rocky start of my dissertation research, and the continual struggles with the Sin3a mouse, you provided constant support and encouragement along the way. As a result of your guidance, I've gained a wealth of perspective on how terrible quadruple transgenic mice are, an appreciation of the importance of properly controlled experiments, and a newfound respect for the horrifying effects of nuclease activity on the brain. I will carry this with me always.

To the Abel lab- you have had my back for the past 7 years and it's been one heck of a ride. Through all of the frustration and heartbreak of science, it's the community of fellow travelers that gets you through. Whether you need another soul who understands how it is to emerge from the

mouse facility after your 1,068th trial of water maze, or the sympathetic ear of someone who has also watched their research project crash and burn, they always know that what you really need is a funny video or a strategic application of tape to the back of your shirt. By maintaining a high level of foolishness and camaraderie in the lab, the p values of 0.06 are a little easier to accept. Thank you. I want to especially thank Jen and Nicola for their help with building this dissertation your faith in my abilities may not have entirely been misplaced.

I am especially grateful for the help and support of my buddy Morg. You've stuck with me through the ups and downs, and further downs of the Sin3a project. Together we tamed the devil mouse and extracted his dark secrets. Thanks, buddy.

Finally, I am incredibly grateful for my family. For my mom, who encouraged me to go into science, my dad who piqued my interest in the natural world, my brothers and sisters and sister-in-law and nieces and aunts uncles and grandparents who support me on this crazy path that I'm on, and also my cat Bill who stays up with me when I'm trying to hit a deadline. For my archnemesis, Dave, who stuck with me through all the late nights and crazy weeks. He always knew that I would make it here someday. Thank you for your patience and understanding.

ABSTRACT

MOLECULAR-GENETIC MECHANISMS OF MEMORY FORMATION IN MOUSE MODELS OF NEURODEVELOPMENTAL AND NEUROPSYCHIATRIC DISORDERS

Hannah Schoch

Ted Abel

Neurodevelopmental and neuropsychiatric disorders are a significant and expanding global health crisis. Many individuals affected by these disorders have social and cognitive symptoms represent significant sources of ongoing disability that are refractory to available treatment options. The search for cures and therapies for disorders fundamentally requires an understanding of the core neuropathology and insight into the underlying molecular mechanisms at work. In this dissertation, I describe experiments that we performed to explore molecular and genetic mechanisms underlying memory impairment and enhancement in mice. Synaptic structural proteins form a critical and adjustable framework that supports recruitment of neurotransmitter receptors and facilitates signal transduction. In **Chapter 2**, we explored a role for the autism-related gene Protocadherin 10 (*Pcdh10*) as a key regulator of dendritic spine morphology and synapse elimination. We found that mice with reduced PCDH10 have deficits in amygdala function, including impairments in conditioned fear, social interactions and gamma synchrony, as well as increased density of immature filopodia-type spines. In the second part of this dissertation, we showed that the co-repressor SIN3A is a negative regulator of memory formation. In **Chapter 3**, we demonstrated that reducing levels of SIN3A enhances in long-term memory and hippocampal synaptic plasticity, and

increases expression of *Homer1*, a gene encoding a post-synaptic density protein that regulates signaling through metabotropic glutamate receptors. In **Chapter 4**, we identified contextual fear deficits in transgenic mice expressing Cre recombinase in forebrain neurons. These results expand our understanding of molecular mechanisms of memory formation, and identify new therapeutic targets for improving cognitive function.

TABLE OF CONTENTS

LIST OF ILLUSTRATIONS

CHAPTER 1: GENETIC APPROACHES TO MODELING NEURODEVELOPMENTAL AND NEUROPSYCHIATRIC DISORDERS

Neurodevelopmental and neuropsychiatric disorders are a significant and expanding global health crisis. The Center for Disease Control estimates that 1 in 6 children in the US are diagnosed with a developmental disorder, and 1 in 13 children have a learning disability (CDC, 2010). Many individuals affected by neurodevelopmental and neuropsychiatric disorders have social and cognitive symptoms that can strongly impact their ability to live independently and function in society. Cognitive deficits, in particular, represent significant sources of ongoing disability that are refractory to available treatment options. One significant barrier to development of treatment options is a lack of promising therapeutic targets. The search for cures and therapies for disorders fundamentally requires an understanding of the core neuropathology and insight into the underlying molecular mechanisms at work. Many neurodevelopmental disorders have a complicated etiology involving a complex combination of environmental contributions, developmental insults, and genetic lesions. The search for molecular mechanisms is no simple task, but it has been facilitated by technological advances in genetic research.

Genetic linkage is one relatively clear-cut way to study disease risk and susceptibility, as it is a stable and long-lasting marker. Unlike environmental exposure and developmental events, genetic mutations are stable across the lifespan of the individual and can be easily identified through non-invasive genetic screens. Given the advances in gene sequencing technology, the primary challenge lies in identifying risk genes. Genome-wide association studies (GWAS) and haplotype mapping have provided a wealth of predictive power in linking genes and point mutations to disease susceptibility. Researchers are able to break down, isolate, and study the role of identified genes, and probe how loss or mutation of these gene products and other interacting factors in the pathway may contribute to the disorder. Through genetic manipulation, model

organisms carrying mutations linked to a genetic disorder can be created, allowing for an intimate dissection of the contributions of individual genes and providing opportunities for screening and testing therapeutic agents.

1.1. Strategies for modeling neurodevelopmental and neuropsychiatric disorders in rodents

Rodents are a versatile model system for modeling genetic disorders affecting cognition and other complex behaviors. Rodents display a wide variety of complex behaviors, both natural and trained, and their rapid generation time and large litters make them highly amenable to genetic studies. Many genetic engineering tools have been developed to manipulate the rodent genome to model human genetic lesions, particularly in the mouse. The advent of mouse transgenesis and gene knockout technology in the 1980s has led to explosive gains in our understanding of the genetic basis of both neurological and somatic disease (Hanahan 2007). More recently, gene knockout and transgenic techniques have been refined in the rat, a model system amenable to studies of higher-level cognitive function, social transmission of learned behavior, and complex social behaviors (Ko and Evenden 2009, Day et al. 2003, Bruchey et al. 2010, Aisner and Terkel 1992, Rutte and Taborsky 2007, Seyfarth and Cheney 2013).

The combination of gene modification in rodents and the advent of human medical genetics has paved the way for the development of highly specific genetic models designed to closely mimic human genetic disorders. Patients with neurodevelopmental disorders have been widely examined in GWAS, where the genomes of affected individuals, and frequently that of siblings and parents, are screened for over-represented mutations or chromosomal abnormalities that might be linked to the disorder

(Talkowski et al. 2012). The autism spectrum disorder (ASD) field in particular has taken a strong interest in identifying genes that might increase susceptibility to developing the disorder (State and Sestan 2012, Morrow et al. 2008, Sanders et al. 2012, Michaelson et al. 2012). This has led to the development of multiple lines of genetically modified mice carrying mutations in conserved genes and regions identified in GWAS studies. Studies in these animals have greatly enhanced our understanding of the molecular basis of ASD, and spawned clinical trials of potential therapeutic agents (Belmonte et al. 2004). The two main approaches to study the genetic basis of human neurodevelopmental disorders have been gene knockouts, and more recently, epigenetic manipulations.

1.2. Gene knockout models

One of the first steps in investigating the function of a gene linked to a neurodevelopmental or neuropsychiatric disorder is often experimentally removing it from the genome. Genes can be physically removed from the mouse genome by full or partial deletion of the DNA sequence. Methods for conditionally deleting DNA sequences include homologous recombination using a targeted DNA construct, and enzyme based conditional deletion systems such as the Cre/LoxP system (**Fig. 1.1**). In addition to deletion systems, the insertion of novel DNA sequence can also be used to disrupt expression at a gene locus, leading to reduced or absent expression of the targeted gene. Mice carrying a gene deletion, “knockout” mice, can then be used to study the role of the gene in brain development and organization, neuronal structure and function, and cognitive and behavioral phenotypes.

Studies of gene knockout mice have been very informative in the study of single gene disorders. These are identified in a subset of genetic studies in human subjects in which a single common genetic basis for a disorder is found. Knockout mice are a good model

for single gene disorders because the conserved mutation or deletion can be engineered in the mouse to create a fairly translational model that can provide further understanding of role of the targeted gene in the pathophysiology of the human disorder. Studies of this model not only provide insight into the molecular basis of a disorder, but also generate important basic knowledge of the functions of the gene and gene products in the animal. Importantly, basic knowledge of the molecular mechanisms underlying a neural disorder is critical for identifying drug targets and designing therapeutic approaches.

1.2.1. Advances in genetic models of neurodevelopmental disorders

Identifying the genetic basis of neurodevelopmental disorders has been successful in certain monogenic disorders. Mutations and copy number variants affecting the gene encoding the liver enzyme phenylalanine hydroxylase lead to neurological symptoms including seizures, social impairment and intellectual disability, as well as other medical issues (Gentile et al. 2010, Rolle-Daya et al. 1975, Lenke et al. 1980). Genetic screening combined with an understanding of the underlying biological pathways involved has led to a steep drop in neurological effects. Affected infants who are diagnosed early and adhere to a diet low in phenylalanine show near-normal brain development and cognitive ability (Smith and Knowles 2000, Janzen and Nguyen 2010, Pietz et al. 1998). Neurological conditions arising from metabolic or peripheral (rather than central) nervous system dysfunction can be more amenable to therapeutic approaches, particularly in the case of dietary causes.

1.2.2. Significant challenges remain

Unfortunately, most neurodevelopmental disorders lack effective therapeutic options, even in cases where the genetic and molecular basis of a disorder is known. Many

monogenic neurological disorders with a clearly defined neuronal and molecular pathology lack effective treatment options. The following overview of therapeutic challenges focuses on two neurodevelopmental disorders with well-defined genetic components but very limited therapeutic promise to date: schizophrenia and Fragile X disorder.

Schizophrenia is typically labeled a psychiatric rather than a neurodevelopmental disorder, but longitudinal studies have unmasked a set of early cognitive and behavioral symptoms in prodromal children who go on to get diagnosed as young adults (Reichenberg et al. 2010, Fuller et al. 2002). A complex and heterogeneous disorder, schizophrenia is typically diagnosed with the emergence in adolescence and early adulthood of positive psychotic symptoms such as hallucinations, delusions, and paranoid ideation, as well as motor effects including stereotypy or catatonia. Negative symptoms such as abnormal social behavior and cognitive impairments in verbal and working memory appear much earlier (Fuller et al. 2002, Reichenberg et al. 2010). Studies in young children affected by ASD suggest that intensive behavioral therapy early in life can improve cognitive and social functioning (Dawson et al. 2010, Warren et al. 2011). The presence of progressive white matter loss, behavior issues, and early verbal IQ deficits in children and adolescents who eventually receive a diagnosis of schizophrenia highlights the need for early detection and intervention (Fuller et al. 2002, Reichenberg et al. 2010, Ho et al. 2007, Jones et al. 1997).

A high degree of heritability is observed with schizophrenia, with an increased risk of as much as 64% observed in siblings of affected individuals that points to a strong genetic component (Lichtenstein 2009). Mutations in the transmembrane protein Neuregulin1 (NRG1) and its receptor ERBB4 have been linked to schizophrenia in multiple human

genetic linkage studies (Li et al. 2006, Walsh et al. 2008, Law et al. 2006). A synaptic protein involved in brain development and synaptic function, NRG1 in mice regulates synapse formation and maintenance, neurotransmitter receptor expression, and neuronal firing patterns and oscillations in the brain (Ehrlichman et al. 2009, Barz et al. 2014, Chen 2008, Xie et al. 2004, Gu et al. 2005). Loss or reduction of NRG1 leads to cognitive, social, and communication deficits in both humans and in mouse models (Ehrlichman et al. 2009, Barz et al. 2014, Chen et al. 2008, Egan et al. 2001, Kircher et al. 2009, Krug et al. 2010), supporting a strong link between disruption of NRG1 signaling and endophenotypes of schizophrenia.

Despite advances in clinical genotyping and gene sequencing technologies and extensive studies in pre-clinical rodent models, no specific treatment solutions are available to schizophrenia patients found to be carrying disease-associated polymorphisms in the *Nrg1* gene. Available therapies for schizophrenia include typical and atypical antipsychotics that largely address positive symptoms (Elis et al. 2013). Although addressing positive symptoms is critically important, the remaining negative symptoms are often a significant source of ongoing disability for patients for which no therapeutic options exist. Recombinant NRG1 peptides had been used to manipulate neurotransmitter receptor expression and firing patterns of cultured neurons almost a decade ago and have since been used in clinical studies for cardiac injury and cancer treatment, but moving therapeutic agents across the blood-brain barrier is a significant obstacle to both peptide and small-molecule based therapies in the CNS (Gao et al. 2010, Britten et al. 2004, Xie et al. 2004, Gu et al. 2005). Oddly, there is no evidence that existing NRG1 compounds are being considered as a therapeutic option for schizophrenia patients carrying *Nrg1* mutations. In 10 years of published pre-clinical

studies of these compounds, no studies have investigated CNS function. Improved communication between basic and clinical researchers and across research fields is critical in order to develop targeted therapies for genetic disorders.

In ASD, significant advances have been made in the quest for treatment options in Fragile X syndrome, a single gene disorder characterized by intellectual disability, seizure, withdrawal, altered motor coordination and repetitive behaviors, and connective tissue abnormalities (Rodgers et al. 2001, Kidd et al. 2013). Anatomical differences in the brains of FX patients include increases in white matter density in cortical and hippocampal regions as well as the corpus callosum, as well as defects in cortical dendritic spine morphology including increased spine density and elevated prevalence of immature long, filopodia-like spines (Hallahan et al. 2011, Irwin et al. 2000). An overwhelming majority of FX patients carry mutations in coding or regulatory regions associated with the X chromosomal gene locus *Fmr1*, which encodes the Fragile X mental retardation protein (FMRP) (Crawford et al. 2001, **Section 1.3.1**). Knockout mice lacking *Fmr1* show behavioral and structural changes similar to phenotypes observed in FX individuals, including impairments in cognitive and motor tasks, defects in dendritic spines, and impaired synaptic plasticity (Bernardet and Crusio 2006, Boda et al. 2014, Comery et al. 1997, Huber et al. 2002, Zhao et al. 2005). A high degree of phenotypic similarity between human probands and mouse models has facilitated detailed mechanistic studies of FMRP in the brain. FMRP is an mRNA binding protein that mediates transport and translational regulation of synaptic activity-regulated mRNA transcripts. Loss of FMRP is associated with over-production of synaptic proteins (including ARC/ARG3, PSD-95, CAMKIIα, PCDH10, and MAP1B), a mechanism that is

thought to underlie synaptic defects observed in *Fmr1* KO mice (Bassell and Warren 2008).

Activity-dependent translation of synaptic mRNA transcripts is regulated in part by signaling pathways downstream of metabotropic glutamate receptors, particularly mGluR5 (Bhakar et al. 2012). Pharmacological inhibition or genetic knockdown of mGluR5 rescues behavioral, synaptic plasticity, and spine structural phenotypes in *Fmr1* KO mice, supporting a dominant role of aberrant mGluR5 activity in the pathophysiology of Fragile X (deVrij et al. 2008, Levenga et al 2011, Bhakar et al. 2012). Interestingly, other pharmacological interventions aimed more specifically at reducing protein synthesis show mixed success in normalizing synaptic plasticity in *Fmr1* KO mice, an outcome that hints at additional roles for mGluR5 in FX besides regulation of protein synthesis (Osterweil et al. 2012, Nosyreva et al. 2006). Clinical trials are currently underway to test efficacy of mGluR5 antagonist compounds as potential therapeutic agents for improving symptoms of FX, but outcomes have been variable (Berry-Kravis 2014, Jacquemont et al. 2014).

In addition to difficulties with developing novel targeted therapeutics, the timing of therapeutic intervention may be critically important. Genetic disorders can derail critical developmental processes occurring within discrete windows of time. Environmental manipulations such as maternal immune activation or acute lead exposure starkly illustrate the long-lasting effects of brief exposure of the developing brain to injurious conditions (Lanphear et al. 2005, Patterson et al. 2010, Brown and Derkits 2010). Social and intellectual changes associated with neurodevelopmental and neuropsychiatric disorders can occur quite early in childhood, and imaging studies suggest that neurostructural changes that accompany disorders such as ASD and schizophrenia are

present early in life during critical periods of verbal and social development (Reichenberg et al. 2010, Fuller et al. 2002, Wolff et al. 2012, Ho et al. 2007, Landa et al. 2007). Studies in a schizophrenia model mouse carrying an inducible genetic manipulation suggest that even with full suppression of a genetic defect, adult animals may experience an incomplete recovery and retain certain types of cognitive deficits (**Fig. 1.2**, Kelly et al. 2008). These studies highlight the need to expand studies of rodent models to expand our understanding of early neurodevelopmental processes and how disruption of these processes may be a critical and treatment-refractory source of behavioral and cognitive changes observed in adult animals.

1.2.3. Multi-gene disorders and gene-environment interactions

One significant challenge in the study of genetic disorders is the presence of multiple genetic and non-genetic risk factors present in many disorders. Many individuals with neurodevelopmental disorders are described as having 'idiopathic' disorders where a clear cause cannot be identified. Our inability to understand the pathogenesis of these disorders likely reflects a complicated disease mechanism involving interaction of environmental factors combined with multiple rare alleles. This "perfect storm" type of disease risk is very difficult to predict using GWAS and epidemiological studies because individual risk genes and factors do not confer susceptibility to the general population. Exploration of multi-gene and gene-environment interactions in model systems is only starting to be explored in basic research. Complex genetic models will be a difficult challenge for neuroscience research in the upcoming decades, but is certain to provide important new insights into mitigating risk and severity of genetic disorders, and open new avenues of research into the ultimate cure: prevention.

1.3. Epigenetic models

A second category of genetic disorders are not driven by mutations within the gene coding sequence, rather they affect regulatory sequences that affect expression, processing or stability of the gene transcript. Regulatory regions of the genome are a substrate for a wide variety of covalent 'epigenetic' modifications of both DNA and the associated histone proteins. Epigenetic modifications form a stable code that can exert a strong influence on the expression of the genome by regulating the biochemical and structural properties of chromatin. Epigenetic modifications are most often studied in the context of DNA methylation and post-translational modification of histones, but can include nucleosome remodeling and incorporation of histone variants (Kouzarides, 2007; Maze et al., 2013). Post-translational modification of histone N-terminal tails is a complex and tightly regulated process that has been linked to regulation of key aspects of gene expression including timing and levels of transcriptional activation, mRNA splicing, and poly-A site selection (Kouzarides, 2007; Maze et al., 2013; Sims et al., 2007; Zhou et al., 2012). Epigenetic modifications are a central mechanism for regulating chromatin structure and gene expression in the brain.

1.3.1 Epigenetic regulatory mechanisms in neurodevelopmental disorders

Disruption of epigenetic regulation has been implicated in multiple neurodevelopmental, neuropsychiatric and neurodegenerative disorders (Abel and Zukin, 2008; Fischer et al., 2010; Peixoto and Abel, 2013). Mutation, insertion, or deletion events in regulatory regions of genes can strongly affect recruitment of regulatory proteins, type and amount of epigenetic modifications in these regions, and ultimately transcriptional activation at the affected locus. Expansion of a nearby CpG island, a regulatory DNA sequence that can be methylated, has been linked to decreased expression at the *Fmr1* gene locus,

the causative gene in the autism-spectrum disorder Fragile X syndrome. Reduced or absent Fragile X mental retardation protein (FMRP) expression in the brain results in cognitive deficits, altered social behavior, and aberrant dendritic spine morphology in both human patients and mouse models (Comery 1997, Bernardet and Crusio 2006). Abnormal DNA methylation patterns have also been found in individuals with ASD and other neurological disorders, particularly affecting the promoter region of the gene for methyl-CpG binding protein 2 (MECP2). MECP2 is the causative gene in Rett Syndrome, a neurodevelopmental disorder affecting motor function, social behavior, and cognition. MECP2 itself is not a synaptic protein, rather it functions in the nucleus as a transcription factor and epigenetic regulator, binding methylated DNA and recruiting co-repressor complexes to regulate transcription of genes involved in neuronal development and function (Yasui et al. 2007, Hite et al. 2009). Indeed, numerous transcriptional and epigenetic regulatory proteins have been identified in gene linkage studies for neurodevelopmental and neuropsychiatric disorders, a fact that emphasizes the need to identify and understand the contributions of epigenetic mechanisms in neuronal function (Schoch and Abel, 2014). Many gene linkage studies have identified disease-linked haplotypes residing outside of coding regions, supporting the idea that regulatory DNA sequences may provide critical new insight into the basis of genetic disorders (Nica et al. 2010). Epigenetic regulation in the brain is only beginning to be explored in basic research, and the clinical implications of these findings for neurological disease have yet to be fully realized.

A wide array of histone- and DNA-modifying enzymes have been identified as critical regulators of neuronal function, memory formation, and as causative agents in neurodevelopmental and neuropsychiatric disorders. Much of the research in epigenetic

regulation of cognition has focused on the regulation of co-activator complexes and histone acetyltransferase (HAT) enzymes involved in increasing acetylation of histone lysine residues including H3K9, H3K14, H3K27 and H4K8, marks often associated with increased chromatin accessibility and active gene expression (Abel and Zukin, 2008; Borrelli et al., 2008; Fischer et al., 2007; Peixoto and Abel, 2013). Fewer studies address positive and negative regulation of gene expression by lysine methylation of histones; a modification that functions as a binding surface for protein interactions (Bannister and Kouzarides, 2011). Overall, little is known in the brain about how changes in histone acetylation and methylation mediate negative regulation of gene expression and silencing by co-repressor complexes.

1.3.2. Co-repressors regulate cognitive processes

Co-repressors assemble multi-protein complexes containing structural, chromatin-binding, and DNA- and histone-modifying enzymes that suppress transcription. Catalytic components are assembled around structural proteins, and bound to DNA or histones by chromatin-binding proteins (**Fig 1.3A**). Gene silencing is associated with the removal of activating epigenetic marks, such as acetylation or H3K4 methylation of histones; or through addition of repressive epigenetic marks including DNA methylation and histone methylation at H3K9, H3K27, and H3K36 (Bannister and Kouzarides, 2011). Co-repressor complexes frequently contain multiple catalytic components involved in both addition and removal of epigenetic modifications, suggesting that gene silencing may involve combinatorial or serial effects on modifications across multiple residues and substrates (**Fig. 1.3B**) (Bannister and Kouzarides, 2011; Kouzarides, 2007; Maze et al., 2013). Studies of histone modifications indicate that the presence of certain marks can regulate the modification of other residues, even across histones (Kouzarides, 2007).

Thus, the diversity of catalytic activities within individual co-repressor complexes is likely a critical aspect of their function.

Early studies of co-repressor function in yeast and cell culture models found that co-repressors regulate critical cellular functions from cell growth to differentiation, signal transduction and apoptosis, but the functions of many co-repressors in the brain are very poorly understood (Kato et al., 2011; McDonel et al., 2009). Few biochemical studies of co-repressor complexes have been conducted in neuronal cells. Much of our knowledge regarding the functional properties of co-repressors in mammalian systems has come from the fields of cancer research and developmental biology, where alterations in the function or localization of co-repressors were linked to aberrant regulation of growth, cell morphology, and tissue organization (Kumar et al., 2005; Lai and Wade, 2011; McDonel et al., 2009). In the adult brain, which is primarily populated with post-mitotic, terminally differentiated cells, we are only beginning to appreciate the important roles co-repressors play in signal transduction, plasticity, and cellular memory. Epigenetic mechanisms are engaged by and critically important for mnemonic and cognitive functions in the brain (Peixoto et al. 2013; Schoch et al. 2014; Mahan et al. 2012). In the context of these uniquely neuronal processes, the function and composition of co-repressors in the brain may not be equivalent to those of non-neuronal tissues. Additionally, the expression of neuron-specific components of co-repressor complexes strongly hints at the existence of specialized functions for these complexes in the brain (Palm et al., 1998; Potts et al., 2011; Vogel-Ciernia et al., 2013). Multiple co-repressors have been linked to dynamic changes in gene expression and neuronal activity-dependent regulation, but the specific roles co-repressors play in the brain are only starting to be uncovered (Chen et al., 2003; Ebert et al., 2013; Youn and Liu, 2000a).

Further studies of co-repressors and their function in neuronal tissue are needed to ascertain whether unique functions for these complexes exist within the nervous system, especially with regard to dynamic mechanisms of transcriptional repression/de-repression following neuronal activity.

Many core and accessory components of co-repressor complexes have been linked through genomic studies to neurodevelopmental and neurological disorders, but there is an overall lack of functional studies directly addressing the role of co-repressors in cognitive processes (Peixoto et al. 2013; Schoch et al. 2014). Future studies of the composition and function of co-repressors in the brain are likely to provide powerful insights into gene regulation and how its disruption can lead to neurological and cognitive disorders.

1.3.3. Co-repressors and their function in the brain

NCOR The nuclear receptor co-repressor NCOR plays critical roles both in neural development and in cognitive processes in the adult brain. NCOR assembles a multi-protein co-repressor complex (**Fig. 1.3B**) that interacts with nuclear receptor transcription factors and represses expression of their target genes (**Fig. 1.4A**). NCOR and its sister repressor, silencing mediator of retinoic acid and thyroid hormone receptors (SMRT/NCOR2), were discovered as reversible repressors that interact with the ligand-binding domain of T3 thyroid hormone receptors and are released by T3 (**Fig. 1.5A**).These co-repressors have been shown to bind to a wide range of nuclear receptors (NR) including the retinoid receptors and NR4A family of orphan nuclear receptors, and the methyl CpG binding protein MeCP2 (Codina et al., 2004; Ebert et al., 2013; Hörlein et al., 1995; Kato et al., 2011). NCOR forms a complex that binds

HDAC3, the SIN3A co-repressor (discussed below), and the H3K9/H3K36 demethylase JMJD2A (Ishizuka and Lazar, 2005; Nagy et al., 1997; Zhang et al., 2005).

Repression by NCOR is necessary for both neural development and memory storage in the adult brain. Regulation of neuronal genes through the retinoid receptors (RAR/RXR) by NCOR is a critical component of neuronal function from the earliest stages of development (Gilbert and Lasley, 2013). In the mature brain, disruption of NCOR-regulated TR- and NR4A-dependent gene expression has been linked to cognitive dysfunction and memory impairment in human disorders and rodent models (Bono et al., 2004; Gilbert and Lasley, 2013; Hawk et al., 2012; Hawk and Abel, 2011; Xing et al., 2006). A recent study identified an NCOR-binding domain on MeCP2 that is affected by multiple mutations linked to Rett syndrome, a neurodevelopmental disorder characterized by severe motor and cognitive disability (Lyst et al., 2013). Elimination of a critical phosphorylation site within the NCOR-binding domain of MECP2 recapitulates motor and lethality endophenotypes associated with loss of MECP2 function, but the impact of this mutation in cognitive functioning is not known (Ebert et al., 2013; Lyst et al., 2013).Mutation analysis of NCOR identifies HDAC3 as a critical component of the NCOR complex in the brain (McQuown et al., 2011). Mice carrying a point mutation in the HDAC3-interaction domain of NCOR show enhanced hippocampus-dependent object location memory, indicating that histone deacetylation by the NCOR complex is a key negative regulator of hippocampal gene expression during memory consolidation (**Fig. 1.4**) (McQuown et al., 2011).

In addition to HDAC3, NCOR recruits epigenetic regulators SIN3A and JMJD2A, but the roles of these regulators in the NCOR complex are not well understood. SIN3A and JMJD2A both bind to the N-terminal RD1 repression domain of NCOR and exhibit

repressor activity in reporter assays, but it is not clear whether these interactions are co-occurring or mutually exclusive (Nagy et al., 1997; Zhang et al., 2005). JMJD2A appears to play a complex role in transcriptional regulation as a remover of both repressive H3K9me and permissive H3K36me modifications via its dual Jumonji demethylase domains. The SIN3A co-repressor has also been linked to both activating and repressive functions through its many catalytic binding partners (discussed below)(Silverstein and Ekwall, 2005). Without knowing which enzymatic components of the SIN3A-HDAC complex are present in association with NCOR, it is difficult to guess what impact the complex may have on the regulation of NCOR target genes. Future studies of NCOR and SIN3A co-repressors will provide important insights into mechanisms of gene repression in the brain, and the roles it plays in both development and cognition.

NuRD In addition to histone modifications, nucleosome repositioning is linked to gene regulation thought regulation of chromatin structure and DNA accessibility. Recent studies of chromatin remodeling complexes have uncovered a complex ATP- dependent mechanism by which these complexes uncouple the DNA from the histone surface to allow for looping of DNA and mono-directional sliding of the nucleosome along the DNA (Allen et al., 2013; Tang et al., 2010). One nucleosome repositioning complex involved chromatin compaction is the NuRD complex. A multi-functional complex containing both chromatin remodeling and histone modifying activities, the NuRD complex has been linked to rapid heterochromatin formation by nucleosome compaction via the MI-2/CHD3/4 ATPase/helicase, and histone deacetylation by HDAC1/HDAC2 (**Fig. 1.3B**)(Allen et al., 2013). The catalytic activity of the NuRD complex is directed to chromatin by H3K9me-binding plant homology domain s (PHD) on MI-2, the transcription

factor binding metastasis-associated gene family (MTA1-3), and by methyl CpG binding domain proteins MBD2 and MBD3, which bind methylated and hydroxyl-methylated DNA respectively (Allen et al., 2013; Yildirim et al., 2011). Depletion of MI-2 increases chromatin accessibility and induces DNA demethylation, demonstrating a role for the NuRD complex as a critical component of heterochromatin maintenance (Gao et al., 2009).

The role of the NuRD complex in the brain is not well studied, but it has recently been indirectly linked to regulation of neuronal gene expression and cognitive function (Schoch et al. 2014). A novel CHD ATPase/helicase family member CDH5 is highly enriched in the brain, where it forms a NuRD-like complex that includes HDAC1/HDAC2 and MBD3 and regulates the expression of neuronal genes in cultured neurons (Potts et al., 2011). Mutations in members of the MBD gene family (including MBD2 and MBD3) have been identified in individuals with ASD, suggesting that NuRD complex association with methylated DNA is important for neural development (Cukier et al., 2012, 2010; Murgatroyd and Spengler, 2012). Genetic deletion studies of MBD family members in mice have identified autism-related behavioral phenotypes in mice lacking MBD1, but MBD2 and MBD3 KO mice have not been behaviorally characterized (Allan et al., 2008; Allen et al., 2013; Hendrich et al., 2001). Although the role NuRD-mediated chromatin compaction in memory formation is unclear, chromatin opening by the nucleosome repositioning Brg1-associated factor (BAF) complex (mammalian SWI/SNF) is critically important for memory formation. Loss of neuron-specific BAF complex subunit BAF53b impairs synaptic plasticity and long-term memory consolidation in the hippocampus (Vogel-Ciernia et al., 2013b).Further studies of the NuRD complex in neuronal function

and in behaving animals are needed to gain a more thorough understanding of its role in neural development and cognition.

SIN3A The Switch-insensitive 3a (SIN3A) co-repressor complex is a massive 1.5-2 MDa transcriptional regulatory complex that interacts with a wide array of epigenetic regulatory proteins with critical roles in brain development and cognition. Originally discovered as a suppressor of mating-type switching in yeast, SIN3A is a scaffold protein with multiple protein interaction domains through which it binds a core group of structural proteins along with HDAC1 and HDAC2, and a number of DNA- and protein-modifying enzymes (**Fig. 1.3B**) (Nasmyth et al., 1987; Silverstein and Ekwall, 2005; Williams et al., 2011). SIN3A is critically important for embryonic development, and constitutive loss of *Sin3a* leads to peri-implantation lethality (Dannenberg et al., 2005). There is a dearth of studies of SIN3A in the brain; however, we show in **Chapter 3** that SIN3A is a negative regulator of both memory formation and synaptic plasticity.

SIN3A recruits a wide array of epigenetic modifiers that have been linked to memory and cognition both in human genetic disorders and rodent models. The classic role for the Sin3a complex is transcriptional silencing through the deacetylation of histones mediated by HDAC1/2. Blockade of HDAC activity and loss of HDAC2 (but not HDAC1) both increase synaptic connectivity and enhance long-term memory in rodents (Guan et al., 2009).In addition to transient repression by deacetylase activity, Sin3a co-repressor complexes have also been linked to long-term silencing and heterochromatin formation through Sin3a-HDAC structural protein SDS3, and the H3K9 methyltransferase SETDB1(David et al., 2003; Yang et al., 2003). SETDB1 activity is implicated in the neuropathology of rodent models of Huntington's disease and Rett syndrome, and mutations in SETDB1 have been linked to ASD (Akbarian and Huang, 2009; Cukier et

al., 2012; Jiang et al., 2011; Ryu et al., 2006). Mice conditionally over-expressing SETDB1 in the forebrain have altered emotional responses, but perform normally in cognitive tasks (Jiang et al., 2010). A unique addition to the Sin3a co-repressor complex, OGT, catalyzes serine and threonine N-acetyl O-glycosylation, a reversible monosaccharide post-translational modification that is abundant in the brain (Khidekel et al., 2007). O-glycosylation has been linked to structural and functional changes in key transcriptional proteins, including RNA polymerase II and cyclic AMP response element binding protein CREB (Ranuncolo et al., 2012; Rexach et al., 2012; Wells et al., 2003).

In addition to its roles in gene silencing, Sin3a core complex interacts with factors that have been linked to positive transcriptional regulation during memory formation. The SET1/MLL family of histone methyltransferase stably associate with the Sin3a complex via host cell factor 1 (HCF1) and catalyzes H3K4 tri-methylation, an activating mark that acts as a binding surface for methyl-lysine binding proteins involved in the assembly of the pre-initiation complex and mRNA splicing machinery at the promoter, and the maintenance of active gene expression (Sims and Reinberg, 2006; Sims et al., 2007; Wysocka et al., 2003; Yokoyama and Wang, 2004). In addition to binding positive transcriptional regulators, methylation at H3K4 also blocks recruitment of the H3K9me-binding MI-2 subunit of the NuRD chromatin remodeling complex (Allen et al., 2013; Nishioka et al., 2002). Changes in H3K4 histone methylation have also been linked to activity dependent DNA demethylation and release of methyl-CpG binding protein MECP2 from the promoter CpG islands of memory-related genes *Zif268* and *Bdnf* (Gupta et al., 2010). The MLL family of H3K4 methyltransferases has been directly linked to intellectual disability in multiple human genetic disorders (Murgatroyd and Spengler, 2012; Ng et al., 2010). Mice with reduced MLL have less H3K4 methylation in

the hippocampus and impaired long-term memory (Gupta et al., 2010). A role for SIN3A in both positive and negative transcriptional regulation is supported by genome-wide expression studies showing that loss of SIN3A is associated with bidirectional changes in expression of its target genes (Cowley et al., 2005; Dannenberg et al., 2005; van Oevelen et al., 2010).

A recently discovered epigenetic modification of DNA involves hydroxylation of 5-methyl-cytosineto5-hydroxy-methyl-cytosine (hmC), a reaction catalyzed by the TET family of hydroxylases (Zhang et al., 2010).Studies of methyl-binding proteins suggest that hmC may fulfill a role that is analogous but distinct to that of mC, as a substrate for hmC-binding proteins including MBD3 of the NuRD complex(Allen et al., 2013; Yildirim et al., 2011). Over-expression studies of TET1 reduces DNA methylation, but the relationship between hmC and DNA demethylation has not been determined (Zhang et al., 2010). Recent studies identified TET1 as a SIN3A binding partner, suggesting that hydroxyl-methylation may be yet another way that the Sin3a complex is able to influence the association of epigenetic and transcriptional regulators with DNA(Williams et al., 2011). The function of TET1 in DNA demethylation and chromatin remodeling in the brain remains an open question. Future studies of TET1 in behavioral and cognitive functioning are a crucial next step in understanding the role of TET1 and hmC in the brain.

The Sin3a-HDAC co-repressor complex is recruited to chromatin through association with its transcription factor binding partners, many of which have been linked to neurodevelopmental disorders with cognitive symptoms. SIN3A interacts with a variety of transcription factors, including neural-restrictive silencing factor (REST/NRSF), MECP2, and myocyte enhancer factor 2(MEF2). Constitutive silencing by REST is

critical for suppressing expression of neuronal genes in non-neuronal tissues, but the role of SIN3A as a co-repressor of REST in the brain is not understood (Ballas et al., 2005). The methyl-CpG binding protein MECP2 is well studied as a repressor of memory-related genes including *Bdnf* and *Zif268* in the brain (Chen et al., 2003; Gupta et al., 2010). Loss of activity-dependent repression by MECP2 in rodent models is also associated with deficits in memory, motor behavior, and in the structure and function of synapses, but the roles of MECP2 in cognition and transcriptional regulation are complex and not entirely clear (Collins et al., 2004; Li et al., 2011; Moretti et al., 2006; Nelson et al., 2011, 2006). The transcription factor MEF2 interacts with SIN3A in an activity-regulated manner, and bi-directionally regulates the expression of genes involved in memory and synaptic plasticity (**Fig. 1.5B**) (Cole et al., 2012; Flavell et al., 2008). Expression of a constitutively-active form of MEF2 that lacks the SIN3A interaction domain impairs memory and dendritic spine growth, supporting a role for SIN3A-MEF2 in memory formation (Cole et al., 2012). Though SIN3A associates with a wide diversity of transcription factors and epigenetic modifiers implicated in neuronal function, the role of SIN3A in the brain is only beginning to be explored.

CoREST A relative newcomer to the co-repressor family of transcriptional regulators is CoREST. CoREST (KIAA0071) was discovered by two groups screening for repressors that interact with HDAC2 and REST (Andrés et al., 1999; Humphrey et al., 2001). CoREST is best known as a complex that mediates deacetylation by HDAC1 and HDAC2, but more recently, H3K4 demethylation activity was discovered in the CoREST complex via lysine specific demethylase 1 (LSD1) (**Fig. 1.3B**)(Hakimi et al., 2002; Lee et al., 2005). The DNA-binding co-factor BRCA2-associated factor 35 (BRAF35), regulates repression activities of the CoREST complex by directly binding to RE1 elements.

(Hakimi et al., 2002). In contrast to the co-repressor complexes with dual regulatory activities discussed previously, CoREST appears to have only silencing activity.

CoREST is a versatile repressor linked to both chronic and transient repression of neuronal genes. In non-neuronal cells with high REST expression, CoREST and the SIN3A-HDAC complex bind to paired repressor domains on REST and stably silence the expression of neuronal genes (Lakowski et al., 2006a). Gene knockdown studies of CoREST in the developing mouse brain highlight a critical role for this co-repressor complex in the development of cortical pyramidal neurons, and in the maintenance of cortical neuronal precursors (Fuentes et al., 2012). Depletion of CoREST or SIN3A in non-neuronal cells increases expression of neuron-specific genes (Dannenberg et al., 2005; Lee et al., 2005; van Oevelen et al., 2010). Interestingly, activity-dependent expression of REST isoforms was found in post-mitotic neurons in the adult brain, but the function of REST/CoREST in the mature brain is not known (Palm et al., 1998). In the absence of REST, CoREST is still able to bind RE-1 elements through the HMG DNA binding domain of BRAF35, but SIN3A recruitment is lost (Hakimi et al., 2002; Lakowski et al., 2006b). In addition to REST, CoREST interacts with the methyl CpG binding protein MECP2, where it has been linked to activity-dependent regulation of gene expression during memory consolidation (**Fig. 1.5C**, **Section 1.3.6**) (Chen et al., 2003; Guy et al., 2011; Kavalali et al., 2011). Additional studies of CoREST and its associated factors are needed to understand the role of this co-repressor in the brain.

1.3.4. Complexity and synergism within co-repressor complexes

Co-repressor complexes recruit a wide variety of epigenetic modifiers, and the impact of this diversity on the function of the complexes is frequently not clear. Much of the

literature on co-repressors focuses on identifying catalytic and transcription factor binding partners (Allen et al., 2013; Silverstein and Ekwall, 2005). Simply identifying proteins that can interact with a co-repressor provides limited information about the function of the complex. Very little work has been done to determine whether a co-factor is constitutively present or conditionally recruited to a complex. Knowledge of the composition of a complex is critical to the understanding of its function because transient accessory components can impart significant variation in the function of the complex. For example, the presence of both activating and repressive epigenetic modulators NCOR and SIN3A calls into question the 'repressor' status of these complexes, and hints at the existence of multiple subtypes of these complexes with different regulatory outcomes. Detailed structural and functional studies of co-repressor complexes and their interacting proteins are sorely needed to gain an accurate understanding of how these complexes can influence the expression of their target genes.

Studies of histone modification patterns suggest that certain marks are highly dependent on the presence or absence of other modifications, but the role of co-repressors in synergistic coordination of histone modifying enzymes has not yet been explored (Bannister and Kouzarides, 2011). The modification of lysine 9 of H3 is one example of how coordination of multiple epigenetic regulatory enzymes within a single complex could have important implications for the regulatory outcome. Coupling HDAC1/2 with the histone methyltransferase SETDB1 in the Sin3a complex would allow for efficient H3K9 deacetylation to expose the lysine residue for subsequent methylation by SETDB1. On the other hand, methylation of H3K4 by SIN3A-associated SET1 is functionally antagonistic to H3K9meand blocks recruitment of H3K9me-binding proteins. It is likely that SETDB1 and SET1 are found in distinct subtypes of the Sin3a complex;

however, the existence of functional variants of the Sin3a complex has yet to be demonstrated. It is imperative to expand the focus of future studies of epigenetic regulation beyond individual enzymes and single modifications into the larger context of multi-protein complexes regulating chromatin accessibility and protein recruitment.

1.3.5. Not just silencing: co-repressors as dynamic regulators of gene expression

Gene promoters typically contain multiple conserved sequence elements bound by transcriptional regulators to collectively influence expression levels at the locus. Genetic studies of conserved regulatory sequences suggest that multiple transcription factors can mediate highly divergent patterns of expression at a promoter. Especially striking is the recruitment of common repressors to mediate two distinct patterns of silencing at a single gene locus. CoREST/SIN3A regulation has been linked to both constitutive silencing (REST) and activity-regulated repression (MECP2) at the *Bdnf* and *Zif268* loci (Ballas et al., 2005; Chen et al., 2003; Gupta et al., 2010). Both repressor complexes were found at two distinct regulatory sites, a REST-bound repressor element 1 (RE1) site and a MECP2-bound CpG island (Ballas et al., 2005). In non-neuronal cells, repressor complexes were found at both sites and expression was strongly inhibited (Ballas et al., 2005). In neurons, constitutive silencing by REST was relieved, leaving plastic repression through the activity-regulated MECP2 (Ballas et al., 2005). These studies suggest that repressor complexes may function as adaptable silencing modules that fulfill a wide range of roles depending on the transcription factors with which they associate.

1.3.6. Activity-dependent gene regulation by co-repressors

Activity-induced activation of gene expression in neurons is best understood in the context of regulation of HATs and histone acetylation; however, studies of HDAC

inhibitor compounds and activity-regulated repressor proteins suggest that relief of repression is a critical component of gene regulation in the brain. The nuclear receptor field has thoroughly demonstrated that co-repressor complexes can be responsive to signal transduction pathways. Ligand-mediated release of NCOR co-repressor from nuclear hormone receptors is required to expose the transactivation domain of the receptor to co-activator binding (**Fig. 1.5A**). In neurons, signaling is frequently propagated to the nucleus via the effects of calcium influx on calcium-binding proteins and kinase activity. The activity-regulated transcription factor MEF2 regulates in turn the expression of numerous neuronal genes, including *Bdnf, Homer1, Egr1,* and *Nurr1* (Flavell et al., 2008). MEF2 alternates between recruitment of either the SIN3A-HDAC co-repressor or the co-activator p300 via a calcium dependent switching mechanism (**Fig. 1.5B**). At rest, MEF2 transactivation is inhibited by the binding of CABIN1, a molecular switch that recruits the SIN3A-HDAC complex (Youn and Liu, 2000a). In the presence of calcium, calmodulin binds to CABIN1 and dissociates it from MEF2, alleviating repression by SIN3A, and freeing the MEF2 domain to bind the co-activator/ HAT p300 (Youn and Liu, 2000b). In addition to calcium-binding proteins, co-repressor activity can also be regulated by phosphorylation, as is the case for MECP2.

MEPC2 has long been associated with chronic repression and maintenance of methylated DNA, but recent discoveries strongly suggest that both DNA methylation and MECP2 are dynamically regulated (Adachi and Monteggia 2014). Recent studies suggest that the activity of repressor protein MECP2 is regulated by neuronal activity and calcium signaling (Guy et al., 2011). At promoters with methylated CpG islands, MECP2 has been associated with histone deacetylation and transcriptional silencing, presumably through interactions with repressive SIN3A, NCOR and CoREST complexes

(**Fig 1.5C**). Phosphorylation of MECP2 is associated with bi-directional changes in affinity of MECP2 for methyl-cytosine, and is reported to occur following neuronal activity (Chen et al., 2003; Ebert et al., 2013; Guy et al., 2011; Li et al., 2011; Tao et al., 2009).

Interestingly, gain- and loss-of-function studies support a role for MECP2 in transcriptional activation at promoters lacking methylated CpG islands as a binding partner for cyclic AMP response element binding protein CREB; however, the function of MeCP2-CREB interactions in gene regulation has not yet been elucidated (Chahrour et al., 2008). One could speculate about a possible role for MECP2 in recruiting an activating SIN3A/HDAC/SET1 complex to locally increase H3K4 methylation, but this hypothesis has yet to be tested (**Fig. 1.5C**). Further studies of the dual roles of MEF2, MeCP2, and the Sin3a-HDAC complex as bidirectional regulators of transcription will yield important new insights into activity-dependent gene regulation, and its dysfunction in neurodevelopmental disorders.

1.3.7. Co-repressors: looking forward

Co-repressor complexes regulate chromatin structure and transcriptional regulation with a wide array of epigenetic modifications. In the brain, epigenetic modifications and chromatin dynamics are highly plastic, and are an integral and fundamental component of neuronal responses to developmental and environmental signals. Studies of transcription factors and regulatory factors associated with co-repressor complexes have uncovered evidence of highly dynamic regulation of repression by SIN3A and CoREST complexes in response to calcium influx, a mechanism long associated with positive regulators, but only recently linked to repression. Evidence that individual co-repressors can fulfill a range of roles from activity-regulated repression to long-term stable silencing is opening up exciting new avenues for discovery.

Although co-repressors themselves are relatively poorly studied in the brain, many transcription factors and catalytic enzymes associated with co-repressor complexes have strong connections to neuronal function, and neurodevelopmental and cognitive disorders. A recurring theme in disease models with co-repressor dysfunction is altered recruitment of proteins to chromatin. All of the complexes discussed herein are involved in either regulation of histone or DNA methylation (NCOR, SIN3A, CoREST) or contain components that bind to methylated histones (NuRD) or methylated or hydroxyl-methylated DNA (NuRD, SIN3A, CoREST). Surprisingly, the role of these complexes as regulators of chromatin-binding proteins has not been well studied. Much of what is known about transcriptional regulation by histone- and DNA-binding proteins came from studies of tumor suppressors in cancer research, but many of these same molecules are being identified as causative agents in neurodevelopmental disorders. Increased dialogue and collaboration between the fields of neuroscience and cancer biology could be highly beneficial to the study of epigenetic basis of memory and synaptic function.

1.4. Summary and future directions

Cognitive deficits are a disabling feature of many neurodevelopmental and neuropsychiatric disorders, and are refractory to many of the available treatment options. Here, we discussed rodent genetic models as a key tool to uncover molecular mechanisms underlying cognitive deficits, and identify novel targets and strategies for drug discovery. In **Chapter 2**, I use a gene knockout model to examine behavioral, cognitive and synaptic functioning in mice lacking a copy of ASD candidate gene *Pcdh10*. One promising avenue for cognitive enhancement lies in the contributions of epigenetic regulatory complexes, particularly silencing complexes, as both causative agents and potential therapeutic targets for neurodevelopmental and neuropsychiatric

disorders. In **Chapter 3**, I use a gene knockdown model to show that the co-repressor *Sin3a* is a negative regulator of memory formation and synaptic plasticity in mice. Finally, in **Chapter 4**, I identify limitations to a currently available conditional gene deletion system in rodents. Together, these studies expand our knowledge of synaptic and epigenetic mechanism of memory formation, and highlight the role of synaptic structural proteins as key targets of genetic regulation in memory formation.

Chapter 1 Figure legends

Figure 1.1. Conditional targeted recombination using the Cre-loxP system. A. Gene knock-in of loxP recognition sites flank the exon targeted for deletion (red). **B.** During Cre-mediated recombination, the intervening sequence between the two loxP sites is arranged into a crossover configuration. **C.** Recombination event results in excision and repair of parent strand, and creation of a circular loop of DNA containing the targeted sequence.

Figure 1.2. Cognitive and neurostructural phenotypes in a schizophrenia mouse model depend on temporal pattern of transgene expression. In mice conditionally overexpressing the G protein alpha S subunit, contextual memory, PPI and brain volume phenotypes depend on what stage of life overexpression occurred. Contextual memory deficits result from developmental changes associated with overexpression in juvenile animals, and these deficits are stable through adulthood despite transgene suppression. PPI deficits persist with constitutive overexpression, but can be rescued by transient suppression during either development or adulthood. Volumetric differences in the striatum are readily produced in animals that overexpress in adulthood. Interestingly, striatal volume changes induced during overexpression in juvenile animals fail to recover following transgene suppression in adulthood. (adapted from Kelly et al. 2008)

Figure 1.3. Structure and composition of co-repressor complexes. A. Co-repressor complexes are composed of structural co-repressor backbones bound to epigenetic modifier effector proteins, and recruited to chromatin by DNA- or histone-binding proteins. **B.** Factors associated with NCOR, NuRD, SIN3A, and CoREST co-repressor complexes, including both core components and accessory co-factors.

Figure 1.4. NCOR regulates long-term memory consolidation via HDAC3. A. Wild-type NCOR complex binds HDAC3 and SIN3A co-repressor, and represses transcription of genes regulated by nuclear receptors. **B.** Mutant NCOR carries a single point mutation in the deacetylase activating domain (DADm) that blocks HDAC3 binding. **C.** DADm mutant mice exhibit enhanced memory in the hippocampus-dependent object location memory task. DADm mice display robust discrimination under sub-threshold training conditions that do not induce long-term memory in wild-type animals. (adapted from McQuown et al. 2011.)

Figure 1.5. Predicted roles for co-repressor complexes in dynamic gene regulation. A. NCOR recruits HDAC activity both directly and indirectly through association with the SIN3A co-repressor. Unliganded nuclear receptors are transcriptionally silent, and are associated with elevate H3K9 methylation and reduced H3K4me and AcH3. Ligand binding induces dissociation of NCOR and recruitment of the histone acetyltransferase p300. **B.** MEF2 alternates between co-repressor recruitment and co-activator recruitment in an activity-dependent manner. The calcium-responsive co-factor CABIN1 binds both MEF2 and SIN3A under basal conditions. **C.** Methyl-DNA bound MECP2 associates with multiple co-repressors, including CoREST and SIN3A. Neuronal activity-dependent phosphorylation of multiple residues on MECP2 alters its affinity for mC. MECP2 can interact with CREB at promoters lacking DNA methylation, but positive transcriptional regulation by MECP2 has not been demonstrated. One potential mechanism for positive regulation could involve SIN3A and the H3K4 methyltransferase SET1.

Chapter 1 Figures

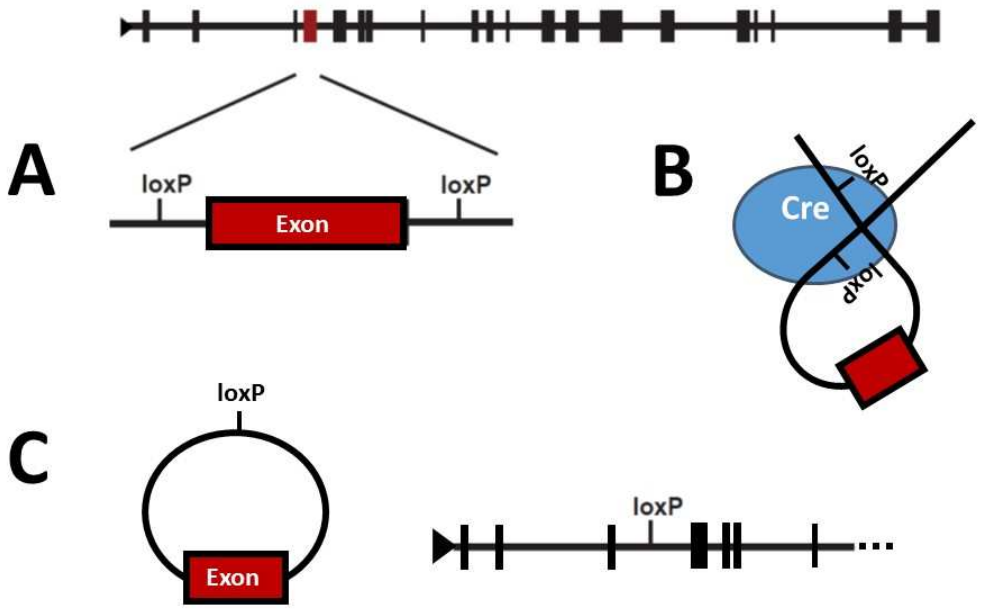

Figure 1.1

GαS transgene expression	Constitutive	Adult only	Developmental
	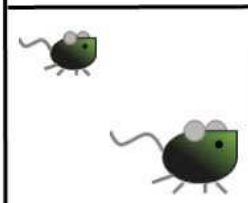	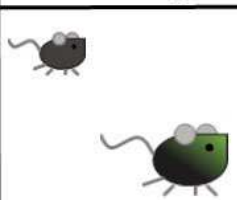	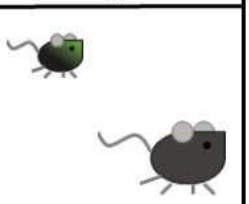
Phenotype:			
Contextual Fear Memory	**Impaired**	**Intact**	**Impaired**
Startle/PPI	**Impaired**	**Intact**	**Intact**
Striatum volume	**Reduced**	**Reduced**	**Reduced**

Figure 1.2

A

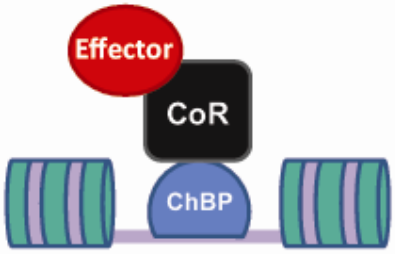

B

Co-Repressor Complex	NCOR	NuRD	SIN3A	CoREST
Effector	HDAC3 HDAC1/2 JMJD2A	MI-2 HDAC1/2	HDAC1/2 SETDB1 SET1 OGT	HDAC1/2 LSD1
Structural	NCOR SIN3A	p66 RBBP7/4	SIN3A SDS3 SAP18/30 RBBP7/4	COREST
Chromatin Binding	NR4A TR ER/AR RAR/RXR MECP2	MI-2 MBD2/3 MTA1-3	MECP2 REST MEF2 HCF1 NR/NCOR	REST MECP2 BRAF35

Figure 1.3

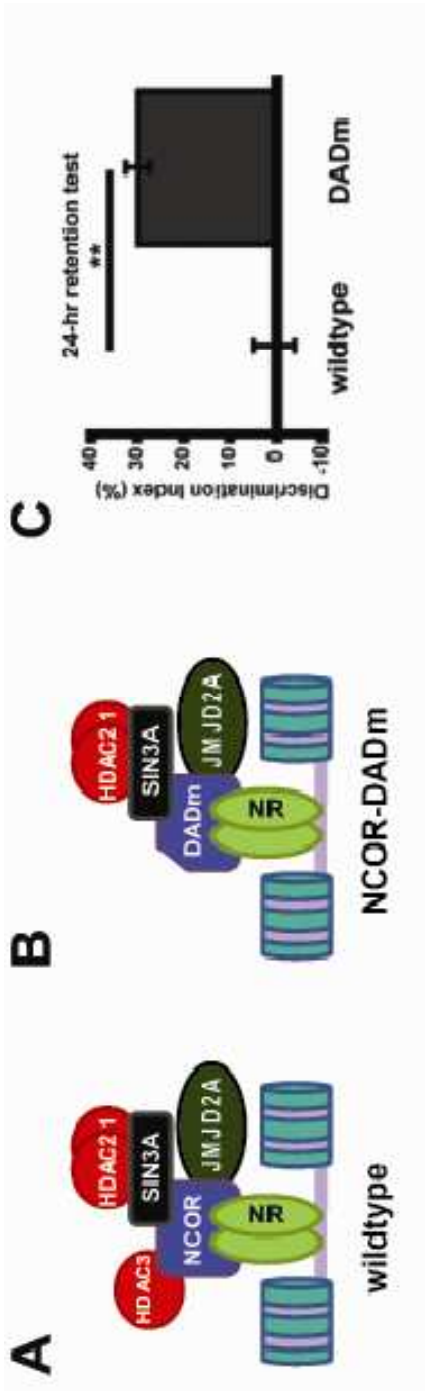
A
HDAC2 1
SIN3A
JMJD2A
HD AC3
NCOR
NR
wildtype
B
HDAC2 1
SIN3A
JMJD2A
DADm
NR
NCOR-DADm
C
24-hr retention test
**
Discrimination Index (%)
40
30
20
10
0
-10
wildtype
DADm

Figure 1.4

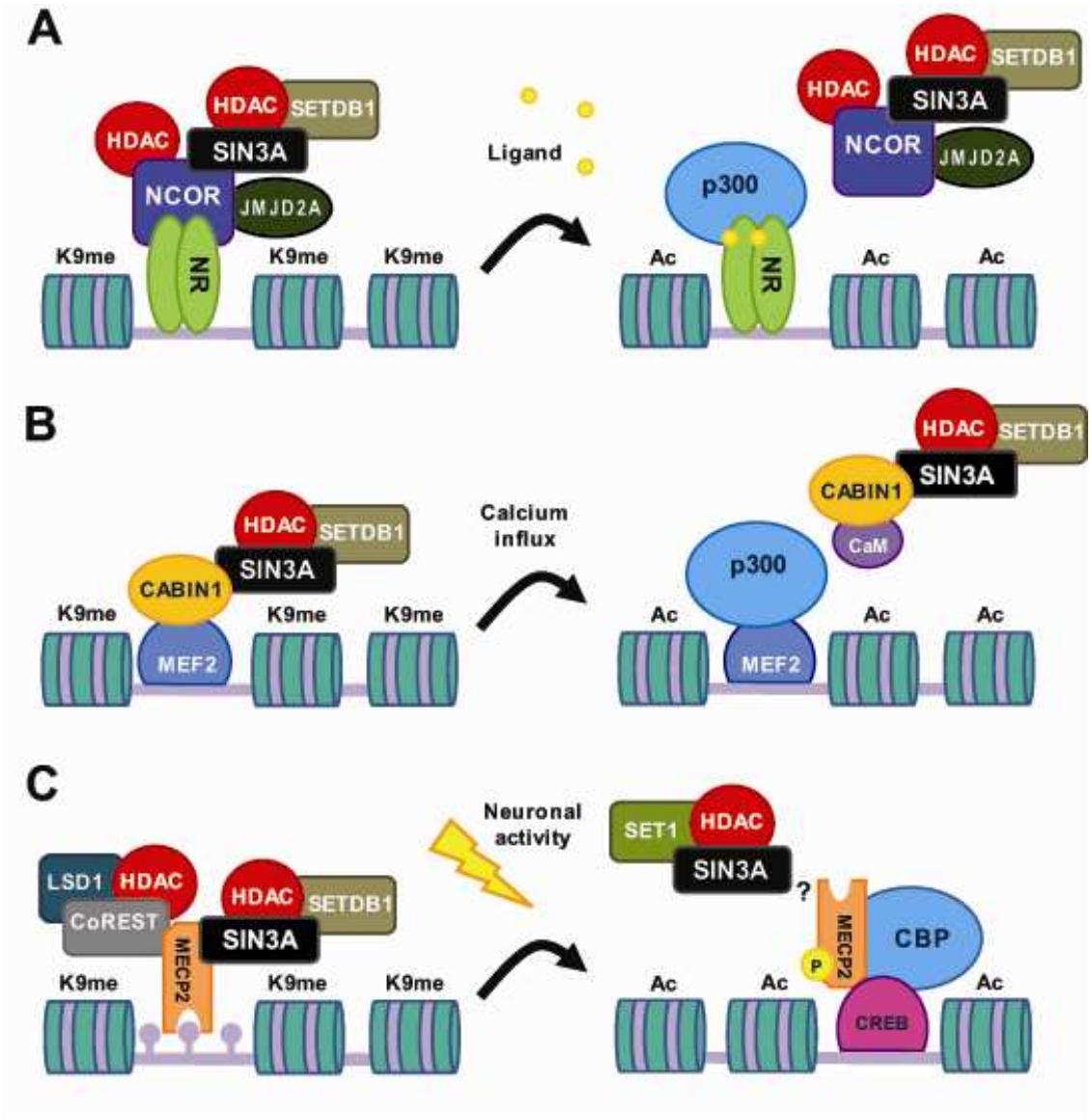
A
HDAC
SETDB1
HDAC
SIN3A
NCOR
JMJD2A
NR
K9me
K9me
K9me
Ligand
HDAC
SETDB1
HDAC
SIN3A
NCOR
JMJD2A
p300
NR
Ac
Ac
Ac
B
HDAC
SETDB1
SIN3A
CABIN1
K9me
K9me
K9me
MEF2
Calcium influx
HDAC
SETDB1
SIN3A
CABIN1
CaM
p300
Ac
Ac
Ac
MEF2
C
LSD1
HDAC
CoREST
HDAC
SETDB1
SIN3A
MECP2
K9me
K9me
K9me
Neuronal activity
SET1
HDAC
SIN3A
?
MECP2
P
CBP
Ac
Ac
Ac
CREB

Figure 1.5

AUTHOR CONTRIBUTIONS

This chapter was written by H. Schoch, with suggestions from T. Abel, and J. Tudor.

Parts of this chapter are contained in a published review: Schoch H, Abel. "Co-repressors and memory storage." (2014) Neuropharmacology, 80: 53-60.

CHAPTER 2: MALE-SPECIFIC SOCIAL AND COGNITIVE DEFICITS IN MICE HAPLOINSUFFICIENT FOR *PCDH10*

Abstract

Behavioral and cognitive impairments in individuals with autism spectrum disorder (ASD) have been attributed to abnormal neuronal connectivity in the developing brain, but the molecular basis of these deficits is largely unknown. Human genetic studies have implicated several members of the cadherin / protocadherin superfamily of genes in autism spectrum disorders (ASD), including *Protocadherin 10 (PCDH10)*, a member of the δ2 subfamily of non-clustered protocadherin genes. Previous reports indicate that *Pcdh10* plays a role in prenatal axon outgrowth, as well as synapse elimination, but its effects on social behavior and cognitive function, phenotypes highly relevant to ASD, are unknown. Here we show that male mice lacking one copy of *Pcdh10* (male *Pcdh10*$^{+/-}$ mice) have behavioral deficits in social approach and conditioned fear, and have abnormal spine morphology and impaired gamma activity in the amygdala. Social deficits in *Pcdh10*$^{+/-}$ males can be rescued with acute treatment with the NMDAR partial agonist d-cycloserine. Our studies reveal that Pcdh10$^{+/-}$ mice have male-specific synaptic and behavioral deficits consistent with amygdala dysfunction, and establish *Pcdh10*$^{+/-}$ mice as a novel genetic model for investigating structural and behavioral changes relevant to ASD.

2.1 Introduction

Reduced tendency to seek out and engage in social interactions is a highly disabling and treatment refractory core feature of autism spectrum disorders (ASD) that disrupts growth of social cognition and social skills during the sensitive developmental period of childhood (Dawson et al., 2002; Jones et al., 2008; Chevallier et al., 2012). The genetic and neurobiological bases of impaired sociability in ASD are both diverse and poorly understood, but multiple lines of evidence from structural imaging, post-mortem brain analysis, and genetic risk genes point to abnormal synaptic connectivity as a key neurobiological feature of ASD that may underlie both social and cognitive impairments (Bakhtiari et al 2012, Wolff et al. 2012, Irwin et al. 2001, Gilman et al. 2011). Human linkage studies have identified multiple ASD-associated genes that are implicated in the structure and function of neuronal synapses (Toro et al. 2010, Gilman et al. 2011, Morrow et al. 2008). Accumulating evidence has strongly implicated variants in the cadherin and protocadherin superfamily of calcium-dependent neural cell adhesion molecules genes in ASD (O'Roak, 2012, Camacho, 2012). Deletions affection the protocadherin 10 gene *Pcdh10* and the regulatory region near *Pcdh10* have been associated with ASD, suggesting that it may play a role in the pathophysiology of the disorder (Morrow et al., 2008; Bucan et al., 2009).

PCDH10, also known as OL-protocadherin, is a member of the δ2 subfamily of non-clustered protocadherins is highly expressed in the brain (Kim et al. 2011, Hirano et al. 1999). *Pcdh10* is an activity-regulated gene expressed throughout much of the postnatal mouse brain, with high levels of expression in olfactory and limbic regions,

including the basolateral amygdala (Hirano et al., 1999; Aoki et al., 2003). In neurons, PCDH10 functions in a molecular pathway with Fragile X mental retardation protein (FMRP) and myocyte enhancer factor 2 (MEF2), to regulate the stability of the post-synaptic density following neuronal activity (Tsai et al 2012). FMRP binds *Pcdh10* mRNA transcripts and transports them to the synapse (Dictenberg et al. 2008, Tsai et al. 2012). At the synapse, PCDH10 has been linked to both spinogenesis and synapse elimination. A synaptic transmembrane protein, PCDH10 interacts with Nck-associated protein 1 (Nap1) to recruit the WAVE actin polymerization complex, a mechanism that has been linked to lamellipodia extension and spinogenesis in neurons (Nakao Takeichi 2010 and Pilpel and Segal 2005). Following neuronal activity, PCDH10 facilitates proteosomal degradation of postsynaptic density protein 95 (PSD-95) and is required for MEF2-induced synapse elimination (Tsai et al., 2012). The role of PCDH10 in regulating spine dynamics downstream of FMRP supports the intriguing idea that synaptic abnormalities observed in Fragile X syndrome, which often has an ASD-like phenotype, might be attributed in part to effects of FMRP loss on the trafficking and regulation of PCDH10.

Here we use a gene knockout mouse model to investigate the role of *Pcdh10* in modulating social behavior, cognition, and connectivity phenotypes relevant to ASD. We demonstrate a role for *Pcdh10* as a regulator of social and cognitive functioning, which likely exerts its effects through modulation of synaptic connectivity in the amygdala.

2.2 Methods

Animal Housing

All mice were cared for in accordance with the National Academy of Sciences Guide for the Care and Use of Laboratory Animals and all animal procedures were approved by the University of Pennsylvania Institutional Animal Care and Use Committee (IACUC).*Pcdh10*$^{+/-}$mice in which the first exon of *Pcdh10* had been replaced with a *lacZ-neo* selection cassette were obtained from Shinji Hirano and Masatoshi Takeichi (Kochi Medical School and RIKEN Center for Developmental Biology, Japan) (Uemura et al., 2007). The mice had been backcrossed to a C57BL/6N genetic background for more than 15 generations (personal communication from Shinji Hirano). Male *Pcdh10*$^{+/-}$ mice were crossed with female C57BL/6J (B6) mice, to generate wild-type (*Pcdh10*$^{+/+}$) or heterozygous null (*Pcdh10*$^{+/-}$) offspring. The mouse line was maintained by consecutive generations of crossing *Pcdh10*$^{+/-}$ males with B6 females. The mice that underwent behavioral testing were the offspring of at least two consecutive backcrosses to C57BL/6J. Same-sex littermates were weaned into group-housing with 2 - 5 per cage in a temperature and humidity controlled environment in a 12-hour light-dark cycle. All mice had access to food and water *ad libitum*. Behavioral testing and tissue collection were conducted during the light phase.

Behavior

Social Approach Test (SAT). Naïve mice underwent the SAT, a test of sociability (tendency to seek social interaction) in a 3-chambered apparatus in a darkened behavioral testing room, using methods described previously (Fairless et al., 2012). The two end chambers of the testing apparatus, separated by a middle chamber, each contained an empty, transparent, perforated Plexiglas cylinder. For the initial 10 minutes of the SAT, each *Pcdh10*$^{+/-}$ or wild-type test mouse was allowed to freely explore the three chambered apparatus (*Phase 1*). Following this habituation phase, a non-social

stimulus (paperweight) was placed into one cylinder and a social stimulus mouse (an adult male A/J that had been gonadectomized prior to 4 weeks of age and had been habituated to being in the cylinders on 3 previous, consecutive days) was placed simultaneously in the other cylinder and the test mouse was allowed to explore the apparatus and cylinders for the next 10 minutes (*Phase 2*). Immediately following Phase 2, the cylinders were removed so that the test mouse could freely interact with the stimulus mouse and the paperweight for 10 minutes (*Phase 3*). The time that each test mouse spent in each chamber and spent in sniffing each cylinder, as well as the distance each mouse traveled was scored in each Phase, using the automated behavioral analysis system, TopScan (CleverSysInc, Reston, VA, USA) (Fairless et al., 2011). Within each sex, time spent sniffing the cylinders was compared using repeated measures analysis of variance (rmANOVA). ANOVA interactions that were $p < 0.05$ underwent *post hoc* tests (Bonferroni-Dunn).

Olfactory habituation-dishabituation. This test of ability to detect and differentiate odors (Yang and Crawley, 2009) was performed under infrared lighting in an otherwise darkened room. Mice were allowed to acclimate for 30 minutes to a clean testing cage, and then were presented with a sequence of different odorant-dipped cotton swabs that were lowered into the cage for 2 min each, with 1 min intervals between presentations of swabs. The order of odorants presented--each presented 3 consecutive times--was the following: water, almond, vanilla, soiled mouse bedding from an unfamiliar same-sex mouse, soiled mouse bedding from an unfamiliar opposite sex mouse. The time that the test mouse spent sniffing each swab was measured.

Fear conditioning. Animals were singly housed one week prior to training, and conditioned as previously described (Hawk et al., 2011). Briefly, animals were handled 2 min per day for three consecutive days, followed by a single training session in enclosed rectangular conditioning chambers. Contextually conditioned animals were exposed to the conditioning context for 148 s, followed by a 2 s 1.5mA footshock. Cue conditioned animals were exposed to the context for 120s, a 60 dB tone was presented for 30s, which co-terminated with a 2 s 1.5mA footshock. Animals were removed from the chambers 30s after receiving the footshock, and tested for memory retention after 24 hrs. Contextually conditioned animals were returned to the training context for a single 5 min context test. Cue conditioned animals were tested in a new room and were placed in a novel round or triangular chambers with solid floors and a novel odorant (lemon dish soap) for 3 min of exploration (pre-CS) followed immediately by 3 min conditioned cue presentation (CS). Training and test sessions were recorded and freezing behavior was measured using automated scoring software (Clever Systems, Reston, VA, USA).

Open field. Naïve group housed mice were exposed to a 41 x 41 cm white open field (San Diego Instruments, San Diego, CA, USA) for 30 min as previously described (Kelly et al., 2008). Horizontal ambulatory activity was calculated for center (greater than 5cm from apparatus wall) and peripheral (within 5cm of apparatus wall) zones. For center, periphery and total movement, each sex was separately compare by genotype using an unpaired two-tailed t-test.

Elevated zero maze test. The Plexiglas zero maze had a width of 2 inches and outside circumference of 79 inches. It consisted of open quadrants and two closed quadrants. In this test of anxiety-like behavior (Tarantino et al., 2000), each mouse was allowed to

investigate the apparatus for 5 minutes. The Viewpoint Tracking System was used to calculate time spent in the open quadrants vs. in the closed quadrants and numbers of transitions between the quadrants. Genotypes were compared using one-way ANOVA.

Accelerating rotarod. To assess motor coordination and balance, mice were placed on a turning rotarod that accelerated from 0 to 40 revolutions per minute over the course of 5 minutes (Crawley, 2007). Each trial ended when the mouse fell off of the rotarod to a table top several inches below or when 5 minutes elapsed. There were 10 consecutive trials, with 5 minute inter-trial intervals. Time that each mouse remained on the rotarod in each trial was measured. Genotypes were compared across training using repeated measures ANOVA.

Novel object recognition. Group housed mice were trained and tested as previously reported (Oliviera et al, 2010). Briefly, mice were handled for 2 min per day for 3 consecutive days, followed by five consecutive days of 5 min habituation sessions in the empty experimental arena. On training day, animals were exposed to two identical objects placed near the center of the arena and allowed to freely explore the objects for 15 min. Twenty-four hours after training, one familiar object explored during training and one novel object was placed in the arena and animals were allowed to explore the objects for a single 15 min test session. Test sessions were scored by a trained observer blind to the genotypes of the animals for exploratory sniffing in which the animal's snout is within approximately 4mm of an object. Preference for the novel object was expressed as the fraction of the total exploration time an animal spent sniffing the novel object. Genotype effects for each sex were calculated using unpaired two-tailed t-tests.

Neuronal reconstruction and spine counts

Male mice were sacrificed and whole brains were removed, rinsed in PBS, and Golgi impregnation was conducted using the FD Rapid GolgiStain kit (FD Neurotechnologies, Columbia, MD, USA) according to manufacturer's instructions. After 5 days of impregnation in kit solution A/B, brains were placed in solution C twice for 24hrs each. Brains were frozen and 100um coronal sections were taken on a cryostat. Sections were mounted on gelatin coated slides and were protected from light and thoroughly dried at room temperature over 7 or more days. Slides were developed according to the manufacturer's instructions, and coverslipped using Permount mounting medium (Thermo-Fisher). Clearly-stained amygdala neurons with visible spines were manually reconstructed using Neurolucida neuron tracing software (MBF Bioscience, Williston, VT). Traced neurons with multiple dendrites over 140 µm in length were selected for spine counts. Proximal (within 100 µm of the soma) and distal (within 100 µm of the terminus) dendritic regions (50 µm length) were identified on long dendrites, and all visible spines within the 50 µm region were manually identified and counted by type (Hering and Sheng 2001, Yuste and Bonhoeffer 2004). A maximum of two dendrites each with proximal and distal regions were counted on each neuron. Average spine counts of each type per 50 µm were calculated for each genotype. Percent filopodial type was calculated as filopodial spines / total spines for each region.

Electrophysiology

VSD experiments were performed according to previous studies (Carlson and Coulter, 2008). Following isoflurane anesthesia, mice were decapitated. The brain was extracted and coronal amygdalar slices 350 µm thick were cut using an Integraslice 7550 PSDS vibrating microtome (Campden Instruments, Lafayette, IN) in ice-cold sucrose artificial

cerebrospinal fluid (ACSF), in which NaCl was replaced with an equiosmolar concentration of sucrose. ACSF consisted of 130 mM NaCl, 3 mM KCl, 1.25 mM NaH2PO4, 26 mM NaHCO3, 10 mM glucose, 1 mM MgCl2, and 2 mM CaCl2 (pH 7.2-7.4 when saturated with 95% O2 and 5% CO2). Slices were then transferred to a static interface chamber (34℃) for 30 min and kept at 22- 25℃ thereafter. The osmolarity of all solutions was 305-315 mOsm.

Slices were stained for 15 min with 0.125 mg/ml (in ACSF) of the voltage sensitive dye di-3-ANEPPDHQ (D36801, Invitogen), and imaged in an oxygenated interface chamber using an 80 x 80 CCD camera recording at a 1 kHz frame rate (NeuroCCD: RedShirtImaging, Decatur, GA). Epi-illumination was provided by a custom LED illuminator. Slices were continuously bathed in ACSF. Amygdalar stimulation using burst of 4-40-mA, 200-ms pulses were administered with the electrode placed in the most dorsal region of the lateral amygdala (LA). After initial electrode placement and establishment of slice viability, baseline responses with control ASCF were elicited by either 12 burst stimulus trials, each separated by 40 s.

To analyze VSD data, a data processing program was created in IGOR (Wavemetrics, Lake Oswego, OR). Regions of Interest (ROI) were chosen according to a standardized anatomy of the amygdala. The lateral amygdala (LA) was chosen to be the dorsal most region of the structure. This region, however, did not include the area where the electrode was placed to avoid including direct stimulation into the analysis. The basolateral amygdala (BLA) was chosen to be ventral medial to the LA. The striatum was chosen to be dorsal medial to the LA. Fluorescence-changes are calculated as the percent change in fluorescence divided by the resting fluorescence (%dF/F0). Colored

images were generated in IGOR on 12-trial-averages. For gamma power analysis data was imported into Matlab (Mathworks), and processed with the open source tool box (Oostenveld, Fries, Maris, & Schoffelen, 2011). Time-locked averaged data were transformed to time frequency space using Morlet wavelets previously used in in-vivo electrophysiology experiments (Gandal et al., 2010) to allow calculation of evoked power. To quantify changes in power, the region of the steady-state GAMMA was observed on the time-frequency plot, and the integral calculated of the response using in house scripts.

Data analysis

The behavioral data and structural are presented as mean ±SEM. Statistical tests were conducted using SPSS (IBM, Armonk, NY) software.

2.3 Results

2.3.1 Pcdh10$^{+/-}$ males exhibit reduced sociability.

To determine whether social behavior is altered in *Pcdh10*$^{+/-}$ mice, we tested male and female juvenile *Pcdh10*$^{+/-}$ mice and wildtype (WT) littermates in the three-chambered social approach task (Sankoorikal et al. 2006, Fairless et al. 2013). Relative to male WT littermates, male *Pcdh10*$^{+/-}$ mice spent less time sniffing the social cylinder in the presence of the stimulus mouse in Phase 2 (**Fig. 2.1A**; rmANOVA: phase $F_{1,26}$= 34.8, $p<0.0001$; genotype $F_{1,26}$=8.4, $p<0.01$, and phase*genotype $F_{1,26}$=10.4, $p<0.01$; Bonferroni *post hoc* wild-type by phase $p<0.05$, phase 2 by genotype $p<0.01$). There were no differences in exploration of the non-social cylinder during Phase 1 or 2 by male mice (**Fig. 2.1B**; rmANOVA: phase $F(1,26)=0.38$ $p>0.05$, genotype $F(1,26)=3.37$, $p>0.05$). Interestingly, there was no significant difference between female WT

littermates and female *Pcdh10*$^{+/-}$ mice in sniffing the social cylinder or in Phase 2 (**Fig. 2.1C**, rmANOVA: genotype $F(1,23)=4.2$ $p>0.05$), nor were differences found in non-social exploration in female mice (**Fig. 2.1D**; rmANOVA $F(1,23)= 24.55$, $p<0.0001$, Bonferroni *post hoc* wild-type by phase $p<0.05$, *Pcdh10*$^{+/-}$ by phase $p<0.05$). Because olfactory function is critically important for social investigation in this task and Pcdh10 is highly expressed in the olfactory bulb, male and female Pcdh10 mice were tested for anosmia using the olfactory habituation-dishabituation task. Males and females of both genotypes showed robust exploration in response to presentation of social and non-social odors, and similar rates of habituation to repeated presentations (**Fig.2.2**, rmANOVA: male genotype $F(1,14)=0.765$ $p>0.05$; female genotype $F(1,14)=1.8$ $p>0.05$). This pattern of responses indicates that basic olfactory acuity and discrimination is intact in *Pcdh10*$^{+/-}$ mice. Altogether, these data show reduced social approach and social sniffing behavior specifically in male *Pcdh10*$^{+/-}$ mice that is not attributable to an olfactory deficit.

2.3.2 Impaired fear memory in Pcdh10$^{+/-}$ males.

Intellectual disability affects approximately 40% of individuals with ASD and is a core phenotype of Fragile X syndrome particularly in males with Fragile X syndrome (AADDMN, Pederson et al. 2012, Brodkin 2008). To investigate the role of Pcdh10 in associative learning, we tested adult *Pcdh10*$^{+/-}$ mice and WT littermates for conditioned fear memory. Processing of contextual and auditory cue stimuli rely on anatomically distinct pathways (hippocampal, and auditory/thalamic respectively), but associative pairing of cue stimuli to a footshock experience requires amygdala circuitry (Phillips and LeDoux 1992, Muller LeDoux 1997, Marschner 2008, Goosens Maren 2001, Newton et al. 2004).

Contextual fear memory relies on both hippocampus and amygdala circuits (Phillips and LeDoux 1992, Kim Faneslow 1993). When we conditioned mice to contextual cues, *Pcdh10*$^{+/-}$ males showed reduced freezing behavior basally prior to footshock, as well as upon exposure to the conditioned context (**Fig.2.3A**. two-way ANOVA: phase $F(1, 22)= 99.82$, $p<0.001$; genotype $F(1,22)= 13.21$, $p<0.001$). By contrast, no difference in freezing behavior was observed in *Pcdh10*$^{+/-}$ females (**Fig.2.3B**. two-way ANOVA: phase $F(1,19)= 51.75$, $p<0.001$).

Auditory tone cued fear memory relies on inputs from cortical/thalamic and brainstem auditory nuclei to the amygdala (Muller and LeDoux 1997, Rogan LeDoux 1997, Newton et al. 2004). During the cued fear test, *Pcdh10*$^{+/-}$ males respond to the tone presentation, but have reduced freezing responses compared to wild type animals (**Fig.2.3C**. two-way ANOVA: phase $F(2,18)= 43.58$, $p<0.001$; genotype $F(1,19)= 10.13$, $p<0.01$); genotype*phase $F(2,18)= 3.27$, $p<0.05$). *Pcdh10*$^{+/-}$ females show a generalized reduction in freezing behavior compared to wild-type females that is not specific to tone presentation (**Fig.2.3D**. two-way ANOVA: phase $F(2,20)= 78.61$, $p<0.001$; genotype $F(1, 21)= 6.75$, $p<05$; phase*genotype $F(2, 20)= 1.67$, $p<0.2$). These results indicate that male *Pcdh10*$^{+/-}$ mice have impairments in cued conditioned fear that are likely to reflect alternations in amygdala function, given the known role of amygdala circuits in this learning paradigm.

2.3.3 No alteration in anxiety-related behaviors or motor coordination.

Social behavior and conditioned fear performance can be influenced by changes in motor function or anxiety-like behavior. When adult *Pcdh10*$^{+/-}$ mice were tested for

anxiety-like behavior and locomotor activity in the open field test, no significant genotype differences were observed in center or peripheral exploration, nor were differences in total ambulatory movements found for either sex (**Fig. 2.4**. unpaired t-test: center $p<0.2$, periphery $p<0.3$, total $p<0.6$). Similarly, no differences were observed in anxiety-like behavior in the elevated zero maze test (**Fig. 2.5A, B**. one-way ANOVA: genotype males $F(1,24)=0.275$ $p>0.05$, females $F(1,16)=0.003$ $p>0.05$), or motor function in the accelerating rotarod test (**Fig. 2.5C, D**. rmANOVA: genotype males $F(1,24)=3.4$ $p>0.05$, females $F(1,16)=0.404$ $p>0.05$) in juvenile *Pcdh10*$^{+/-}$ males or females. Together, these results show a lack of basal changes in locomotor or anxiety-like behaviors in *Pcdh10*$^{+/-}$ mice.

2.3.4 Object recognition memory is intact in Pcdh10$^{+/-}$ mice.

Because the conditioned fear deficits displayed by male *Pcdh10*$^{+/-}$ mice suggest specific impairment in fear memory, we next explored whether the mice were impaired in a non-fear based memory task. Object recognition memory is a relatively non-aversive cognitive task in which animals are allowed to explore two identical objects, followed by a discrimination test with one familiar object and one novel object (Oliviera, 2010). This task engages perirhinal cortical circuits involved in discriminating objects using sensory features (Norman and Eacott, 2004; Winters and Bussey, 2005). In this task, both male and female *Pcdh10*$^{+/-}$ mice were able to discriminate between novel and familiar objects (**Fig.2.6**. t-test: males $p<0.8$, females $p<0.93$). *Pcdh10*$^{+/-}$ males and females were also tested in the hippocampus-dependent spatial version of the Morris water maze (Broadbent et al. 2006, Lattal et al. 2001). No genotype differences were found in latency to find the hidden platform either during acquisition or in the probe trial, suggesting that hippocampal function is intact (**Fig. 2.7**, t-test: male wild-type $p<0.03$,

male Pcdh10+/- $p<0.05$; female wild type $p<0.001$, female Pcdh10+/- $p<0.001$). These data suggest that *Pcdh10*$^{+/-}$ males have specific cognitive deficits affecting amygdala-dependent fear memory circuits but not affecting hippocampal spatial memory, cortical recognition memory, novelty detection, or interaction with non-social objects.

2.3.5 Abnormal dendritic spines in amygdala of Pcdh10$^{+/-}$ males.

Both social approach and cued fear tasks strongly engage amygdala circuits, and are impaired in *Pcdh10*$^{+/-}$ males (Rogan LeDoux 1997, Felix-Ortiz and Tye 2014, Marschner 2008). Because *Pcdh10* has been linked to spine elimination, we hypothesized that the behavioral deficits we observe may be related to changes in spine density in the amygdala of *Pcdh10*$^{+/-}$ mice. To visualize amygdala dendrites and spines, brains from wild-type and *Pcdh10*$^{+/-}$ males were stained using Golgi impregnation. When dendritic arbors were reconstructed (**Fig. 2.8A**) and spines counted (**Fig. 2.8B**), there was no significant genotype effects on the number of dendrites or branch points (**Fig. 2.8C**. unpaired t-test: dendrites $p<0.24$, branches $p<0.79$), but spine density was increased in *Pcdh10*$^{+/-}$ dendrites (**Fig. 2.8D**. unpaired t-test: $p<0.03$). When we separated spines into categories by morphological characteristics (Hering and Sheng 2001, Yuste and Bonhoeffer 2004), we found that *Pcdh10*$^{+/-}$ dendrites contain a higher percentage of thin, elongated filopodia-like spines compared to wild-type dendrites (**Fig. 2.8E**. unpaired t-test: $p<0.04$). The change in spine density in *Pcdh10*$^{+/-}$ dendrites appears to be driven primarily by the increased number of filopodial-type spines, an immature spine morphology (Ziv and Smith 1996, Petrak et al. 2006) and to a lesser extent by increased mushroom-type spines (**Fig. 2.9**. unpaired t-test: filopodia $p<0.003$, mushroom $p<0.05$).

2.3.6 Reduced LA-BLA transmission of gamma coherence in Pcdh10$^{+/-}$ slices.

White matter structural changes observed in schizophrenia and ASD are thought to underlie changes in functional connectivity and temporal binding of regional brain activity, particularly in the gamma frequency range (Ye et al. 2014, Wolff et al. 2012, Wilson et al. 2007, Gandal et al. 2010, Khan et al. 2013). Alterations in gamma activity in the amygdala have been linked to impairments in social cognition and fear processing (Das et al. 2007, Williams et al. 2009). To determine whether functional connectivity is altered in *Pcdh10*$^{+/-}$ amygdala circuitry, voltage sensitive dye was used to optically record the transmission of stimulation-evoked activity from lateral amygdala to its functional targets. The lateral amygdala was stimulated at gamma frequency and spread of evoked response, or changes in fluorescence, to neighboring basolateral amygdala (BLA) and ventral caudate (STR) was imaged (**Fig. 2.10A**). Peak evoked responses and gamma-band activity in the BLA and STR were analyzed. Evoked responses in BLA and STR regions of interest (**Fig. 2.10B**) were analyzed for peak response amplitude, and gamma-band activity. No differences were found in the amplitude of responses in amygdala or striatal regions (**Fig. 2.10C**); however, *Pcdh10*$^{+/-}$ slices showed significant reduction in BLA high-frequency gamma power (**Fig. 2.10D, E**). Interestingly, the impairment in gamma transmission was limited to LA-BLA connections, and no differences were found in gamma responses in the striatum. These results provide further evidence suggesting that abnormal synaptic and network connectivity amygdala circuits involving the basolateral amygdala underlie the impairments in social behavior and fear learning observed in *Pcdh10*$^{+/-}$ males.

2.3.7 Rescue of social deficits in Pcdh10$^{+/-}$ males with NMDAR activation.

Impaired social behavior and reduced gamma frequency responses have been described in mouse models with reduced NMDAR expression (Meilnik et al. 2014,

Gandal et al. 2012). One therapeutic agent that has shown promise in improving sociability in both animal models and human individuals with ASD is the NMDAR partial agonist d-cycloserine (dCs) (Posey et al. 2004, Burket et al. 2013, Deutsch et al. 2012). To determine this NMDAR partial agonist could rescue sociability in *Pcdh10*$^{+/-}$ mice and WT littermates were treated with an acute, systemic injection of saline or dCs 30 min prior to social approach testing. Treatment with dCs rescued the deficit in social sniffing seen in *Pcdh10*$^{+/-}$ males (**Fig. 2.11A**), but had no effect on social sniffing in wild-type littermates. Exploration of the non-social cylinder (**Fig. 2.11B**) and locomotor activity (**Fig. 2.11C**) were not affected by dCs in *Pcdh10*$^{+/-}$ mice and WT littermates, indicating that dCS treatment did not elicit non-specific changes in exploratory behavior or locomotor output.

2.4 Discussion

Social and cognitive deficits are major behavioral phenotypes of autism spectrum disorder as well as Fragile X syndrome but the neural circuitry and molecular changes underlying these phenotypes are not fully understood. Reduced expression of Fragile X protein FMRP disrupts trafficking and translation of mRNAs encoding multiple synaptic structural and functional proteins, including *Protocadherin 10.* Here we showed that male mice lacking a single copy of *Pcdh10* exhibit reduced social approach behavior and associative fear learning, as well as altered structure and function of synaptic connections in the amygdala.

2.4.1 Behavioral deficits in Pcdh10+/- males implicate amygdala dysfunction

Behavior and cognitive phenotypes in *Pcdh10*$^{+/-}$ males are remarkably limited to reduced social approach and investigation, as well as deficit in cued fear conditioning. Male

Pcdh10$^{+/-}$ mice exhibit profound impairments in the social choice task, showing similar exploratory behavior toward empty cylinders compared to cylinders containing a live mouse. Reduced social approach behavior has been observed in multiple genetic and environmental models of ASD (Peca et al. 2011, Penagarikano et al. 2011, Ehninger et al. 2010, Kirsten et al. 2010), but interpretation of this behavior has frequently been complicated by accompanying changes in locomotor activity (Penagarikano et al. 2011) and anxiety-like behaviors (Peca et al. 2011). Despite robust expression of *Pcdh10* in striatal and BLA regions, locomotor activity, anxiety like behavior are not altered in *Pcdh10*$^{+/-}$ males. Inputs from the BLA to ventral hippocampus and from VTA to Nucleus accumbens (N.Acc) have been proposed as a key pathways likely mediating negative and positive modulation of social behaviors in mice respectively (Felix-Ortiz and Tye 2013, Gunaydin et al. 2014). Inputs from NAcc to BLA have been identified as key modulators of reward seeking behavior (Ciano and Everitt 2004), supporting the role of the BLA as a central regulator of emotional valence during social interactions. Further dissection of the functional circuitry underlying amygdala and striatal regulation of social approach behavior is needed to gain a more complete understanding of the roles these regions play in social motivation and social avoidance behaviors.

Intellectual disability is a principal feature of Fragile X syndrome, and is often present in individuals with ASD (AADDMN, Pederson et al. 2012, Brodkin 2008). *Pcdh10*$^{+/-}$ males exhibit memory impairments that are strikingly specific to associative fear conditioning. Both cued and contextual fear conditioning tasks rely on BLA integration of aversive stimuli with predictive cues (contextual features, auditory tone, odors) for associative learning (Phillips and LeDoux 1992, Muller et al.1997, Marschner 2008, Goosens et al. 2001). The presence of male specific deficits in both types of associative fear learning

strongly implicates BLA dysfunction, as it is a common neuroanatomical substrate for both tasks. The absence of impairment in object recognition and spatial water maze tasks furnish additional support for regional specificity of the cognitive deficits.

2.4.2 Structural and functional connectivity impaired in the amygdala.

Alterations in maturation of synaptic connections and organization of major white matter tracts have been observed in the brains of individuals with ASD both developmentally and in adulthood (Bakthiari et al. 2012, Wolff et al. 2012, Hutsler et al. 2010). Dendritic spine processes are dynamic, highly plastic structures with structural and functional properties that are highly dependent on neuronal activity (Leuner and Shors 2004, Matsuzaki et al. 2004). We show that amygdala neurons from adult male *Pcdh10*$^{+/-}$ mice have increased spine density, and that this effect largely reflects an increase in long filamentous spines. Dendrites with a dense covering of long, thin filopodia-type spines have been described in adult neurons from individuals with Fragile X syndrome and *Fmr1* KO mice (Irwin et al. 2001, Comery et al. 1997), but it is unclear whether increases in spine density and immature filopodia-type spines seen in adults reflect lingering circuit-level effects of aberrant spine maturation and pruning during development, or are driven by ongoing disruption of homeostatic regulation of spine function. Future studies of the role of *Fmr1 and Pcdh10* in regulation of synaptic structure and function in adult neurons are needed to address these open questions.

Increased spine density and extension of filopodial processes has been observed with pharmacological and genetic manipulations that impair synaptic plasticity, synaptic transmission, or acutely block NMDAR activity (Chen et al. 2014, Petrak et al. 2005, Lin

and Constantine-Paton. 1998). Elongation of spine necks is correlated with reduced charge transfer between spine head and the parent dendrite (Harris and Stevens 1989), suggesting that long filamentous spines are less effective at synaptic transmission. In amygdala slices from *Pcdh10*$^{+/-}$ males, we observed impaired transmission of the high-frequency gamma activity from LA to BLA. EEG and MEG studies in human subjects have linked deficits in evoked amygdala gamma oscillations to impaired social cognition and fear association (Das et al. 2007, Williams et al. 2009). Reduced evoked gamma activity has been observed along with social and cognitive deficits in mice with reduced NMDAR activity (Gandal et al. 2012). In *Pcdh10* males, enhancing activation of NMDARs with the glycine site agonist dCS rescued the social approach deficit observed in juvenile mice. Together, these results suggest that reduced synaptic efficacy, particularly in the amygdala, underlie the behavioral deficits we observe in *Pcdh10*$^{+/-}$ males.

2.4.3 Sex differences are an important feature of ASD models.

A striking feature of this study is the stark sex difference observed in social and cognitive functioning. ASD is more common in males than females, but the basis of this sex difference in susceptibility is poorly understood (Werling and Geschwind 2013, Baron-Cohen et al. 2011). X-linked disorders, such as Fragile X, predictably show strong sex differences, but the majority of ASD-associated genes, including *Pcdh10*, are autosomal (Morrow et al.2008, State and Sestan 2012). These differences raise intriguing questions about the nature of sex differences, particularly in disorders with early, pre-pubertal onset (Wolff et al. 2012, Hartley and Sikora 2009). Two prevailing theories for molecular sources of sex differences (sex-linked genes and exposure to sex hormones) represent related but distinct opportunities for gene x gene and gene x environment

(hormone) interactions. Organizational effects of the pre-natal testosterone surge on the brains of male fetuses represent an early window for neuroendocrine effects on neural development (Lutchmaya et al. 2002, Knickmeyer and Baron-Cohen 2006). In rodents, male pups undergo a surge in testosterone around birth that organizes sexually dimorphic effects on both behavior and brain structures (Isgor and Sengelaub 1998, Olioff and Stewart 1978, Handa et al. 1985). Despite the prominent sex differences in ASD incidence and the large body of knowledge on sex differences in neuronal structure and behavior in rodent models, studies of sex differences in rodent ASD models are surprisingly limited. Exploration the existence of sex differences in ASD models along with studies of their molecular and genetic underpinnings, will be critical steps toward understanding of the nature and source of the male predominance ASD, and ultimately provide clues to a powerful source of resilience.

Chapter 2 Figure Legends

Figure 2.1. Male-specific reduction in social approach behavior in juvenile *Pcdh10*$^{+/-}$ mice. **A.** Social exploration is impaired in juvenile male *Pcdh10*$^{+/-}$ mice and wildtype (WT) littermates (rmANOVA: Phase- $F(1,26)= 34.8$, $p<0.0001$; Genotype $F(1,26)=8.4$, $p<0.01$, and phase*genotype $F(1,26)=10.4$, $p<0.01$). Wild-type males, but not *Pcdh10*$^{+/-}$ males, spent more time sniffing the social cylinder containing the novel mouse in Phase 2 than the empty cylinder in Phase 1 (*Bonferroni post hoc: $p<0.05$). *Pcdh10*$^{+/-}$ males spent less time sniffing the social cylinder during Phase 2 than wild-type males ($^{+}$Bonferroni post hoc $p<0.01$). **B.** No difference in exploration of a novel object by wild-type and Pcdh10$^{+/-}$ males during either Phase 1 or Phase 2 (rmANOVA, no main effect of time $F(1,26)=0.38$ $p>0.05$, no main effect of genotype $F(1,26)=3.37$, $p>0.05$). **C.** No difference in social exploration in juvenile wild-type and *Pcdh10*$^{+/-}$ females. Both genotypes display increased exploration of the social cylinder in Phase 2 compared to Phase 1 (rmANOVA $F(1,23)= 24.55$, $p<0.0001$, * Bonferroni post hoc $p<0.05$). **D.** No difference in exploration of a novel object by wild-type and *Pcdh10*$^{+/-}$ females during either Phase 1 or Phase 2 (rmANOVA, no main effect of genotype $F(1,23)=4.2$ $p>0.05$).

Figure 2.2. Olfactory habituation dishabituation in juvenile *Pcdh10*$^{+/-}$ and WT mice. **A.** Juvenile male wild-type (n=13) mice do not show a significant difference in sniffing times when compared with Pcdh10$^{+/-}$ (n=13) males (rmANOVA: trial $F(1,14 = 52.9$, $p>0.05)$, nor they do not show a significant difference between groups when exposed to the odor stimuli (rmANOVA: genotype $F(1,14)=0.765$ $p>0.05$ not significant). **B**. Both juvenile female WT (n=9) and Pcdh10$^{+/-}$ (n=9) mice show an overall change in sniffing times (rmANOVA: trial $F(1,14 = 26.7$, $p<0.001)$; however they do not show a significant

difference between groups when exposed to the odor stimuli (rmANOVA: genotype F(1,14)=1.8 p>0.05 not significant).

Figure 2.3. Male-specific deficits in conditioned fear memory in Pcdh10+/- mice. **A.** *Pcdh10*$^{+/-}$ males exhibited reduced freezing when tested 24hrs after contextual fear conditioning (two-way ANOVA: phase F(1, 22)= 99.82, p<0.001; genotype F(1,22)= 13.21, p<0.001). **B.** Both WT and *Pcdh10*$^{+/-}$ females exhibited high levels of freezing when tested in the conditioned context (two-way ANOVA: phase F(1,19)= 51.75, p<0.001). **C.** *Pcdh10*$^{+/-}$ males showed reduced freezing to the tone compared to wild-type littermates when tested for tone cued fear 24hrs after conditioning (two-way ANOVA: phase F(2,18)= 43.58, p<0.001; genotype F(1,19)= 10.13, p<0.01); genotype*phase F(2,18)= 3.27, p<0.05). **D.** *Pcdh10*$^{+/-}$ females exhibit a general reduction in freezing in the cued fear task (two-way ANOVA: phase F(2,20)= 78.61, p<0.001; genotype F(1, 21)= 6.75, p<05; phase*genotype F(2, 20)= 1.67, p<0.2).

Figure 2.4. No differences in anxiety or locomotor behaviors in *Pcdh10*$^{+/-}$ mice.

A. No differences in spontaneous locomotor activity, or in exploration of center and peripheral regions of the open field by adult Pcdh10$^{+/-}$ males (t-test: center p<0.2, periphery p<0.3, total p<0.6). **B.** No difference in locomotor activity or center or peripheral exploration by adult Pcdh10$^{+/-}$ females (t-test: center p<0.2, periphery p<0.9, total p<0.5)

Figure 2.5. Juvenile *Pcdh10*$^{+/-}$ mice show no differences in anxiety-like behavior or motor function. A. Elevated Zero maze. There is no significant difference in the percent of time juvenile male WT (n=13) or *Pcdh10*$^{+/-}$ (n=13) spent in closed or open arms in the elevated zero maze (one-way ANOVA (1,24)=0.275 p>0.05 not significant).

B. There is no significant difference in the percent of time juvenile female WT (n=9) or *Pcdh10*$^{+/-}$ (n=9) spent in closed or open arms in the elevated zero maze (one-way ANOVA (1,16)=0.003 p>0.05). **C.** No significant differences in performance of male juveniles on the accelerating rotarod (rmANOVA: genotype F(1,24)=3.4 p>0.05). D. There is no significant difference between juvenile female WT (n=9) and Pcdh10+/- (n=9) mice in latency to fall from the rotarod (rmANOVA: genotype F(1,16)=0.404 p>0.05).

Figure 2.6. Object recognition memory is intact in Pcdh10+/- mice. A. No difference in novel object recognition in male *Pcdh10*$^{+/-}$ mice (t-test: p<0.8). **B.** No difference in object recognition memory in female Pcdh10$^{+/-}$ mice (t-test: p<0.93).

Figure 2.7. Spatial navigation memory in the water maze is intact. No differences in latency to locate the hidden platform in male (**A**) or female (**B**) *Pcdh10*$^{+/-}$ mice during acquisition of the spatial water maze. Both male (**C**) and female (**D***) Pcdh10*$^{+/-}$ mice show significant preference for the target quadrant (formerly containing the platform) and reduced preference for the quadrant opposite the target during the probe trial (t-test: male wild-type p<0.03, male Pcdh10+/- p<0.05; female wild type p<0.001, female Pcdh10+/- p<0.001).

Figure 2.8. Increased filopodia-type spines on amygdala neurons of Pcdh10+/- males. A. Representative dendritic reconstructions from amygdala neurons from wild-type and Pcdh10$^{+/-}$ males. **B.** Representative dendritic lengths from BLA neurons from wild-type and Pcdh10$^{+/-}$ males. **C.** No difference in number of dendrites or dendritic branch points in Pcdh10$^{+/-}$ neurons (t-test: dendrites p<0.24, branches p<0.79). **D.**

Increased spine density in Pcdh10$^{+/-}$ dendrites (t-test: p<0.03). **E.** Increased filopodia-type spines in Pcdh10$^{+/-}$ dendrites (t-test: p<0.04).

Figure 2.9. Change in spine density is driven by increases in filopodia and mushroom type spines. A. Average number of spines counted in each morphological category in 50um regions of wild-type and *Pcdh10*$^{+/-}$ amygdala neurons. Significant increases in mushroom type (ttest: p<0.05) and filopodia type (ttest: p<0.003) spines were detected in Pcdh10$^{+/-}$ dendrites.

Figure 2.10. *Pcdh10*$^{+/-}$ mice exhibit BLA-specific impairment for the transmission of gamma-band power, but not amplitude of EPSP. A) Grey scale image of amygdala coronal slice showing the lateral amygdala (LA), basolateral amygdala (BLA) and striatum (STR), electrode placement and regions of interest. Color images show peak VSDi responses following direct stimulation of the LA amygdala in slices from wild-type and *Pcdh10*$^{+/-}$ males. **B)** Kinetics of fluorescence changes in response to 4 stimuli at 40Hz over time are shown from ROIs in the BLA and STR. Traces from wild-type mice are shown in black and *Pcdh10*$^{+/-}$ are shown in red. **C)** The lack of peak differences in these representative traces are reflected in the group data (n=5). **D)** In contrast, taking the integral of the gamma-band response (30-50Hz) over time in both BLA and STR, showed specific reduction in the ability of the BLA to mount a gamma-band response to high frequency LA activity. **E)** This is specific to the LA -> BLA circuit, as functional connectivity to the striatum remains unaffected (bottom).

Figure 2.11. NMDAR agonist d-cycloserine rescues social impairment in *Pcdh10*$^{+/-}$ males. A. Social exploration is improved in juvenile Pcdh10$^{+/-}$ males after acute d-cycloserine (dCS, 32mg/kg) treatment. Both genotypes show a significant increase in

exploration of the social cylinder during Phase 2 when it contains a novel mouse, compared Phase 1 when it is empty (rmANOVA, main effect of phase $F(1,34= 186.2$, $p<0.0001$). During Phase 2, acute dCS treatment increases social exploration in $Pcdh10^{+/-}$ males ($Pcdh10^{+/-}$ saline n= 9 vs. $Pcdh10^{+/-}$ dCS n=9, Bonferroni Dunn *post hoc* p=0.01) but does not alter exploration in wild-type males. **B.** Treatment with dCS does not alter exploration of the non-social cylinder. **C.** Locomotor activity is not altered by dCS treatment. During Phase 2, exposure to the social and non-social stimuli reduces locomotor activity in both wild-type and $Pcdh10^{+/-}$ males (rmANOVA, significant main effect of phase, $F (1,34)=82.9$, $p<0.001$). However, there is no significant difference in locomotor activity between juvenile wild-type and $Pcdh10^{+/-}$ males treated with saline or dCS 32mg/kg (rmANOVA, main effect of genotype $F (1,34)=6.5$ $p=0.02$, no significant interaction genotype*treatment $(F1,34)=1.3$, $p>0.05$).

Chapter 2 Figures

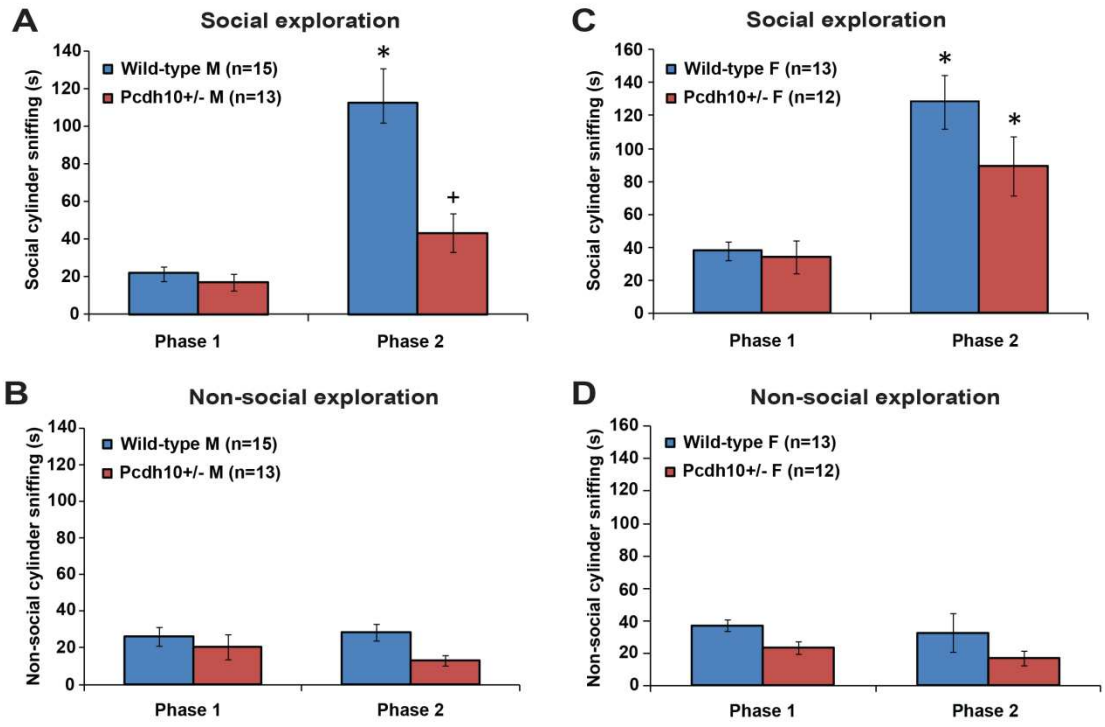

Figure 2.1

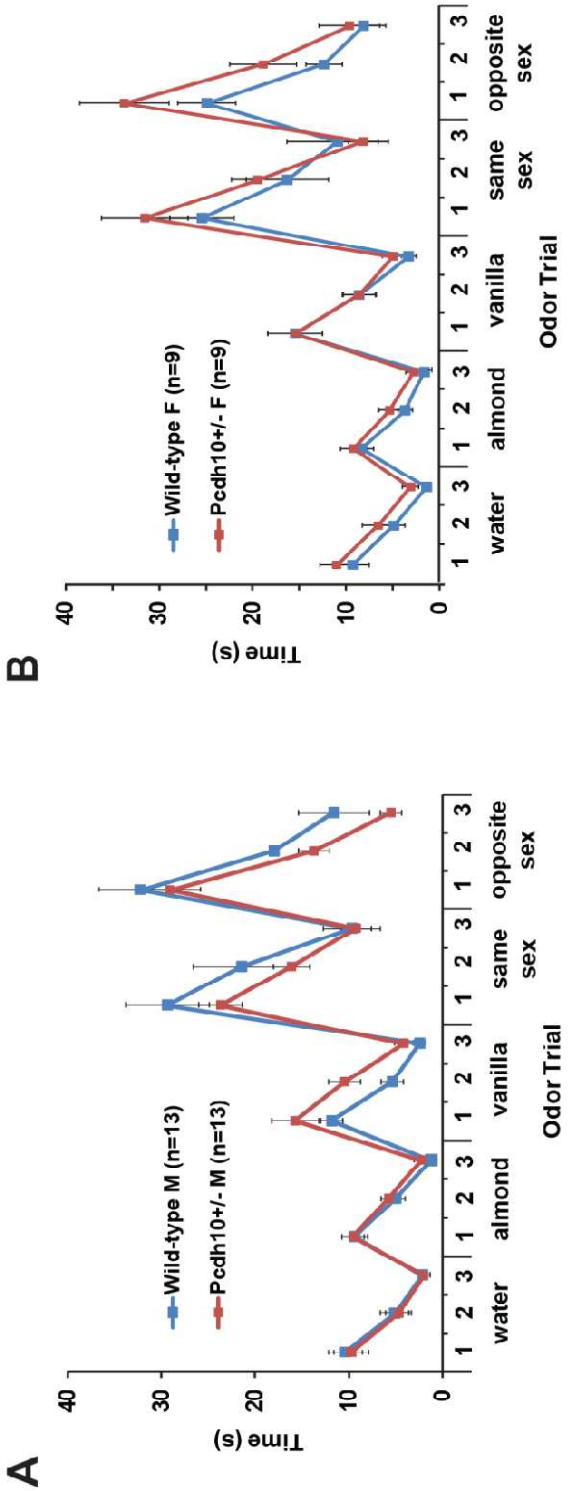
A
B
Time (s)
Wild-type M (n=13)
Pcdh10+/- M (n=13)
Wild-type F (n=9)
Pcdh10+/- F (n=9)
water
almond
vanilla
same sex
opposite sex
Odor Trial

Figure 2.2

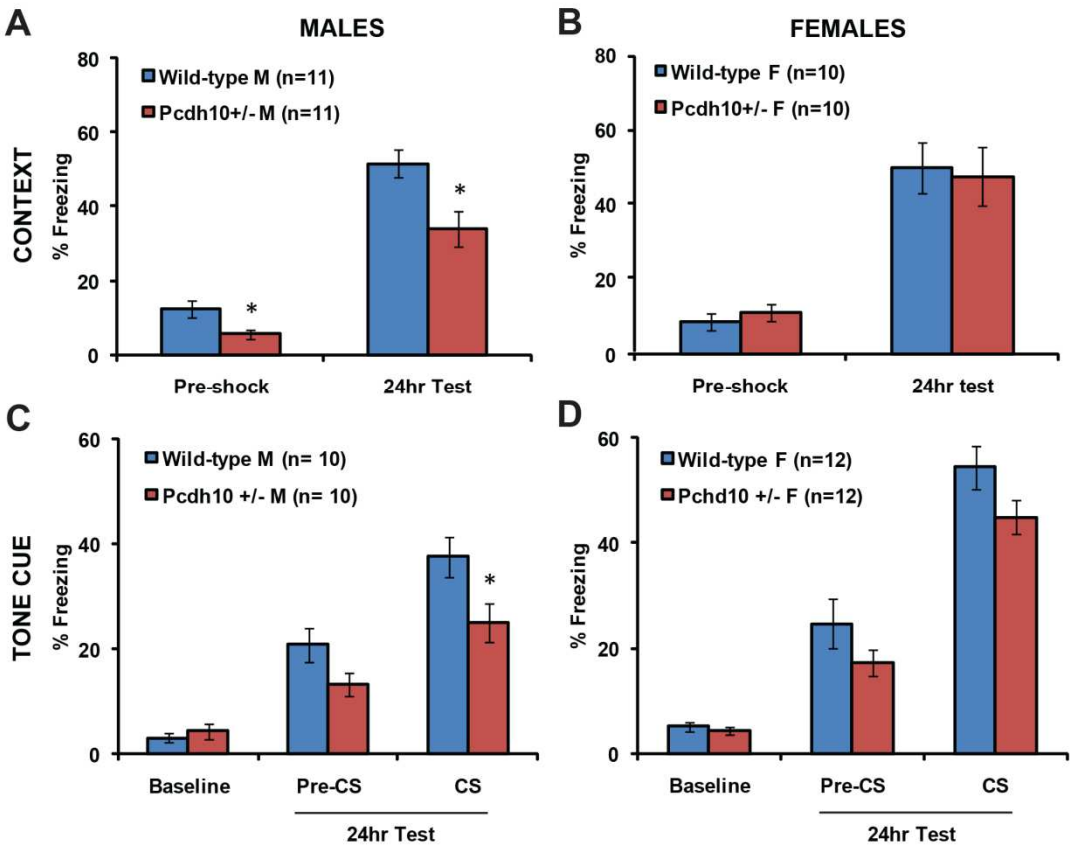
A
MALES
Wild-type M (n=11)
Pcdh10+/- M (n=11)
CONTEXT
% Freezing
80
60
40
20
0
*
*
Pre-shock
24hr Test
B
FEMALES
Wild-type F (n=10)
Pcdh10+/- F (n=10)
% Freezing
80
60
40
20
0
Pre-shock
24hr test
C
Wild-type M (n= 10)
Pcdh10 +/- M (n= 10)
TONE CUE
% Freezing
60
40
20
0
*
Baseline
Pre-CS
CS
24hr Test
D
Wild-type F (n=12)
Pchd10 +/- F (n=12)
% Freezing
60
40
20
0
Baseline
Pre-CS
CS
24hr Test

Figure 2.3

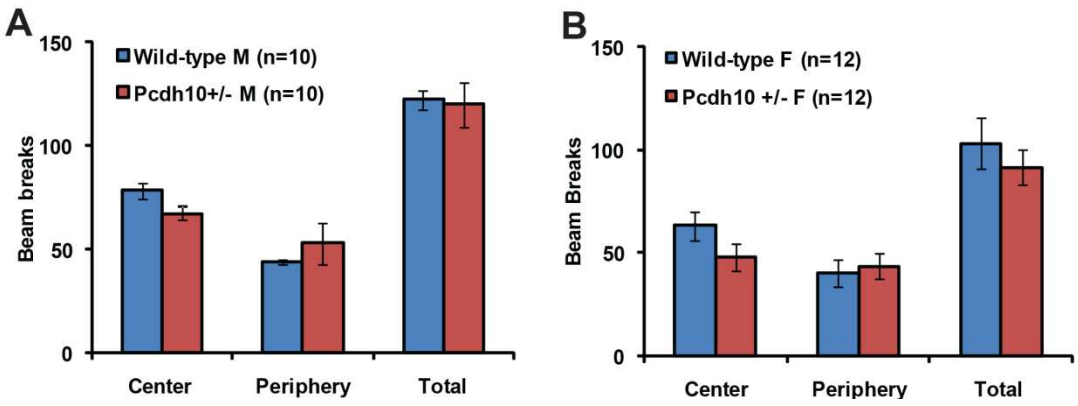
A
150
100
50
0
Beam breaks
Wild-type M (n=10)
Pcdh10+/- M (n=10)
Center
Periphery
Total
B
150
100
50
0
Beam Breaks
Wild-type F (n=12)
Pcdh10 +/- F (n=12)
Center
Periphery
Total

Figure 2.4

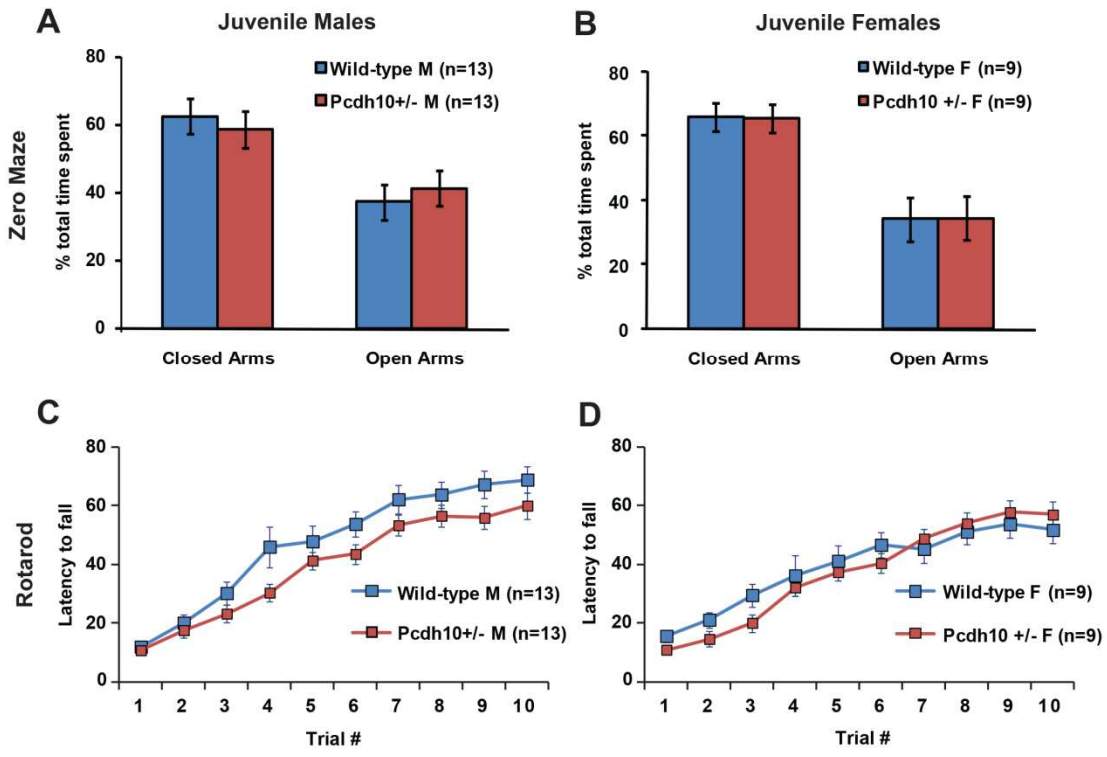
A
Juvenile Males
Zero Maze
% total time spent
Wild-type M (n=13)
Pcdh10+/- M (n=13)
Closed Arms
Open Arms
B
Juvenile Females
% total time spent
Wild-type F (n=9)
Pcdh10 +/- F (n=9)
Closed Arms
Open Arms
C
Rotarod
Latency to fall
Wild-type M (n=13)
Pcdh10+/- M (n=13)
Trial #
D
Latency to fall
Wild-type F (n=9)
Pcdh10 +/- F (n=9)
Trial #

Figure 2.5

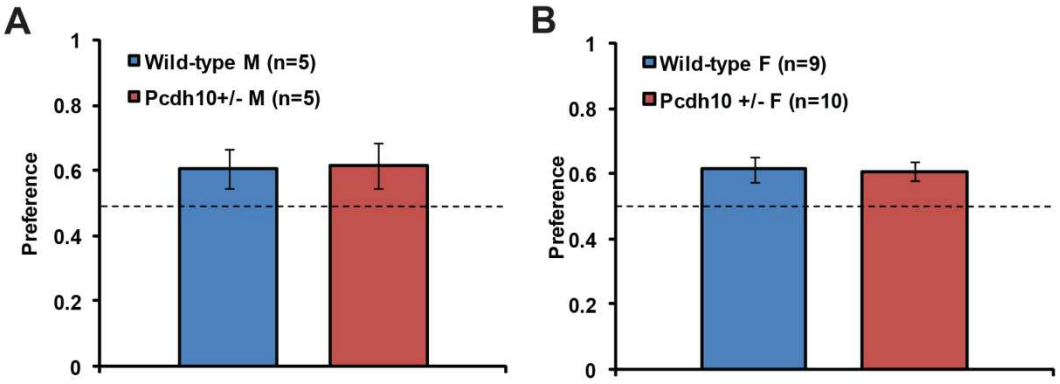
A
Wild-type M (n=5)
Pcdh10+/- M (n=5)
Preference
1
0.8
0.6
0.4
0.2
0
B
Wild-type F (n=9)
Pcdh10 +/- F (n=10)
Preference
1
0.8
0.6
0.4
0.2
0

Figure 2.6

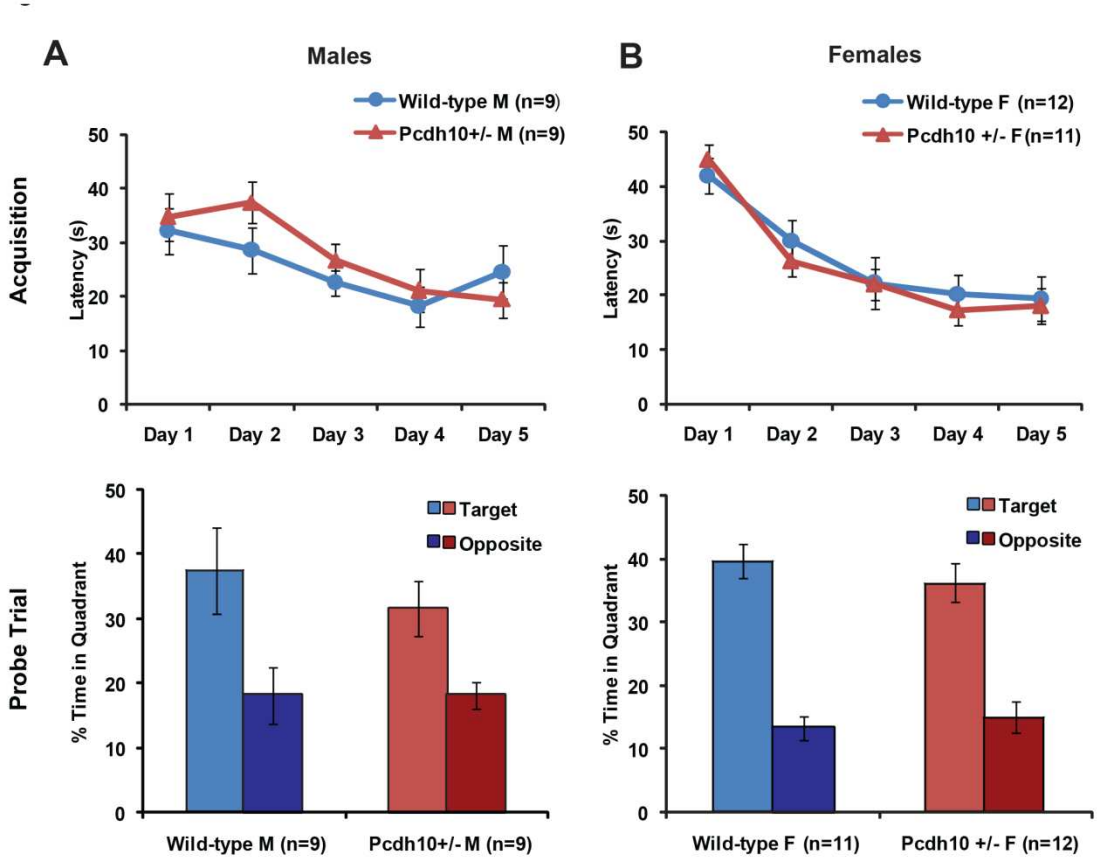
A
Males
Wild-type M (n=9)
Pcdh10+/- M (n=9)
Acquisition
Latency (s)
50
40
30
20
10
0
Day 1
Day 2
Day 3
Day 4
Day 5
B
Females
Wild-type F (n=12)
Pcdh10 +/- F (n=11)
Latency (s)
50
40
30
20
10
0
Day 1
Day 2
Day 3
Day 4
Day 5
Probe Trial
% Time in Quadrant
Target
Opposite
50
40
30
20
10
0
Wild-type M (n=9)
Pcdh10+/- M (n=9)
% Time in Quadrant
Target
Opposite
50
40
30
20
10
0
Wild-type F (n=11)
Pcdh10 +/- F (n=12)

Figure 2.7

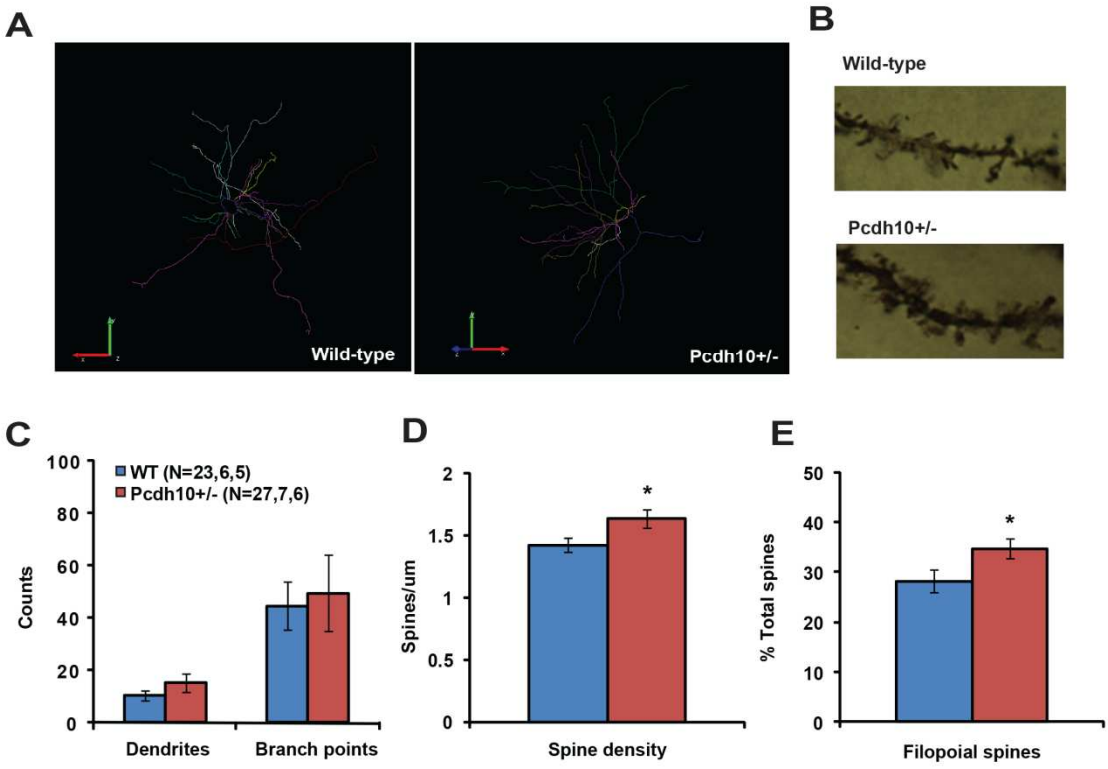
A
Wild-type
Pcdh10+/-
B
Wild-type
Pcdh10+/-
C
WT (N=23,6,5)
Pcdh10+/- (N=27,7,6)
Counts
100
80
60
40
20
0
Dendrites
Branch points
D
Spines/um
2
1.5
1
0.5
0
*
Spine density
E
% Total spines
50
40
30
20
10
0
*
Filopoial spines

Figure 2.8

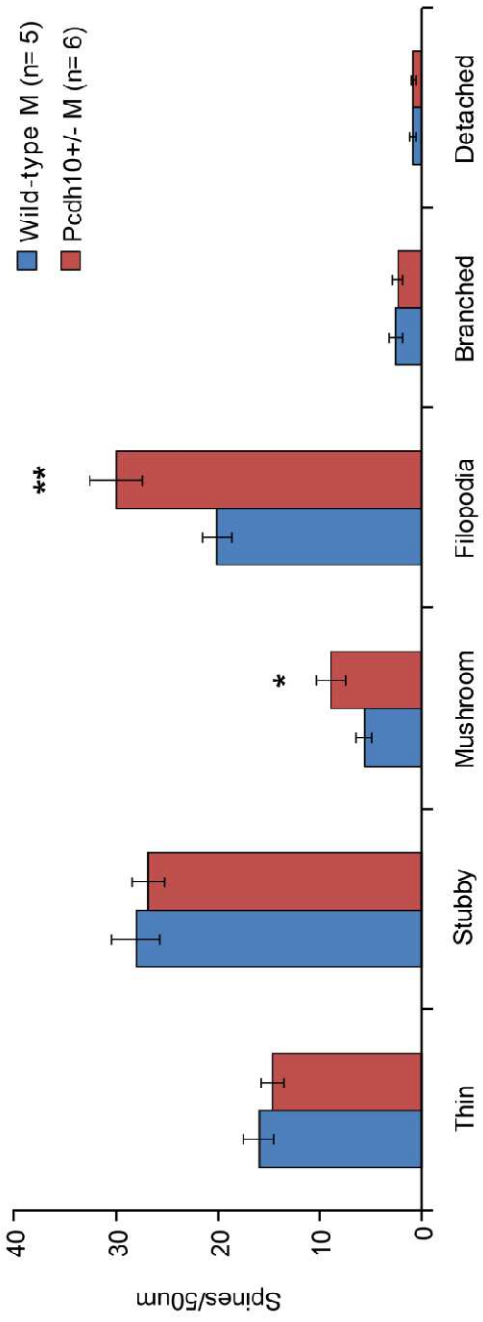
Wild-type M (n= 5)
Pcdh10+/- M (n= 6)
Spines/50um
0
10
20
30
40
Thin
Stubby
Mushroom
Filopodia
Branched
Detached
*
**

Figure 2.9

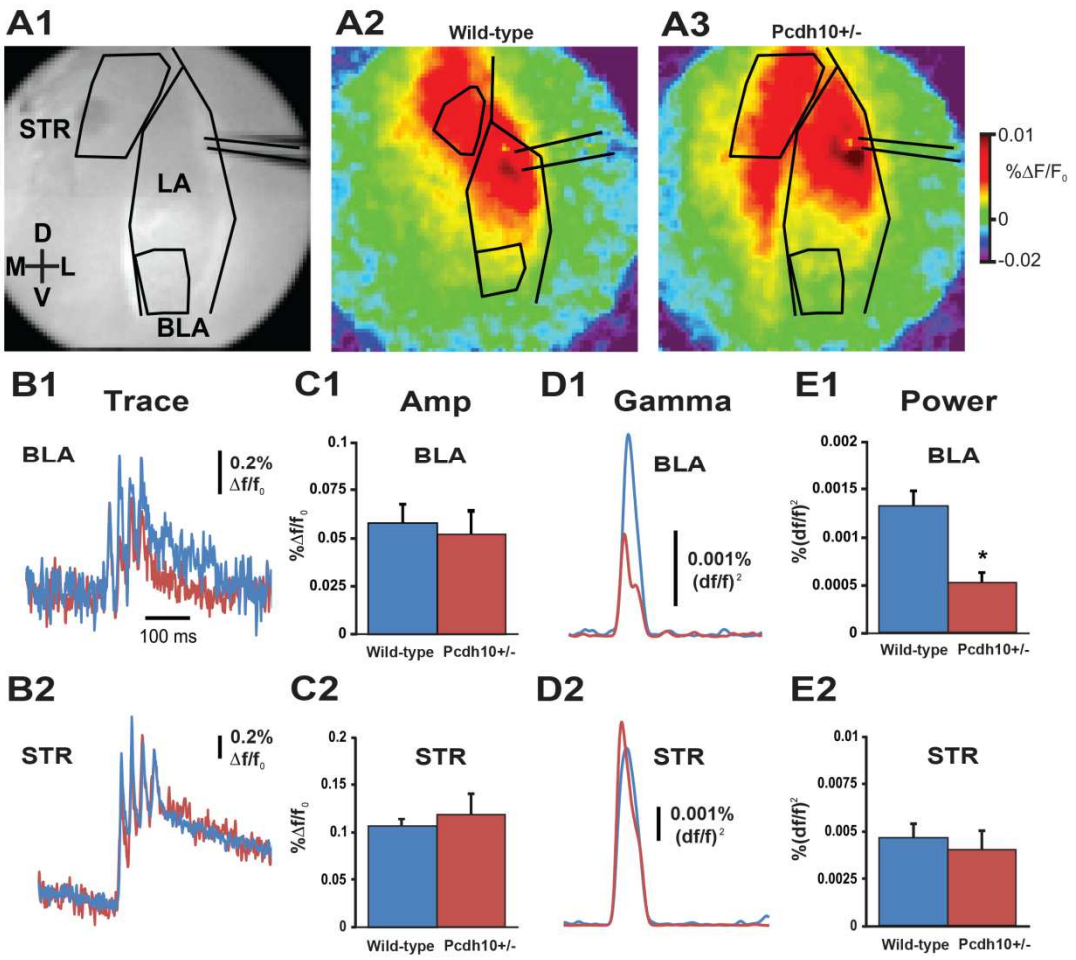
A1
A2
Wild-type
A3
Pcdh10+/-
STR
LA
BLA
D
M
L
V
0.01
%ΔF/F0
0
-0.02
B1
Trace
C1
Amp
D1
Gamma
E1
Power
BLA
0.2%
Δf/f0
100 ms
%Δf/f0
0.001%
(df/f)2
%(df/f)2
*
Wild-type
Pcdh10+/-
B2
C2
D2
E2
STR

Figure 2.10

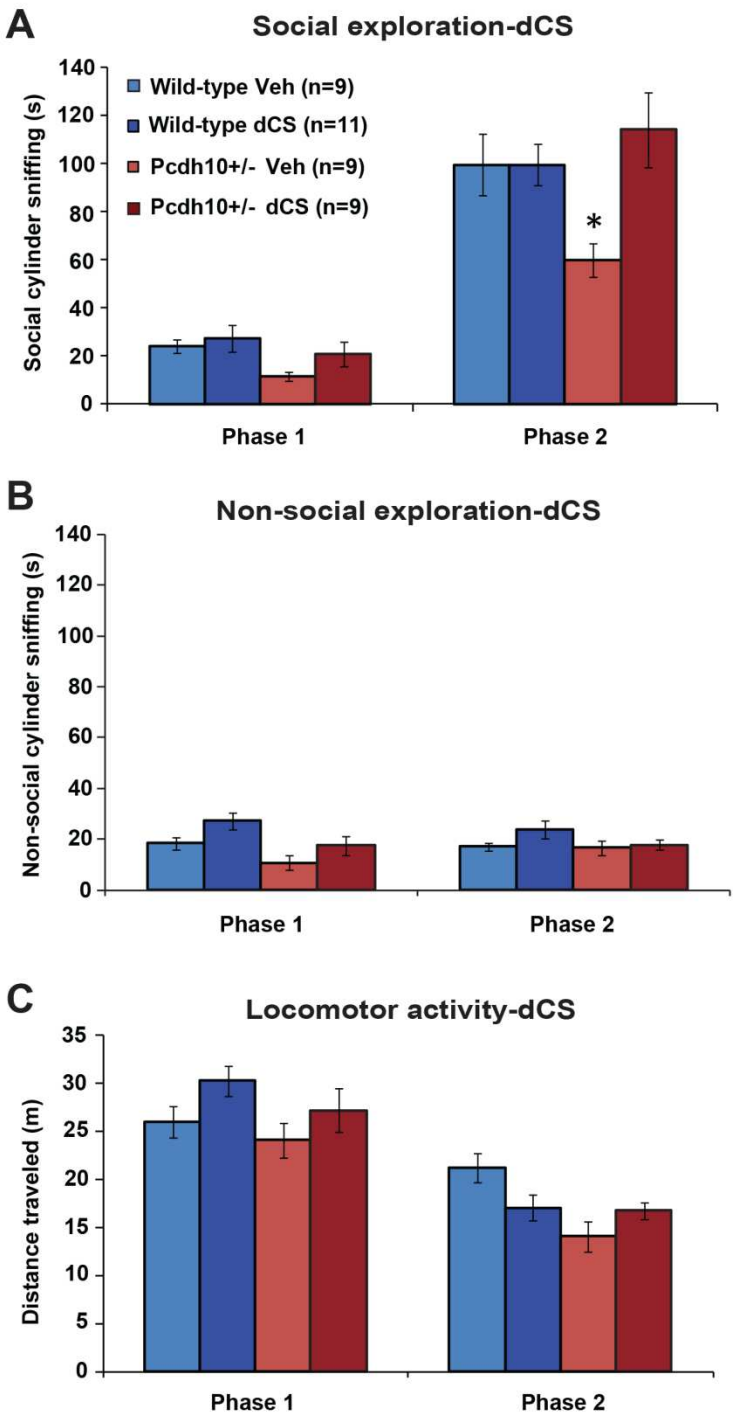
A
Social exploration-dCS
Social cylinder sniffing (s)
140
120
100
80
60
40
20
0
Wild-type Veh (n=9)
Wild-type dCS (n=11)
Pcdh10+/- Veh (n=9)
Pcdh10+/- dCS (n=9)
*
Phase 1
Phase 2
B
Non-social exploration-dCS
Non-social cylinder sniffing (s)
140
120
100
80
60
40
20
0
Phase 1
Phase 2
C
Locomotor activity-dCS
Distance traveled (m)
35
30
25
20
15
10
5
0
Phase 1
Phase 2

Figure 2.11

ACKNOWLEDGEMENTS

The studies contained in this chapter were supported by the Pennsylvania Department of Health (SAP # 4100042728) (R.T.S.), 1P50MH096891 subproject 6773 (E.S.B. and T.A.), National Institutes of Health Grants R01MH080718 (E.S.B.), ARRA supplement 3R01MH080718-03S1 (E.S.B.), and McMorris Autism Research Program. H. Schoch was supported by NIH Training Grant T32-MH017168.

AUTHOR CONTRIBUTIONS

This chapter was written by H. Schoch, with suggestions from E. Brodkin, T. Abel, and R White. E. Brodkin, T. Abel, H. Schoch, A. Kreibich, R. White, G. Carlson, D. Feldmeyer, A. Bannerjee, and C.G. Hahn conceived and designed the experiments. H. Schoch, A Kreibich and H. Dow conducted behavioral testing. H. Schoch performed spine analysis. R. White and D. Bohorquez conducted electrophysiology experiments. A. Bannerjee performed Western blots. E. Brodkin, T. Abel, G. Carlson, and C.G. Hahn directed the studies. I thank J. Tudor and N. Grissom for discussions and critically reading the manuscript.

This chapter is being prepared for submission: Schoch H, Kreibich AS*, White R, Bohorquez D, Bannerjee A, Dow H, Li H, Hirano S, Takeichi M, Schultz RT, Feldmeyer D, Hahn CG, Carlson GC, Abel T, Brodkin ES. "Social and cognitive deficits in male mice haploinsufficient for Protocadherin 10 (Pcdh10), an autism associated gene."*

CHAPTER 3: THE TRANSCRIPTIONAL CO-REPRESSOR SIN3A REGULATES HIPPOCAMPAL SYNAPTIC PLASTICITY VIA HOMER1/MGLUR5 SIGNALING

Abstract

Long-term memory depends on the control of activity-dependent neuronal gene expression, which is regulated by epigenetic modifications. The epigenetic modification of histones is orchestrated by the opposing activities of two classes of regulatory complexes: permissive co-activators and silencing co-repressors. Much work has focused on co-activator complexes, but little is known about the co-repressor complexes that suppress the expression of plasticity-related genes. Here, we define a critical role for the co-repressor SIN3A in memory and synaptic plasticity showing that post-natal neuronal deletion of *Sin3a* enhances hippocampal long-term potentiation and long-term contextual fear memory. SIN3A regulates the expression of a specific set of genes encoding proteins in the post-synaptic density. Loss of SIN3A increases expression of the synaptic scaffold *Homer1*, alters the mGluR1α- and mGluR5-dependence of long-term potentiation, and increases activation of extracellular signal regulated kinase (ERK) in the hippocampus after learning. Our studies define a critical role for co-repressors in modulating neural plasticity and memory consolidation and reveal that Homer1/mGluR signaling pathways are central molecular mechanisms for memory enhancement.

3.1 Introduction

Long-term memory consolidation and hippocampal long-term potentiation depend on activity-dependent neuronal gene expression, which is in turn regulated by epigenetic mechanisms such as post-translational histone modification (Fischer, Sananbenesi, Mungenast, & Tsai, 2010; Peixoto & Abel, 2013). Histone acetylation is associated with transcriptional activation, and both histone acetylation and expression of acetylation-regulated genes are increased during memory consolidation (Levenson et al., 2004; Mahan et al., 2012; Maze, Noh, & Allis, 2013; Peixoto & Abel, 2013). Acetylation levels

are determined by the activity of histone acetyltransferase (HAT) and histone deacetylase (HDAC) enzymes, which are recruited to chromatin by association with co-activator and co-repressor proteins (Guan et al., 2009; McQuown et al., 2011; Vecsey et al., 2007). For example, HATs such as CBP and p300 are recruited by the transcription factor and co-activator protein CREB in response to signaling cascades triggered by synaptic activity (Vo & Goodman, 2001). The CREB-CBP/p300 complex can regulate transcription through HAT activity as well as association with other plasticity-related transcription factors , and genetic studies have demonstrated critical roles for CREB, CBP, and p300 in memory and synaptic plasticity (Alarcón et al., 2004; Oliveira, Wood, McDonough, & Abel, 2007; Vecsey et al., 2007). On the other hand, HDACs and other histone-modifying effector enzymes are recruited by co-repressor proteins such as NCoR, SIN3A, MI-2 (NuRD), and CoREST (Schoch & Abel, 2014, **Chapter 1.3.3**). In neurons, co-repressors have been linked to dynamic and activity-dependent regulation of gene expression and neuron-specific components of co-repressor complexes have also been described (Schoch & Abel, 2014), suggesting that these proteins may play a large role in regulating transcription-dependent plasticity. However, few studies have directly addressed the function of the co-repressor proteins in memory and plasticity.

SIN3A is a highly-conserved co-repressor protein that is expressed throughout the brain, both in neuronal and in non-neuronal cells. Through its histone-interacting domain (HID), SIN3A recruits a core complex that includes the histone binding proteins RBAP46/48, stabilizing proteins SAP18/20 and SDS3, and the Class I HDAC enzymes HDAC1 and HDAC2 (Grzenda, Lomberk, Zhang, & Urrutia, 2009; Silverstein & Ekwall, 2005) (**Fig.1.3)**. Four paired-amphipathic helix (PAH) domains mediate the binding of the

SIN3A-HDAC complex to numerous transcription factors, DNA binding factors, and other co-repressor proteins, facilitating the dynamic recruitment of SIN3A to chromatin (Grzenda et al., 2009; Silverstein & Ekwall, 2005). The binding partners of the SIN3A-HDAC complex include several factors linked to neuronal function and cognition, including MEF2, MECP2, NCoR, REST, and CoREST(Schoch & Abel, 2014; Silverstein & Ekwall, 2005). Members of the core SIN3A complex, especially HDAC2, have also been shown to regulate memory and plasticity (Bahari-Javan et al., 2012; Guan et al., 2009). These findings suggest that the SIN3A co-repressor complex is in a position to act as a critical regulator of neuronal function and cognition, but this co-repressor and its function in the mature nervous system have not been studied.

Pharmacological inhibition of HDAC enzymes has been shown to facilitate robust enhancements in long-term memory as well as in long-term potentiation(Alarcón et al., 2004; Levenson et al., 2004; Vecsey et al., 2007). Although a number of acetylation-regulated genes have been identified in these studies, it remains to be defined what downstream mechanisms mediate the enhancement of LTP and memory at the level of synaptic function. Similarly, while HDAC2 has been identified as a negative regulator of memory and plasticity in the hippocampus(Guan et al., 2009), the mechanisms by which it is recruited to its regulatory targets and ultimately leads to changes in synaptic function has received little attention. Interestingly, blocking the HDAC binding site on the co-repressor NCOR recapitulates the effect of HDAC inhibitor drugs on object memory, highlighting the critical role for co-repressors in bringing epigenetic regulators to gene loci (McQuown et al., 2011). Here, we address the function of co-repressors in memory storage and synaptic plasticity by conditionally deleting the co-repressor SIN3A in excitatory neurons, demonstrating a role for the SIN3A-HDAC co-repressor complex as

a negative regulator of memory and plasticity that exerts its downstream effects through the synaptic scaffold protein Homer1 and the Group I metabotropic glutamate receptors.

3.2 Methods

Mice

Mutant mice with a forebrain-specific deletion of *Sin3a* were generated by crossing mice homozygous for a loxP-flanked exon 4 of the *Sin3a* gene (*Sin3a*$^{L/L}$)(Dannenberg et al., 2005) with mice carrying the CaMKIIα-Cre transgene (L7ag#13) (Dragatsis & Zeitlin, 2000) and heterozygous for a loxP-flanked exon 4 of Sin3a (CaMKIIα-Cre; *Sin3a*$^{+/L}$) to produce CaMKIIα-Cre; *Sin3a*$^{L/L}$ (Sin3aNH) mice and control littermates. Deletion and premature stop codons were confirmed in cDNA from Sin3aNH hippocampus by PCR across the deletion site using the following primers- Exon 2 F: CAGCAGTTTCAGAGGCTCAAG and Exon 6 R: GGGCATACACCTCTTGCTCA. Amplified products were separated by gel electrophoresis, purified, and sequenced. In Sin3aNH, a full length *Sin3a* product and a single recombined *Sin3a* product were identified (data not shown). All genotypes produced from this mating were examined in fear conditioning. No differences were observed among genotypes with the exception of Sin3aNH mice, so all other genotypes were grouped for controls in the presented data. Experimenters were blind to the genotypes of the mice during collection of behavioral and electrophysiological data. CaMKIIα-Cre line L7ag#13 expresses Cre recombinase throughout the forebrain including the hippocampus, cortex, and amygdala with the majority of recombination occurring postnatally(Dragatsis & Zeitlin, 2000). These Sin3aNH mice were produced after more than 6 generations of backcrossing of the loxP-flanked *Sin3a* allele and more than 9 generations of backcrossing the CaMKIIα-Cre transgene into C57BL/6J.

Genotyping was performed using PCR with allele-specific primers. To identify mice bearing floxed alleles of the *Sin3a* gene, PCR was performed with the following primers: 3A-4 5'-AGC CAG CCC TGA GAC TAG TGA TAA AC-3', 3A-6: 5'-GGG GGA ATG CTG TGT TTT AGG TAT G-3'. PCR reactions were performed using RedExtract-N-Amp (Sigma, R4775) with the following thermal cycles parameters: 94°C for 15 min, [94°C for 30 s, 55°C for 30 s, 72°C for 30 s] x 50 cycl es, 72°C for 10 min. For CaMKII-Cre genotyping, PCR was performed with the following primers: Cre1 5'-CTG CCA CGA CCA AGT GAC AGC-3', Cre2 5'-CTT CTC TAC ACC TGC GGT GCT-3', Bglob1 5'-CCA ATC TCC TCA CAC AGG ATA GAG AGG GCA GG-3', Bglob2 5'-CCT TGA GGC TGT CCA AGT GAT TCA GGC CAT CG-3'. Thermal cycling parameters were as follows: 94° C for 3 min, [94°C for 45 s, 61°C for 45 s, 72°C for 60 s] x 30 cycles, 72°C for 10 min.

Mice were maintained under standard conditions consistent with National Institute of Health guidelines for animal care and use, and were approved by the Institutional Animal Care and Use Committee of the University of Pennsylvania. Mice were maintained on a 12 hr light-dark cycle and provided with food and water in their home cages *ad libitum.* Animals were group housed in cages of 2-5 littermates except for fear conditioning experiments. For fear conditioning, animals were moved from group housing to single housing 1 week prior to training. Behavioral testing, tissue collection, and electrophysiology were conducted on 2-6 month old male and female animals during the light portion of the cycle.

Immunoblots

Hippocampal lysation and immunoblotting were conducted as previously described (Hawk et al., 2012). Mice were cervically dislocated, and hippocampi were quickly dissected and flash frozen on dry ice. Hippocampi were homogenized at 4°C in 500 µL of cell lysis solution (10 mM HEPES pH 7.9, 1 mM EDTA, 1.5 mM $MgCl_2$, 10 mM KCl, 1% protease inhibitor cocktail (Sigma), 1 mM DTT), and nuclei were pelleted by 20 min centrifugation at 1000 x g at 4°C. Nuclear pellet s were resuspended in 100 µL of nuclear lysis buffer (20 mM HEPES pH 7.9, 0.2 mM EDTA, 1.5 mM $MgCl_2$, 400 mM KCl, 25% glycerol, 1% protease inhibitor cocktail (Sigma), 1mM DTT). After 30 min incubation on ice, samples were centrifuged at 4°C for 20 min at 1000 x g. Protein concentrations of the supernatants were quantified by the Bradford method (Biorad). Nuclear protein samples were prepared using 20 µg fractionated protein combined with NuPage LDS sample buffer and 2-mercaptoethanol (Invitrogen) and incubated for 5 min at 100°C. Proteins were separated on a 3-8% Bis-T ris gel (Novex, Life Technologies) for 1 hr and transferred to a PVDF membrane for immunoblotting. Membrane was blocked with 5% milk/PBST for 2 hrs at room temperature (RT), and incubated with anti-SIN3A (Sigma,S6695) 1:500 in 2% milk/PBST at 4°C o vernight. Membrane was washed three times in PBST for 10 min and incubated with anti-rabbit HRP conjugated secondary antibody (sc-2004, Santa Cruz Biotechnology) 1:1000 in 2% milk/PBST for 2 hr at RT. After three 10 min washes in PBST, the membrane was incubated for 1 min in ECL Western Blotting Detection Reagent (GE Healthcare) and developed on film. For detection of β tubulin control band, antibody was removed from the blot using Restore Western Blot Stripping Buffer (Thermo Scientific) according to the manufacturer's instructions. The membrane was re-blocked and re-probed with anti- β tubulin antibody (Sigma, T4026) using the same blotting protocol.

Gene expression

Hippocampal RNA was purified and cDNA was prepared as previously described (Hawk et al., 2012). Following contextual conditioning, hippocampal dissections were performed on ice, and tissue stored in RNA Later (Qiagen) at -80°C until RNA extraction. RNA was isolated by Trizol extraction and purified using an RNeasy kit (Qiagen) according to the manufacturer's instructions. RNA concentration was measured using a NanoDrop spectrophotometer (ThermoFisher Scientific). Template cDNA was synthesized from 1 µg total RNA using the RETROscript kit (Ambion). Reactions were conducted at 44°C for 1 hr, heat in activated at 100°C for 10min, and the final products were diluted in water to a final concentration of 2 ng/µL. Real time qPCR was performed on the Viia7 Real Time PCR platform (Applied Biosystems) in 5uL reactions consisting of 4.5 ng cDNA, 2.5 µL Fast SYBR Green master mix (Applied Biosystems), and 250nM forward and reverse primers. Samples that did not amplify were excluded from analysis. Values were normalized to three housekeeper genes (Gapdh, ActB, ActG), and relative quantification was calculated using a ΔΔCt method as described previously (Vecsey et al., 2007). Relative gene expression is reported as the fold difference in mean values for distinct biological replicates.

Behavior

Fear conditioning was conducted as previously described (Hawk et al., 2012). For contextual conditioning, naïve 2- to 6-month old male and female Sin3a NH (CaMKIIα-Cre; *Sin3a*$^{L/L}$*)* and control (CaMKIIα-Cre; *Sin3a*$^{L/+}$*, and Sin3a*$^{L/L}$*)* mice were placed in a novel training chamber for 180 s and a single 2 s, 0.75 mA foot shock was administered after 148 s. Contextual fear testing was conducted 1 hr or 24 hrs after training, by re-

exposing the animals to the trained context for 5 min. Cued fear conditioning was conducted using a similar training procedure as contextual fear, with the addition of a 30 s tone presentation starting at 120 s. Cued fear testing was conducted in a novel conditioning chamber with altered floor covering, odor, and dimensions. Mice were exposed to the novel context for 3 min, followed immediately by 3 min of tone presentation. Freezing behavior during contextual and cued testing was scored by computer using FreezeScan software (Clever Systems). Freezing levels for all groups was examined for normality using Shapiro-Wilk test. Normally distributed data sets were compared using two-way ANOVA, with significance levels of $p < 0.05$. Non-parametric data were compared using independent samples Kruskal-Wallis test, with p value significance level of 0.05. For all conditioning experiments, animals with responses two standard deviations above or below the group mean were excluded from the analysis as outliers. Mice were tested in the elevated zero maze with a single 5 min exposure in which the animals were allowed to freely explore the maze. Time spent in open and closed quadrants of the maze were scored manually by a trained observer blind to the genotypes of the animals. A two-tailed independent samples t-test was used to compare genotypes for open and closed areas. For all behavioral tasks, testing order was designed so that mice of different sexes were not in the testing room at the same time. Testing chambers were thoroughly cleaned between each session to minimize odor cues.

Immunohistochemistry

Transcardial perfusions and immunohistochemical stainings were conducted as previously described (Havekes et al., 2012). Sections incubated rabbit anti-phopsho-ERK1/2 (Cell Signaling, AB9101). Phosphatase inhibitors were included in the fixative

and all buffers (Havekes et al., 2012). Cell counts were conducted as described (Havekes et al., 2012) by a trained observer blind to grouping. Groups were compared using a one-tailed independent samples t-test.

Electrophysiology

Recordings: To assess the effects of conditional *Sin3a* mutation on LTP, 2- to 6-month old male and female Sin3a NH (CaMKIIα-Cre; *Sin3a*$^{L/L}$*)* and control (*Sin3a*$^{L/L}$*)* mice we killed by cervical dislocation and their hippocampi quickly dissected out into ice-cold oxygenated artificial CSF (aCSF;124 mM NaCl, 4.4 mM KCl, 1.3 mM MgSO4•7H2O, 1 mM NaH2PO4•H2O, 26.2 mM NaHCO3, 2.5 mM CaCl2•2H2O, 10 mM D-glucose). Transverse hippocampal slices were cut 400µm thick using a tissue chopper (Stoelting Co., Wood Dale, IL), placed in an interface chamber, and perfused with oxygenated aCSF at 28.0℃ at a flow rate of 1 mL/min. Slices were allowed to recover for at least 2 hours before beginning electrophysiological recordings. Single-pathway recordings were made using a single bipolar stimulating electrode made from nichrome wire (A-M Systems, Sequim, WA) placed in the stratum radiatum and used to elicit action potentials in the axons of CA3 pyramidal neurons. Field potentials (fEPSPs) were recorded using an aCSF-filled glass microelectrode (A-M Systems) with a resistance between 1 and 5 MΩ placed in the stratum radiatum region of CA1. Data collection was handled by Clampex software (Molecular Devices, Palo Alto, CA) and was analyzed using Clampfit software (Molecular Devices). The peak fEPSP amplitude induced by the stimulating electrode was required to be at least 5 mV, and stimulus intensity during the recording was set to produce a response of 40% of the maximum fEPSP amplitude. Test stimulation occurred once every minute. Baseline responses were recorded for 20 minutes before LTP induction or drug application. To examine early-phase LTP (E-LTP)

one 1-second, 100 Hz train of stimuli was applied through the stimulating electrode. To examine late-phase LTP (L-LTP) four 1-second, 100 Hz trains of stimuli were delivered 5 min apart. Recordings continued for at least 160 min after LTP induction. The initial slope of the recorded fEPSPs were normalized to the average of the 20 baseline traces and expressed as percentages of this baseline value.

Drugs: All drugs used in the electrophysiology experiments were mixed as stock solutions and stored as individual aliquots at -20° C. The HDAC inhibitor Trichostatin A (TSA; AG Scientific) was mixed as a 16.5 mM stock solution in 50% ethanol (Vecsey et al., 2007), and diluted to a final concentration of 1.65 µM in aCSF. The mGluR5 antagonist MPEP and the mGluR1α antagonist LY367385 were purchased from AbCam. MPEP was mixed as a 5 mM stock solution in ddH_2O and diluted to a final concentration of 40 µM in aCSF. LY367385 was mixed as a 50 mM stock solution in equimolar NaOH, and diluted to a final concentration of 100 µM in aCSF. The RNA synthesis inhibitor actinomycin D was dissolved in DMSO at a stock concentration of 50 mM, and was diluted to a final concentration of 25 µM in aCSF(Vecsey et al., 2007). Drug application was initiated 20 min prior to induction and lasted for 10 min (mGLuR antagonists) or for the duration of the recording (TSA and Actinomycin-D).

Statistical analyses: Initial slope of the fEPSP was used to quantify synaptic potentiation, normalized to the averaged value of the 20-minute baseline. Only one slice per animal was included in any treatment condition. Within each LTP experiment, recordings were made from multiple slices from each mouse whenever possible to reduce the number of animals used. The order of treatment was determined randomly on each day of

recording. Sample sizes were not predetermined using statistical methods, but the sample sizes in our experiments are similar to those reported in similar previously published research from our lab and others(Havekes et al., 2012; Vecsey et al., 2007). To evaluate potential differences in paired-pulse facilitation a repeated measures ANOVA was used with genotype and inter-stimulus interval as factors and the facilitation ratio as the dependent variable. For evaluation of input–output characteristics, an independent samples t-test was performed comparing the average linear regression slopes for control mice and Sin3aNH mice. Potential differences in the maximum fEPSP slope were evaluated using an independent samples t-test. Between-group differences in LTP maintenance were determined using a repeated measures ANOVA on the final 20 minutes of the recordings, followed by Tukey's *post-hoc* test when appropriate(Vecsey et al., 2007). Normality and variance of LTP data were checked to determine suitability for analysis by ANOVA. Normality of the data was evaluated by Shapiro-Wilk tests and examination of normal probability plots of the residuals. Variance was evaluated by examination of residual plots of observed versus fitted values. All statistical analyses were performed using STATISTICA software (StatSoft Inc.; Tulsa, OK). Significance for all tests was set at $p < 0.05$. In all related figures, significance is indicated by $*p < 0.05$, $**p < 0.01$, and $***p < 0.001$.

3.3 Results

3.3.1 Deletion of *Sin3a* from forebrain excitatory neurons enhances long-term potentiation

To explore the role of SIN3A in synaptic plasticity and memory consolidation, we used the Cre-loxP system to conditionally delete the *Sin3a* gene in forebrain excitatory neurons **(Fig. 3.1A)**. SIN3A protein levels are reduced by approximately 50% in the

hippocampus of Sin3a neuronal hypomorphs (Sin3aNH) relative to control animals (ANOVA: $F_{(1,10)}$= 32.74, $p < 0.001$) **(Fig. 3.1B,C)**. SIN3A binds HDAC1 and HDAC2, and mediates transcriptional repression through interactions with multiple transcription factors and epigenetic regulatory proteins that have been linked to both positive and negative regulation of gene transcription (**Fig. 3.1D)**.

HDAC inhibition enhances hippocampal long-term potentiation (LTP), transforming short-term LTP into long-lasting, transcription-dependent LTP (Levenson et al., 2004; McQuown et al., 2011). Because SIN3A is a scaffold protein that recruits both HDAC1 and HDAC2 to sites of transcriptional regulation, we hypothesized that reduced neuronal *Sin3a* would mimic the effects of HDAC inhibition and enhance hippocampal LTP. Initially, we tested basal synaptic properties, paired-pulse facilitation, and synaptic stability at the Schaffer collateral synapses of area CA1. We found that these electrophysiological properties were unchanged in the Sin3aNH mice, indicating that synaptic transmission and the stability and health of slices are not affected by reduced neuronal *Sin3a* (**Fig. 3.2**). In hippocampal slices from wild-type control mice, a single tetanus (1 sec, 100 Hz) induces short-lasting LTP that typically returns to baseline levels within one or two hours after stimulation(Havekes et al., 2012; Vecsey et al., 2007). In slices from Sin3aNH mice, the same weak stimulus produces sustained potentiation that is significantly higher than in controls (controls, n = 6, avg. of fEPSP slope over final 20 min = 101.25 ± 2.03 %; Sin3aNH, n = 6, avg. of fEPSP slope over final 20 min = 151.72 ± 10.88 %; repeated measures ANOVA: genotype, $F_{(1,10)}$ = 7.713, p = 0.0195; **Fig. 3.3A**). Further, this LTP enhancement in Sin3aNH slices is blocked by the transcription inhibitor Actinomycin D **(Fig. 3.4)**. Given the enhancement in hippocampal LTP by *Sin3a*

deletion, we next investigated the ability of an HDAC inhibitor to further enhance LTP in Sin3aNH mice. As has been demonstrated previously(Vecsey et al., 2007), the combination of a single tetanus and administration of the HDAC inhibitor Trichostatin A (TSA) enhances LTP in wild-type control slices (controls + veh, n = 4, avg. fEPSP slope = 99.71 ± 7.24%; controls + TSA, n = 6, avg. fEPSP slope = 155.01 ± 9.47%; repeated measures ANOVA: genotype, $F_{(1,16)} = 10.604$, $p = 0.005$; treatment, $F_{(1,16)} = 5.111$, $p = 0.038$; genotype × treatment interaction, $F_{(1,16)} = 5.151$, $p = 0.037$; Tukey's *post-hoc*, controls + veh vs. controls + TSA, $p = 0.026$**; Fig. 3.3B**). However, in Sin3aNH mice, TSA administration did not enhance LTP compared to vehicle-treated slices (Sin3aNH + veh, n = 4, avg. fEPSP slope = 168.82 ± 2.05%; Sin3aNH + TSA, n = 6, avg. fEPSP slope = 169.34 ± 17.4%; Tukey's *post-hoc*, Sin3aNH + veh vs. Sin3aNH + TSA, $p = 0.999$; **Fig. 3.3C**). Further, LTP in Sin3aNH slices was significantly greater than in vehicle-treated control slices but was similar to TSA-treated control slices (repeated measures ANOVA with Tukey's *post-hoc* test: control + veh vs. Sin3aNH + veh, $p = 0.012$; control + veh vs. Sin3aNH + TSA, $p = 0.006$; control + TSA vs. Sin3aNH + veh, $p = 0.894$; control + TSA vs. Sin3aNH + TSA, $p = 0.862$**; Fig. 3.3D**). The occlusion of the effects of TSA on LTP in Sin3aNH mice and the similarity of LTP enhancement by *Sin3a* deletion to LTP enhancement by HDAC inhibitor treatment suggest that the changes we observe here in synaptic plasticity are a phenocopy of HDAC inhibition, and that the enhanced LTP phenotypes share a common underlying mechanism.

3.3.2 Reduced Sin3a in forebrain excitatory neurons enhances hippocampal long-term memory

To determine whether reduction of neuronal *Sin3a* impacts memory consolidation, we tested associative memory in Sin3aNH animals using the contextual fear conditioning

paradigm. First, we tested long-term memory in Sin3aNH and wild type control animals in the foreground contextual fear paradigm, a cognitive task that engages the hippocampus(Maren & Fanselow, 1997; Trifilieff et al., 2006). Sin3aNH animals show enhanced long-term memory compared to controls when tested 24 hrs after conditioning (independent samples Kruskal-Wallis, effect of genotype: pre-shock, $p < 0.13$; 24 hr test, $p < 0.008$; **Fig. 3.5A**). Consolidation of long-term (24 hr) hippocampal fear memory requires transcriptional activation and translation of new proteins, but 1 hr short-term memory does not(Bourtchouladze et al., 1998; Igaz, Vianna, Medina, & Izquierdo, 2002). When we tested a second naïve cohort of animals for short-term contextual fear memory 1 hr after training, we found no differences in the freezing responses of Sin3aNH and control animals to the training context (two-way ANOVA; genotype $F_{(1,44)} = 0.05$, $p < 0.83$; phase $F_{(1,44)} = 94.1$, $p < 0.001$**; Fig. 3.5B**). Previous studies of fear learning circuitry suggest that associative fear conditioning to a tone cue is dependent on the amygdala, but not on the hippocampus (Maren, 2005; Phillips & LeDoux, 1992). When we conditioned a third cohort of Sin3aNH animals in the tone cued fear task, no differences were seen in either baseline freezing pre-CS, or during CS tone presentation (two-way ANOVA: genotype $F_{(1,22)} = 0.1$, $p < 0.77$; phase $F_{(1,22)} = 21.0$, $p < 0.001$)**; Fig. 3.5C**). This finding suggests that the memory enhancements observed are specifically due to changes in hippocampal function. As a next step, we examined mice for anxiety-related behaviors in the elevated zero maze. Sin3aNH mice show increased time spent in the open sections (independent samples t-test, $p < 0.01$) compared to controls, a result suggestive of decreased anxiety in the Sin3aNH animals (**Fig. 3.5D**). The low levels of anxiety-like behaviors in the Sin3aNH mice together with the absence of changes in both 1hr contextual and cued fear responses strongly argue against general fear abnormalities in these animals. Rather, these results indicate that reducing the function

of the SIN3A co-repressor in excitatory neurons enhances hippocampal long-term memory.

3.3.3 Reduction of neuronal SIN3A changes memory-related gene expression and synaptic signaling.

The effects of SIN3A depletion on transcription-dependent forms of long-term memory and synaptic plasticity support a role for the SIN3A-HDAC complex in regulating the expression of genes involved in neuronal plasticity. We focused our studies on specific gene loci linked to memory and synaptic plasticity that were shown by others to be regulated by both HDAC2 and SIN3A (NHGRI ENCODE)(Guan et al., 2009; Kundaje et al., 2012). To investigate whether expression of these candidate target genes is altered in Sin3aNH mice, we collected hippocampal tissue from Sin3aNH and control animals 1 hr after contextual fear conditioning and measured mRNA transcript levels by quantitative RT-PCR. Neuronal depletion of SIN3A alters mRNA expression of a subset of HDAC2-regulated synaptic genes, increasing levels of transcripts encoding synaptic scaffold *Homer1* and cyclin-dependent kinase *Cdk5* (Student's t-test: *Homer,1* $p < 0.001$; *Cdk5,* $p < 0.02$; *Gria1,* $p < 0.26$; *Grin2a,* $p < 0.61$; *Grin2b,* $p < 0.02$; *CaMKIIα,* $p < 0.34$; **Fig. 3.6A**). Homer1 and Cdk5 are implicated in memory consolidation and both proteins function in a common pathway regulating the localization and function of type I mGluRs, so we further investigated the role of HOMER1 and mGluR signaling in the Sin3aNH animals (Mahan et al., 2012; Orlando et al., 2009). Two classes of HOMER1 isoforms modulate mGluR signaling at the synapse (Shiraishi-Yamaguchi & Furuichi, 2007). Long Homer1 isoforms promote mGluR signaling and recruit mGluRs to the post-synaptic density (Mao et al., 2005; Tu et al., 1999; Xiao et al., 1998). Short isoforms of Homer1 act in a dominant negative manner to uncouple mGluRs from the post-synaptic density

and from downstream effector molecules (Bottai et al., 2002; Kammermeier & Worley, 2007). A more detailed examination of *Homer1* mRNA expression in Sin3aNH animals revealed an increase in expression across the *Homer1* locus, including regions specific to both short isoforms (Homer1a-specific UTR following exon 5, and Ania-3 specific exon A) and long isoforms (exon 10) (Student's t test: exon 1, $p < 0.02$; Homer1a, $p < 0.01$; Ania-3, $p < 0.08$; exon10, $p < 0.01$; **Fig. 3.6B** and **Fig. 3.7C and D**). These data provide evidence of synaptic changes that accompany *Sin3a* deletion, and suggested a mechanism that could support the memory and plasticity phenotype observed in Sin3aNH mice through changes in Group I mGluR function.

The Group I mGluRs (mGluR1α and mGluR5), have been shown to play important roles in several forms of memory and synaptic plasticity (Jia et al., 1998; Manahan-Vaughan & Braunewell, 2005; Ménard & Quirion, 2012; Neyman & Manahan-Vaughan, 2008), and are upstream of a number of signaling pathways that contribute to plastic processes **(Fig. 3.8A)**, including intracellular Ca^{2+} release, IP3/DAG signaling and PKC activation, ultimately leading to the phosphorylation and activation of ERK1/2(Anwyl, 2009; Piers et al., 2012). Compounds that facilitate activation of mGluR5 enhance performance in rodent learning paradigms(Ayala et al., 2009; Balschun, Zuschratter, & Wetzel, 2006; Uslaner et al., 2009). Because the reduction of forebrain SIN3A was accompanied by the enhancement of long-term memory and long-term potentiation, as well as the upregulation of both *Homer1* and *Cdk5* mRNA levels, we hypothesized that the observed memory and LTP enhancements could be attributed to increased function of synaptic Type 1 mGluRs. We chose to assay levels of ERK1/2 phosphorylation after contextual fear conditioning as an initial test of the memory-related signaling cascades downstream of the Group I mGluRs. ERK phosphorylation is essential for memory

formation and synaptic plasticity (Thomas & Huganir, 2004; Trifilieff et al., 2006), is regulated by mGluR1α/5 activity (Mao et al., 2005), and is necessary for Homer1/mGluR-mediated enhancement of LTP (O'Riordan, Gerstein, Hullinger, & Burger, 2014). We measured activation of ERK signaling pathways in hippocampal neurons one hour after contextual fear conditioning using immunostaining for phosphorylated ERK1/2 in sections from both Sin3aNH and control mice **(Fig. 3.6C** and **Fig. 3.9)**. Quantification of the immunostained cells revealed a higher number of phospho-ERK1/2 positive cells in area CA1, but not in area CA3 or in the dentate gyrus (DG), of Sin3aNH mice compared to control littermates (n =10 for each group; CA1 t-test, $p = 0.0296$; CA3 t-test, $p = 0.46$; DG, t-test, $p = 0.0864$; **Fig. 3.6 D**). These results suggest that a reduction in neuronal Sin3a leads to elevated expression of the mGluR scaffold Homer1, and increased activity in mGluR signaling pathways.

3.3.4 Reduction of neuronal Sin3a changes mGluR contributions to long term potentiation

Changes in *Homer1* expression have been linked to changes in synaptic plasticity, and previous studies have shown that increasing the expression of long-form Homer1 alters signaling through mGluR1α/mGluR5 in long-lasting forms of synaptic plasticity (Gerstein, O'Riordan, Osting, Schwarz, & Burger, 2012; Klugmann et al., 2005). Late phase LTP in wild-type hippocampal slices requires activity of both mGluR1 and mGluR5, but slices expressing long isoform *Homer1c* exhibited a form of LTP that did not require mGluR1 signaling(Gerstein et al., 2012). To investigate whether the changes we observed in *Homer1* expression in the Sin3aNH mice affect the contributions of mGluR1α and mGluR5 to synaptic plasticity, we induced L-LTP using spaced 4-train stimulation in the presence of either the mGluR1α antagonist LY367385 or the mGluR5 antagonist

MPEP(Neyman & Manahan-Vaughan, 2008). When slices from wild type control mice and Sin3aNH mice were stimulated with this protocol in the absence of drug treatment no differences in LTP were observed, indicating L-LTP maintenance is not changed by *Sin3a* depletion **(Fig. 3.10)**. In slices from wild type control mice, antagonizing either of the Type I mGluRs reduced LTP compared to vehicle-treated slices (controls + veh, n=6, avg. fEPSP slope = 182.24 ± 4.67%; controls + LY367385, n = 5, avg. fEPSP slope = 121.82 ± 20.67%; controls + MPEP, n = 5, avg. fEPSP slope = 120.96 ± 6.56%; repeated measures ANOVA: genotype, $F_{(1,28)} = 17.894$, $p = 0.00023$; treatment, $F_{(2,28)} = 20.453$, $p = 0.000003$; genotype × treatment interaction, $F_{(2,28)} = 7.924$, $p = 0.0019$; Tukey's *post-hoc* test, controls + vehicle vs. controls + MPEP, $p = 0.018$; controls + vehicle vs. controls + LY367385, $p = 0.008$**; Fig. 3.11A)**. In slices from Sin3aNH mice, the administration of MPEP significantly reduced LTP, while antagonism of mGluR1α with LY367385 did not have a significant effect on potentiation (Sin3aNH + veh, n = 5, avg. fEPSP slope = 192.29 ± 17.4%; Sin3aNH + LY367385, n = 6, avg. fEPSP slope = 213.12 ± 7.62%; Sin3aNH + MPEP, n = 7, avg. fEPSP slope = 116.06 ± 10.94%; Tukey's *post-hoc* test, Sin3aNH + vehicle vs. Sin3aNH + MPEP, $p = 0.0002$; Sin3aNH vehicle vs. Sin3aNH + LY367385, $p = 0.999$; Sin3aNH + LY367385 vs. Sin3aNH + MPEP, $p = 0.0002$**; Fig. 3.11B)**. These results indicate that LTP in Sin3aNH mice is independent of mGluR1α but requires mGluR5, suggesting that increased long Homer1 levels result in very specific changes in the function of the Group I mGluRs at CA1 synapses.

3.4 Discussion

Inhibition of HDAC activity enhances memory and facilitates neuronal plasticity(Peixoto & Abel, 2013). However, the precise molecular mechanisms by which these

manipulations ultimately affect synaptic and neuronal function are not understood, and the identification of functional effector genes targeted by HDAC inhibition has been challenging. Here, we targeted the co-repressor SIN3A, a scaffolding protein that coordinates a multi-functional co-repressor complex containing several histone-modifying enzymes including HDAC1 and HDAC2. Mice carrying a conditional neuronal depletion of *Sin3a* have reduced levels of protein in the hippocampus. We observed that chronic reduction of SIN3A is accompanied by enhanced hippocampal synaptic plasticity and memory formation, mimicking the effects of acute HDAC inhibitor administration. These enhancements in memory and plasticity are accompanied by increased expression of several neuronal genes regulated by HDAC2 and SIN3A, including *Homer1* and *Cdk5*. We observed an increase in expression of constitutively expressed long isoforms of *Homer1,* which organize group I mGluRs at the synapse, and increased phosphorylation of ERK, a downstream target of group I mGluRs. Alterations in Homer1 and mGluR functioning has profound effects on synaptic structure, plasticity, and cognition (Ayala et al., 2009; Gerstein et al., 2012; Klugmann et al., 2005; Ménard & Quirion, 2012).

The upregulation of *Homer1* and the observed shift in the requirements for Group I mGluR signaling in Sin3aNH L-LTP indicate that the enhancements we observed in hippocampus-dependent memory and hippocampal synaptic plasticity may be attributable to a change in Homer1/mGluR5 signaling at the synapse, and suggest a model by which these changes could occur. Long isoforms of Homer1 bind to the intracellular C-terminal tails of the Group I mGluRs and linking them to the postsynaptic density in dendritic spines (Tu et al., 1999; Xiao et al., 1998a). Under baseline conditions both mGluR1α and mGluR5 are linked to the postsynaptic density through interactions with long Homer1b/c **(Fig. 3.8A)**., Group I mGluRs are associated with several key

signaling pathways associated with memory and plasticity (Ayala et al., 2009; Mao et al., 2005; Ménard & Quirion, 2012), and under baseline conditions the activation of both mGluR1α and mGluR5 are necessary for long-term potentiation (Neyman & Manahan-Vaughan, 2008) (**Fig. 3.12**). In Sin3aNH mice, higher levels of long-form Homer1b/c may recruit more mGluR5 to the postsynaptic density **(Fig. 3.8B)**. Such an increase in synaptic mGluR5 could reduce the requirement for mGluR1α in LTP, and could also facilitate LTP enhancement via increases in $[Ca^{2+}]i$(Ayala et al., 2009; Kotecha et al., 2003; Mao et al., 2005), downstream signaling through PKC and ERK (Ayala et al., 2009; Kotecha et al., 2003; Mao et al., 2005), and even NMDA receptor potentiation through Src kinase (Kotecha et al., 2003) (**Fig. 3.12**).

Pharmacological inhibition of HDAC enzymes could be an important component of future therapies for not only at improving cognition, but also treating cognitive and neurodegenerative disorders(Abel & Zukin, 2008; Fischer et al., 2010). One of the major obstacles to developing HDAC inhibitor drugs as neural therapeutic agents is a lack of understanding of basic molecular mechanisms driving the synaptic and behavioral effects of these compounds. Here, we show that neuronal depletion of the HDAC-coordinating co-repressor SIN3A alters the expression of HDAC-regulated genes as well as Group I mGluR function and downstream signaling through ERK, and these effects on mGluR5/Homer1 signaling likely mediate the enhancements in memory and plasticity observed in Sin3aNH mice. Indeed, it has recently been demonstrated that increasing mGluR signaling via positive allosteric modulators enhances hippocampal long-term potentiation, long-term depression, and long-term memory consolidation in rodents(Ayala et al., 2009), while disruption of Group I mGluR function has been implicated in many cognitive and neurological disorders that may also be influenced by histone acetylation (including anxiety disorder, Fragile X syndrome, Parkinson's disease,

and schizophrenia)(Nicoletti, Bockaert, & Collingridge, 2011; Piers et al., 2012; Szumlinski, Kalivas, & Worley, 2006). These findings provide evidence linking mGluR signaling at the synapse to epigenetic mechanisms regulating gene expression for the first time, paving the way for novel therapeutics to treat cognitive deficits.

Chapter 3 Figure Legends

Figure 3.1. Sin3a neuronal hypomorphs have reduced levels of SIN3A in the hippocampus.

A. Structure of murine *Sin3a* locus with exon 4 highlighted. Recombination via CaMKIIα promoter-driven Cre at one or more $Sin3a^{LoxP}$ alleles results in deletion of exon 4 of *Sin3a*. **B.** Sin3aNH mice have decreased SIN3A protein levels (arrows) in the hippocampus by immunoblot. **C.** Quantification of optical density of SIN3A bands (arrows in panel c) normalized to β tubulin loading control (controls n = 6, Sin3aNH n = 5, one way ANOVA, $F_{(1,9)} = 32.74$, ***$p < 0.001$). **D.** The HID domain and four PAH domains of SIN3A mediate interactions with co-factors, epigenetic modifiers, and transcription factors. SIN3A-interacting factors have been linked to both activating (green) and repressive (red) regulation of gene transcription.

Figure 3.2. Sin3aNH conditional mutation does not change basal synaptic properties at the Schaffer collateral synapses. A. Paired-pulse facilitation was unchanged in hippocampal slices from Sin3aNH mice (controls n = 18, Sin3aNH n = 16; repeated measures ANOVA: genotype, $F_{(1,32)} = 0.364$, $p = 0.55$; genotype × interval interaction, $F_{(4,128)} = 0.769$, $p = 0.547$). **B.** Input-output relationships were not different in Sin3aNH mice compared to wild type controls (controls n = 18, Sin3aNH n = 16; independent samples t-test on average of regression slopes, $t_{(1,32)} = 1.324$, $p = 0.189$). **C.** The maximum amplitude of fEPSP slopes recorded in slices from Sin3aNH mutant mice and wild type control animals were not significantly different (controls n = 18, Sin3aNH n = 16; independent samples t-test, $t_{(1,32)} = 0.11$, $p = 0.913$). **D.** Baseline synaptic response in the absence of stimulation is not altered in Sin3aNH mutants when

compared to wild type controls (controls, n = 3, avg. fEPSP slope = 94.32 ± 7.78%; Sin3aNH, n = 3, avg. fEPSP slope = 95.12 ± 6.58%; repeated measures ANOVA: genotype, $F_{(1,4)} = 0.092$, $p = 0.777$).

Figure 3.3. Neuronal deletion of SIN3A enhances hippocampal LTP. A. LTP was induced by a single 100 Hz, 1 s duration stimuli (indicated by arrow). LTP maintenance was significantly enhanced in Sin3aNH mice (controls, n = 6, avg. of fEPSP slope over final 20 min = 101.25 ± 2.03 %; Sin3aNH, n = 6, avg. of fEPSP slope over final 20 min = 151.72 ± 10.88 %; repeated measures ANOVA: genotype, $F_{(1,10)} = 7.713$, $^*p = 0.0195$). **B.** In control slices, perfusion with 1.65 µM TSA enhanced 1-train LTP compared to vehicle (controls+veh, n = 4, avg. fEPSP slope = 99.71 ± 7.24%; controls+TSA, n = 6, avg. fEPSP slope = 155.01 ± 9.47%; repeated measures ANOVA: genotype, $F_{(1,16)}=10.604$, $p = 0.005$; treatment, $F_{(1,16)}= 5.111$, $p = 0.038$; genotype×treatment interaction, $F_{(1,16)}= 5.151$, $p = 0.037$; Tukey's *post-hoc*, controls+veh vs. controls+TSA, $^*p = 0.026$). **C.** In Sin3aNH slices, TSA administration did not enhance LTP compared to vehicle (Sin3aNH+veh, n = 4, avg. fEPSP slope = 168.82±2.05%; Sin3aNH + TSA, n = 6, avg. fEPSP slope = 169.34 ± 17.4%; Tukey's *post-hoc*, Sin3aNH+veh vs. Sin3aNH+TSA, $p = 0.999$). **D.** Average fEPSP slopes over final 20 minutes from all groups. No significant difference was observed between control + TSA, Sin3aNH+veh, and Sin3a+TSA groups; these groups all displayed higher potentiation than control+veh slices (repeated measures ANOVA, Tukey's *post-hoc*, control+veh vs. Sin3aNH+veh, $^*p = 0.012$; control+veh vs. Sin3aNH+TSA, $^{**}p = 0.006$; control+TSA vs. Sin3aNH+veh, $p = 0.894$; control+TSA vs. Sin3aNH+TSA, $p = 0.862$).

Figure 3.4. Enhanced LTP in Sin3aNH slices is transcription-dependent. Following a 20 minute baseline recording, hippocampal slices from Sin3aNH mutant mice were

perfused with the RNA synthesis inhibitor Actinomycin-D (ActD, 25 μM) or vehicle (0.05 % DMSO) in aCSF for the remainder of the recording period. A single 1 sec, 100 Hz tetanus was delivered at 40 minutes (indicated by arrow). LTP in vehicle-treated Sin3aNH slices was significantly higher than in ActD treated slices, indicating that transcription is necessary for the LTP enhancement observed in Sin3aNH mutant mice (Sin3aNH + vehicle, n = 4, avg. fEPSP slope = 168.32 ± 17.74%; Sin3aNH + ActD, n = 4, avg. fEPSP slope = 110.55 ± 6.23%; repeated measures ANOVA: treatment, $F_{(1,6)} = 9.430$, $*p = 0.022$).

Figure 3.5. Sin3aNH mice have enhanced long-term memory. **A.** Sin3aNH animals have enhanced 24 hr long-term memory for contextual fear conditioning (n = 34 control, n = 32 Sin3aNH, independent samples Kruskal-Wallis test, effect of genotype: pre-shock $p < 0.13$; 24 hr test $**p < 0.008$). **B.** No effect of Sin3a reduction on 1 hr short-term memory for contextual fear conditioning (n = 10 control, n = 12 Sin3aNH; two-way ANOVA, genotype, $F_{(1,44)} = 0.05$, $p < 0.83$; phase, $F_{(1,44)} = 94.1$, $p < 0.001$). **C.** Cued fear long-term memory is not altered in Sin3aNH animals (n = 6 control, n = 7 Sin3aNH; two-way ANOVA: genotype, $F_{(1,22)} = 0.1$; $p < 0.77$; phase, $F_{(1,22)} = 21.0$, $p < 0.001$). **D.** In the elevated zero maze, Sin3aNH mice spend more time in the open arms (n =12 per group; independent samples t-test, $t_{(1,22)} = 3.342$, $**p < 0.01$), and less time in the closed arms (t-test, $**p < 0.01$) compared to wild-type control animals.

Figure 3.6. Reduction in SIN3A increases *Homer1* expression and affects signaling cascades downstream of mGluR. **A.** Expression of genes regulated by HDAC2 and SIN3A in hippocampus of Sin3aNH mice 1hr after fear conditioning. Levels of *Homer1* (unpaired t-test, n = 7 per group; $t_{(1,12)} = -6.448$, $***p < 0.001$) and *Cdk5* ($t_{(1,12)} = -2.836$, $*p < 0.02$) are increased relative to controls, and the level of *Grin2b* is decreased ($t_{(1,12)} =$

3.038, * $p < 0.02$). **B.** Expression of *Homer1* exons encoding both short (*Homer1a*) and long (containing exon 10) isoforms is elevated in Sin3aNH mice (n = 7 control, n = 6 Sin3aNH; unpaired t-test, Exon 1 $t_{(1,11)} = -2.877$ *$p < 0.02$; Homer1a $t_{(1,11)} = -3.313$, **$p < 0.01$; Ania-3 $t_{(1,11)} = -2.146$, $p < 0.08$; Exon 10 $t_{(1,11)} = -3.251$ **$p < 0.01$). **C.** Representative images of hippocampal area CA1 showing cells stained for somatic ERK p42/44 in a Sin3aNH mouse and a control littermate one hour after contextual fear conditioning. Scale bar = 0.1 mm. **D.** Quantification of pERK-positive neurons is dorsal hippocampus following contextual fear conditioning shows a significantly higher number of cells positive for ERK p42/44 in CA1, but not CA3 or DG, of Sin3aNH mice compared to control littermates (n = 10 per group; t-test, CA1 *$p = 0.0296$; CA3 $p = 0.46$; DG $p = 0.0864$).

Figure 3.7 Expression of Homer1 exons and mGluR1/5 transcripts. A. mRNA expression of individual exons of Homer1 in control and Sin3aNH mutant hippocampi 1hr after training in contextual fear (t-test, *$p < 0.05$, **$p < 0.01$). **B.** Expression of mGluR5 mRNA is reduced in Sin3aNH mutants 1hr after contextual fear training (t-test, *$p < 0.05$). **C.** Exon structure of *Homer1* and neuronally expressed *Homer1* mRNA transcripts. **D.** Gene structure of *Homer1* in RefSeq in UCSC genome browser (dark purple). ChIPseq analysis of SIN3A binding and histone H3K27 acetylation Homer1 locus in CH12 murine B cell lymphoma cell line and melanocyte cells (MEL) from the TFBS ChIP-seq conducted by ENCODE/Stanford/Yale (NHGRI ENCODE data; Kundaje et al., 2012). Called peaks are indicated in black and grey bars (significant enrichment **$p < 0.01$ compared to input DNA control) above the signal (blue) for each cell line.

Figure 3.8. A model for enhanced synaptic plasticity and mGluR5 function with the deletion of *Sin3a*. A. In wild type mice, both mGlur1α and mGluR5 are required for

the maintenance of hippocampal LTP. Group I mGluRs may be found clustered at glutamatergic synapses by interactions with long-form Homer1 proteins, linking them to the post-synaptic density and ionic glutamatergic receptors through other scaffolding proteins such as Shank, GKAP, and PSD95. While there is debate over the exact mechanisms distinct to or shared by mGluR1α and mGluR5 in CA1 pyramidal neurons, the Group I mGluRs are associated with several downstream pathways and signaling mechanisms involved in both memory and LTP. These include release of Ca^{2+} from internal stores and increase in $[Ca^{2+}]i$ via IP3R signaling; potentiation of NMDA receptor currents through Src kinase; and activation of PKC and the ERK signaling cascade. **B.** A possible mechanism underlying memory and LTP enhancement in Sin3aNH mutant mice: Neuronal deletion of *Sin3a* is accompanied by changes in expression of several HDAC-regulated genes encoding synaptic proteins, including increased *Homer1* and *Cdk5* expression. Increased levels of long-form Homer1b/c facilitate recruitment and clustering of mGluR5 at the postsynaptic density, while increased Cdk5 leads to greater levels of phosphorylation of the C-terminal tails of mGluRs, enhancing mGluR5/long-form Homer1 interaction and contributing further to localization of mGluR5 at the PSD. The increase in synaptically-located mGluR5 could contribute to enhanced LTP through increased $[Ca^{2+}]i$ and increased signaling via downstream pathways, and reduce the necessity of mGluR1α signaling at the synapse.

Figure 3.9. Phospho-ERK immunostaining in hippocampal sections following contextual fear conditioning. Representative images of hippocampal areas CA3 and DG in sections from control mice **(A, C)** and Sin3aNH **(B, D)** that were immunostained for phospho-ERK1/2. Scale bars indicate 0.1 mm. Quantification of phospho-ERK

positive cells in these regions found no significant effect of genotype (n=10 for each group; CA3 t-test, $p = 0.46$; DG, t-test, $p = 0.0864$).

Figure 3.10. L-LTP is not affected by conditional neuronal *Sin3a* deletion. Four trains of stimulation spaced five minutes apart (indicated by arrows) induces L-LTP of similar magnitude in both wild type control slices and slices taken from Sin3aNH mice (controls, n = 5, avg. fEPSP slope = 143.1 ± 9.22%; Sin3aNH, n = 6, avg. fEPSP slope = 146.59 ± 19.01%; repeated measures ANOVA: genotype, $F_{(1,9)} = 0.028$, $p = 0.879$).

Figure 3.11. Reduction in SIN3A affects the role of mGluR signaling in hippocampal LTP. A. In control animals, LTP induced by four spaced trains of stimulation is impaired by the administration of the mGluR1α antagonist LY367385 or the mGluR5 antagonist (controls + veh, n = 6, avg. fEPSP slope = 182.24 ± 4.67%; controls + LY367385, n = 5, avg. fEPSP slope = 121.82 ± 20.67%; controls + MPEP, n = 5, avg. fEPSP slope = 120.96 ± 6.56%; repeated measures ANOVA: genotype, $F_{(1,28)} = 17.894$, $p = 0.00023$; treatment, $F_{(2,28)} = 20.453$, $p = 0.000003$; genotype × treatment interaction, $F_{(2,28)} = 7.924$, $p = 0.0019$; Tukey's *post-hoc* test, controls + vehicle vs. controls + MPEP, $*p = 0.018$; controls + vehicle vs. controls + LY367385, $**p = 0.008$). **B.** In Sin3aNH slices, application of an mGluR5 antagonist impairs spaced 4-train LTP, while antagonizing mGluR1α has no effect (Sin3aNH + veh, n = 5, avg. fEPSP slope = 192.29 ± 17.4%; Sin3aNH + LY367385, n=6, avg. fEPSP slope = 213.12 ± 7.62%; Sin3aNH + MPEP, n = 7, avg. fEPSP slope = 116.06 ± 10.94%; Tukey's *post-hoc* test, Sin3aNH+ vehicle vs. Sin3aNH + MPEP, $***p = 0.0002$; Sin3aNH vehicle vs. Sin3aNH + LY367385, $p = 0.999$; Sin3aNH + LY367385 vs. Sin3aNH + MPEP, $***p = 0.0002$).

Figure 3.12. Reduction in SIN3A affects the requirement for type I mGluR signaling during plasticity. Synaptic plasticity engages both major type I mGluRs in the hippocampus, leading to influx of calcium from intracellular and extracellular sources, activation of downstream calcium-responsive kinase cascades, and transcriptional activation. Both type mGluR1 and mGluR5 activate common downstream calcium signaling mechanisms. Blockade of mGluR1 in control animals leads to reduced overall calcium influx, reduced kinase activity, and failure of transcriptional activation necessary for late phase plasticity. In Sin3aNH animals, expanded signaling through mGluR5 is able to support signal transduction and engage transcription in the presence of mGluR1 blockade. Because mGluR5 is the more abundant type I receptor in the hippocampus, blockade of mGluR5 leads to insufficient pathway activation and impaired synaptic plasticity in both control and Sin3aNH animals.

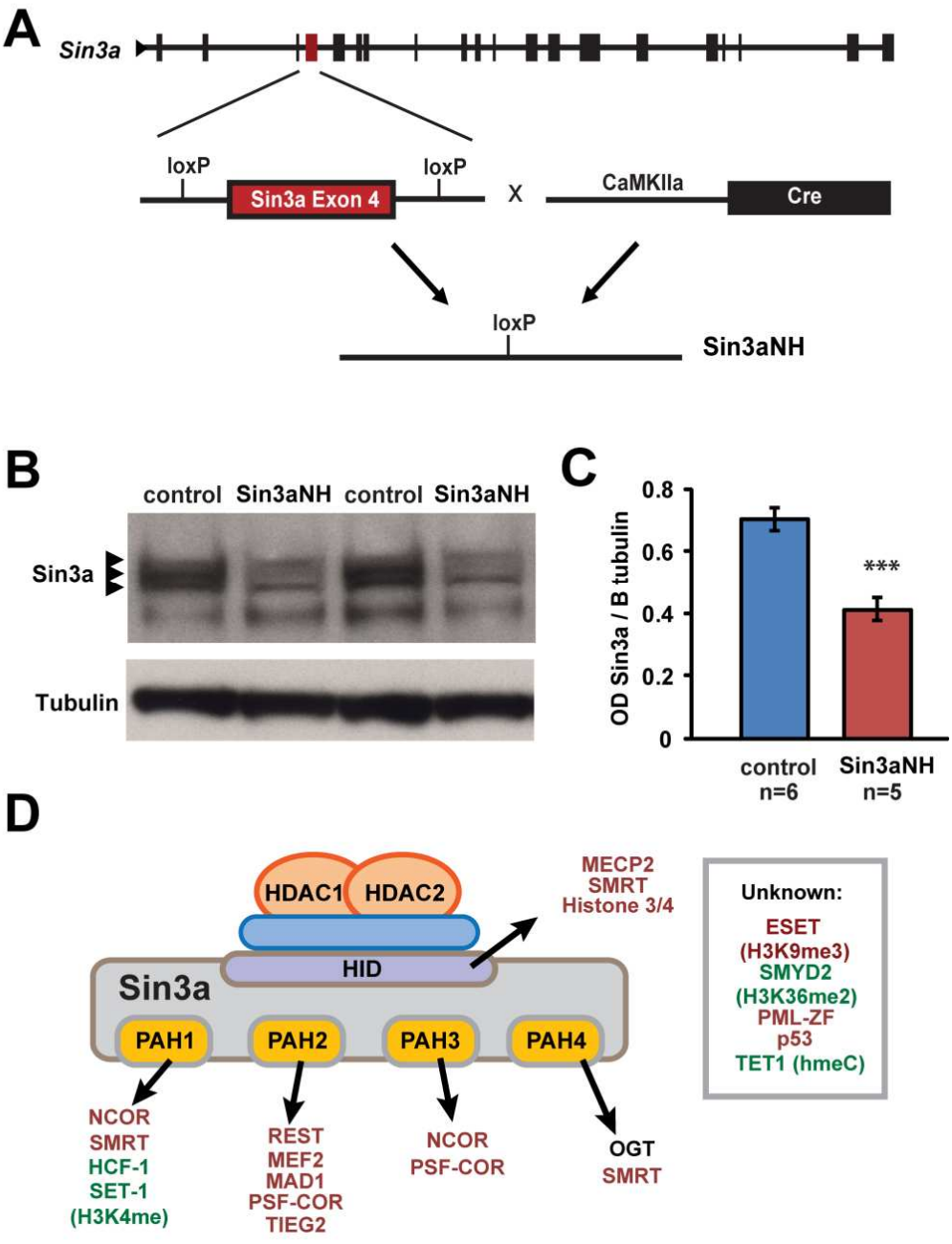
A
Sin3a
loxP
Sin3a Exon 4
loxP
X
CaMKIIa
Cre
loxP
Sin3aNH
B
control
Sin3aNH
control
Sin3aNH
Sin3a
Tubulin
C
OD Sin3a / B tubulin
0.8
0.6
0.4
0.2
0
***
control
n=6
Sin3aNH
n=5
D
HDAC1
HDAC2
HID
Sin3a
PAH1
PAH2
PAH3
PAH4
MECP2
SMRT
Histone 3/4
Unknown:
ESET
(H3K9me3)
SMYD2
(H3K36me2)
PML-ZF
p53
TET1 (hmeC)
NCOR
SMRT
HCF-1
SET-1
(H3K4me)
REST
MEF2
MAD1
PSF-COR
TIEG2
NCOR
PSF-COR
OGT
SMRT

Figure 3.1

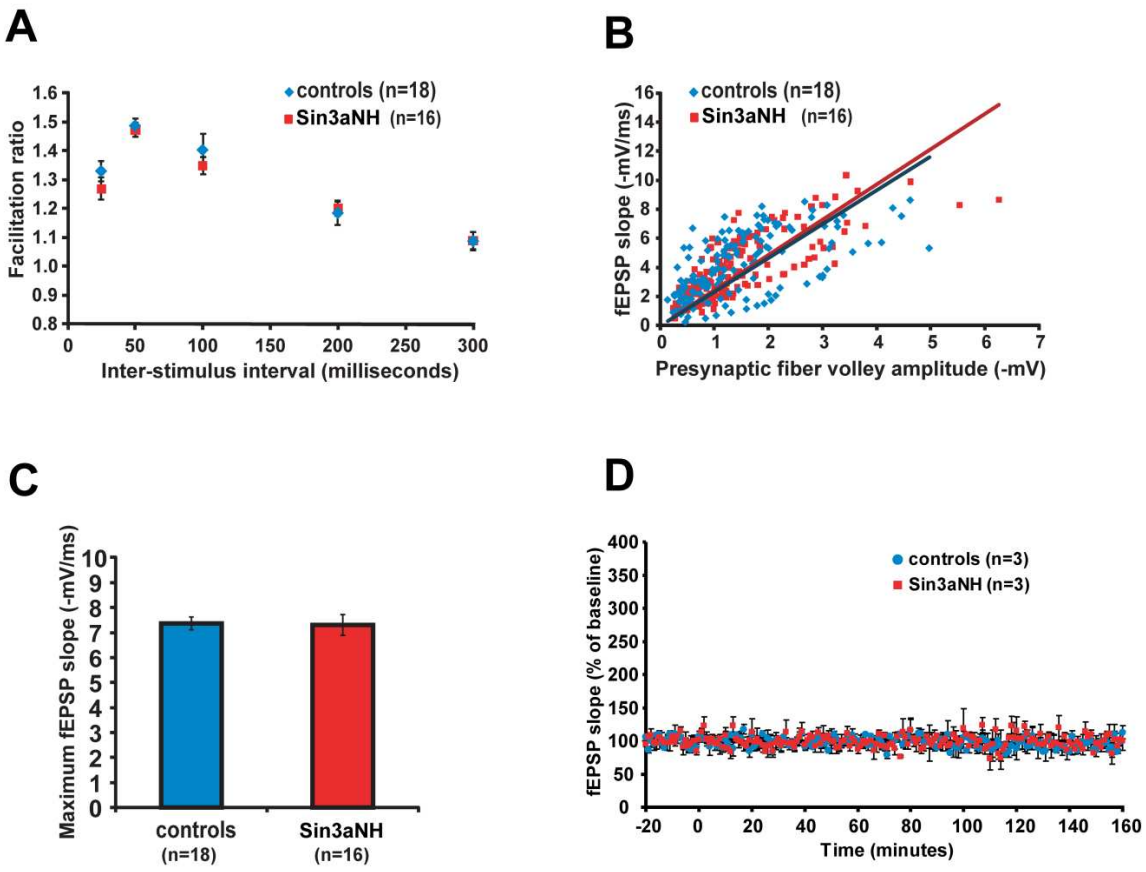
A
controls (n=18)
Sin3aNH (n=16)
Facilitation ratio
Inter-stimulus interval (milliseconds)
B
controls (n=18)
Sin3aNH (n=16)
fEPSP slope (-mV/ms)
Presynaptic fiber volley amplitude (-mV)
C
Maximum fEPSP slope (-mV/ms)
controls
(n=18)
Sin3aNH
(n=16)
D
controls (n=3)
Sin3aNH (n=3)
fEPSP slope (% of baseline)
Time (minutes)

Figure 3.2

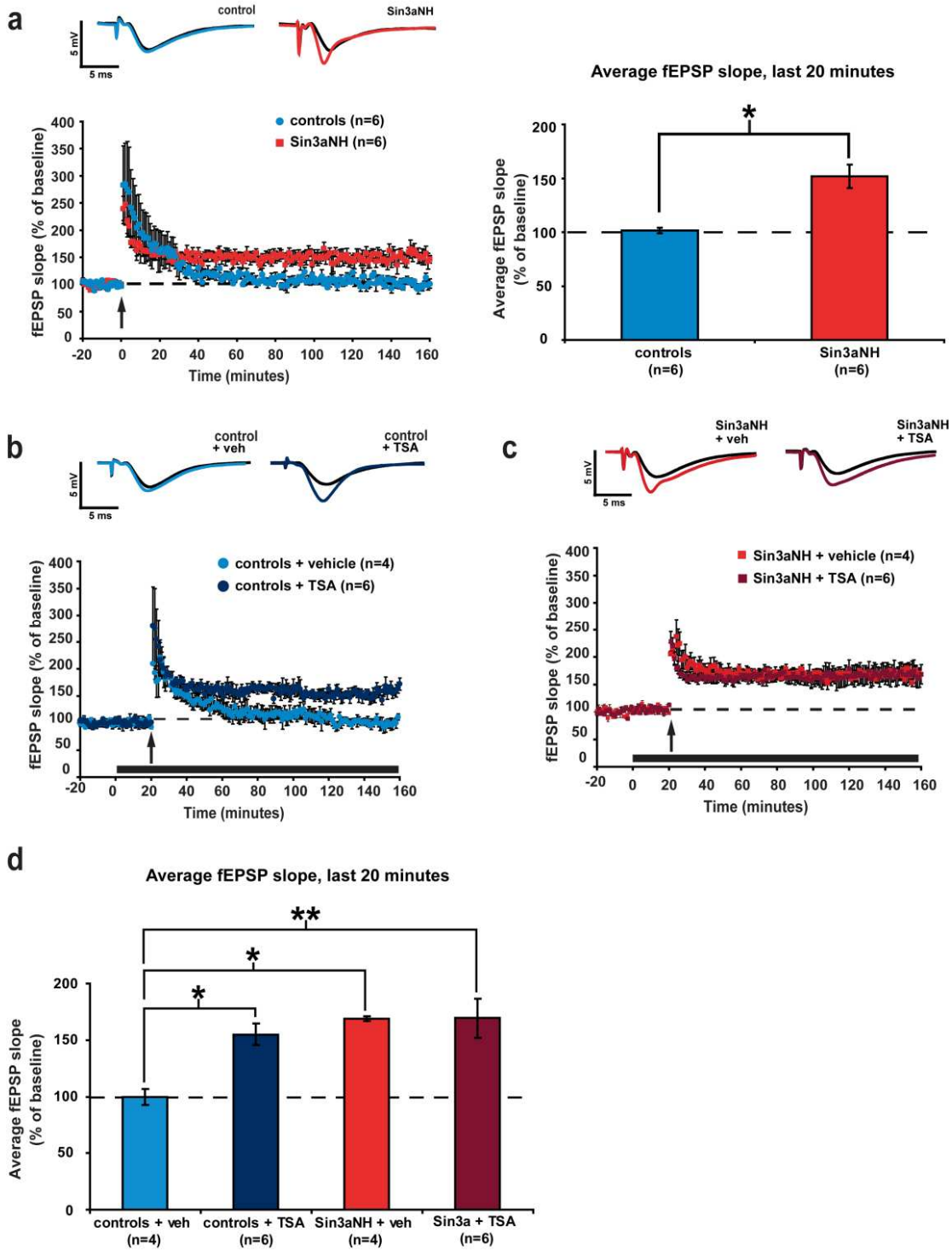
a
control
Sin3aNH
5 mV
5 ms
controls (n=6)
Sin3aNH (n=6)
fEPSP slope (% of baseline)
Time (minutes)
Average fEPSP slope, last 20 minutes
Average fEPSP slope (% of baseline)
controls (n=6)
Sin3aNH (n=6)
b
control + veh
control + TSA
controls + vehicle (n=4)
controls + TSA (n=6)
c
Sin3aNH + veh
Sin3aNH + TSA
Sin3aNH + vehicle (n=4)
Sin3aNH + TSA (n=6)
d
Average fEPSP slope, last 20 minutes
controls + veh (n=4)
controls + TSA (n=6)
Sin3aNH + veh (n=4)
Sin3a + TSA (n=6)

Figure 3.3

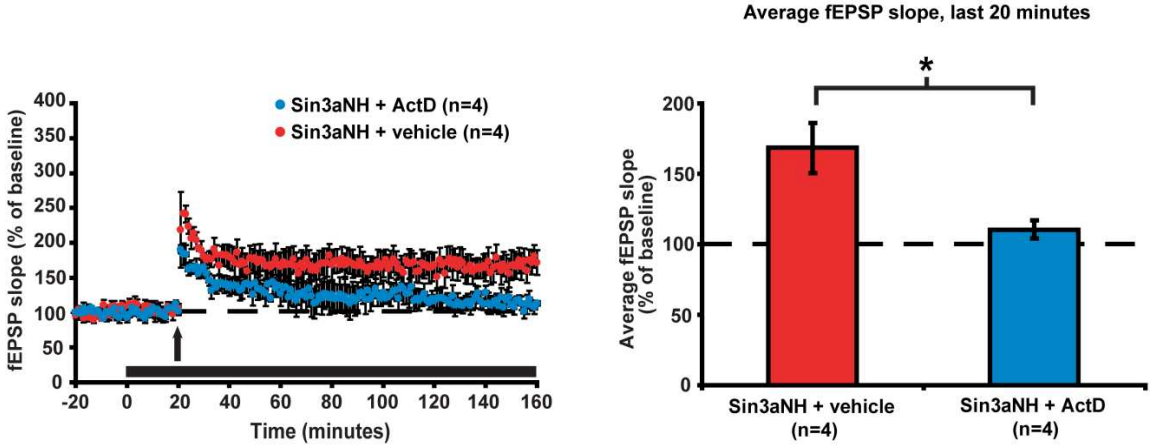
Sin3aNH + ActD (n=4)
Sin3aNH + vehicle (n=4)
fEPSP slope (% of baseline)
Time (minutes)
Average fEPSP slope, last 20 minutes
Average fEPSP slope (% of baseline)
*
Sin3aNH + vehicle (n=4)
Sin3aNH + ActD (n=4)

Figure 3.4

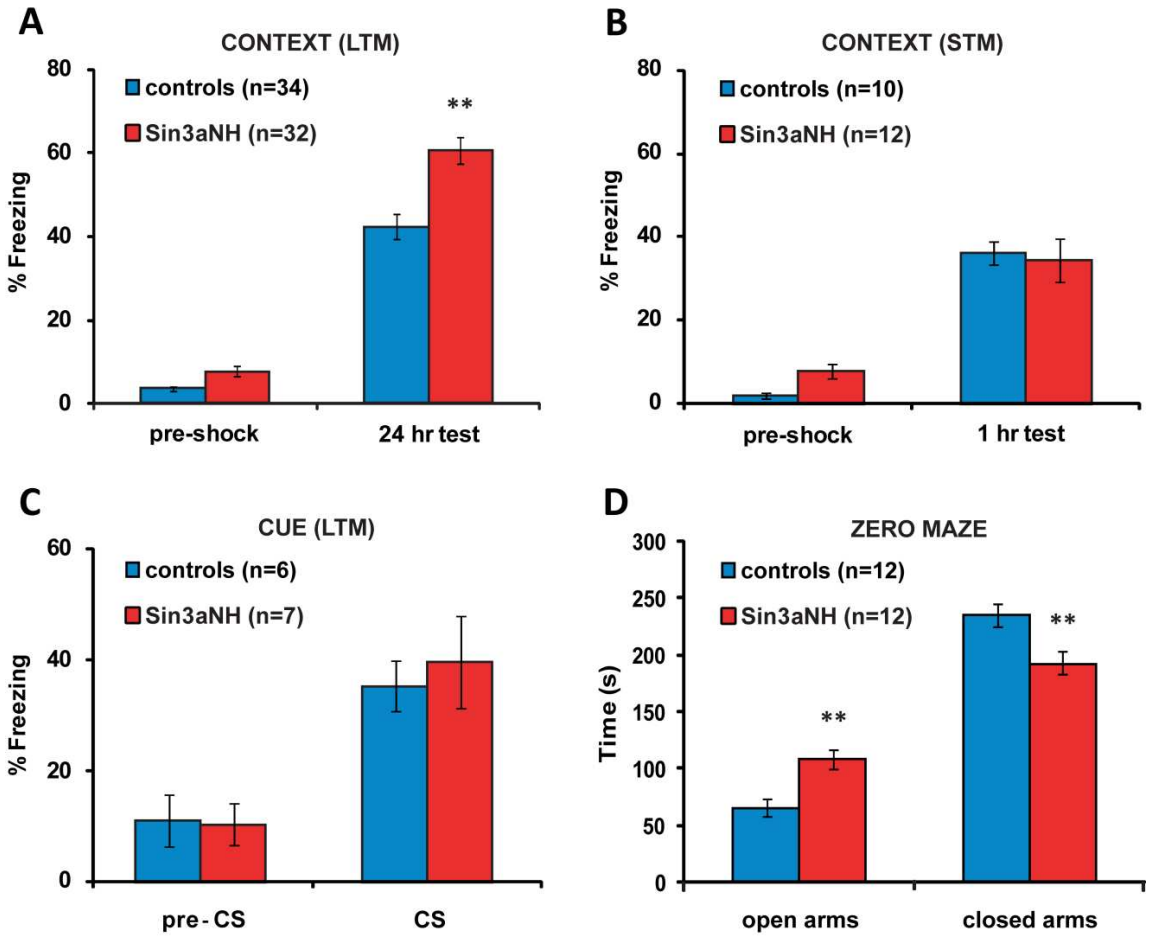
A
CONTEXT (LTM)
controls (n=34)
Sin3aNH (n=32)
**
% Freezing
80
60
40
20
0
pre-shock
24 hr test
B
CONTEXT (STM)
controls (n=10)
Sin3aNH (n=12)
% Freezing
80
60
40
20
0
pre-shock
1 hr test
C
CUE (LTM)
controls (n=6)
Sin3aNH (n=7)
% Freezing
60
40
20
0
pre-CS
CS
D
ZERO MAZE
controls (n=12)
Sin3aNH (n=12)
**
**
Time (s)
300
250
200
150
100
50
0
open arms
closed arms

Figure 3.5

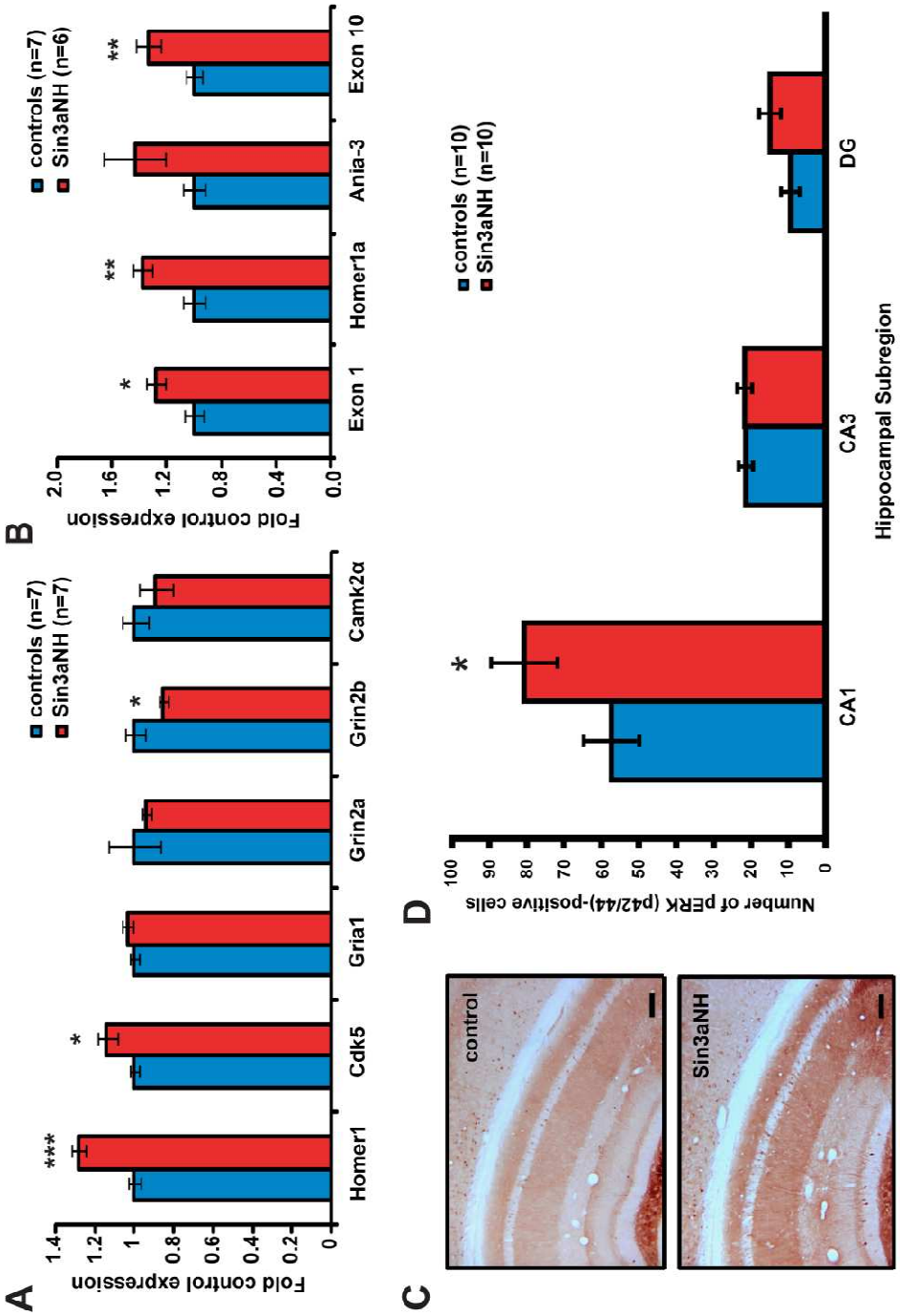
A
controls (n=7)
Sin3aNH (n=7)
Fold control expression
1.4
1.2
1
0.8
0.6
0.4
0.2
0
***
*
*
Homer1
Cdk5
Gria1
Grin2a
Grin2b
Camk2α
B
controls (n=7)
Sin3aNH (n=6)
Fold control expression
2.0
1.6
1.2
0.8
0.4
0.0
*
**
**
Exon 1
Homer1a
Ania-3
Exon 10
C
control
Sin3aNH
D
controls (n=10)
Sin3aNH (n=10)
Number of pERK (p42/44)-positive cells
100
90
80
70
60
50
40
30
20
10
0
*
CA1
CA3
DG
Hippocampal Subregion

Figure 3.6

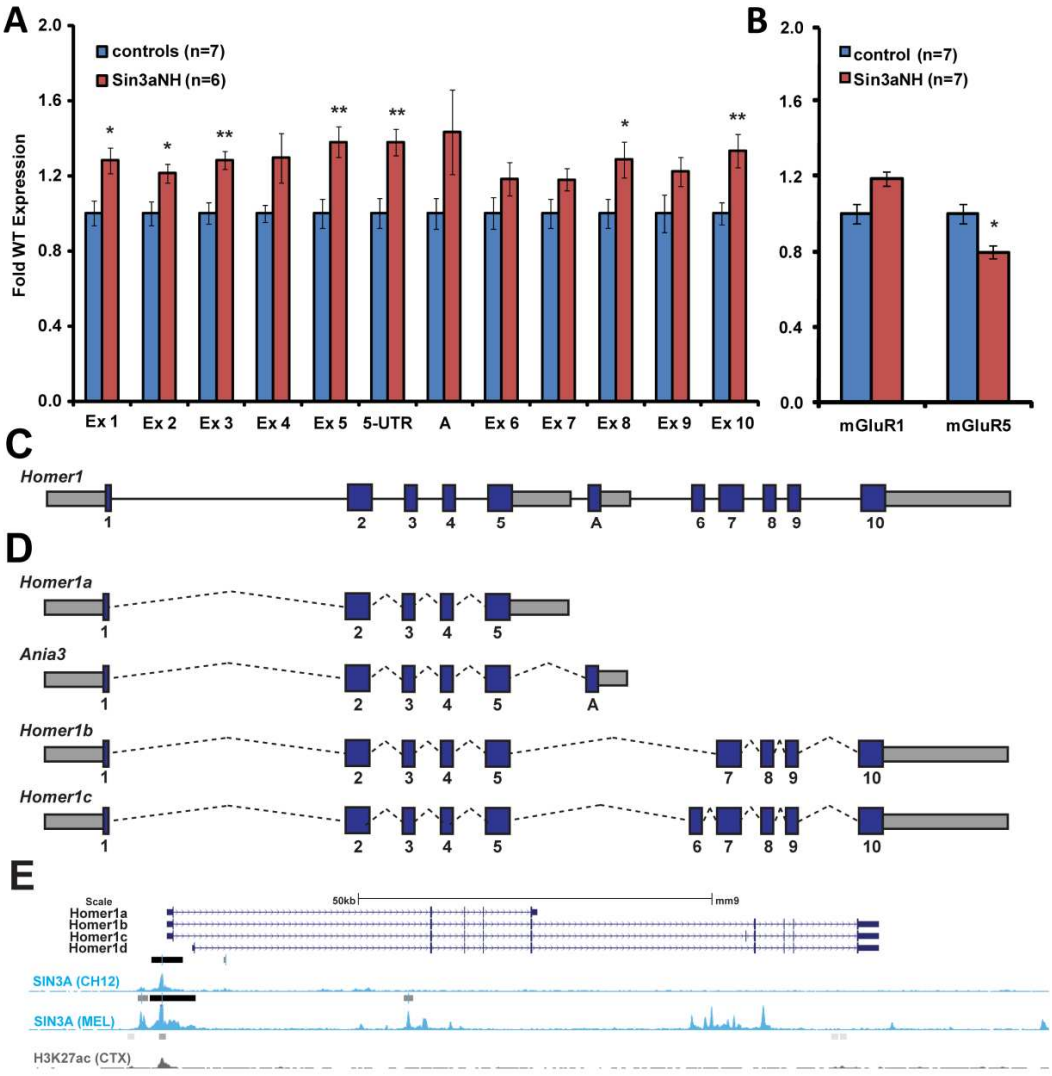
A
B
C
D
E
controls (n=7)
Sin3aNH (n=6)
Fold WT Expression
Ex 1
Ex 2
Ex 3
Ex 4
Ex 5
5-UTR
A
Ex 6
Ex 7
Ex 8
Ex 9
Ex 10
control (n=7)
Sin3aNH (n=7)
mGluR1
mGluR5
Homer1
Homer1a
Ania3
Homer1b
Homer1c
Scale
50kb
mm9
Homer1a
Homer1b
Homer1c
Homer1d
SIN3A (CH12)
SIN3A (MEL)
H3K27ac (CTX)

Figure 3.7

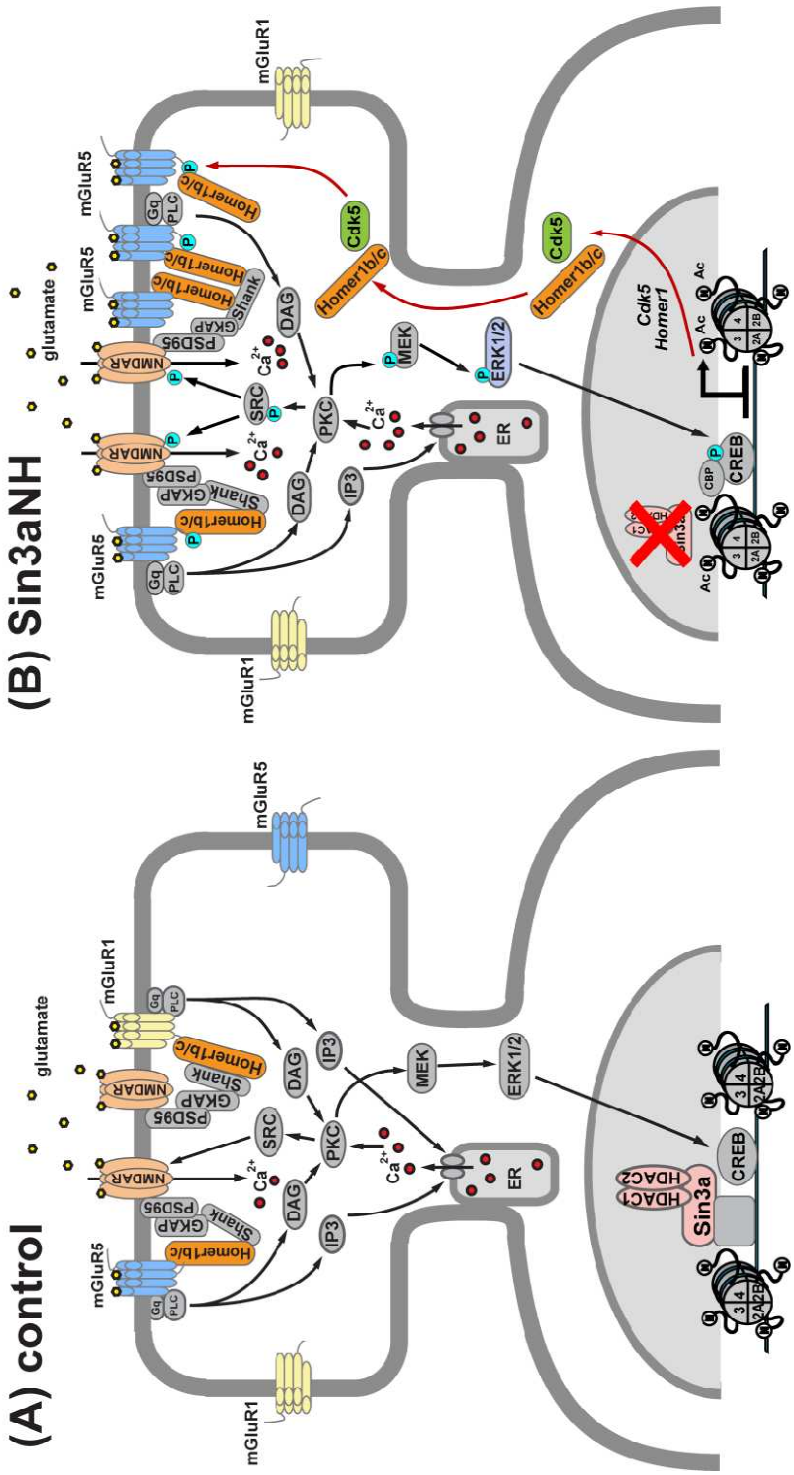
(B) Sin3aNH
(A) control
glutamate
mGluR1
mGluR5
Gq
PLC
Homer1b/c
Shank
GKAP
PSD95
NMDAR
Ca2+
SRC
DAG
IP3
PKC
ER
MEK
ERK1/2
Cdk5
Homer1b/c
Cdk5
Homer1
CBP
CREB
HDAC1
HDAC2
Sin3a
Ac
2A
2B
3
4

Figure 3.8

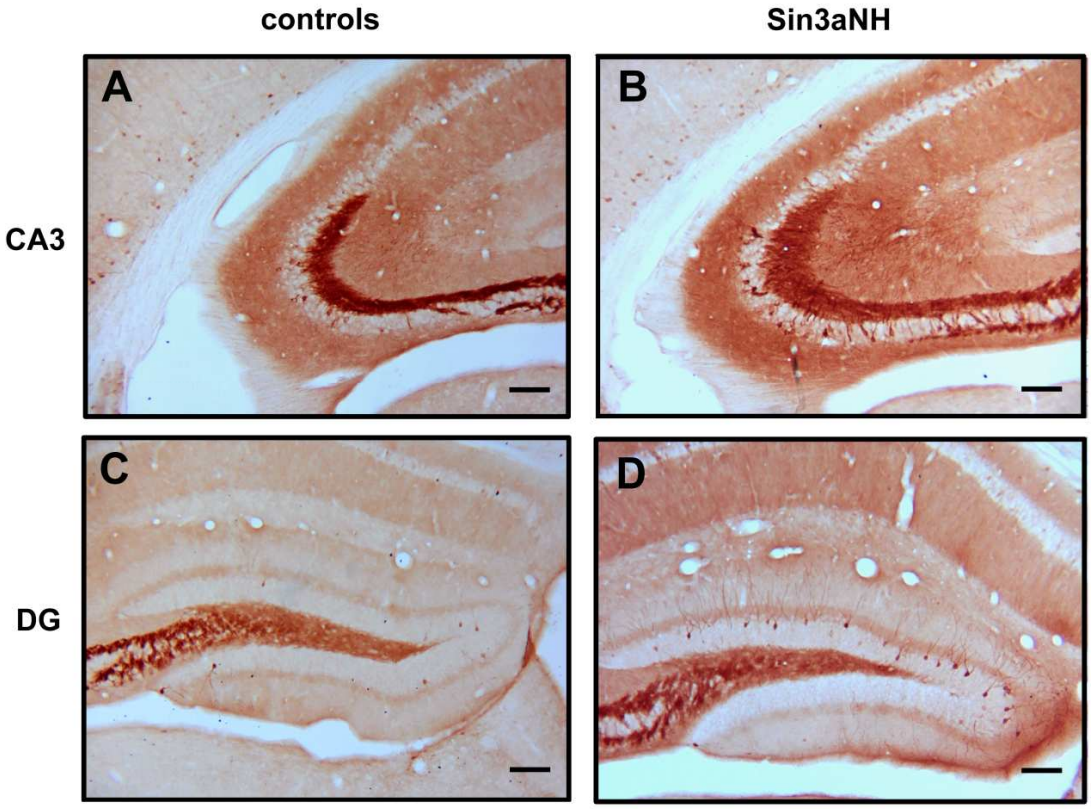

Figure 3.9

Average fEPSP slope, last 20 minutes
Average fEPSP slope, (% of baseline)
200
150
100
50
0
controls (n=5)
Sin3aNH (n=6)
fEPSP slope (% of baseline)
400
350
300
250
200
150
100
50
0
-20
0
20
40
60
80
100
120
140
160
Time (minutes)
Sin3aNH (n=6)
controls (n=5)

Figure 3.10

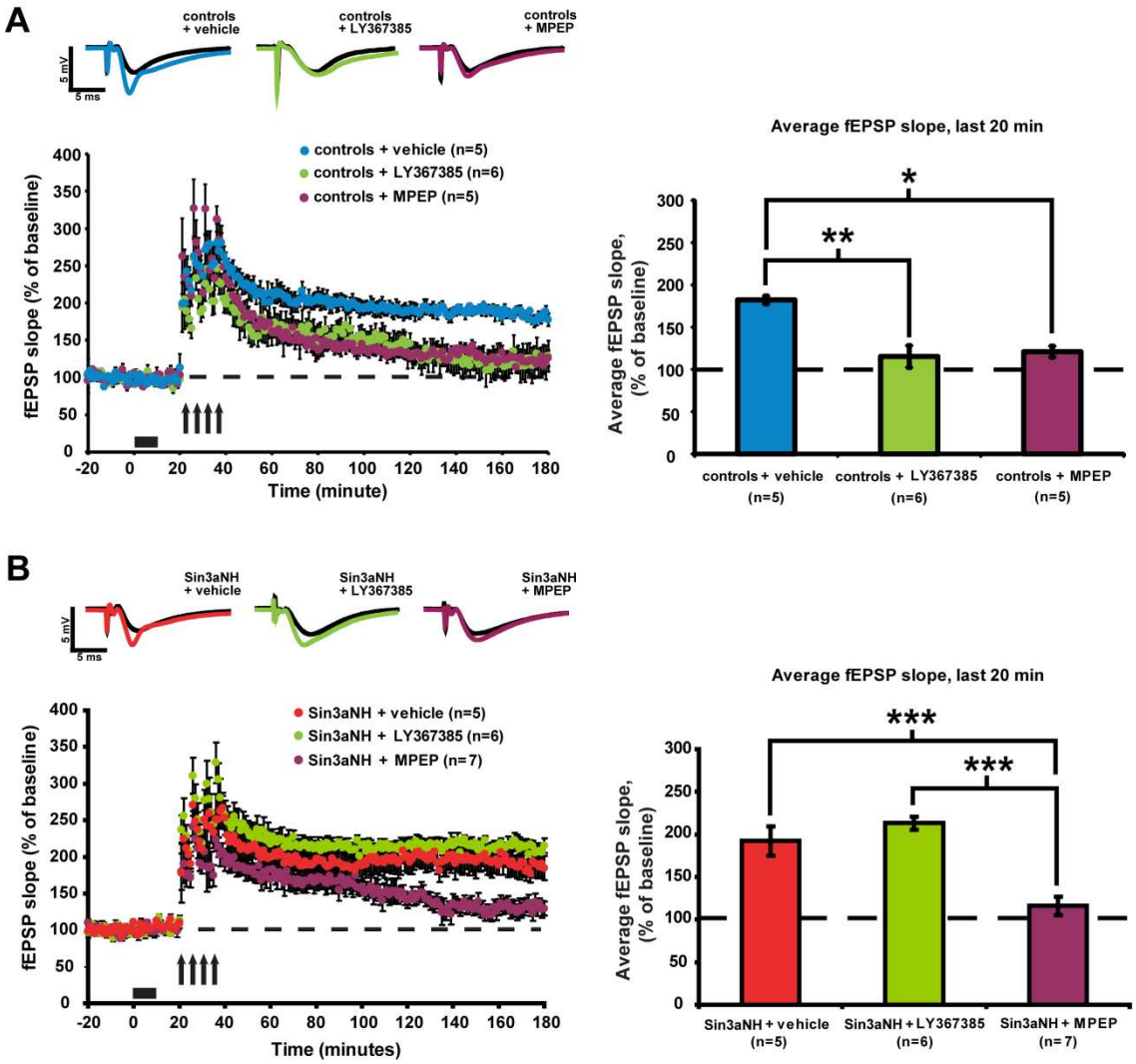
A
controls + vehicle
controls + LY367385
controls + MPEP
5 mV
5 ms
controls + vehicle (n=5)
controls + LY367385 (n=6)
controls + MPEP (n=5)
fEPSP slope (% of baseline)
Time (minute)
Average fEPSP slope, last 20 min
Average fEPSP slope, (% of baseline)
*
**
controls + vehicle (n=5)
controls + LY367385 (n=6)
controls + MPEP (n=5)
B
Sin3aNH + vehicle
Sin3aNH + LY367385
Sin3aNH + MPEP
5 mV
5 ms
Sin3aNH + vehicle (n=5)
Sin3aNH + LY367385 (n=6)
Sin3aNH + MPEP (n=7)
fEPSP slope (% of baseline)
Time (minutes)
Average fEPSP slope, last 20 min
Average fEPSP slope, (% of baseline)
***
***
Sin3aNH + vehicle (n=5)
Sin3aNH + LY367385 (n=6)
Sin3aNH + MPEP (n=7)

Figure 3.11

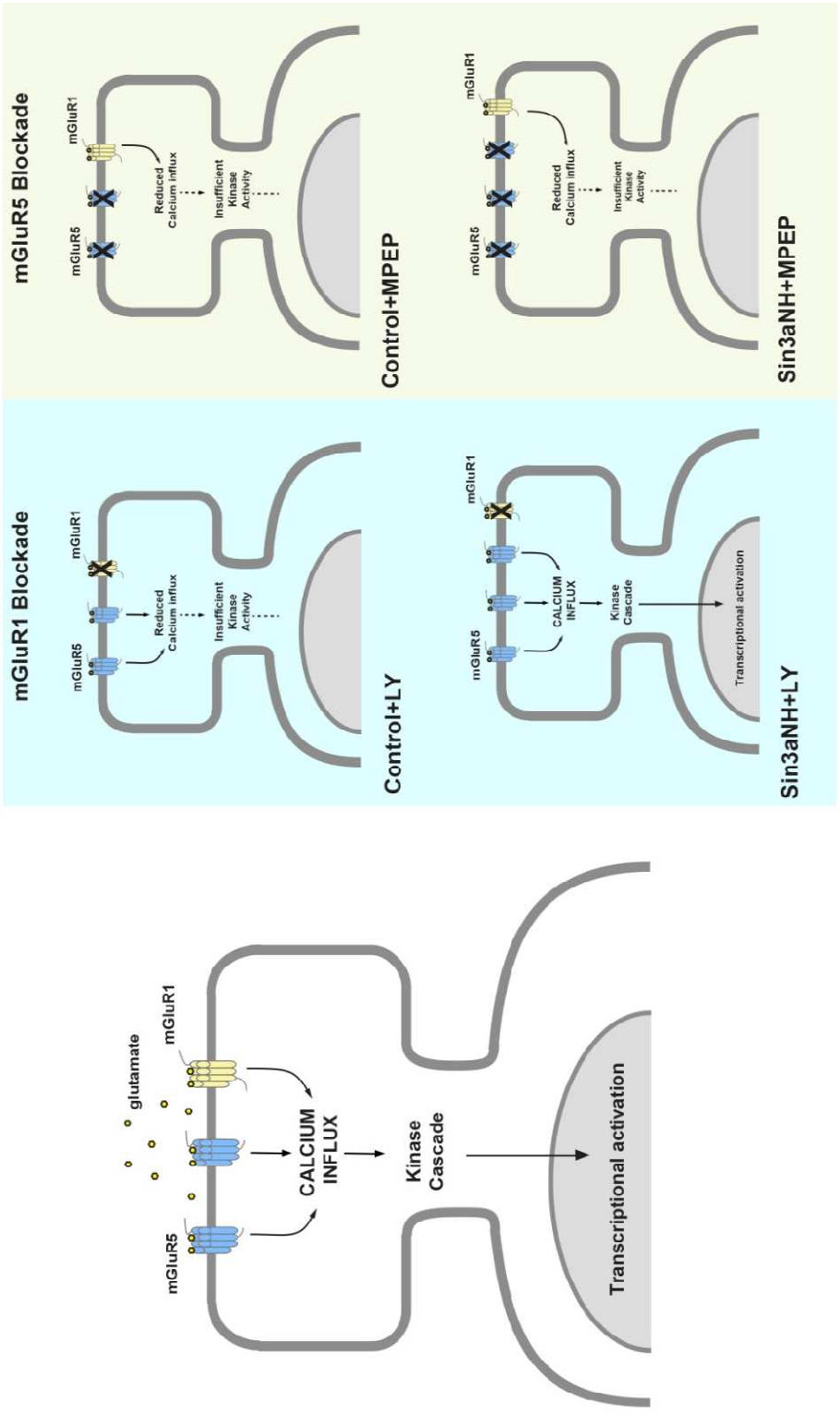
mGluR5 Blockade
mGluR1
mGluR5
Reduced Calcium influx
Insufficient Kinase Activity
Control+MPEP
Sin3aNH+MPEP
mGluR1 Blockade
Control+LY
Sin3aNH+LY
CALCIUM INFLUX
Kinase Cascade
Transcriptional activation
glutamate

Figure 3.12

ACKNOWLEDGEMENTS,

H. Schoch was supported by NIH Training Grant T32-MH017168. M. Bridi was supported by a predoctoral NRSA fellowship from the NINDS (1F31NS079019). The work was also supported by NIH Grant R01-MH087463 to T. Abel. R. DePinho kindly provided the $Sin3a^{LoxP}$ mouse line.

AUTHOR CONTRIBUTIONS

This chapter was written by H. Schoch and M. Bridi, with suggestions from T. Abel, C. Florian, J. Hawk, and K.P Giese. T. Abel, M. Bridi, H. Schoch, J. Hawk and C. Florian conceived and designed the experiments. M. Bridi conducted gene expression experiments and all electrophysiology experiments. H. Schoch conducted mouse behavioral tests, gene expression experiments, and Western blots. C. Florian conducted mouse behavior tests. Shane Poplawski conducted gene expression experiments. R. Havekes conducted the Erk experiment. T. Abel directed the studies. We thank Dr. K. P. Giese, L. Peixoto, and J.Tudor for discussions and critically reading the manuscript.

This chapter is under revision at Journal of Clinical Investigation: Bridi M, Schoch H*, Florian C, Poplawski SG, Hawk JD, Giese KP, Havekes R, Abel T. "Transcriptional co-repressor SIN3A regulates hippocampal synaptic plasticity via Homer1/mGluR5 signaling"*

CHAPTER 4: COGNITIVE DEFICITS IN MICE EXPRESSING CRE RECOMBINASE IN FOREBRAIN EXCITATORY NEURONS.

Abstract

Cre recombinase is the predominant site-specific recombinase tool for conditional gene deletion approaches in transgenic rodent models. Phenotypes associated with off-target Cre recombinase activity have been described in cultured cells and peripheral tissues, but Cre-specific phenotypes have not been identified or explored in the brain. Here, we find sex-specific contextual fear memory deficits in transgenic mice expressing Cre in forebrain excitatory neurons.

4.1 Introduction

Conditional gene deletion systems have revolutionized genetic research across multiple disciplines. The bacteriophage P1 site-specific recombination system, Cre-loxP, has developed into the primary tool for viral and transgene-mediated conditional gene deletion in rodents and has been used in multiple other research organisms (Schmidt et al. 2000, Sauer 1991, Coppoolse et al. 2003, Siegel and Hartl 1996, Thummel et al. 2005, Abremski and Hoess 1984). The double-stranded DNA recombinase Cre is required to transition the phage genome from the linear dsDNA contained in the viral particle to a circular plasmid in the bacterial host. Cre binds the terminal loxP recognition sites of the linearized genome, and induces a recombination event to yield a circular genome and ligated linear end fragments (Abremski and Hoess, 1984). To adapt this system for conditional gene deletion in other organisms, homotypic loxP sites sharing the same orientation are inserted into gene loci in positions flanking exon sequences (**Fig. 1.1A)**. Upon binding to Cre, a crossover event is induced such that the intervening sequence between the loxP sites is excised into a circular loop, and the cut ends of parent strand are ligated (Hoess and Abremski 1984, **Fig. 1.1**). Alternately, heterotypic sites with opposite orientations can be used to induce inversion of the

targeted sequence (Oberdoerffer et al. 2003) Expression of Cre recombinase under a cell type-specific promoter allows for tissue restricted deletion events.

The success of Cre as a research tool hinges on specificity in acting on its intended target, but it has long been known that cryptic sequences similar to loxP sequences can be found throughout yeast, plant, and mouse genomes, and that these cryptic sites are active and undergo Cre-mediated recombination (Sauer 1992, Coppoolse et al. 2003, Thyagarajan and Calos 2000, Semprini et al. 2007). Studies of off-target effects of Cre-mediated recombination have uncovered increased cell cycle arrest and increased incidence of double strand breaks, chromosome fusions, and aneuploidy in cultured mouse embryonic fibroblasts (MEFs) (Loonstra et al. 2001). Genotoxic effects of Cre expression have also been observed in mouse models. Chromosomal aberrations and sterility were fully penetrant in transgenic mice expressing Cre in post-meiotic spermatids, indicating that DNA damage and chromosome instability require recombinase activity, and occur in non-dividing tissues (Schmidt et al. 2000). In addition to genome instability, Cre activity has been linked to changes in the cAMP/protein kinase A (PKA) signaling pathway in MEFs. Increased expression of the PKA inhibitor PKI, decreased phosphorylation of PKA targets p40/42 ERK and CREB, and altered expression of cAMP/CREB regulated genes *Nur77, Nurr1, Il-6*, and *Dusp1* were observed in Cre expressing MEFs (Gangoda et al. 2012).

Hippocampal learning and memory processes are sensitive to changes in PKA signaling and cell division (Abel et al. 1997, Bourtchouladze et al. 1998). Disruption of adult neurogenesis and PKA activity have been linked to deficits in contextual fear memory (Saxe et al. 2006, Winocur et al. 2006). Based on these potential off-target effects of Cre, we examined contextual fear memory in mice expressing Cre in forebrain neurons.

4.2 Methods

Mouse lines

Transgenic mice expressing Cre recombinase under the control of CaMKIIα promoter sequence were bred from three lines. CaMKIIα-Cre L7ag#13 (Dragatsis and Zeitlin 2000), CaMKIIα-Cre transgene R4ag#11, and CaMKIIα-Cre T29-1 (Tsien et al. 1996), each with more than 9 generations of backcrossing the CaMKIIα-Cre transgene into C57BL/6J. CaMKIIα-Cre males from each line were bred to C57/BL6j wild-type females to produce CaMKIIα-Cre hemizygous mice and non-transgenic wild-type littermates.

Genotyping was performed using PCR with allele-specific primers. To identify mice bearing CaMKII-Cre transgenes, PCR was performed with the following primers: Cre1 5'-CTG CCA CGA CCA AGT GAC AGC-3', Cre2 5'-CTT CTC TAC ACC TGC GGT GCT-3', Bglob1 5'-CCA ATC TCC TCA CAC AGG ATA GAG AGG GCA GG-3', Bglob2 5'-CCT TGA GGC TGT CCA AGT GAT TCA GGC CAT CG-3'. Thermal cycling parameters were as follows: 94°C for 3 min, [94°C for 45 s, 61°C for 45 s, 72°C for 60 s] x 30 cycles, 72°C for 10 min. Mice were maintai ned under standard conditions consistent with National Institute of Health guidelines for animal care and use, and all procedures were approved by the Institutional Animal Care and Use Committee of the University of Pennsylvania. Mice were maintained on a 12 hr light-dark cycle and provided with food and water in their home cages *ad libitum.* Animals were group housed in cages of 2-5 littermates except for fear conditioning experiments. For fear conditioning, animals were moved from group housing to single housing 1 week prior to training. Behavioral testing was conducted on 2- to 6-month old male and female

animals during the light portion of the cycle. Experimenters were blind to the genotypes of the mice during collection of behavioral data.

Immunohistochemistry

Transcardial perfusions and immunohistochemical stainings were conducted as previously described (Havekes et al., 2012). Briefly, coronal sections were incubated with rabbit anti-Cre (gift from C. Kellendonck), and developed using avidin-biotin horseradish peroxidase complex (ABC kit; Vector Laboratories, 1:500) and stained with 0.02% diaminobenzidine (DAB). Staining was initiated with 100uL 0.1% hydrogen peroxide, and terminated with multiple rinses in PBS.

Fear conditioning

Fear conditioning was conducted as previously described (Hawk et al., 2012). For contextual conditioning, naïve 2- to 6-month old male and female CaMKIIα-Cre mice and wild-type siblings were placed in a novel training chamber for 180 s and a single 2 s, 0.75 mA foot shock was administered after 148 s. Contextual fear testing was conducted 1 hr or 24 hrs after training, by re-exposing the animals to the trained context for 5 min. Freezing behavior during contextual training and testing was scored by computer using FreezeScan software (Clever Systems). For all behavioral tasks, testing order was designed so that mice of different sexes were not in the testing room at the same time. Testing chambers were thoroughly cleaned between each session to minimize odor cues. Results are presented as group means with SEM. Animals with responses two standard deviations above or below the group mean were excluded from the analysis as outliers. Groups were compared across test phases using two-way ANOVA, with

significance levels of $p < 0.05$. Genotype effects within phases were compared using unpaired t-tests.

4.3 Results

4.3.1 Forebrain expression of Cre recombinase in transgenic mouse lines.

Expression patterns of CaMKIIα Cre transgenic mouse lines differ among animals with the same transgene insert. CaMKIIα L7 Cre and CaMKIIα R4 Cre lines were created using the same gene construct (Dragatsis and Zeitlin, 2000), but are derived from different founder animals. We found differential expression among the L7 and R4 lines in brain regions engaged by the contextual fear task (Phillips and LeDoux. 1992). In the L7 line, Cre is expressed more widely throughout the hippocampus, including areas CA1, CA3, and the dentate gyrus (DG) **(Fig. 4.1A)**. In the amygdala, there is widespread expression of Cre throughout the BLA in L7 Cre animals **(Fig. 4.1B)**. In the R4 line, Cre is expressed in CA1 and DG in the hippocampus, but is not expressed in CA3 **(Fig. 4.1C)**. In the BLA, Cre is expressed widely in R4 animals **(Fig. 4.1D)**. In the T29-1 line, Cre is expressed in all subregions of the hippocampus in adult animals (Zeng et al. 2001). In the amygdala, Jackson Laboratories uses a Rosa 26 flox β galactosidase reporter line to show sparse Cre activity that is not present in all cell types (Jackson Laboratories, http://cre.jax.org/Camk2a/Camk2a-creNano.html). Further characterization of Cre expression in the amygdala is needed to determine which cell populations actively express the transgene.

4.3.2 Line-specific contextual fear deficits in CaMKIIα Cre transgenic lines

Transgenic and viral Cre constructs used in studies of hippocampal function frequently contain a CaMKIIα promoter sequence to drive targeted recombination events in excitatory pyramidal cells in the hippocampus. To determine whether expression of Cre

recombinase throughout the forebrain affects basal performance in hippocampus-dependent learning tasks, we bred mice that were hemizygous for a CaMKIIα Cre transgene and lacked any targeted floxed alleles. Thus we have Cre mice and their non-transgenic wild-type siblings for long-term memory tests in the contextual fear conditioning task. We tested three lines of transgenic CaMKIIα Cre mice: L7, R4, and T29-1.

CaMKIIα L7 Cre mice show mild memory deficits when tested for long-term contextual fear memory 24hrs after conditioning. Baseline freezing levels prior to conditioning is not different in L7 Cre animals compared to non-transgenic WT siblings, but L7 animals show reduced freezing when they are re-exposed to the conditioned context 24hrs after training (t-test: baseline $p<0.96$, 24hr test $*p<0.04$. **Fig. 4.2A**). The observed difference is small and does not hold up to comparisons of genotypes across the two phases (two-way ANOVA: genotype $F_{1,116} = 3.19$, $p<0.08$, phase $F_{1,116} = 4.51$, $p<0.001$, genotype*phase $F_{1,116} = 2.98$, $p<0.09$). When the test session is examined more closely in one minute bins, L7 animals consistently show reduced freezing levels across all bins (rmANOVA: genotype $F_{1,232} = 4.51$, $p<0.04$, minute $F_{1,232} = 6.75$, $p<0.001$, genotype*minute $F_{1,232} = 0.34$, $p<0.85$, **Fig. 4.2B**). When we separate animals by sex, we find that the Cre group difference in freezing levels is strongly driven by reduced freezing levels in male L7 animals (two-way ANOVA: genotype $F_{1,73} = 2.95$, $p<0.1$, phase $F_{1,73} = 81.83$, $p<0.001$, genotype*phase $F_{1,73} = 3.49$, $p<0.07$; ttest: baseline $p<0.91$, 24hr test $p<0.052$. **Fig. 4.2C**). In comparison, female L7 animals freeze at levels similar to wild-type females during the 24hr context test (two-way ANOVA: genotype $F_{1,86} = 0.66$, $p<0.43$, phase $F_{1,86} = 106.92$, $p<0.001$, genotype*phase $F_{1,86} = 0.58$, $p<0.46$; ttest: baseline $p<0.30$, 24hr test $p<0.47$. **Fig. 4.2D**).

When the CaMKIIα R4 Cre transgenic line was tested for contextual fear memory, severe deficits were observed in Cre transgenic mice. Prior to conditioning, baseline freezing levels in R4 mice is comparable to non-transgenic siblings, but when animals are tested for contextual memory, R4 mice exhibit significantly reduced freezing behavior (two-way ANOVA: genotype $F_{1,41} = 5.2$, $p<0.03$, phase $F_{1,41} = 116.53$, $p<0.001$, genotype*phase $F_{1,41} = 4.24$, $p<0.05$; t-test: baseline $p<0.76$, 24hr test *$p<0.03$. **Fig. 4.3A**). R4 Cre animals show reduced freezing early in the testing period, but this difference disappears over time (rmANOVA: genotype $F_{1,23} = 1.17$, $p<0.3$; minute $F_{1,4} = 2.41$, $p<0.055$; genotype*minute $F_{1,4} = 2.56$, $p<0.05$, **Fig. 4.3B**). Interestingly, the freezing deficits observed in the R4 Cre line are strikingly sex-dependent. Male R4 Cre animals show robust freezing deficits at the 24hr test compared to wild-type males (two-way ANOVA: genotype $F_{1,24} = 8.46$, $p<0.008$, phase $F_{1,24} = 116.34$, $p<0.001$, genotype*phase $F_{1,24} = 8.43$, $p<0.008$; t-test: baseline $p<0.76$, 24hr test *$p<0.02$. **Fig. 4.3C**). In contrast, contextual fear memory in female R4 cre mice is not impaired (two-way ANOVA: genotype $F_{1,13} = 0.71$, $p<0.42$; phase $F_{1,13} = X$, $p<0.001$; genotype*phase $F_{1,13} = 0.17$, $p<0.69$; t-test: baseline $p<0.53$, 24hr test $p<0.46$. **Fig. 4.3D**).

In CaMKIIα T29-1 Cre mice, contextual fear memory was found to be intact. No differences were seen between T29-1 and wild-type mice in baseline freezing levels, nor during the contextual memory test (two-way ANOVA: genotype $F_{1,84} = 1.47$, $p<0.23$, phase $F_{1,84} = 411.1$, $p<0.001$, genotype*phase $F_{1,84} = 3.3$, $p<0.08$; t-test: baseline $p<0.39$, 24hr test *$p<0.12$. **Fig. 4.4A**). Freezing levels in T29-1 mice were not significantly different from wild-type mice over the five minute test (rmANOVA: genotype $F_{1,168} = 2.74$, $p<0.11$; minute $F_{1,168} = 2.14$, $p<0.08$, genotype*minute $F_{1,168} = 0.57$, $p<0.69$, **Fig. 4.4B**). Male T29-1 mice exhibited slightly enhanced freezing during the test phase

(two-way ANOVA: genotype $F_{1,62} = 3.3$, $p<0.08$; phase $F_{1,62} = 389.63$, $p<0.001$; genotype*phase $F_{1,62} = 5.65$, $p<0.03$; t-test: baseline $p<0.26$, 24hr test *$p<0.09$. **Fig. 4.4C**). Freezing responses in female T29-1 animals are not different from wild-type responses (two-way ANOVA: genotype $F_{1,40} = 0.66$, $p<0.43$, phase $F_{1,40} = 230.59$, $p<0.001$, genotype*phase $F_{1,40} = 0.374$, $p<0.55$; t-test: baseline $p<0.69$, 24hr test $p<0.48$. **Fig. 4.4D**).

4.4 Discussion

The Cre-loxP system for conditional genetic manipulation can be a useful tool, but care should be taken in experimental design to avoid Cre lines with off-target phenotypes that compromise interpretation of the results. Here we showed that Cre expression alone impaired performance in the contextual fear task in a line-specific manner. Despite similar transgenic inserts (Dragatsis and Zeitlin 2000, Tsien et al. 1996), the Cre lines in this study show slightly different expression patterns that likely reflect a combination of copy number and insertion site effects that are specific to each line. All three transgenic lines express Cre in area CA1 of the hippocampus, but patterns of expression in hippocampal areas CA3 and DG, and in the cortex differ between lines (Tsien et al. 1996, Figure 1). Differential patterning and expression particularly in amygdala nuclei and in the hippocampal CA3 subregion, may underlie the line-specific nature of the memory deficits.

Specific molecular mechanisms underlying the effects of Cre recombinase activity on cells have not been studied in depth. Significant effects of Cre expression, such as aneuploidy and DNA-damage-induced cell cycle arrest, have been demonstrated in non-neuronal cells (Loonstra et al. 2001), and may underlie the memory deficits observed in L7 and R4 Cre mice. In all three lines studied, Cre expression is present to various

degrees in the dentate gyrus (**Fig. 4.1**; see also Jackson Laboratories), a site of adult neurogenesis. Experimental manipulations, such as x-irradiation, that induce genomic damage and arrest neurogenesis in the hippocampus lead to deficits in hippocampal memory, including contextual fear memory (Leuner et al. 2002, Saxe et al. 2006, Winocur et al. 2006, Drew et al. 2010). Titration experiments in non-neuronal cells showed that effects of Cre activity on proliferation are dose-dependent (Loonstra et al. 2001), suggesting that effects of insertion site and copy number on transgene expression levels will likely have a strong influence on whether Cre-specific phenotypes emerge.

In addition to effects on neurogenesis, chromosomal rearrangements and double strand breaks in mature neurons may disrupt epigenetic regulatory processes or interrupt coding sequences of genes critical for memory formation. In MEFs, Cre activity led to reduced expression of multiple genes linked to memory and plasticity in the hippocampus, including *Nur77*, *Nurr1*, Rgs2, and Pkib (Gangoda et al. 2012, Hawk and Abel. 2011, Han et al. 2006). Differences in DNA accessibility among cell types may also influence off-target recombination rates, leading to tissue-specific effects of Cre expression. Because Cre is a site-specific recombinase, gene loci situated in chromosomal regions with higher incidence of cryptic loxP sequences would be predicted to be more vulnerable to recombination events than gene loci in regions with fewer cryptic sequences. Bioinformatic analysis of predicted cryptic loxP sites in the murine genome could be used to predict vulnerability of individual gene loci to off-target Cre recombination events.

A candidate molecular signaling pathway likely altered by Cre expression in the brain is the cAMP/PKA pathway. MEFs expressing Cre exhibit increased expression of protein

kinase A inhibitor PKIβ, reduced PKA activity, reduced phosphorylation of PKA target protein CREB, and altered expression of genes involved in neuronal activity and memory (Gangoda et al. 2012). The specific mechanism by which Cre expression led to changes in PKA signaling in the study is not known, but it is dependent on the recombinase activity of Cre (Gangoda et al. 2012). Experimental reduction of PKA activity using inactive cAMP analogs or transgenic expression of dominant-negative regulatory subunits impairs contextual fear memory at the 24hr time point (Bourtchouladze et al. 1998). Cre-mediated reduction of PKA signaling raises serious concerns about studies that use Cre transgenic lines or viral delivery of Cre to study memory or circuitry in the hippocampus. Additional studies are needed to uncover and characterize molecular mechanisms underlying effects of Cre expression on gene regulation and PKA signaling pathways.

The male-specific cognitive deficits in CaMKIIα Cre L7 and R4 mice are the first example of sex differences in off-target effects of Cre expression. Sex differences in spatial memory have been described in humans and rodents (Mizuno and Giese 2010, Driscoll et al. 2005), but it is unclear how these mechanisms might be affected by Cre expression. In rodents, sex differences in fear conditioning have been linked to alterations in molecular signaling pathways and expression of memory-related genes, suggesting that the process of memory formation occurs differently in males and females at a molecular level (Gresack et al. 2009, Mizuno et al. 2006, Mizuno et al. 2007). Sex hormones have been shown to increase cAMP levels (Rosner et al. 1999), and regulate the expression of PKI genes (Frasor et al. 2006, Zhou et al. 2010), supporting a role for sex hormones in mediating the sex-specific effects of Cre expression on memory. Enhanced signaling through the estrogen receptor in female animals could potentially

attenuate the effects of Cre expression on PKA signaling by stimulating cAMP production, and decreasing expression of PKI. Future studies of molecular mechanisms underlying sex differences in memory formation, and mechanisms underlying effects of Cre expression in the brain will provide important insight into the process of memory consolidation and highlight important limitations inherent in Cre-mediated conditional recombination tools.

Chapter 4 Figure Legends

Figure 4.1. Expression pattern of CaMKIIα Cre transgenic lines in the hippocampus and amygdala. A. Cre is expressed strongly in CA1 and the DG, and lightly in CA3 in the dorsal hippocampus of adult CaMKIIα L7 Cre mice. **B.** Cre is expressed in the lateral and basolateral nuclei of the amygdala in CaMKIIα L7 Cre mice. **C.** In adult CaMKIIα R4 Cre mice, Cre is expressed strongly in area CA1 and in the DG of the dorsal hippocampus, but it is not expressed in area CA3. **D.** CaMKIIα R4 Cre mice express Cre in the lateral and basolateral amygdala.

Figure 4.2. Mild impairment of contextual fear memory in CaMKIIα L7 Cre mice. A. L7 cre mice show reduced freezing when tested for contextual fear 24hrs after conditioning (two-way ANOVA: genotype $F_{1,116} = 3.19$, $p<0.08$, phase $F_{1,116} = 4.51$, $p<0.001$, genotype*phase $F_{1,116} = 2.98$, $p<0.09$; ttest: baseline $p<0.96$, 24hr test *$p<0.04$. **B.** Over the five minute exposure to the conditioned context, L7 Cre mice show a general reduction of freezing across the testing period (rmANOVA: genotype $F_{1,232} = 4.51$, $p<0.04$, minute $F_{1,232} = 6.75$, $p<0.001$, genotype*minute $F_{1,232} = 0.34$, $p<0.85$). **C.** When separated by sex, male L7 Cre mice exhibit a strong trend toward freezing deficits during the test (two-way ANOVA: genotype $F_{1,73} = 2.95$, $p<0.1$, phase $F_{1,73} = 81.83$, $p<0.001$, genotype*phase $F_{1,73} = 3.49$, $p<0.07$; ttest: baseline $p<0.91$, 24hr test $p<0.052$.) **D.** Female L7 Cre mice freeze at levels similar to wild-type mice during both baseline and test conditions (two-way ANOVA: genotype $F_{1,86} = 0.66$, $p<0.43$, phase $F_{1,86} = 106.92$, $p<0.001$, genotype*phase $F_{1,86} = 0.58$, $p<0.46$; ttest: baseline $p<0.30$, 24hr test $p<0.47$.)

Figure 4.3. CaMKIIα R4 Cre male mice exhibit contextual long-term fear memory deficits. **A.** R4 Cre mice exhibit robust freezing deficits when tested for long-term contextual fear memory (two-way ANOVA: genotype $F_{1,41} = 5.2$, $p<0.03$, phase $F_{1,41} = 116.53$, $p<0.001$, genotype*phase $F_{1,41} = 4.24$, $p<0.05$; t-test: baseline $p<0.76$, 24hr test *$p<0.03$.) **B.** R4 Cre mice show reduced freezing levels early in the contextual test phase when compared to wild-type mice (rmANOVA: genotype $F_{1,23} = 1.17$, $p<0.3$; minute $F_{1,4} = 2.41$, $p<0.055$; genotype*minute $F_{1,4} = 2.56$, $p<0.05$). **C.** Male R4 Cre exhibit significantly reduced freezing levels during the test session (two-way ANOVA: genotype $F_{1,24} = 8.46$, $p<0.008$, phase $F_{1,24} = 116.34$, $p<0.001$, genotype*phase $F_{1,24} = 8.43$, $p<0.008$; t-test: baseline $p<0.76$, 24hr test *$p<0.02$). **D.** Freezing levels in female R4 Cre mice is not different from wild-types during baseline or test sessions (two-way ANOVA: genotype $F_{1,13} = 0.71$, $p<0.42$; phase $F_{1,13} = 34.5$, $p<0.001$; genotype*phase $F_{1,13} = 0.17$, $p<0.69$; t-test: baseline $p<0.53$, 24hr test $p<0.46$).

Figure 4.4. Contextual fear memory is intact in CaMKIIα T29-1 Cre mice. A. In baseline and contextual fear test sessions, freezing levels in T29-1 Cre mice are not significantly different from wild-type freezing levels (two-way ANOVA: genotype $F_{1,84} = 1.47$, $p<0.23$, phase $F_{1,84} = 411.1$, $p<0.001$, genotype*phase $F_{1,84} = 3.3$, $p<0.08$; t-test: baseline $p<0.39$, 24hr test $p<0.12$.) **B.** Over the 5 minute test session, T29-1 Cre mice freeze at levels comparable or slightly higher than wild-type animals (rmANOVA: genotype $F_{1,168} = 2.74$, $p<0.11$; minute $F_{1,168} = 2.14$, $p<0.08$, genotype*minute $F_{1,168} = 0.57$, $p<0.69$). **C.** Male T29-1 Cre mice show a small trend to increased freezing during the test session compared to wild-type males (two-way ANOVA: genotype $F_{1,62} = 3.3$, $p<0.08$; phase $F_{1,62} = 389.63$, $p<0.001$; genotype*phase $F_{1,62} = 5.65$, $p<0.03$; t-test: baseline $p<0.26$, 24hr test $p<0.09$). **D.** Female T29-1 Cre mice exhibit freezing levels

that are not different from that of wild-type females during both baseline and test sessions (two-way ANOVA: genotype $F_{1,40} = 0.66$, $p<0.43$, phase $F_{1,40} = 230.59$, $p<0.001$, genotype*phase $F_{1,40} = 0.374$, $p<0.55$; t-test: baseline $p<0.69$, 24hr test $p<0.48$).

Chapter 4 Figures

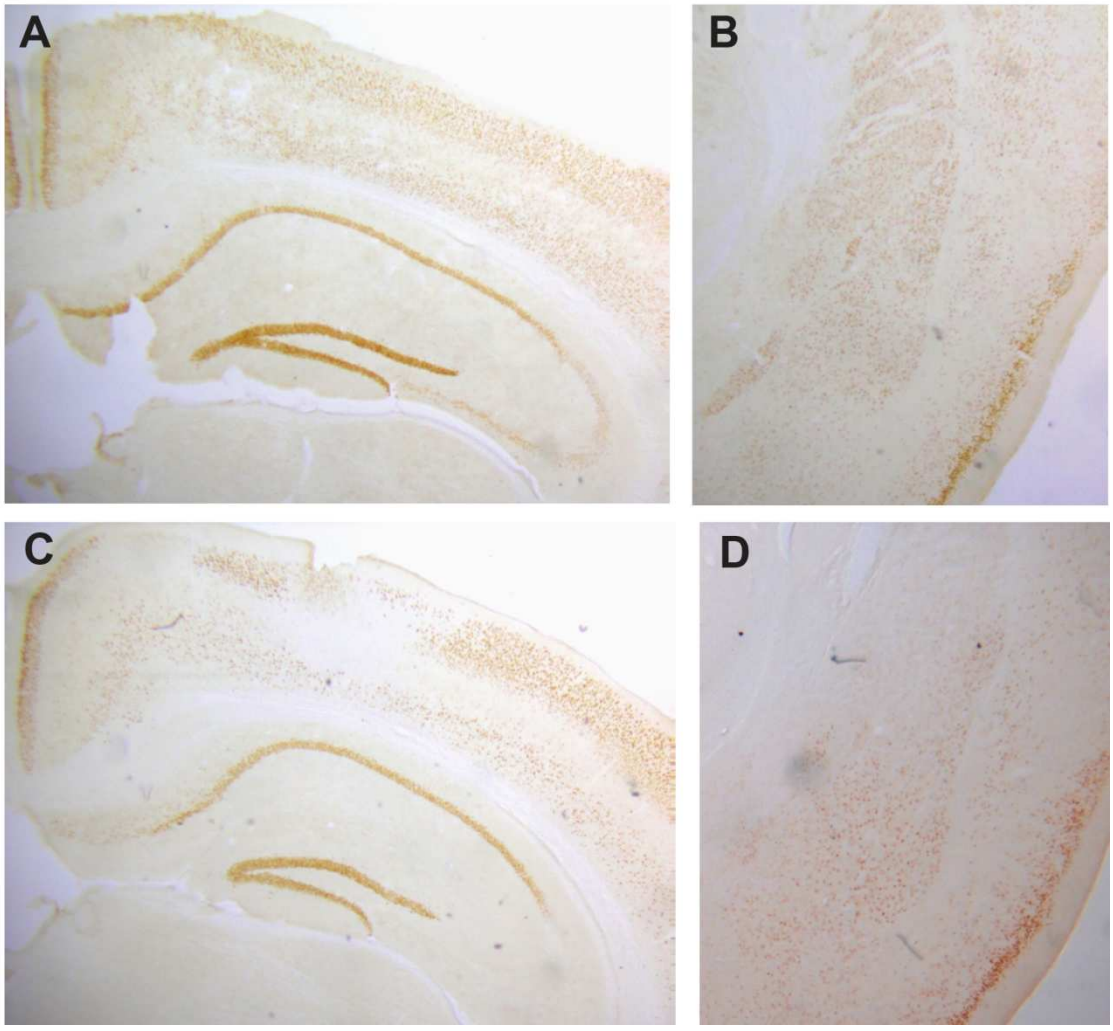

Figure 4.1

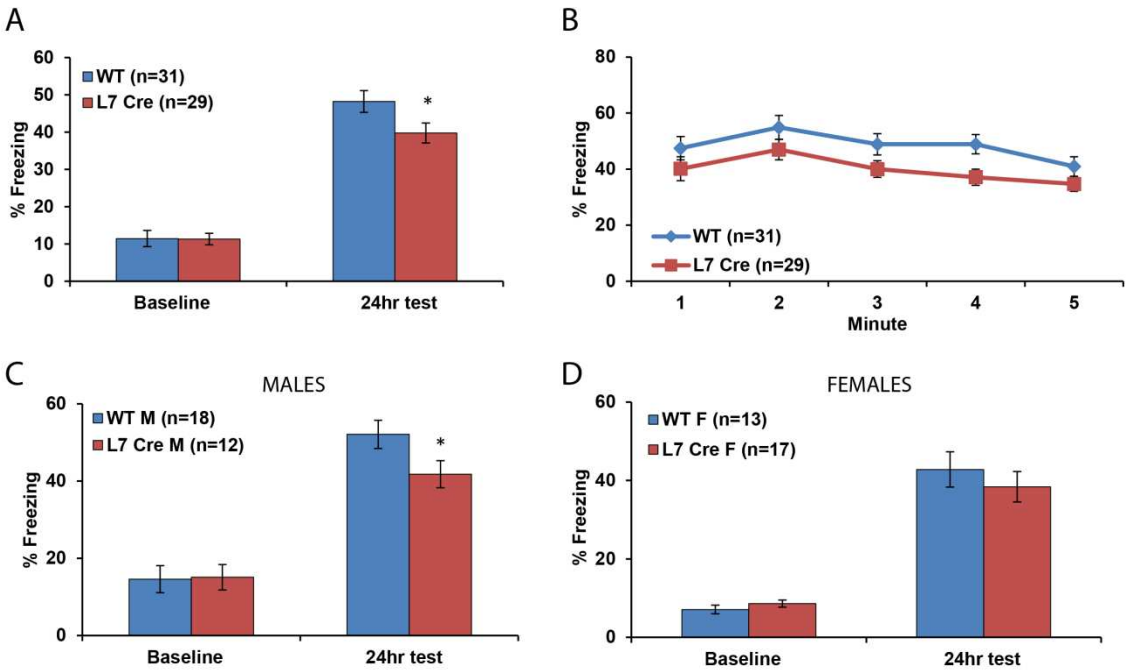
A
WT (n=31)
L7 Cre (n=29)
% Freezing
Baseline
24hr test
*
B
% Freezing
WT (n=31)
L7 Cre (n=29)
Minute
C
MALES
WT M (n=18)
L7 Cre M (n=12)
% Freezing
Baseline
24hr test
*
D
FEMALES
WT F (n=13)
L7 Cre F (n=17)
% Freezing
Baseline
24hr test

Figure 4.2

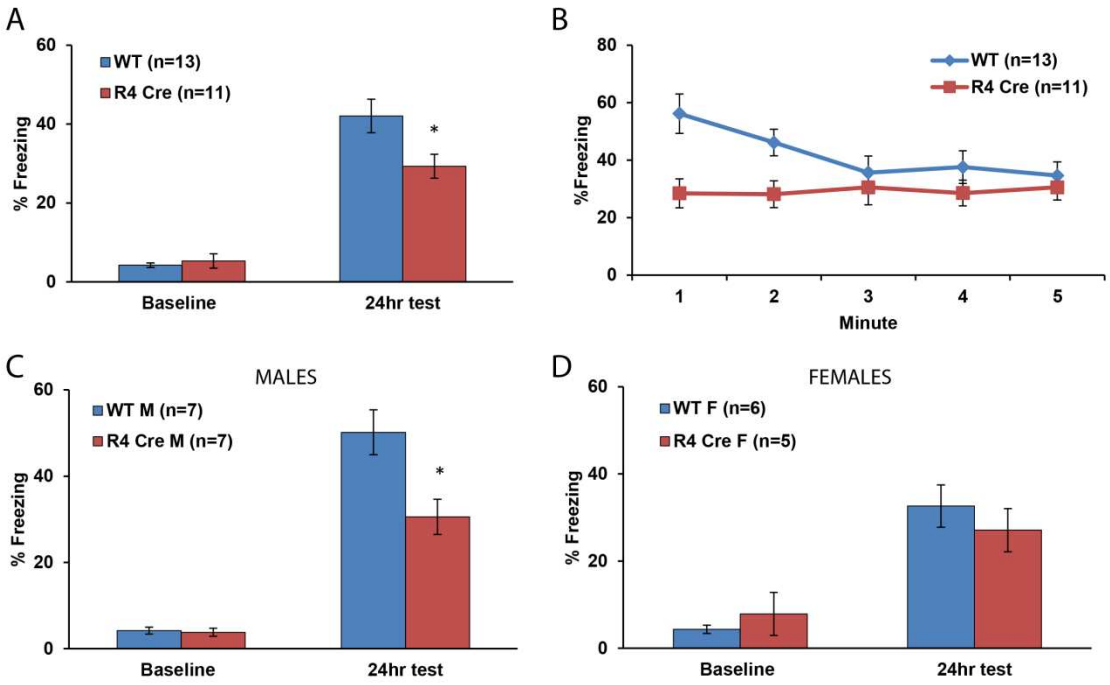
A
WT (n=13)
R4 Cre (n=11)
% Freezing
Baseline
24hr test
B
WT (n=13)
R4 Cre (n=11)
%Freezing
Minute
C
MALES
WT M (n=7)
R4 Cre M (n=7)
% Freezing
Baseline
24hr test
D
FEMALES
WT F (n=6)
R4 Cre F (n=5)
% Freezing
Baseline
24hr test

Figure 4.3

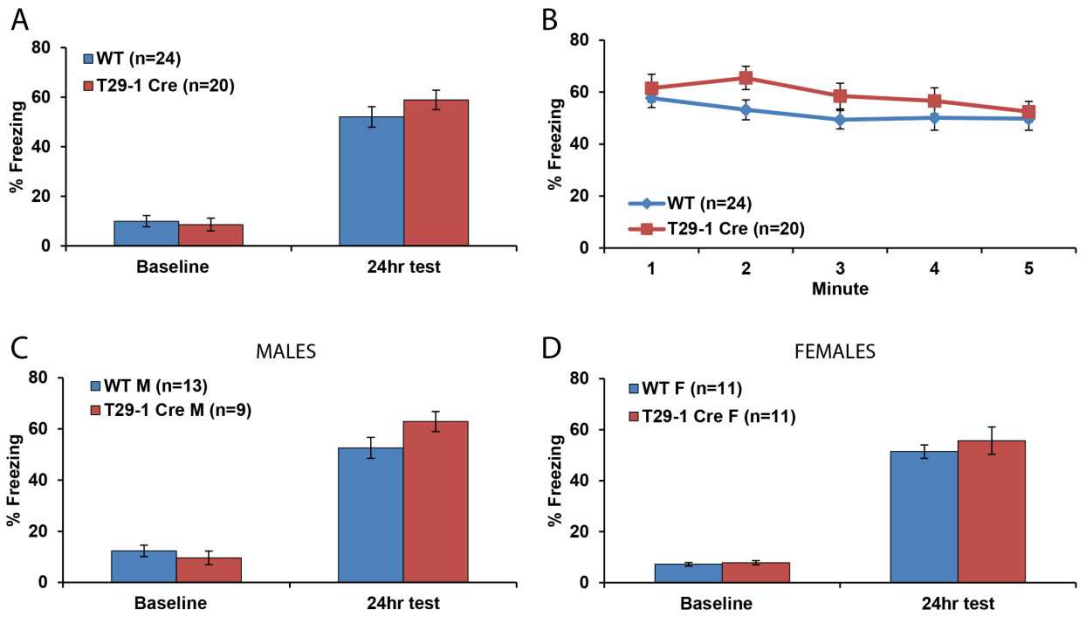
A
WT (n=24)
T29-1 Cre (n=20)
% Freezing
Baseline
24hr test
B
% Freezing
WT (n=24)
T29-1 Cre (n=20)
Minute
C
MALES
WT M (n=13)
T29-1 Cre M (n=9)
% Freezing
Baseline
24hr test
D
FEMALES
WT F (n=11)
T29-1 Cre F (n=11)
% Freezing
Baseline
24hr test

Figure 4.4

AUTHOR CONTRIBUTIONS

This chapter was written by H. Schoch with suggestions from T. Abel, J. Tudor, and N. Grissom. T. Abel, M. Wimmer, and H. Schoch conceived and designed the experiments. M. Wimmer conducted the immunostaining, and H. Schoch performed the behavioral experiments.

This chapter is part of a manuscript in preparation for submission.

CHAPTER 5: GENERAL DISCUSSION AND FUTURE DIRECTIONS

Cognitive deficits are a highly disabling, and poorly understood aspect of many neurodevelopmental disorders for which there are no effective treatment options. Biochemical and genetic studies aimed at expanding our understanding of the molecular basis of cognition are a critical first step to identify targets for therapeutic agents and design successful treatment strategies. In this dissertation, we used two approaches to explore the genetic basis of cognitive functioning: first using a single gene knockout model to validate a predicted ASD susceptibility gene, and secondly targeting a transcriptional regulatory complex that coordinates expression of genes critical for memory formation. We also uncovered a significant complication with one of the predominant genetic tools for conditional gene deletion in rodents.

5.1 Understanding cognitive deficits in neurodevelopmental disorders using a candidate gene approach

In **Chapter 2**, we validated Pcdh10 as a key molecule that regulates synaptic structure in the amygdala, and found that loss of one allele of *Pchd10* led to deficits in social behavior and amygdala-dependent learning. Previously, genome-wide association studies of families with high incidence of ASD identified a novel copy number variation (CNV) affecting a region near multiple genes encoding members of the cadherin and protocadherin superfamilies, including *Pcdh10* (Morrow et al. 2008). Because the CNV is more than 500kb downstream of the nearest protocadherin locus (*Pcdh10*) and did not include promoter or coding regions of the proposed candidate genes, it was unclear whether the deletion was likely to alter expression levels at these loci. Additionally, *Pcdh10* is a novel ASD candidate gene with limited genetic and molecular studies to support a link to the disorder. To address a possible role for *Pcdh10* in the

pathophysiology of ASD, functional studies are needed to demonstrate a role for PCDH10 in endophenotypes associated with the disorder.

Because many neurodevelopmental disorders have complicated etiology likely involving multiple genetic and environmental factors, identification and validation of candidate genes and molecular pathways is critical to gain an understanding of central mechanisms. Studies of PCDH10 function in the brain are limited, but functional studies link it to the Fragile X mental retardation protein FMRP (Tsai et al. 2012). *Pcdh10* is a regulatory target of FMRP linked to regulation of post-synaptic density stability and synapse number, key neuronal processes disrupted in Fragile X disorder (FX) (Tsai et al. 2012). In **Chapter 2**, we used genetically modified mice to show that loss of a single copy of *Pcdh10* resulted in cognitive deficits and social withdrawal behaviors, as well as alterations in structural and functional properties of synaptic connections that are remarkably similar to phenotypes observed in mice lacking FMRP expression. These studies provide further evidence that *Pcdh10* regulates structural and functional properties of synapses, consistent with it being a functional target of FMRP that supports consolidation of emotional memory in the amygdala.

PCDH10 is a newly identified functional target of FMRP, and it is unknown whether it plays a role in the pathophysiology of FX. Knockdown experiments in primary cultured neurons from wild-type mice support a role for PCDH10 in dendritic spine elimination that is disrupted by aberrant translation elongation factor EF1α in *Fmr1* KO mice, leading to increased spine density (Tsai et al. 2012). In $Pcdh10^{+/-}$ mice, increased spine density and reduced gamma synchrony in amygdala neurons mirror structural and functional changes in *Fmr1* KO cortical neurons, hinting at a common mechanism, yet important mechanistic differences are predicted in the two mouse lines. *Fmr1* KO mice exhibit

increased mGluR5 activity and overactive translation machinery- key functional changes proposed to underlie changes in spine density and synaptic plasticity (Tsai et al. 2012, Iliff et al. 2012). In contrast, PCDH10 has yet to be linked to either translational regulation or mGluR5 activity. We could start to address these possibilities by measuring protein translation rates in Pcdh10$^{+/-}$ tissue using a protein synthesis reporter system such as puromycin labeling. Additionally, western blot experiments measuring activation of signaling molecules downstream of type I mGluRs such as PLC (see **Fig. 3.7**) would indicate whether activity of mGluR5 was altered in Pcdh10$^{+/-}$ tissue. Further dissection of synaptic mechanisms underlying synaptic phenotypes in Pcdh10$^{+/-}$ and *Fmr1* KO neurons is a critical next step in understanding molecular pathways underlying changes in spine density in *Fmr1* KO mice as well as the role of PCDH10 in spine elimination.

In **Chapter 2**, we also showed that social deficits in juvenile Pcdh10$^{+/-}$ males could be rescued by treatment with the NMDAR partial agonist d-cycloserine (dCS). Experimental reduction of NMDAR subunit NR1 levels yields deficits in social approach and fear learning, as well as impaired gamma synchrony in mice (Dzirasa et al. 2009, Halene et al., 2009). This array of phenotypes is highly similar to behavioral and electrophysiological changes in Pcdh10$^{+/-}$ mice, suggesting that reduced expression of NR1 could underlie the social deficts and therapeutic response we observed. To test this hypothesis, we are currently measuring synaptic levels of NMDAR subunits in subcellular fractions isolated from amygdala tissue of Pcdh10$^{+/-}$ mice. Preliminary results suggest that levels of NR1 protein are reduced in the post-synaptic density of Pcdh10$^{+/-}$ mice (A. Bannerjee, unpublished results).

PCDH10 facilitates degradation of PSD95, a synaptic structural protein involved in clustering NMDARs and AMPARs at the PSD (Tsai et al. 2012, Yan et al. 2014); however, the reduction in NR1 protein levels suggested by our preliminary studies is not entirely consistent with the current model of PCDH10 function. In the Huber model (Tsai et al. 2012), knockdown of PCDH10 levels in cultured primary cortical neurons leads to stabilization of PSD95 and spine preservation. Increased synaptic PSD95 is associated with increased spine density and increased AMPAR-mediated synaptic transmission (El-Husseini et al. 2000, Beique and Andrade 2002). In our mouse, reduced PCDH10 is associated with increased spine density but the dCS rescue and NR1 protein levels suggest a mechanism involving NDMAR hypofunction. We did not observe a change in amplitude of field responses in the BLA (**Fig. 2.10C**); suggesting that reduced NMDAR function may be accompanied by increased activation of other receptor types, including AMPARs. To unravel this mechanism, more specific dissection of NMDAR/AMPAR function is needed. Whole cell patch clamp recordings designed to distinguish NMDAR activity from AMPAR activity will provide a critical functional readout of the relative activity of these receptor types, and indicate whether one or both currents are altered in $Pcdh10^{+/-}$ neurons. Additionally, Western blots for synaptic and total levels of PSD95 in $Pcdh10^{+/-}$ amygdala tissue will indicate whether reduction of PCDH10 in our mouse affects levels of PSD95. Because the current model of PCDH10 function is based off of experiments conducted in cultured cortical neurons harvested from neonatal mice, important molecular differences between tissues and developmental stages explain the different patterns of electrophysiological and protein changes we observe in 30d old mice. In rodents, expression of NMDAR subunits and functional properties of the resulting channels are highly dynamic during the first post-natal week (Monyer et al. 1994). Certain experiments in our study were conducted in juvenile mice (social testing,

protein levels, electrophysiology), while other experiments were conducted in adult animals (cognitive tasks, spine counts). Additional studies of PSD composition, dendritic spine morphology, and electrophysiological properties of $Pcdh10^{+/-}$ neurons from mice of different ages will provide important insight into the function of PCDH10 and its regulation of structural and functional properties of synapses across development.

A major theme from **Chapter 2** is that exploration of molecular pathways containing existing ASD-associated proteins is not only critical for understanding pathological processes, but is also a strategy for discovering novel candidates. In a molecular pathway that is a critical mechanism underlying ASD phenotypes, major regulatory and enzymatic factors should be investigated as potential risk genes by merit of their essential role in the pathway. In the FMRP-PCDH10 pathway, modification of PSD95 by the ubiquitin ligase murine double minute 2 (MDM2) is a critical step upstream of its degradation. An oncogene best studied for its role in promoting degradation of the tumor suppressor p53, MDM2 is only beginning to be explored in the context of neuronal function and cognition (Tsai et al. 2012, Richmany et al. 2013). Existing pharmacological tools for inhibiting MDM2-mediated degradation of p53 could potentially be used to experimentally stabilize PSD95 (Rew et al. 2012). Future studies of MDM2 and its role in synaptic structure and memory formation will provide insight into this novel mechanism for regulating a major post-synaptic structural protein.

5.2 Gene silencing is a critical regulatory mechanism during memory formation.

Gene expression is a tightly regulated process that is a required step in the formation of memory traces in the brain. Loss of activity-dependent gene regulatory factors has been

observed in multiple neurodevelopmental and neuropsychiatric disorders with associated cognitive dysfunction (**Section 1.3)**. Studies of histone deacetylases and HDAC inhibitor drugs have uncovered strong potential in epigenetic regulation of gene expression as promising strategy for cognitive enhancement. In **Chapter 3**, we identified Sin3a as a gene silencing complex that represses expression of synaptic genes, and acts as a negative regulator of memory and synaptic plasticity in the hippocampus. We showed that Sin3a neuronal hypomorph mice exhibit enhancements in long-term contextual fear memory, and late-phase LTP. The memory enhancement was accompanied by increased expression of *Homer1* a gene that encodes a synaptic scaffolding protein involved in regulating signaling through type I mGluRs. Increased expression of long isoforms of HOMER1 and enhanced signaling through mGluR5 have both been linked to enhancements in memory consolidation and long-lasting forms of synaptic plasticity (Klugmann et al. 2008, Gerstein et al. 2012, Ayala et al. 2009). In Sin3aNH animals, we also see an enhanced role for mGluR5 in maintenance of L-LTP and increased activation of mGluR5 downstream target ERK. Our findings are consistent with a role for SIN3A in regulating memory and plasticity via HOMER1/mGluR5 signaling pathways.

The link we discovered between enhanced synaptic plasticity and changes in synaptic mGlur signaling is a unique and significant step forward in our understanding of the role of epigenetic modifiers in memory enhancement models. Previous studies of memory-related HDACs including HDAC2 and HDAC3 found structural and functional changes in synapses, as well as enhanced memory consolidation in hippocampal tasks, but the mechanism by which these HDAC proteins regulate synaptic function has remained elusive (Guan et al. 2009, McQuown et al. 2011). Studies of gene targets of HDAC inhibitors during memory consolidation have led to the identification of a key transcription

factor, yet have yielded little insight into synaptic mechanisms (Vecsey et al. 2007, McQuown et al. 2011, Mahan et al. 2012). Given the level of interest directed toward cognitive enhancement, and the strong and consistent nature of memory enhancement phenotypes associated with HDAC inhibition, the current lack of mechanistic understanding of its molecular underpinnings is disquieting.

Mechanisms of memory enhancement

In our study, we take a novel approach by targeting a large co-repressor complex with multi-modal functions affecting multiple histone and DNA modifications, an approach that strongly deviates from previous studies exclusively focused on histone acetylation. Epigenetic modifying enzymes are frequently found in regulatory complexes with other modifiers, where carefully coordinated synergistic activity is likely a critical component of their function (**Section 1.3**). By targeting the scaffold protein at the heart of the complex, we are able to explore the function of the entire Sin3a co-repressor complex (**Fig. 3.1**). This approach allowed us to uncover a molecular mechanism not affected by acute blockade of HDAC function alone. We observed elevated levels of long *Homer1* transcripts in Sin3aNH animals 1hr after contextual conditioning; however, levels of long Homer1 isoforms are not altered at the same time point in animals treated with the HDAC inhibitor TSA (**Fig. A.1**). This is a critical discovery, because if future studies find that the memory enhancements observed in Sin3aNH mice do depend on increased expression of long Homer1 isoforms, then the enhancements operate via a different mechanism from that of acute HDAC inhibitor treatment. Two possible epigenetic mechanisms could explain the memory enhancements in Sin3aNH animals.

First, a single one-hour blockade of HDACs may be too brief to fully reverse effects of stable silencing machinery, such as the SIN2A complex. Histone acetylation is known to be an important regulator of the *Homer1* locus in the hippocampus. A transient increase in acetylated H3 at the common promoter of *Homer1* following contextual conditioning is associated with induction of only short isoform *Homer1a* expression, and not long isoforms *Homer1b/c* (Mahan et al.2012). These findings suggest that long and short *Homer1* isoforms are regulated by different mechanisms, and that extended HDAC inhibitor treatment may be needed to re-organize epigenetic mechanisms that regulate long Homer1 isoforms. The SIN3A complex facilitates deacetylation through the activity of three main catalytic partners: HDAC1, HDAC2, and HDAC3. HDAC2 and HDAC3 both independently enhance memory and plasticity (McQuown et al. 2011, Guan et al. 2009), and it is not known which co-repressor(s) mediate these effects. If changes in Homer1/mGLuR5 signaling in Sin3aNH mice are due to loss of HDAC activity, memory enhancements in Sin3aNH and HDAC2/3 KO mice likely occur through the same mechanism. Although possible, it is unlikely that multiple groups studying constitutive HDAC KO mice failed to uncover this mechanism. To test for a common mechanism, gene expression studies in HDAC2 and HDAC3 KO mice focused on levels of *Homer1* isoforms, followed by functional studies of mGluR5 activity are be needed to determine whether *Homer1* expression and mGluR5 signaling is altered with long-term loss of HDAC recruitment.

A more parsimonious interpretation of the inability of TSA to affect long *Homer1* expression implicates a novel mechanism of memory enhancement in Sin3aNH mice that is not dependent on histone acetylation. Binding partners of the SIN3A co-repressor include modulators of both histone and DNA methylation (**Fig. 3.1**). H3K9

methyltransferase activity via SIN3A binding partner SETDB1 engages repressive machinery including nucleosome compaction via the NuRD complex helicase Mi-2, and DNA methylation through recruitment of HP1α/DNMT1 (**Section 1.3**). The promoter region of *Homer1* contains a CpG island that overlaps with the predicted peak binding site for SIN3A in non-neuronal cells that can function both as a substrate for DNA methylation, and a subsequently as a binding site for MeCP2, a methyl-DNA binding factor that recruits DNMT1 and the SIN3A and CoREST co-repressors (**Fig. 1.5**). This intriguing theory suggests that we have discovered a novel mechanism of memory enhancement that is separate from effects of HDAC manipulations, and engages histone and/or DNA methylation mechanisms. Additional studies of epigenetic regulation of Homer1 locus in both wild-type and Sin3aNH mice are needed to explore open questions concerning the role of large complexes such as the SIN3A co-repressor as multi-modal regulators of epigenetic landscapes at gene loci. Immuno-precipitation experiments in Sin3aNH and control mice to measure levels of activating (AcH3, H3K4me) and repressive (H3K9me) histone marks, as well as DNA methylation at the SIN3A binding site on the *Homer1* promoter will provide critical insight into the pertinent catalytic activities of the SIN3A complex at this locus. If changes in DNA methylation are observed, studies to probe for SETDB1 and MeCP2 localization can be followed up by conditional knockdown studies to identify the key factor(s) involved in regulating long *Homer1* transcription. Changes in levels of hydroxymethycytosine mediated by SIN3A binding partner TET1 are unlikely to be a central mechanism for memory enhancement, as contextual memory is not affected in TET1 KO mice (Rudenko et al. 2013).

Unraveling epigenetic regulation Homer1 locus by SIN3A

Future studies of the localization and epigenetic regulatory functions of the SIN3A complex under baseline conditions compared to learning conditions are an important next step in getting a more complete picture of SIN3A function in the brain. Our studies of gene expression changes in Sin3aNH mice were all conducted in tissue collected from trained animals (**Fig. 3.6**). Upcoming experiments measuring baseline expression of long and short *Homer1* isoforms in tissue collected from naïve Sin3aNH and control animals will determine whether the increase in long isoforms is related to activity-dependent processes. The *Homer1* locus contains a single promoter and transcription start site from which short (*Homer1a* and *Ania-3*) and long (*Homer1b/c*) isoforms are differentially expressed via alternative splicing and poly-adenylation (poly-A) site selection (Niibori et al 2007, Flavell et al. 2007, **Fig. 3.7**). Long isoform transcripts containing exons 7-10 are expressed constitutively, and levels are not altered by depolarization events (Bottai et al. 2002, Mahan et al. 2012). Induction of short isoform expression following neuronal activity is thought to occur through an increase in transcription levels combined with a switch to internal poly-A sites in the 3' UTRs of exon 5 and exon A (Bottai et al. 2002, **Figure 3.7**). ChIP seq experiments suggest that histone methylation, SIN3A, and SIN3A binding partner MEF2 are important regulators of alternate splicing and poly-A site selection (Zhou et al. 2012, Flavell et al. 2008).

The regulation of isoform-specific expression at the *Homer1* locus is not understood, but further studies of baseline *Homer1* isoform expression in Sin3aNH animals may provide insight into this mechanism. In Sin3aNH animals, we saw increased expression levels of both short and long *Homer1* isoforms following fear conditioning (**Fig. 3.6**). The simplest explanation of this result involves a mechanism in which SIN3A acts as a braking mechanism slowing the rate of transcriptional activation at the *Homer1* locus. Release of

this braking mechanism in Sin3aNH animals would lead to increased baseline expression of long *Homer1* transcripts in Sin3aNH animals. Higher rates of transcription coupled with intact poly-A site selection would yield the higher rates of short isoform expression we observed in trained animals. Alternately we might find that long isoform levels are not changed under baseline conditions in Sin3aNH animals. This outcome would indicate impairment poly-A site switching, and loss of isoform-specific expression. If this is the case, the results in **Fig. 3.6** reflect activity-dependent induction of both long and short *Homer1* transcripts following contextual conditioning. Because poly-A site selection is a critical process that affects many gene loci involved in neuronal function (Flavell et al. 2008), mis-regulation of this process is unlikely to have beneficial effects on memory formation. It is highly unlikely that both transcriptional output and splicing are mis-regulated in Sin3aNH animals, leading to increased expression of both long and short isoforms at baseline. Aberrant expression of short isoform *Homer1a* is associated with poor cognitive performance and deficits in synaptic plasticity (Manahan et al. 2012, Menard and Quirion 2012, Celiekel et al, 2007, Sala et al. 2003), a pattern that is not consistent with the phenotype of Sin3aNH animals.

Non-epigenetic mechanisms of SIN3A function

In addition to epigenetic regulatory activities, the SIN3A complex also contains non-epigenetic activity mediated by its binding partner O-linked N-acetylglucosamine (O-GlcNAc) transferase (OGT) (**Fig. 3.1**). O-glycosylation is a reversible post-translational modification that can impact the function of transcriptional regulatory machinery on multiple levels. O-glycosylation of key phosphorylation sites on the RNA polymerase II C-terminal domain (CTD) has been linked to retention of Pol II at the TSS (Comer et al. 2001). O-glycosylation also reduces transcriptional activation by CREB. Blocking

glycosylation of a key phosphorylation site on CREB (serine 40 to alanine) leads to increased transactivation of its target genes and enhances contextual fear memory (Rexach et al. 2012). Loss of SIN3A-mediate recruitment of OGT to the Homer1 promoter could result in increased transcriptional activation through one or both of these mechanisms. Should ChIP experiments show that OGT is present at the *Homer1* locus, we could follow up with experiments to determine whether long *Homer1* isoforms are up-regulated in memory-enhanced mice expressing S40A CREB.

Synaptic changes in Sin3aNH mice

Another future direction pertaining to **Chapter 3** is to explore mechanisms underlying synaptic structural and functional effects of increased *Homer1* expression. We showed that increased expression of long Homer1 isoforms was accompanied an expanded role for mGluR5 in synaptic plasticity, and additional electrophysiological studies indicate that signaling through mGluR5 is enhanced (Morgan Bridi, unpublished data). Increased expression of Homer1 is sufficient to enhance memory and increase mGluR5 signaling during LTP (Klugmann et al. 2008, Gerstein et al. 2012), but the synaptic basis of these effects is not understood. In our model, we have only begun to uncover structural and functional changes underlying the memory and plasticity enhancements we observed. Experiments measuring levels and localization of synaptic proteins in Sin3aNH are a critical next step. Validation of protein levels changes in HOMER1 proteins and PSD localization of mGluR5 are critical next steps needed to support our model. Due to the lack of signaling mechanisms specific to mGluR1/5, activation of synaptic and nuclear calcium signaling factors cannot be definitively attributed to activity of mGluR1/5 receptors, and thus cannot be used to validate our model. Despite this drawback, detailed studies of synaptic protein levels and their activity patterns would provide a

valuable window into the molecular changes that support enhanced synaptic plasticity and memory in this model.

Enhancements in memory, plasticity, and ERK signaling are consistent with a mechanism whereby enhanced mGluR5 signaling facilitates memory formation, but do not definitively demonstrate that the increases in Homer1/ mGluR5 signaling underlie the enhancement of plasticity we observed. Classical approaches to demonstrate necessity typically focus on functional blockade, but this is a difficult approach for exploring enhanced functioning. For example, Homer1 and mGluR5 are both critically important for memory formation, so knockout or blockade approaches result in general memory impairments that do not address our mechanism (Ronesi et al. 2008, Mahan et al. 2012, Gerstein et al. 2012, Schulz et al. 2001). What we need is a subtle approach to reduce the excess Homer1/mGluR5 signaling and achieve a 'down-rescue' of the enhanced plasticity in a way that doesn't impair plasticity in our control animals. Carefully controlled titration experiments involving viral knockdown of long Homer1 isoforms or using a soluble peptide to uncouple Homer1-mGluR5 interactions would be the best approach to address this important question.

5.3 Important considerations for genetic models

A key advantage to using rodent genetic models in neuroscience research is the ability to intricately dissect molecular mechanisms underlying cellular, network, and behavioral phenotypes. Despite continual development of increasingly powerful tools, two areas have been consistently overlooked in studies of genetic models of neurodevelopmental disorders: sex differences and limitations of the aforementioned tools. In **Chapter 2** and **Chapter 4**, we found male-specific impairment of memory formation in mice lacking the

autosomal gene *Pcdh10* and also in mice expressing Cre recombinase in forebrain neurons.

In **Chapter 2**, we observed impairments in social behavior and emotional memory in male but not female mice haploinsufficient for *Pcdh10*. Because of the significant and poorly understood predominance of ASD incidence in male children, behavioral and cognitive tasks were conducted in both male and female $Pcdh10^{+/-}$ mice. Oddly, multiple studies of ASD model mice focus exclusively on male animals, and do not consider sex differences (Penagarikano et al. 2011, Jamain et al. 2008, Tsai et al. 2012, Peca et al. 2011). Because we observed sex differences in behavioral responses, we are able to explore the biochemical effects experimentally in our mice. Sex differences are fundamentally related to either sex chromosome complement or activational changes following exposure to steroid sex hormones during gestation and post-puberty. Social changes in juvenile $Pcdh10^{+/-}$ males prior to puberty show reduced social interactions, indicating that sex-differences in social functioning emerge early in life. A pattern of early-onset social differences has also been found in studies of toddlers with ASD, suggesting a possible mechanistic role for sex chromosomes or early exposure to sex hormones before puberty (Landa et al. 2007, Werling and Geschwind 2013, Baron-Cohen et al. 2011).

Prior to onset of puberty, sexual dimorphism can occur through both chromosomal and hormonal mechanisms (Arnold and Chen, 2009). The Y chromosome is dominantly comprised of a 'male-specific' region that is not engaged in crossover events with the X chromosome, and contains multiple genes encoding transcription and translation regulatory proteins (Skaletsky et al. 2003). Several of these Y-specific genes, including the transcription factor *Sry* are expressed in the brain, providing a possible mechanism

by which expression of transcripts and proteins in the brain may be differentially regulated in males (Xu et al., 2002 and 2006; Skaletsky et al., 2003). Expression of *Sry* in the substantia nigra of male rodents is correlated with levels of dopamine production, supporting a role for the Y chromosome in sexual dimorphism in motor and reward functioning (Dewing et al. 2006). Additionally, homologous sex-linked genes show differential expression in male and female mice, with 13 X-linked genes identified by RNA sequencing as incompletely inactivated in XX female mice (Fisher et al., 1990; Yang et al., 2010). Sex-dependent changes in gene expression in the brain have been described in mice at very early time points prior to differentiation of the gonad, providing evidence for the presence of chromosomal or non-gonadal gene regulatory mechanisms (Dewing et al. 2003). In addition to chromosome complement, exposure to sex steroid hormones during the late pre-natal and early post-natal period induces organizational changes in brain structure and function in rodents (de Vries et al. 2014). Sex-specific volumetric changes in the brain have been described for cortical, hypothalamic, and extended amygdala regions in pre-pubertal children, and volumetric changes in the extended amygdala have been linked to developmental testosterone exposure in rodents (Lombardo et al., 2012; del Abril et al.,1987). Additionally, organizational effects of neonatal testosterone exposure have been linked to sex differences in the pattern of estrogen receptor and tyrosine hydroxylase expression in the rodent brain (MacLusky et al. 1997; King et al. 2000). These studies provide strong evidence for effects of chromosome complement and early sex hormone exposure on neuronal gene expression, amygdala volume, and behavioral changes in tasks that engage midbrain dopamine circuits, such as social interaction (Gunaydin et al. 2014).

In our haploinsufficiency model, our Pcdh10$^{+/-}$ animals carry a single copy of the intact *Pcdh10* locus that could be subject to sex-dependent compensatory regulation. Quantitative PCR experiments to measure expression levels of *Pcdh10* in male and female Pcdh10$^{+/-}$ juveniles and adults are an important first step to determine whether levels of PCDH10 are altered in a sex-dependent manner. Future studies to explore emergence of fear memory deficits in Pcdh10$^{+/-}$ mice combined with experimental manipulation of sex chromosome complement and exposure to sex hormones will provide important insight into molecular mechanisms underlying the sex-dependent nature of these deficits. To determine whether sex chromosome complement affects sex dependence of social and memory deficits, we are currently behaviorally characterizing gonadally female XY^{-} Pcdh10$^{+/-}$ mice carrying a mutated copy of the Y chromosome lacking the male organizing locus *Sry* (Arnold and Chen 2009). Additionally, neonatal castration of XX mice carrying a *Sry* transgene would reveal organizational effects of *Sry* expression in the absence of testosterone exposure. To explore effects of hormone exposure early in life, experiments to exogenously manipulate sex hormone effects through gonadectomy with or without sex hormone replacement are also being conducted in Pcdh10$^{+/-}$ male and female animals.

In **Chapter 4**, we found unexpected sexually dimorphic fear memory deficits in mice expressing Cre recombinase. Cognitive deficits have not previously been described in mice only expressing Cre recombinase, and the mechanisms underlying this effect are unclear. Studies of cultured embryonic fibroblasts found reduced cAMP/PKA signaling (Gangoda et al. 2012), but it is not clear whether these changes reflect increased susceptibility at the PKI locus to deleterious effects of Cre, or whether these changes reflect line-specific differences such as a locus-specific effect of the transgene insertion

site. Bioinformatics approaches to identify genomic regions with high incidence of cryptic loxP sequences would provide useful information that could be used to predict gene loci with increased susceptibility to Cre effects, but further efforts to mechanistically explore Cre effects in the brain cross over into the realm of morbid curiosity. Efforts toward improving the tool to reduce deleterious effects are more likely to benefit the field. LoxP flanked Cre transgenes have been put forward as one promising method to reduce the duration of Cre expression and thereby reduce off-target effects (Silver and Livingston, 2001). Sex differences observed in the R4 Cre mice are puzzling, but experiments to uncover sex differences in memory formation would be more useful outside of variable background effects of Cre expression. Studies of sex differences in memory processes in wild-type mice, or in genetic models with sex differences in memory formation, such as $Pcdh10^{+/-}$ mice, will provide novel insights into mechanisms of memory consolidation.

5.4 Concluding remarks

In this dissertation, I explored genetic and epigenetic regulation of synaptic structure and function, and how these factors impact memory consolidation. We explored mechanisms underlying memory impairment in **Chapter 2**, as well as memory enhancement in **Chapter 3**. In both these studies, we traced the memory phenotype back to effects on glutamatergic signaling at the post-synaptic density. PCDH10 is a synaptic protein that has a direct role in the PSD regulating the stability of key structural protein PSD95, and through PSD95, it modulates the localization and function of a wide array of glutamatergic receptors and calcium signaling pathways. Mice haploinsufficient for *Pcdh10* show behavioral and electrophysiological changes highly suggestive of reduced NMDAR function (**Fig. 2.10, 2.11**). In Sin3aNH animals, effects of reduced

SIN3A indirectly modulate synaptic function through epigenetic regulation of synaptic structural protein HOMER1. HOMER1 is a strong modulator of glutamatergic signaling, particularly through type I mGluRs (**Fig. 3.8, 3.12**), and the increased expression of long isoforms we observed is associated with enhanced mGluR5 signaling. At first glance, it appears that the directionality of changes we see in memory neatly align with effects on glutamatergic signaling- impaired signaling in mice with memory deficits and increased signaling in mice with memory enhancement. However, closer inspection of pathological glutamatergic signaling in Fragile X syndrome reveals an important caveat.

Overactive glutamatergic signaling through metabotropic receptors leads to cognitive and synaptic deficits in Fragile X, indicating that the positive relationship between mGluR signaling and cognition observed in Sin3aNH has a limited scope. Cognitive impairment is found both with reduced mGluR signaling observed in schizophrenia and with overabundant mGluR signaling in Fragile X, yielding the classic inverted U-shaped relationship (**Fig. 5.1**). In Sin3aNH animals and animals treated with positive allosteric modulators of mGluR5, there is an expansion of mGluR5 signaling that bolsters memory formation without over-reaching into maladaptive responses. This mechanism of memory enhancement could be a powerful tool for overcoming cognitive deficits, but it is not a magic bullet. Molecular changes underlying the enhanced synaptic plasticity in Sin3aNH animals show many of the same directional changes as synaptic changes observed in Fragile X models (**Fig. 5.2**), suggesting that in *Fmr1* KO mice, reducing expression of SIN3A would be damaging rather than therapeutic. Similarly, reducing SIN3A levels in Pcdh10 haploinsufficient mice may also prove detrimental if the memory and dendritic spine deficits we observed (**Chapter 2**) are mechanistically similar to those of *Fmr1* KO mice. On the other hand, reduced signaling through type I mGluRs has

been observed in schizophrenia models, including Nrg1 mutant mice. Therapeutic approaches to enhance mGluR signaling are promising therapeutic options for the treatment of negative symptoms in schizophrenia.

These studies highlight important challenges in identifying therapeutic targets for neurodevelopmental and neuropsychiatric disorders, and underscore the need for detailed studies addressing molecular mechanisms of synaptic function. Cognition requires a delicate balance of signaling through a wide array of receptors and signaling pathways, therefore therapeutic approaches must therefore be specifically targeted to affected pathways. Careful dissection of structural and signaling processes at the synapse is a critical component both in pathological and therapeutic models. It is through a detailed and careful exploration of the molecular basis of memory formation in synapses that we will gain insight into how to properly develop effective therapeutics to improve cognitive functioning using epigenetic or neuropharmacologic strategies.

Chapter 5 Figure Legends

Figure 5.1. Inverted U-shaped relationship between cognition and mGluR signaling. Signaling through metabotropic glutamate receptors is critical for cognitive processes. Neurodevelopmental and neuropsychiatric disorders such as schizophrenia and Fragile X syndrome are associated with deficient or excess mGluR signaling, respectively. In Sin3aNH mice, enhanced mGluR5 signaling likely reaches a therapeutic threshold above typical levels, but remains below pathological levels observed in Fragile X.

Figure 5.2. Post-synaptic mGluR5 and NMDAR signaling in mouse models. A. Calcium signaling and ERK activity downstream of mGluR5 and the NMDAR activates transcription and translation mechanisms required for long-term memory. **B.** In Sin3aNH mice, increased signaling through mGluR5 increases calcium signaling, leading to increased phosphorylation of ERK, elevated transcriptional activation, and enhanced memory. **C.** In Fmr1 KO mice, increased signaling through mGluR5 leads to increased pERK and increased translation. Over-active transcription leads to reduced post-synaptic responses mediated by AMPAR and voltage gated calcium channels, and impaired memory. **D.** In Pcdh10+/- mice, NMDAR function is decreased, but the amplitude of post-synaptic responses is not altered. Amygdala-dependent memory is impaired. (red = increased, blue = reduced, ? = not determined)

Chapter 5 Figures

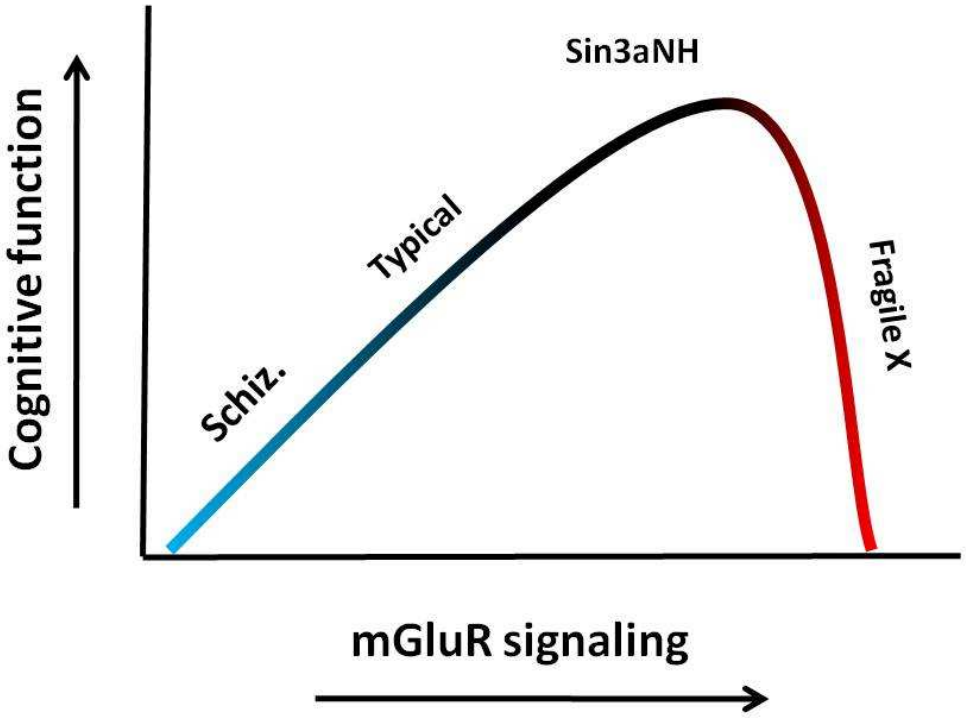

Figure 5.1

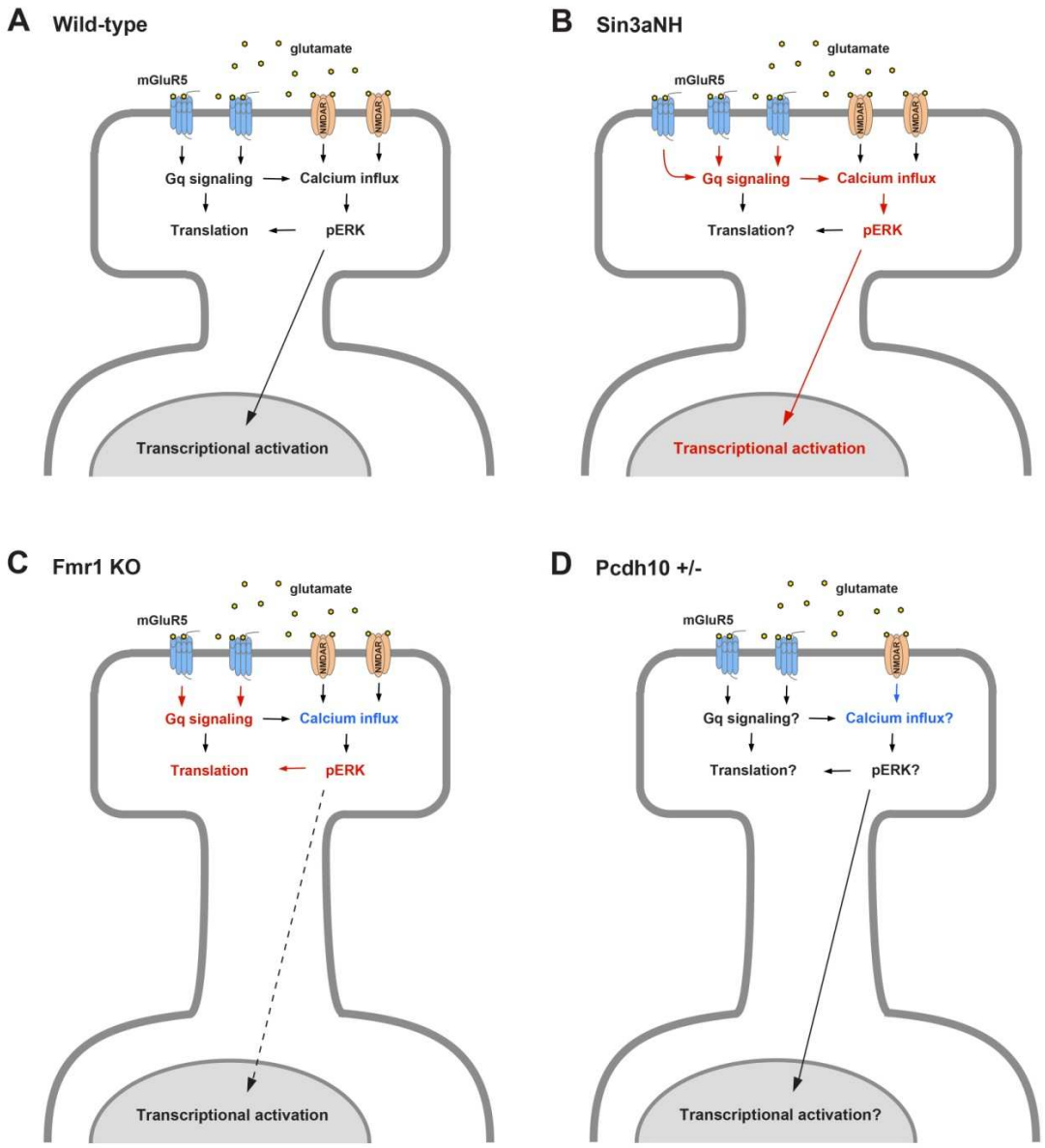
A
Wild-type
glutamate
mGluR5
NMDAR
Gq signaling
Calcium influx
Translation
pERK
Transcriptional activation
B
Sin3aNH
glutamate
mGluR5
NMDAR
Gq signaling
Calcium influx
Translation?
pERK
Transcriptional activation
C
Fmr1 KO
glutamate
mGluR5
NMDAR
Gq signaling
Calcium influx
Translation
pERK
Transcriptional activation
D
Pcdh10 +/-
glutamate
mGluR5
NMDAR
Gq signaling?
Calcium influx?
Translation?
pERK?
Transcriptional activation?

Figure 5.2

AUTHOR CONTRIBUTIONS

This chapter was written by H. Schoch with suggestions from T. Abel, J. Tudor, and N. Grissom.

APPENDIX

In addition to the main directions of my research, expanded my studies into other directions that greatly enhanced my understanding of gene regulation during memory consolidation, as well as increased my knowledge of social behavior in mouse models of autism. Here, I will briefly describe additional studies that are ongoing, part of manuscripts in preparation, or already published.

A1. Short-term regulation of *Homer1* expression in the hippocampus by the HDAC inhibitor Trichostatin A (TSA).

Introduction

Histone acetylation is associated with transcriptional activation, and both histone acetylation and expression of acetylation-regulated genes are increased during memory consolidation (Levenson et al. 2004, Mahan et al. 2012, Maze et al. 2013). Pharmacological blockade of HDAC function is a well-established strategy for memory enhancement in rodents (Vecsey et al.2007, Alarcon et al. 2004, Levenson et al. 2004, McQuown et al. 2011). Previous work from our lab and others has shown that administration of the histone deacetylase inhibitor TSA enhances hippocampal memory, synaptic plasticity, and increases memory-related gene expression (Vecsey et al. 2007, Levenson et al. 2004, Hawk et al. 2011; **Fig. 3.5**). One memory-related gene with increased expression following HDAC inhibitor treatment is *Homer1* (Mahan et al. 2012). Interestingly, we see increased expression of *Homer1* in Sin3aNH mice following contextual conditioning (**Fig. 3.7**), affecting both long and short splice variants (**Fig. 3.8**). Because previous studies only investigated expression of short isoform *Homer1a* following HDAC inhibitor treatment, we examined expression of long *Homer1* isoforms following acute TSA treatment.

Methods

Mice were maintained under standard conditions consistent with National Institute of Health guidelines for animal care and use, and all procedures were approved by the Institutional Animal Care and Use Committee of the University of Pennsylvania. Mice were maintained on a 12 hr light-dark cycle and provided with food and water in their home cages *ad libitum.* Adult male C57BL/6 mice were fitted with bilateral hippocampal guide cannulae as previously described (Hawk et al. 2012). Singly housed mice were handled for three days prior to training in contextual fear conditioning as described in **Section 3.2**. Immediately after training, mice were injected bilateral injections of 1.0uL Trichostatin A dissolved in 50% ethanol, or an equal volume of 50% ethanol (vehicle) as previously described (Hawk et al. 2012). One hour after training, hippocampi were collected, and RNA was isolated as described in **Section 3.2**. Quantitative PCR was performed using Taqman assays targeting exons 3-4 or exons 7-8 of *Homer1* (Applied Biosystems) were used to amplify target isoforms. ΔΔCt values were calculated as described in **Section 3.2**.

Results

Expression levels of long *Homer1* isoforms were differentially affected by acute post-conditioning treatment with TSA. Expression of transcripts containing common exons shared by both long and short *Homer1* isoforms is increased in TSA treated animals compared to vehicle treated animals. In contrast, levels of transcripts containing exons specific to long *Homer1* isoforms is not altered by acute treatment with TSA. These results are consistent with a role for histone acetylation in the regulation of short isoforms of *Homer1* during memory formation, but not long isoforms.

Discussion

In this experiment, we found that regulation of Homer1 isoforms is differentially impacted by acute treatment with the HDAC inhibitor TSA. Activity-regulated short isoform *Homer1a* is up-regulated by TSA treatment, but levels of long Homer1 transcripts containing the common final exon 10 does not change. These results suggest that short and long Homer1 isoforms are regulated by different epigenetic mechanisms following fear conditioning, and that expression of long Homer1 isoforms is not dependent on changes in histone acetylation at this time point.

Contributions

J.D. Hawk and H. Schoch designed the experiment. J.D. Hawk trained the animals and collected the tissue. H. Schoch performed the gene expression assay.

A2. Social behavior not altered in genetic models of autism

Reciprocal social interaction is one of the core features of autism spectrum disorders. Individuals with ASD show atypical frequency and quality of social interactions that emerges early in development and extend into adulthood (Landa et al. 2007, Nacewicz et al. 2006). ASD is a highly heritable disorder, and genomic studies have identified many genetic polymorphisms and copy-number variants (CNVs) associated with the disorder (Michelson et al. 2012, Sanders et al. 2012). Two of the more common polymorphisms linked to syndromic forms of ASD are the 16p11.2 microdeletion

(Fernandez et al. 2010) and variants in the gene contactin associated protein-like 2 (CNTNAP2) (Burbach and van der Zwaag 2008, Alarcon et al, 2008, Arking et al. 2008). Social deficits have been described in CNTNAP2 deficient mice (Penagarikano et al. 2011), but a lack of social phenotypes has been described in mouse models carrying a single copy deletion affecting the conserved murine 16p11.2 region (Horev et al. 2011, Portmann et al. 2014). Here we investigate social approach behavior in mouse models of 16p11.2 microdeletion and CNTNAP2 deficiency.

Methods

Mice were maintained under standard conditions consistent with National Institute of Health guidelines for animal care and use, and all procedures were approved by the Institutional Animal Care and Use Committee of the University of Pennsylvania. Mice were maintained on a 12 hr light-dark cycle and provided with food and water in their home cages *ad libitum.* Mice heterozygous for deletion of the murine conserved locus corresponding to the 16p11.2 human microdeletion (16p11.2 del) (Horev et al. 2011) were obtained from Jackson Laboratories, and bred in house on a mixed B6/129 genetic background. Adult mice 63-77 days of age were tested in social choice. CNTNAP2 knockout mice (Pengarikano et al. 2011) were obtained from Jackson Laboratories, and bred in house on a B6 background. Juvenile mice aged 28-32 days old were tested in social choice. Social testing was conducted as described in **Section 2.2**. Social behavior was scored using Top Scan automatic behavior analysis software, and average time spent sniffing social and non-social cylinders was reported for mice of each sex and genotype combination. Social preference scores were computed for each phase as the fraction of time spent sniffing social cylinder divided by total time spent sniffing both cylinders.

Results

No differences in social approach behavior were observed adult 16p11.2 del males or juvenile CNTNAP2 knockout mice. Male 16p11.2 del mice spend similar amounts of time sniffing the social cylinder during Phase 2 when the stimulus mouse is present (**Fig. A.2A**). Compared to wild-type females, female 16p11.2 del mice show decreased time spent exploring the empty social cylinder and empty non-social cylinder during Phase 1 prior to addition of novel object and novel mouse, and also spend less time sniffing the social cylinder containing the novel mouse during Phase 2 (**Fig. A.2B**). However, when we normalize for differences in overall sniffing and calculate the ratio of time spent interacting with the social cylinder vs non-social cylinders, all groups show significant preference for the social cylinder (**Fig. A.2C**). This result suggests that the differences in total sniffing observed in Phase 1 and Phase2 in female mice reflects a decreased baseline level of exploratory behavior in the deleted animals, and not a difference in sociability. Male and female CNTNAP2 KO mice show robust increases in time spent sniffing the social cylinder in Phase 2 that are not different from wild-type mice (**Fig. A.3**). No genotype differences were found in male or female animals.

Discussion

We observed no significant differences in sociability in male or female animals in either 16p11.2del mice or CNTNAP2 mice. A reduced level of overall sniffing time was found in 16p11.2 del females compared to wild-type females, but no change was observed in preference for the social cylinder. We did not observe changes in sociability in CNTNAP KO males, a finding that contrasts with previous reports of social interaction deficits in male KO animals (Pengarikano et al. 2011). Lack of deficits in juvenile male animals

could indicate a developmental change in sociability in KO males, such that social deficits emerge in adulthood. Additional studies of sociability in both mouse lines across development are in progress, and will provide critical information about the role of these CNVs in the developmental trajectory of social approach behavior in mice.

Author Contributions

This section was written by H Schoch. Experiments were planned by H. Schoch. Experiments were carried out by H. Schoch, M. Zhang, and O. Perez.

Experiments in section A2 are part of a manuscript in preparation.

A3. Object-Location Training Elicits an Overlapping but Temporally Distinct Transcriptional Profile from Contextual Fear Conditioning

Abstract

Hippocampus-dependent learning is known to induce changes in gene expression, but information on gene expression differences between different learning paradigms that require the hippocampus is limited. The bulk of studies investigating RNA expression after learning use the contextual fear conditioning task, which couples a novel environment with a footshock. Although contextual fear conditioning has been useful in discovering gene targets, gene expression after spatial memory tasks has received less attention. In this study, we used the object-location memory task and studied gene expression at two time points after learning in a high-throughput manner using a

microfluidic qPCR approach. We found that expression of the classic immediate-early genes changes after object-location training in a fashion similar to that observed after contextual fear conditioning. However, the temporal dynamics of gene expression are different between the two tasks, with object-location memory producing gene expression changes that last at least 2 hours. Our findings indicate that different training paradigms may give rise to distinct temporal dynamics of gene expression after learning.

Introduction

Long-term memory is critical to our lives, yet the molecular mechanisms that create and stabilize memories are still poorly understood. The hippocampus, which encodes contextual information, has been heavily studied in an effort to better understand these mechanisms. Transcription is required to convert labile short-term memories into stable long-term memories during the period of memory consolidation (Agranoff et al., 1967; Igaz et al., 2002). The expression of many genes is regulated within the first hour after learning in the hippocampus (Hawk et al., 2012; Keeley et al., 2006; Lemberger et al., 2008; Levenson et al., 2004; Lonergan et al., 2010; Ramamoorthi et al., 2011). Epigenetic mechanisms, such as histone acetylation, can modulate this transcription to enhance or dampen long-term memory formation (Alarcon et al., 2004; Guan et al., 2009; Korzus et al., 2004; Levenson et al., 2004; McQuown et al., 2011; Vecsey et al., 2007; Wood et al., 2006; Wood et al., 2005).

Most research into transcriptional regulation in the hippocampus has used contextual fear conditioning as the paradigm to test learning and memory (Barnes et al., 2012; Keeley et al., 2006; Levenson et al., 2004; Mei et al., 2005). This is primarily because

contextual fear conditioning produces a robust memory that has a well-defined time of acquisition due to the requirement of only a single training session (Abel and Lattal, 2001). Although this task has proven useful for dissecting the phases of memory and mapping the transcriptional landscape after learning, it also introduces a footshock that can be stressful to the animal. It is therefore important to study gene expression in other memory tasks that are more similar to the learning events that occur in daily life.

Spatial learning requires the hippocampus and can be measured using the Morris water maze, Barnes maze, or object-location memory (OLM) tasks that do not require a footshock. These spatial tasks are also known to regulate transcription in the hippocampus, including many of the same genes and processes required for contextual fear memory (Bousiges et al., 2010; Cavallaro et al., 2002; Florian et al., 2006; Fordyce et al., 1994; Haettig et al., 2011; Hawk et al., 2011; Klur et al., 2009; McNulty et al., 2012; Pittenger et al., 2002; Vogel-Ciernia et al., 2013). There is evidence that contextual and spatial learning in the hippocampus can utilize different molecular pathways (Mizuno and Giese, 2005), so gene expression may also differ after these two tasks. Like contextual fear memory, OLM is a hippocampus-dependent task (Oliveira et al., 2010). However, the targets and temporal resolution of the gene expression changes after OLM have not been thoroughly studied. The goal of this study was to investigate the transcriptional profile that occurs within the first transcriptional wave after OLM learning (Bourtchouladze et al., 1998; Igaz et al., 2002) and compare this transcriptional profile to that of contextual fear conditioning. Gene expression changes within this window after fear conditioning are typically highest 30 minutes after training and return to baseline by 2 hours (Hawk et al., 2012; Keeley et al. 2006; Peixoto et al., 2013). Using a Fluidigm HD microfluidic high-throughput qPCR system, we examined expression of 96

different candidate genes at both 30 minutes and 2 hours after OLM training in a single experiment. We found that the most commonly studied genes after fear conditioning show a similar profile after OLM. However, OLM produces long-lasting expression changes in a number of genes that are not observed after fear conditioning.

Methods

Subjects

Forty-two C57BL/6J mice were maintained under standard conditions with food and water available *ad libitum*. Adult male mice 3 months of age were kept on a 12-hr light/12-hr dark cycle with lights on at 7AM. All behavioral and biochemical experiments were performed during the light cycle with training starting at approximately 7AM (ZT0). All procedures were approved by the University of Pennsylvania Institutional Animal Care and Use Committee.

Behavior

Object-location memory (OLM) was carried out as previously described (Hawk et al., 2011; Oliveira et al., 2010). Briefly, naïve three month old male C57Bl/6J mice were singly housed for a week and handled for 2 min/day for five consecutive days prior to tissue collection. One animal per behavioral group was trained and dissected each day for 10 total days to allow all animals to be dissected at the same circadian time. Exploration was normal in all mice used in this experiment (data not shown). One animal per training session was tested in a 24hr retrieval test the following day to ensure the

training proceeded correctly. Half of the handled animals received OLM training, and half of the animals were left undisturbed on training day and were sacrificed at the same circadian time points as trained animals. On the day of training, OLM mice were given a single block of four 6 min trials with an inter-trial interval of 3 min. The animals were habituated to an empty arena with a black and white striped spatial cue on one wall in the first trial, followed by three trials of object exposure. Each mouse was exposed to three distinct objects: a rectangular metal tower, a glass bottle, and a white plastic cylinder that were arranged in a V-shaped spatial pattern in the arena. Objects were positioned in the arena with at least two inches of spacing around each object to allow free exploration of all objects. During the ITI, animals were gently removed from the arenas, and the arenas and objects were cleaned with 70% ethanol. Objects were not moved during the ITI. Immediately following the final trial, animals were gently placed in their home cage, and returned to the colony room until tissue collection.

Fear conditioning was performed as previously described (Hawk et al., 2012; Vecsey et al., 2007) with handling for 3 days prior to conditioning. Briefly, the conditioning protocol entailed a single 2-sec, 1.5mA footshock terminating at 2.5 minutes after placement of the mouse in the novel chamber. Mice were left in the chamber for an additional 30 seconds and then returned to their homecage.

RNA isolation

Hippocampi were dissected 30 minutes and 2 hours after the last training session into RNAlater (Qiagen, Valencia, CA) and frozen on dry ice. Tissue was homogenized using

a TissueLyser system and RNA was extracted using the miRNeasy kit (Qiagen) according to the manufacturer's instructions.

cDNA synthesis and high-throughput qPCR

RNA concentration was determined using a NanoDrop spectrophotometer (Thermo Scientific, Waltham, MA) and 1µg RNA was used in each RETROscript (Ambion, Austin, TX) cDNA synthesis reaction with random decamers, 10x RT Buffer and no heat denaturation according to the manufacturer's protocol. Concentrated cDNA was used in a specific target reaction following the manufacturer's recommendations (Fluidigm Corp. South San Francisco, CA). Briefly, Taqman assays for all 96 probes were pooled to a concentration of 0.2X (1:100) and 1.25ul of the pooled assay mix was combined with 2.5ul 2X Taqman Preamp Master Mix (Life technologies, Carlsbad, CA) and 1.25µl cDNA. The preamplification reaction was cycled using the following protocol in a 7500 Fast Real-Time PCR system: 10 min at 95C, then 14 cycles of 95C for 15s followed by 60C for 4min. Preamplified samples were diluted 1:5 using 1X TE. Samples were then delivered to the Molecular Profiling Core at the University of Pennsylvania, where they were run on a 96.96 Dynamic Array IFC on the Biomark HD machine (Fluidigm Corp).

For validation and the 120 minute fear conditioning experiment, cDNA reactions were diluted to 2 ng/ul in water, and real-time RT-PCR reactions were prepared in 384-well optical reaction plates with optical adhesive covers (Life technologies). Each reaction was composed of 2.25µl cDNA (2 ng/ul), 2.5µl 2x Taqman Fast Universal Master Mix (Life Technologies), and 0.25µl of Taqman probe. Reactions were performed in triplicate on the Viia7 Real-Time PCR system (Life Technologies, Carlsbad, CA).

Data analysis

High-throughput qPCR was analyzed using the Fluidigm Real Time PCR Analysis program and Microsoft Excel. Genes with at least one sample having an average Ct ≥20 were discarded as being non-expressed or failed reactions. This included *Dnmt3b*, *Erbb2*, *Esrrg*, *Fosb*, *Hdac1*, *Hdac4*, *Jun*, *Nr6a1*, *Pparg*, and *Trdmt1*, which brought the total number of genes tested to 86. Relative quantification of gene expression between groups was performed using the ΔΔCt method as described previously (Vecsey et al., 2007). The difference between each Ct and the average Ct for that gene was subtracted from the average of three housekeeper genes treated in the same manner. A p-value of 0.01 was used for significance to control for the number of t-tests performed. This p-value cutoff was chosen because we selected genes for analysis that we expected to change, and thus Bonferroni correction is too strict. This 1% chance of a type I error corresponds to one false positive per 100 t-tests. Because 86 t-tests were performed, this p-value would suggest less than 1 false positive in the data, limiting the amount of type I errors introduced by multiple testing.

Results

Immediate Early Genes Are Regulated 30 minutes after OLM training

We chose sixteen representative genes that have been studied 30 minutes after fear conditioning to examine expression profiles 30 minutes after OLM training. The genes were chosen for well-studied expression changes (*Arc*, *Bdnf4, Egr1, Fos, Homer1*),

genes our lab has previously studied [*Fosl2 (Hawk et al., 2012), Gadd45* family (Leach et al., 2012)], or from microarray data (*Btg2*, *Cpeb3*, *Histh2hab*, *Sik1*, *Sox18*, *Tob1*, *Tob2 (Peixoto et al., 2013)*). cDNA samples underwent specific target amplification and were run on a 96.96 Fluidigm Biomark HD plate in triplicate (96 genes, 32 samples). Ten genes were excluded due to too low expression or a failed reaction, bringing the total number of genes tested to 86 (See **Methods** for genes). In all cases, immediate early gene (IEG) expression after OLM mirrored expression after fear conditioning (**Figure A.4**). Previously studied genes including *Arc*, *Bdnf4*, *Egr1*, *Fos* and *Homer1* were upregulated as anticipated (*Arc* 272% $p=4.7x10^{-8}$; *Bdnf4* 53% $p=3.3x10^{-7}$; *Egr1* 225% $p=4.4x10^{-8}$; *Fos* 410% $p=1.2x10^{-10}$; *Homer1* 31% $p=1.4x10^{-4}$) (Keeley et al., 2006; Lonergan et al., 2010; Mahan et al., 2012; Mizuno et al., 2012). The probe against *Homer1* recognizes both *Homer1a* and *Homer1c*, but research from our lab and others suggests that this effect is primarily due to Homer1a (Mahan et al., 2012). Further investigation is required to investigate specific Homer1 isoforms regulated by OLM. Genes that our lab discovered to be regulated after contextual fear conditioning using microarrays (Peixoto et al., 2013), including *Btg2* (27% $p=8.9x10^{-6}$), *Hist2h2ab* (-26% $p=8.8x10^{-4}$), *Sik1* (70% $p=1.3x10^{-5}$), *Sox18* (-21% p=0.002), and *Tob2* (30% p=0.004) showed similar changes after OLM. The genes *Gadd45b* and *Gadd45g* showed increased expression (32% p=0.004, 32% p=0.001) while *Gadd45a* did not (p=0.20), as has been reported previously by our lab and others (Leach et al., 2012; Sultan et al., 2012). This observation suggests that the most commonly studied genes after contextual fear conditioning are similarly regulated after spatial behavioral tasks such as object-location memory.

Nuclear Hormone Receptors Display a Limited Response to OLM

A subset of nuclear hormone receptors are known to be regulated 30 minutes after fear conditioning, including the *Nr4a* family of orphan nuclear receptors (Hawk et al., 2012). We tested all 37 nuclear hormone receptors that are expressed in the hippocampus for changes after OLM training (**Figure A.5**). The Nr4a family of nuclear receptors (*Nr4a1*, *Nr4a2*, *Nr4a3*), which are known to be necessary for long-term fear memory (Hawk et al., 2012; McNulty et al., 2012; McQuown et al., 2011), all displayed increased expression at 30 minutes after OLM. Rev-ErbA (*NR1D1*), COUP-TFII (*NR2F2*), and retinoid X receptor gamma (*Rxrg*) all showed decreased expression at 30 minutes. No other nuclear receptors were observed to respond to spatial learning at this time point or at 120 minutes after OLM (data not shown). This contrasts with the large number of nuclear receptors that our lab observed to change after fear conditioning training in our previous study (Hawk et al., 2012), which included increased expression of 13 nuclear receptor genes between 30 and 120 minutes after training. These results may indicate transcriptional regulation of this class of genes depends on the training paradigm.

Regulators of Transcription Show Limited Changes in Response to OLM

Histone acetylation is known to be a crucial regulator of transcription during memory consolidation (Alarcon et al., 2004; Barrett et al., 2011; Haettig et al., 2011; Korzus et al., 2004; Levenson et al., 2004; McQuown et al., 2011; Vecsey et al., 2007; Wood et al., 2006; Wood et al., 2005). To test whether expression levels of histone acetylation modifying enzymes are regulated by OLM, we tested all histone deacetylases (HDACs, **Figure A.6A**) and 16 histone acetyltransferases (HATs, **Figure A.6B**) representing each class of enzyme, including the HATs CBP and p300 that have been shown to be

essential for memory formation. The probes against *Hdac1* and *Hdac4* did not amplify and were discarded. None of the HATs tested showed a gene expression change, in contrast to previous reports showing changes in expression of CBP, p300 and PCAF after the Morris Water Maze (Bousiges et al., 2010). However, *Hdac7* displayed reduced expression after OLM. HDAC7 is a class IIa HDAC that has not been previously linked to memory formation. This may suggest a novel role for HDAC7 in hippocampus-dependent memory formation. In addition to the regulators of histone acetylation, we chose ten genes that are known to regulate transcription in other ways. None of these genes showed any changes in transcription at 30 minutes after OLM training (**Figure A.7**).

OLM Induces Longer Lasting Gene Expression Changes than Fear Conditioning

In addition to the 30 minute timepoint that has shown such robust changes after fear conditioning, we also tested hippocampal samples taken 2 hours after OLM training to investigate the persistence of these transcriptional changes. Interestingly, a number of genes that are upregulated at 30 minutes remain elevated 2 hours after OLM training. This includes highly induced genes that appear to be slowly returning to baseline, such as *Egr1* and *Fos*, but also genes that maintain a similar level of induction as observed at 30 minutes such as *Bdnf4*, *Fosl2*, *Homer1*, *Nr4a2* and *Nr4a3* (**Figure A.8A**). *Sin3a* was not changed at 30 minutes, but shows a selective change at 2 hours. The gene expression profiles at 30 minutes and 2 hours for *Arc*, *Egr1*, *Fos*, *Nr4a1*, and *Nr4a2* were confirmed by standard 384-well qPCR (data not shown). To test whether these same genes show transcriptional changes after fear conditioning, we prepared cDNA from samples that were collected 2 hours after fear conditioning. None of the genes determined to change 2 hours after OLM showed a significant change 2 hours after fear

conditioning (**Figure A.8B**), indicating a long-lasting gene expression response specific to OLM.

Discussion

In this study, we investigated the transcriptional changes that occur in response to OLM training using powerful high-throughput qPCR technology and compared these changes to fear conditioning. In a single run, we were able to study 96 different genes in 2 different time points after OLM training with n=8 mice per group using microfluidic high-throughput qPCR. This type of throughput, flexibility, and consistency is not possible with any other qPCR technology. In addition to requiring more pipetting steps, standard qPCR would have required the same housekeepers to be run on each individual plate and limited the number of targets that could be tested. Using a high-throughput approach allowed us to reliably determine that gene expression changes after OLM last longer than similar expression changes after contextual fear.

Our study discovered that commonly studied IEGs, such as *Fos* and *Arc*, show similar expression differences after fear conditioning and after OLM, indicating overlap between contextual and spatial learning. In a previous study from our lab (Hawk et al., 2012), we found that a number of nuclear receptors exhibit increased expression after contextual fear conditioning. Our current findings suggest a more limited regulation of this class of genes after OLM. It is unclear whether the wider regulation after fear conditioning is in response to the footshock or whether the timecourse of expression after OLM is different. As seen after fear conditioning, all 3 members of the *Nr4a* family of orphan nuclear receptors were upregulated after OLM. However, while *Nr4a1*

returned to baseline by 2 hours, *Nr4a2* and *Nr4a3* did not, suggesting that different processes may regulate *Nr4a1* than the other two family members. Future studies will aim to determine how expression increases of *Nr4a2* and *Nr4a3* are maintained after OLM training.

It is interesting to note that *Hdac7* and *Sin3a* are regulated by OLM while HATs are not. This may suggest that relieving the negative repression of histone acetylation is a crucial step for long-term memory formation. Although class I HDACs have been heavily implicated in learning and memory (Bahari-Javan et al., 2012; Guan et al., 2009; Hawk et al., 2011; McQuown et al., 2011), class IIa HDACs have received less attention. A study by Agis-Balboa et al. demonstrated that loss of the class IIa member HDAC5 impairs spatial memory (Agis-Balboa et al., 2013), but those experiments used a complete knockout mouse line that has the potential for developmental or extrahippocampal effects. Our study is the first to observe changes in *Hdac7* in response to learning in the hippocampus.

The most intriguing finding of this study was the long-lasting regulation of gene expression 2 hours after OLM, something that is not seen after fear conditioning. It might be expected that the fear of a footshock would produce a stronger transcriptional response in the hippocampus than would the spatial rearrangement of objects. There are a number of potential causes for this disparity, although the most likely explanation is that the multiple training sessions required for OLM induce a stronger response than the single shock training used by our lab for fear conditioning. It would be interesting to test whether a multiple shock fear conditioning protocol induces longer lasting gene expression changes. Also, there could be an association between the novel context and the novel objects formed during OLM training that is not present in fear conditioning.

Testing mice in the context only, introducing novel objects, or altering the number of training trials could determine whether these changes are sufficient to elicit gene expression changes. Further, different molecular mechanisms may regulate contextual and spatial learning (Mizuno and Giese, 2005). Future studies can test for changes at the protein level, although mRNA and protein levels generally agree after learning (Stanciu et al., 2001; Steward et al., 1998). Additional investigation into later time points after OLM training will be required to see if gene expression changes that occur well after fear conditioning (Mizuno et al., 2012) also exist after OLM. It is interesting that not all genes with increased expression at the 30 minute timepoint remain elevated for 2 hours after OLM. Future studies will determine whether specific epigenetic modifications regulate this longer term maintenance of gene expression at particular genes.

Author Contributions

This section was written by Shane Poplawski with suggestions by Ted Abel, Hannah Schoch and Karl Peter Giese. Experiments were planned by Shane Poplawski, Hannah Schoch and Mathieu Wimmer. Experiments were carried out by Shane Poplawski, Hannah Schoch, and Joshua Hawk. Behavioral scoring was performed by Jennifer Walsh. We thank Morgan Bridi, Giulia Porcari, and Robbert Havekes for constructive discussions and editing.

Section A3 was published in: Poplawski SG, Schoch H*, Wimmer M, Hawk JD, Walsh JL, Giese KP, Abel T. "Object-Location Training Elicits an Overlapping, but Temporally*

Distinct Transcriptional Profile from Contextual Fear Conditioning" Neurobiology of Learning and Memory (In press, 2014)

Appendix Figure Legends

Figure A.1. Differential expression of Homer1 isoforms by acute post-training treatment of TSA. Expression of Homer1 transcripts containing exons common to both short and long isoforms is elevated in trained animals that received infusions of TSA, but levels of long Homer1 isoforms containing exons 7-8 are not changed. Graph shows means with error bars denoting SEM (t-tests: * indicates $p<0.05$.)

Figure A.2. Cylinder sniffing is reduced in female 16p11.2 del mice, but social preference is intact. A. Sniffing of social and non-social cylinders in not different in adult male 16p11.2 del mice. **B.** Female 16p11.2 del animals show reduced sniffing behavior during both phases of social choice testing. **C**. No difference in preference scores for sniffing the social cylinder in males or females of either genotype. All graphs show means with error bars denoting SEM (t-tests: * indicates $p<0.05$.).

Figure A.3. Sociability is not altered in juvenile CNTNAP2 knockout mice. A. No differences in exploration of social cylinder during phase 2 in male CNTNAP2 KO mice. **B.** No differences in sniffing of social or non-social cylinders in female CNTNAP2 KO mice. Graphs show means with error bars denoting SEM (t-tests: * indicates $p<0.05$.).

Figure A.4. Classic IEGs Show Expected Expression Changes after OLM Training. 16 genes that are known to be induced 30 minutes after contextual fear conditioning were studied 30 minutes after OLM training. Each gene tested displayed the expression change that would be expected after contextual fear conditioning, indicating these genes may represent a common transcriptional response to learning. All error bars denote s.e.m. and * indicates $p<0.01$.

Figure A.5. Limited Expression Changes of Nuclear Receptors after OLM training. Because of the known involvement of the *Nr4a* nuclear receptor family in memory, we tested expression of all nuclear receptors expressed in the hippocampus 30 minutes after OLM training. The *Nr4a* family displayed increased expression after OLM, while *NR1D1*, *NR2F2*, and *RXRg* had reduced expression. All error bars denote s.e.m. and * indicates $p<0.01$.

Figure A.6. Modifiers of Histone Acetylation Display Limited Regulation after OLM Training. Histone modifying enzymes were tested for expression changes 30 minutes after OLM training. **A.** *Hdac7*, a class IIa HDAC, was the only family member found to change expression after OLM. **B.** No HATs were observed to change expression after OLM. All error bars denote s.e.m. and * indicates $p<0.01$.

Figure A.7. No Changes in Other Transcriptional Regulators after OLM Training. Other genes that can regulate gene expression, including DNMTs, were tested 30 minutes after OLM training. No differences in any gene were observed. All error bars denote s.e.m. and * indicates $p<0.01$.

Figure A.8. OLM Training Induces Long-Lasting Changes in Gene Expression Not Seen after Fear Conditioning. A. Every gene was also tested 2 hours after OLM training to observe the maintenance of transcription. Genes shown in this figure are those that were changed at 2 hours after OLM, all other genes were unchanged. *Sin3a* was the only gene uniquely regulated at the 2 hour time point. **B.** These same genes do not show gene expression changes 2 hours after contextual fear conditioning. All error bars denote s.e.m. and * indicates $p<0.01$.

Appendix Figures

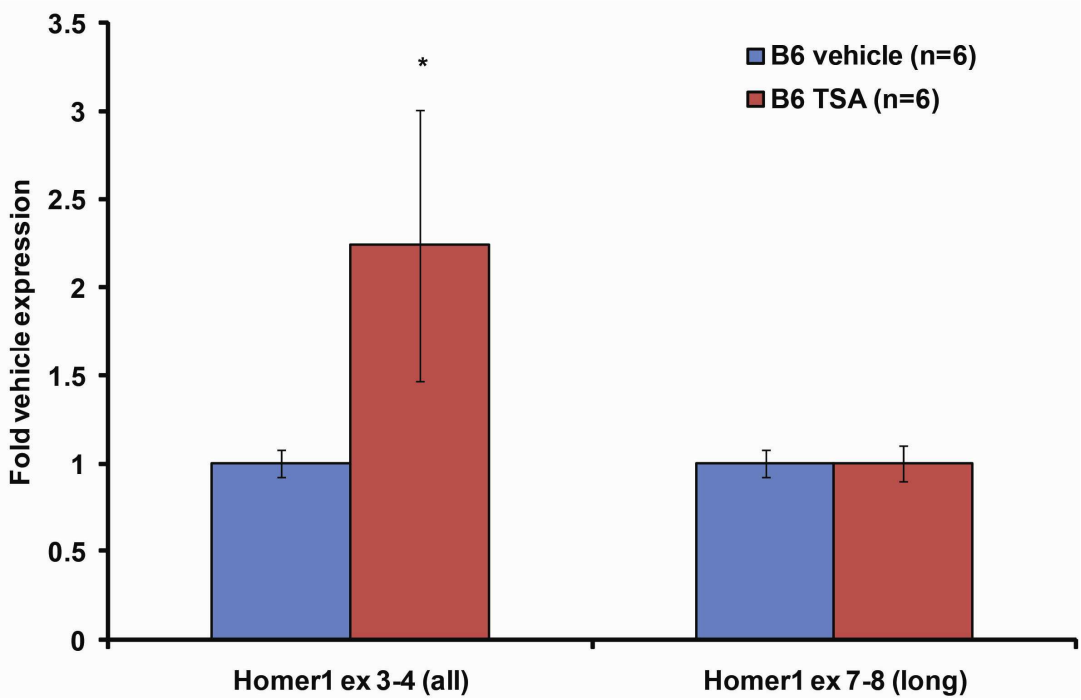

Figure A.1

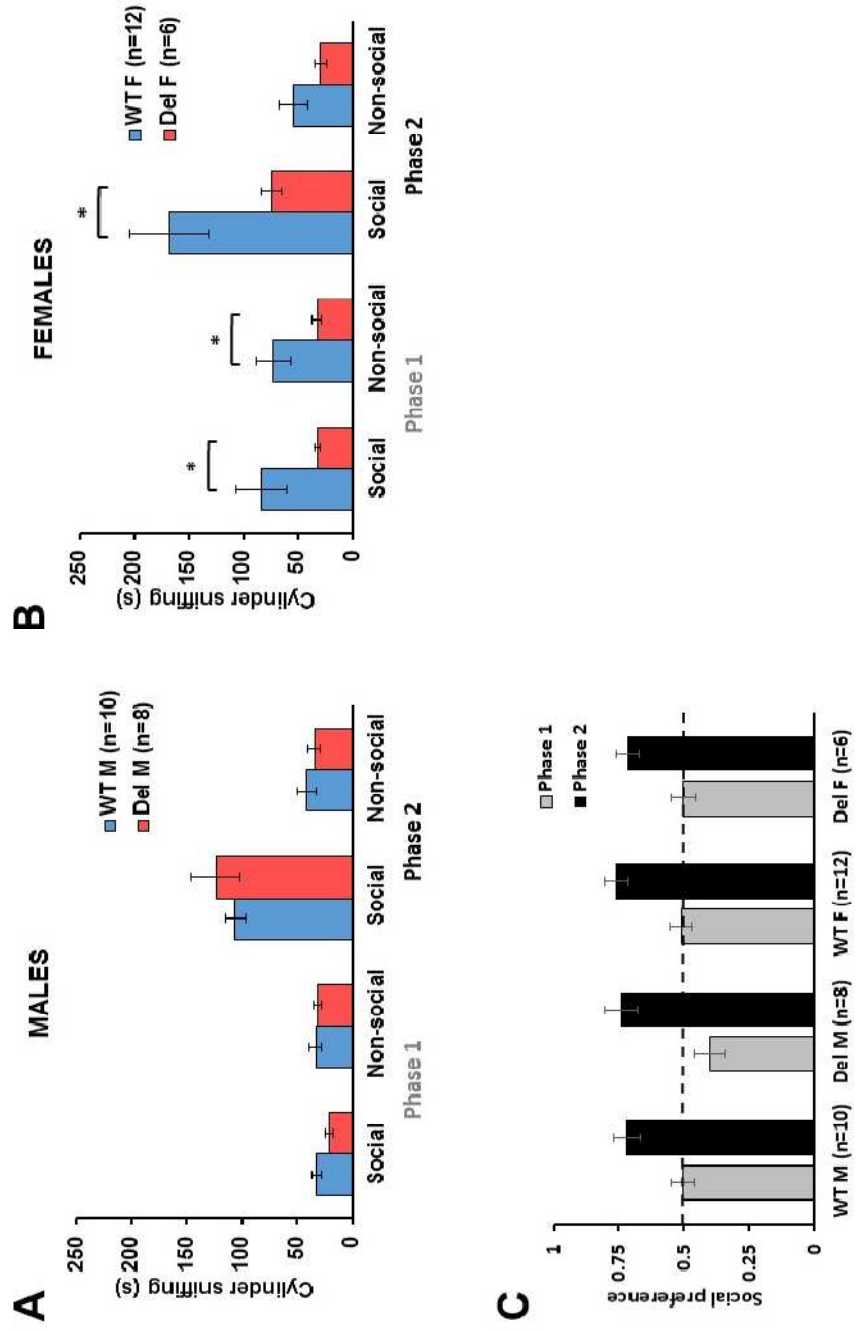
A
MALES
WT M (n=10)
Del M (n=8)
Cylinder sniffing (s)
250
200
150
100
50
0
Social
Non-social
Social
Non-social
Phase 1
Phase 2
B
FEMALES
WT F (n=12)
Del F (n=6)
*
*
*
C
Phase 1
Phase 2
Social preference
1
0.75
0.5
0.25
0
WT M (n=10)
Del M (n=8)
WT F (n=12)
Del F (n=6)

Figure A.2

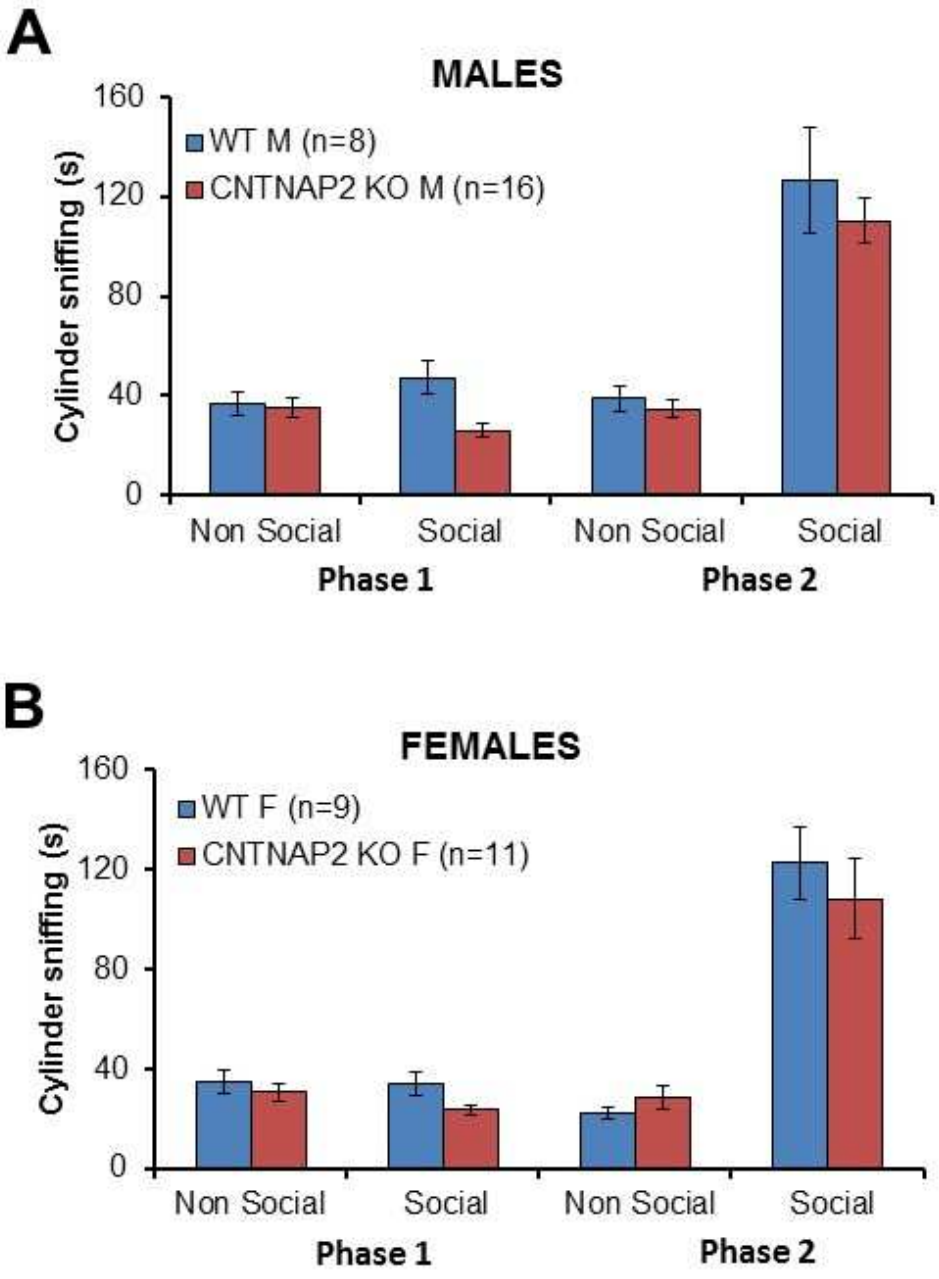
A
MALES
WT M (n=8)
CNTNAP2 KO M (n=16)
Cylinder sniffing (s)
160
120
80
40
0
Non Social
Social
Non Social
Social
Phase 1
Phase 2
B
FEMALES
WT F (n=9)
CNTNAP2 KO F (n=11)
Cylinder sniffing (s)
160
120
80
40
0
Non Social
Social
Non Social
Social
Phase 1
Phase 2

Figure A.3

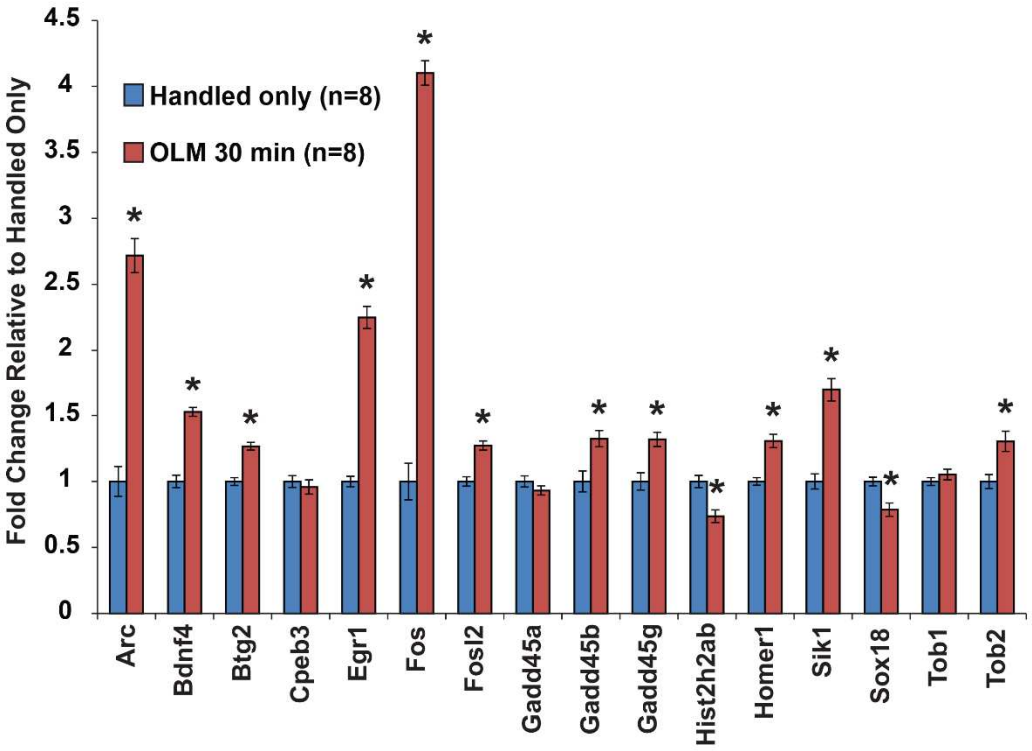
Fold Change Relative to Handled Only
4.5
4
3.5
3
2.5
2
1.5
1
0.5
0
Handled only (n=8)
OLM 30 min (n=8)
*
Arc
Bdnf4
Btg2
Cpeb3
Egr1
Fos
Fosl2
Gadd45a
Gadd45b
Gadd45g
Hist2h2ab
Homer1
Sik1
Sox18
Tob1
Tob2

Figure A.4

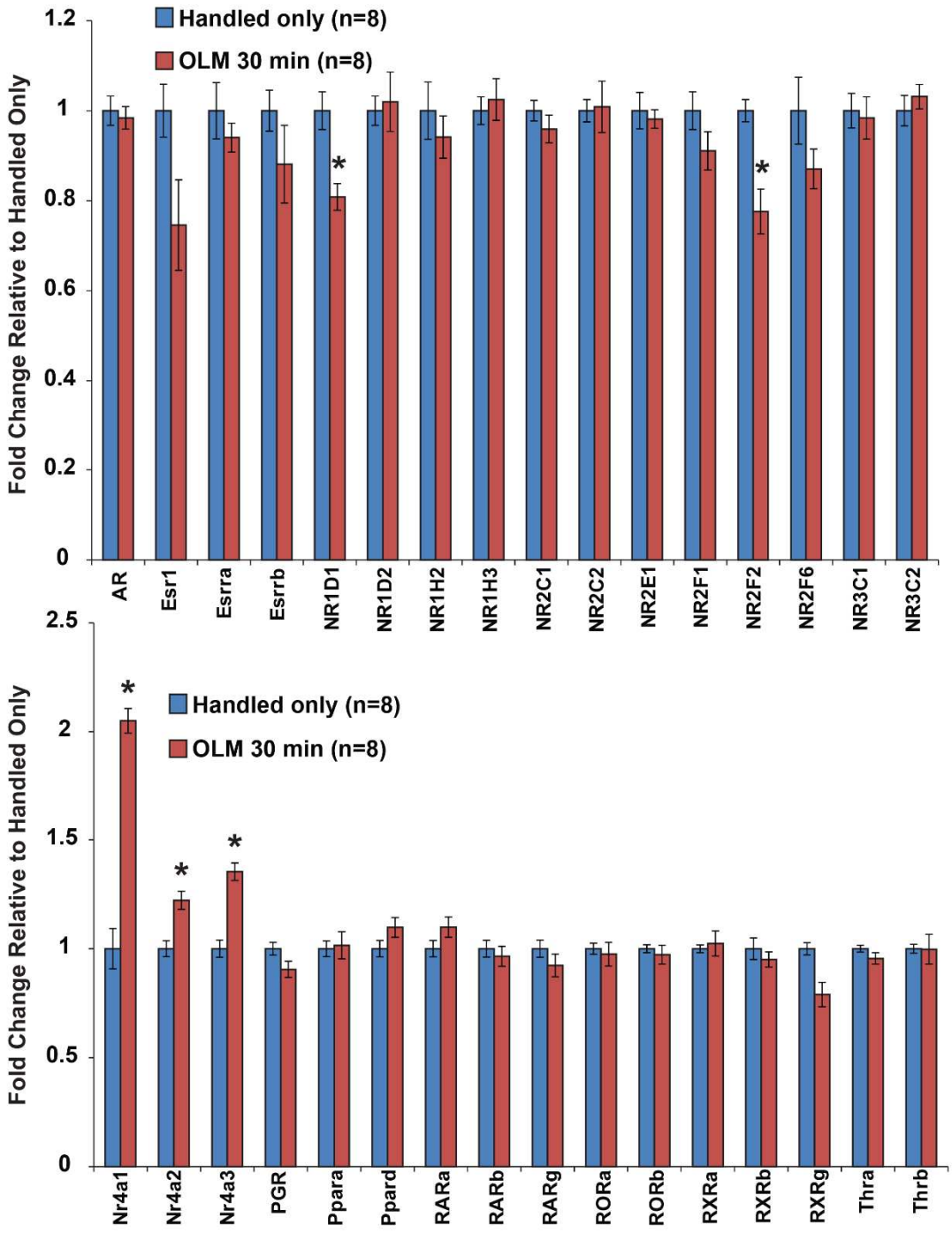
Handled only (n=8)
OLM 30 min (n=8)
Fold Change Relative to Handled Only
1.2
1
0.8
0.6
0.4
0.2
0
AR
Esr1
Esrra
Esrrb
NR1D1
NR1D2
NR1H2
NR1H3
NR2C1
NR2C2
NR2E1
NR2F1
NR2F2
NR2F6
NR3C1
NR3C2
Handled only (n=8)
OLM 30 min (n=8)
Fold Change Relative to Handled Only
2.5
2
1.5
1
0.5
0
Nr4a1
Nr4a2
Nr4a3
PGR
Ppara
Ppard
RARa
RARb
RARg
RORa
RORb
RXRa
RXRb
RXRg
Thra
Thrb

Figure A.5

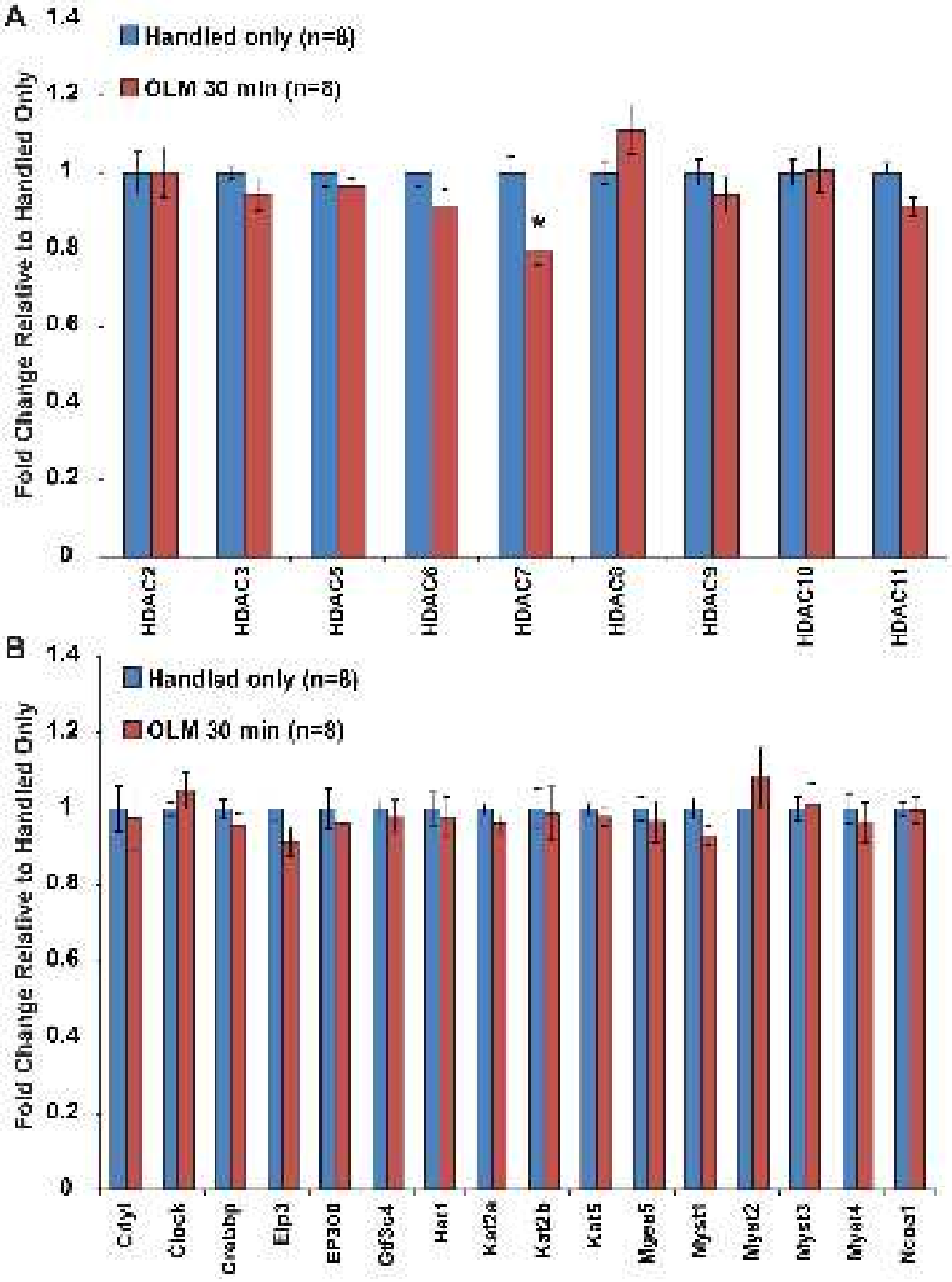
A
Handled only (n=8)
OLM 30 min (n=8)
Fold Change Relative to Handled Only
1.4
1.2
1
0.8
0.6
0.4
0.2
0
*
HDAC2
HDAC3
HDAC5
HDAC6
HDAC7
HDAC8
HDAC9
HDAC10
HDAC11
B
Handled only (n=8)
OLM 30 min (n=8)
Fold Change Relative to Handled Only
Crlyl
Clock
Crebbp
Elp3
EP300
Gtf3c4
Hat1
Kat2a
Kat2b
Kat5
Mgea5
Myst1
Myst2
Myst3
Myst4
Ncoa1

Figure A.6

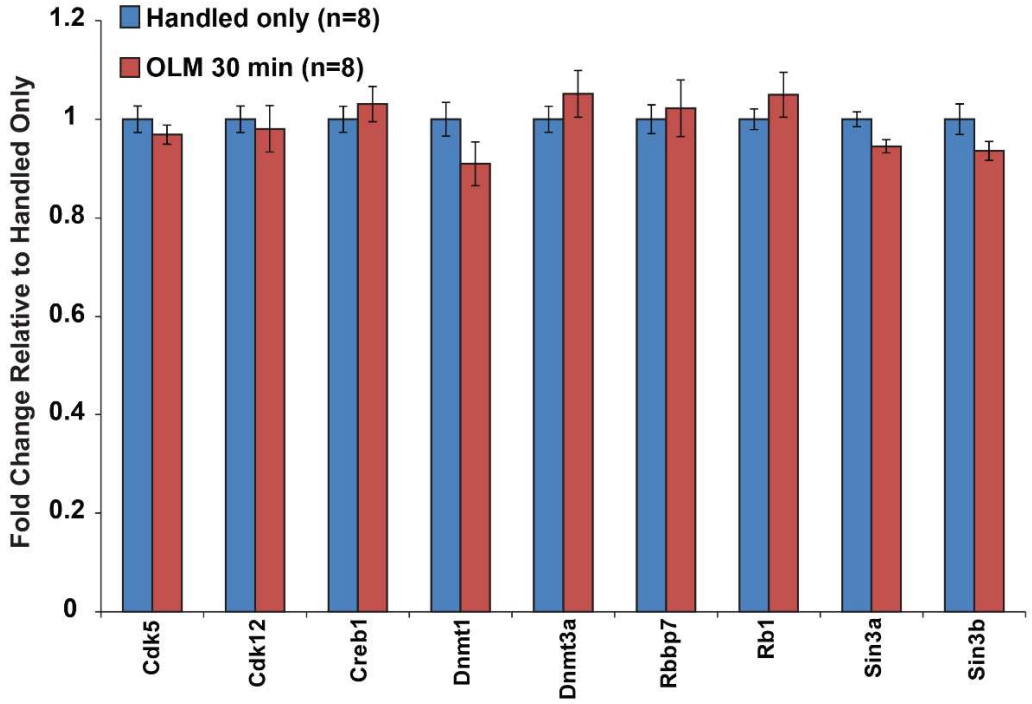
Handled only (n=8)
OLM 30 min (n=8)
Fold Change Relative to Handled Only
1.2
1
0.8
0.6
0.4
0.2
0
Cdk5
Cdk12
Creb1
Dnmt1
Dnmt3a
Rbbp7
Rb1
Sin3a
Sin3b

Figure A.7

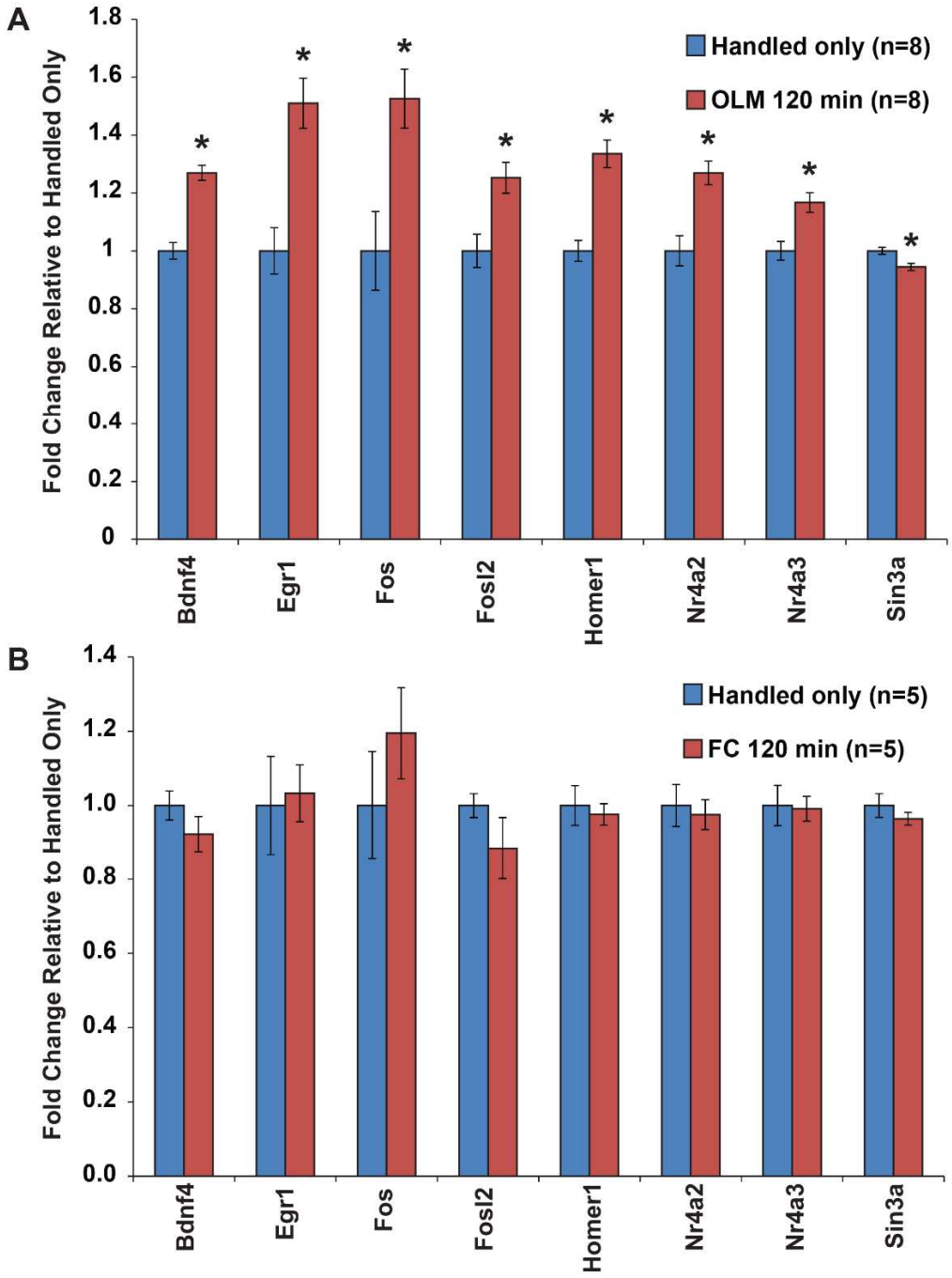
A
Fold Change Relative to Handled Only
1.8
1.6
1.4
1.2
1
0.8
0.6
0.4
0.2
0
Handled only (n=8)
OLM 120 min (n=8)
*
Bdnf4
Egr1
Fos
Fosl2
Homer1
Nr4a2
Nr4a3
Sin3a
B
Fold Change Relative to Handled Only
1.4
1.2
1.0
0.8
0.6
0.4
0.2
0.0
Handled only (n=5)
FC 120 min (n=5)
Bdnf4
Egr1
Fos
Fosl2
Homer1
Nr4a2
Nr4a3
Sin3a

Figure A.8

BIBLIOGRAPHY

Abel, T., Nguyen, P., Barad, M., & Deuel, T. (1997). Genetic demonstration of a role for PKA in the late phase of LTP and in hippocampus-based long-term memory. Cell, 88, 615–626.

Abel, T., & Zukin, R. S. (2008). Epigenetic targets of HDAC inhibition in neurodegenerative and psychiatric disorders. Current Opinion in Pharmacology, 8(1), 57–64. doi:10.1016/j.coph.2007.12.002

Aisner, R., & Terkel, J. (1992). Ontogeny of pine cone opening behaviour in the black rat, Rattus rattus. Animal Behaviour, 327–336.

Akbarian, S., & Huang, H.-S. (2009). Epigenetic regulation in human brain-focus on histone lysine methylation. Biological Psychiatry, 65(3), 198–203. doi:10.1016/j.biopsych.2008.08.015

Alarcón, J. M., Malleret, G., Touzani, K., Vronskaya, S., Ishii, S., Kandel, E. R., & Barco, A. (2004). Chromatin acetylation, memory, and LTP are impaired in CBP+/- mice: a model for the cognitive deficit in Rubinstein-Taybi syndrome and its amelioration. Neuron, 42(6), 947–59. doi:10.1016/j.neuron.2004.05.021

Alarcón, M., Abrahams, B., & Stone, J. (2008). Linkage, Association, and Gene-Expression Analyses Identify CNTNAP2 as an Autism-Susceptibility Gene. The American Journal of Human Genetics, (January), 150–159. doi:10.1016/j.ajhg.2007.09.005.

Allan, A. M., Liang, X., Luo, Y., Pak, C., Li, X., Szulwach, K. E., Zhao, X. (2008). The loss of methyl-CpG binding protein 1 leads to autism-like behavioral deficits. Human Molecular Genetics, 17(13), 2047–57. doi:10.1093/hmg/ddn102

Allen, H. F., Wade, P. a, & Kutateladze, T. G. (2013). The NuRD architecture. Cellular and Molecular Life Sciences: CMLS. doi:10.1007/s00018-012-1256-2

Andrés, M. E., Burger, C., Peral-Rubio, M. J., Battaglioli, E., Anderson, M. E., Grimes, J., … Mandel, G. (1999). CoREST: a functional corepressor required for regulation of neural-specific gene expression. Proceedings of the National Academy of Sciences of the United States of America, 96(17), 9873–8.

Anwyl, R. (2009). Metabotropic glutamate receptor-dependent long-term potentiation. Neuropharmacology, 56(4), 735–740. doi:10.1016/j.neuropharm.2009.01.002

Aoki E, Kimura R, Suzuki ST, Hirano S (2003) Distribution of OL-protocadherin protein in correlation with specific neural compartments and local circuits in the postnatal mouse brain. Neuroscience 117:593-614.

Arking, D. E., Cutler, D. J., Brune, C. W., Teslovich, T. M., West, K., Ikeda, M., … Chakravarti, A. (2008). A Common Genetic Variant in the Neurexin Superfamily Member CNTNAP2 Increases Familial Risk of Autism. American Journal of Human Genetics, (1), 160–164. doi:10.1016/j.ajhg.2007.09.015.

Ayala, J. E., Chen, Y., Banko, J. L., Sheffler, D. J., Williams, R., Telk, A. N., … Conn, P. J. (2009). mGluR5 positive allosteric modulators facilitate both hippocampal LTP and LTD and enhance spatial learning. Neuropsychopharmacology: Official Publication of the American College of Neuropsychopharmacology, 34(9), 2057–71. doi:10.1038/npp.2009.30

Bahari-Javan, S., Maddalena, A., Kerimoglu, C., Wittnam, J., Held, T., Bähr, M., Sananbenesi, F. (2012). HDAC1 regulates fear extinction in mice. The Journal of Neuroscience : The Official Journal of the Society for Neuroscience, 32(15), 5062–73. doi:10.1523/JNEUROSCI.0079-12.2012

Ballas, N., Grunseich, C., Lu, D. D., Speh, J. C., & Mandel, G. (2005). REST and its corepressors mediate plasticity of neuronal gene chromatin throughout neurogenesis. Cell, 121(4), 645–57. doi:10.1016/j.cell.2005.03.013

Balleine, B., & Dickinson, A. (1998). Goal-directed instrumental action: contingency and incentive learning and their cortical substrates. Neuropharmacology, 37, 407–419. Retrieved from http://www.sciencedirect.com/science/article/pii/S0028390898000331

Balschun, D., Zuschratter, W., & Wetzel, W. (2006). Allosteric enhancement of metabotropic glutamate receptor 5 function promotes spatial memory. Neuroscience, 142(3), 691–702. doi:10.1016/j.neuroscience.2006.06.043

Bannister, A. J., & Kouzarides, T. (2011). Regulation of chromatin by histone modifications. Cell Research, 21(3), 381–95. doi:10.1038/cr.2011.22

Bassell, G. J., & Warren, S. T. (2008). Fragile X syndrome: loss of local mRNA regulation alters synaptic development and function. Neuron, 60(2), 201–14. doi:10.1016/j.neuron.2008.10.004

Belmonte, M. K., Cook, E. H., Anderson, G. M., Rubenstein, J. L. R., Greenough, W. T., Beckel-Mitchener, a, … Tierney, E. (2004). Autism as a disorder of neural information processing: directions for research and targets for therapy. Molecular Psychiatry, 9(7), 646–63. doi:10.1038/sj.mp.4001499

Bernardet, M., & Crusio, W. E. (2006). Fmr1 KO mice as a possible model of autistic features. TheScientificWorldJournal, 6, 1164–76. doi:10.1100/tsw.2006.220

Bhakar, A. L., Dölen, G., & Bear, M. F. (2012). The pathophysiology of fragile X (and what it teaches us about synapses). Annual Review of Neuroscience, 35, 417–43. doi:10.1146/annurev-neuro-060909-153138

Bhattacharya, A., Kaphzan, H., Alvarez-Dieppa, A. C., Murphy, J. P., Pierre, P., & Klann, E. (2012). Genetic removal of p70 S6 kinase 1 corrects molecular, synaptic, and behavioral phenotypes in fragile X syndrome mice. Neuron, 76(2), 325–37. doi:10.1016/j.neuron.2012.07.022

Bono, G., Fancellu, R., Blandini, F., Santoro, G., & Mauri, M. (2004). Cognitive and affective status in mild hypothyroidism and interactions with L-thyroxine treatment. Acta Neurologica Scandinavica, 110(1), 59–66. doi:10.1111/j.1600-0404.2004.00262.x

Borrelli, E., Nestler, E. J., Allis, C. D., & Sassone-Corsi, P. (2008). Decoding the epigenetic language of neuronal plasticity. Neuron, 60(6), 961–74. doi:10.1016/j.neuron.2008.10.012

Bottai, D., Guzowski, J. F., Schwarz, M. K., Kang, S. H., Xiao, B., Lanahan, A., … Seeburg, P. H. (2002). Synaptic activity-induced conversion of intronic to exonic sequence in Homer 1 immediate early gene expression. The Journal of Neuroscience : The Official Journal of the Society for Neuroscience, 22(1), 167–75.

Boulware, M. I., Weick, J. P., Becklund, B. R., Kuo, S. P., Groth, R. D., & Mermelstein, P. G. (2005). Estradiol activates group I and II metabotropic glutamate receptor signaling, leading to opposing influences on cAMP response element-binding protein. The Journal of Neuroscience : The Official Journal of the Society for Neuroscience, 25(20), 5066–78. doi:10.1523/JNEUROSCI.1427-05.2005

Bourtchouladze, R., Abel, T., Berman, N., Gordon, R., Lapidus, K., & Kandel, E. R. (1998). Different Training Procedures Recruit Either One or Two Critical Periods for Contextual Memory Consolidation , Each of Which Requires Protein Synthesis and PKA. doi:10.1101/lm.5.4.365

Britten, C. (2004). Targeting ErbB receptor signaling: a pan-ErbB approach to cancer. Molecular Cancer Therapeutics, 1335–1342.

Brodkin ES, Hagemann A, Nemetski SM, Silver LM (2004) Social approach-avoidance behavior of inbred mouse strains towards DBA/2 mice. Brain Research 1002:151-157.

Brown, A., & Derkits, E. (2010). Prenatal infection and schizophrenia: a review of epidemiologic and translational studies. American Journal of Psychiatry, (March), 261–280.

Bruchey, A. K., Jones, C. E., & Monfils, M.-H. (2010). Fear conditioning by-proxy: social transmission of fear during memory retrieval. Behavioural Brain Research, 214(1), 80–4. doi:10.1016/j.bbr.2010.04.047

Bucan M, Abrahams BS, Wang K, Glessner JT, Herman EI, Sonnenblick LI, Alvarez Retuerto AI, Imielinski M, al. e (2009) Genome-wide analyses of exonic copy number variants in a family-based study point to novel autism susceptibility genes. PLoS Genetics 5:e1000536.

Burbach, J., & Zwaag, B. Van Der. (2009). Contact in the genetics of autism and schizophrenia. Trends in Neurosciences, 15–18. Retrieved from http://www.sciencedirect.com/science/article/pii/S016622360800266X

Chahrour, M., Jung, S. Y., Shaw, C., Zhou, X., Wong, S. T. C., Qin, J., & Zoghbi, H. Y. (2008). MeCP2, a key contributor to neurological disease, activates and represses transcription. Science (New York, N.Y.), 320(5880), 1224–9. doi:10.1126/science.1153252

Chapman NH, Estes A, Munson J, Bernier R, Webb SJ, Rothstein JH, Minshew NJ, Dawson G, Schellenberg GD, Wijsman EM (2011) Genome scan for IQ discrepancy in autism: evidence for loci on chromsomes 10 and 16. Human Genetics 129:59-70.

Chen, W. G., Chang, Q., Lin, Y., Meissner, A., West, A. E., Griffith, E. C., … Greenberg, M. E. (2003). Derepression of BDNF transcription involves calcium-dependent phosphorylation of MeCP2. Science (New York, N.Y.), 302(5646), 885–9. doi:10.1126/science.1086446

Chen, Y.-J. J., Johnson, M. a, Lieberman, M. D., Goodchild, R. E., Schobel, S., Lewandowski, N., … Role, L. W. (2008). Type III neuregulin-1 is required for normal sensorimotor gating, memory-related behaviors, and corticostriatal circuit components. The Journal of Neuroscience : The Official Journal of the Society for Neuroscience, 28(27), 6872–83. doi:10.1523/JNEUROSCI.1815-08.2008

Chevallier C, Kohls G, Troiani V, Brodkin ES, Schultz RT (2012) The social motivation theory of autism. Trends in Cognitive Sciences 16:231-239.

Codina, A., Benoit, G., Gooch, J. T., Neuhaus, D., Perlmann, T., & Schwabe, J. W. R. (2004). Identification of a novel co-regulator interaction surface on the ligand binding domain of Nurr1 using NMR footprinting. The Journal of Biological Chemistry, 279(51), 53338–45. doi:10.1074/jbc.M409096200

Cole, C. J., Mercaldo, V., Restivo, L., Yiu, A. P., Sekeres, M. J., Han, J.-H., … Josselyn, S. a. (2012). MEF2 negatively regulates learning-induced structural plasticity and memory formation. Nature Neuroscience, 15(9), 1255–64. doi:10.1038/nn.3189

Collins, A. L., Levenson, J. M., Vilaythong, A. P., Richman, R., Armstrong, D. L., Noebels, J. L., … Zoghbi, H. Y. (2004). Mild overexpression of MeCP2 causes a progressive neurological disorder in mice. Human Molecular Genetics, 13(21), 2679–89. doi:10.1093/hmg/ddh282

Comer, F., & Hart, G. (2001). Reciprocity between O-GlcNAc and O-phosphate on the carboxyl terminal domain of RNA polymerase II. Biochemistry, 7845–7852.

Cowley, S., Iritani, B., Mendrysa, S., Xu, T., Cheng, P., Yada, J., … Eisenman, R. N. (2005). The mSin3A chromatin-modifying complex is essential for embryogenesis and T-cell development. Molecular and Cellular Biology. doi:10.1128/MCB.25.16.6990

Crawford, D., Acuña, J., & Sherman, S. (2001). FMR1 and the fragile X syndrome: human genome epidemiology review. Genetics in Medicine, 3(5), 359–371.

Crawley JN (2007) What's Wrong With My Mouse: Behavioral Phenotyping of Transgenic and Knockout Mice. Hoboken, New Jersey: John Wiley & Sons.

Cukier, H. N., Lee, J. M., Ma, D., Young, J. I., Mayo, V., Butler, B. L., Gilbert, J. R. (2012). The expanding role of MBD genes in autism: identification of a MECP2 duplication and novel alterations in MBD5, MBD6, and SETDB1. Autism Research : Official Journal of the International Society for Autism Research, 5(6), 385–97. doi:10.1002/aur.1251

Cukier, H. N., Rabionet, R., Konidari, I., Rayner-Evans, M. Y., Baltos, M. L., Wright, H. H., … Gilbert, J. R. (2010). Novel variants identified in methyl-CpG-binding domain genes in autistic individuals. Neurogenetics, 11(3), 291–303. doi:10.1007/s10048-009-0228-7

Dannenberg, J.-H., David, G., Zhong, S., van der Torre, J., Wong, W. H., & DePinho, R. a. (2005). mSin3A corepressor regulates diverse transcriptional networks governing normal and neoplastic growth and survival. Genes & Development, 19(13), 1581–95. doi:10.1101/gad.1286905

Dawson G, Carver L, Meltzoff AN, Panagiotides H, McPartland J, Webb SJ (2002) Neural correlates of face and object recognition in young children with autism spectrum disorder, developmental delay, and typical development. Child Development 73:700-717.

Dawson, G., Rogers, S., Munson, J., Smith, M., Winter, J., Greenson, J., Donaldson, A., Varley J. (2010) Randomized, controlled trial of an intervention for toddlers with autism: the Early Start Denver Model. 125:17-23

David, G., Turner, G. M., Yao, Y., Protopopov, A., & DePinho, R. a. (2003). mSin3-associated protein, mSds3, is essential for pericentric heterochromatin formation and chromosome segregation in mammalian cells. Genes & Development, 17(19), 2396–405. doi:10.1101/gad.1109403

De Vries, G.J., Fields, C.T., Peters, N.V., Whylings, J., Paul, M.J. (2014) Sensitive periods for hormonal programming of the brain. Current Topics and Behavioral Neuroscience 16:79-108

Del Abril, A., Segovia, S., Guillamon, A. (1987) The bed nucleus of the stria terminalis in the rat: regional sex differences controlled by gonadal steroids after birth. Developmental Brain Research 32:295-300

Dewing, P., Shi, T., Horvath, S., Vilain, E. (2003) Sexually dimorphic gene expression in mouse brain precedes gonadal differentiation. Molecular Brain Research 118:82-90

Dewing, P., Chiang, C.W.K., Sinchak, K., Chesselet, M., Micevych, P.E., Albrecht, K.H., Harley, V.R., Vilain, E. (2006) Direct regulation of adult brain function by the male specific factor SRY. Current Biology 16:415-20

Dictenberg, J. B., Swanger, S. a, Antar, L. N., Singer, R. H., & Bassell, G. J. (2008). A direct role for FMRP in activity-dependent dendritic mRNA transport links filopodial-spine morphogenesis to fragile X syndrome. Developmental Cell, 14(6), 926–39. doi:10.1016/j.devcel.2008.04.003

Dölen, G., Osterweil, E., Rao, B. S. S., Smith, G. B., Auerbach, B. D., Chattarji, S., & Bear, M. F. (2007). Correction of fragile X syndrome in mice. Neuron, 56(6), 955–62. doi:10.1016/j.neuron.2007.12.001

Driscoll, I., Hamilton, D. a, Yeo, R. a, Brooks, W. M., & Sutherland, R. J. (2005). Virtual navigation in humans: the impact of age, sex, and hormones on place learning. Hormones and Behavior, 47(3), 326–35. doi:10.1016/j.yhbeh.2004.11.013

Ebert, D. H., Gabel, H. W., Robinson, N. D., Kastan, N. R., Hu, L. S., Cohen, S., … Greenberg, M. E. (2013). Activity-dependent phosphorylation of MeCP2 threonine 308 regulates interaction with NCoR. Nature, 499(7458), 341–5. doi:10.1038/nature12348

Egan, M., Goldberg, T., & Gscheidle, T. (2001). Relative risk for cognitive impairments in siblings of patients with schizophrenia. Biological …, 3223(01). Retrieved from http://www.sciencedirect.com/science/article/pii/S0006322301011337

Ehrlichman, R. S., Luminais, S. N., White, S. L., Rudnick, N. D., Ma, N., Dow, H. C., … Siegel, S. J. (2010). Neuregulin 1 transgenic miec display reduced mismatch negativity, contextual fear conditioning, and social interactions. Brain Research Bulletin, 116–127. doi:10.1016/j.brainres.2009.07.065.Neuregulin

Elis, O., Caponigro, J., & Kring, A. (2013). Psychosocial treatments for negative symptoms in schizophrenia: Current practices and future directions. Clinical Psychology Review. S0272735813000895

Ey, E., Leblond, C. S., & Bourgeron, T. (2011). Behavioral profiles of mouse models for autism spectrum disorders. Autism Research: Official Journal of the International Society for Autism Research, 4(1), 5–16. doi:10.1002/aur.175

Fairless AH, Shah RY, Guthrie AJ, Li H, Brodkin ES (2011) Deconstructing sociability, an autism-relevant phenotype, in mouse models. The Anatomical Record (Special Issue: “New Concepts in Developing Brain Disorders--Autism”) 294:1713-1725.

Fairless AH, Dow HC, Kreibich AS, Torre M, Kuruvilla M, Gordon E, Morton EA, Tan J, Berrettini WH, Li H, Abel T, Brodkin ES (2012) Sociability and brain development in BALB/cJ and C57BL/6J mice. Behavioural Brain Research 228:299-310.

Fischer, A., Sananbenesi, F., Mungenast, A., & Tsai, L.-H. (2010). Targeting the correct HDAC(s) to treat cognitive disorders. Trends in Pharmacological Sciences, 31(12), 605–17. doi:10.1016/j.tips.2010.09.003

Fischer, A., Sananbenesi, F., Wang, X., Dobbin, M., & Tsai, L.-H. (2007). Recovery of learning and memory is associated with chromatin remodelling. Nature, 447(7141), 178–82. doi:10.1038/nature05772

Fisher, E.M.C., Bear-Romero, P., Brown, L.G., Ridley, A., McNeill, J.A., Lawrence, J.B., Willard, H.F., Bieber, F.R., Page, D.C. (1990) Homologous ribosomal protein genes on the human X and Y chromosomes: Escape from X inactivation and possible implications for Turner Syndrome. Cell 83:1205-18

Flavell, S. W., Kim, T.-K., Gray, J. M., Harmin, D. a, Hemberg, M., Hong, E. J., … Greenberg, M. E. (2008). Genome-wide analysis of MEF2 transcriptional program reveals synaptic target genes and neuronal activity-dependent polyadenylation site selection. Neuron, 60(6), 1022–38. doi:10.1016/j.neuron.2008.11.029

Fuller, R., & Nopoulos, P. (2002). Longitudinal assessment of premorbid cognitive functioning in patients with schizophrenia through examination of standardized scholastic test performance. American Journal of Psychiatry, (July), 1183–1189.

Gangoda, L., Doerflinger, M., Lee, Y. Y., Rahimi, a, Etemadi, N., Chau, D., … Puthalakath, H. (2012). Cre transgene results in global attenuation of the cAMP/PKA pathway. Cell Death & Disease, 3, e365. doi:10.1038/cddis.2012.110

Gao, H., Lukin, K., Ramírez, J., Fields, S., Lopez, D., & Hagman, J. (2009). Opposing effects of SWI/SNF and Mi-2/NuRD chromatin remodeling complexes on epigenetic reprogramming by EBF and Pax5. Proceedings of the National Academy of Sciences of the United States of America, 106(27), 11258–63. doi:10.1073/pnas.0809485106

Gao, R., Zhang, J., Cheng, L., Wu, X., Dong, W., Yang, X., Zhou, M. (2010). A Phase II, randomized, double-blind, multicenter, based on standard therapy, placebo-controlled study of the efficacy and safety of recombinant human neuregulin-1 in patients with chronic heart failure. Journal of the American College of Cardiology, 55(18), 1907–14. doi:10.1016/j.jacc.2009.12.044

Gerstein, H., O'Riordan, K., Osting, S., Schwarz, M. K., & Burger, C. (2012). Rescue of synaptic plasticity and spatial learning deficits in the hippocampus of Homer1 knockout mice by recombinant Adeno-associated viral gene delivery of Homer1c. Neurobiology of Learning and Memory, 97(1), 17–29. doi:10.1016/j.nlm.2011.08.009

Geurts, A., Cost, G., Freyvert, Y., & Zeitler, B. (2009). Knockout rats via embryo microinjection of zinc-finger nucleases. Science, 2793. Retrieved from http://www.sciencemag.org/content/325/5939/433.short

Gilbert, M. E., & Lasley, S. M. (2013). Developmental thyroid hormone insufficiency and brain development: a role for brain-derived neurotrophic factor (BDNF) Neuroscience, 239, 253–70. doi:10.1016/j.neuroscience.2012.11.022

Gresack, J. E., Schafe, G. E., Orr, P. T., & Frick, K. M. (2009). Sex differences in contextual fear conditioning are associated with differential ventral hippocampal extracellular signal-regulated kinase activation. Neuroscience, 159(2), 451–67. doi:10.1016/j.neuroscience.2009.01.009

Grossman, A. W., Elisseou, N. M., McKinney, B. C., & Greenough, W. T. (2006). Hippocampal pyramidal cells in adult Fmr1 knockout mice exhibit an immature-appearing profile of dendritic spines. Brain Research, 1084(1), 158–64. doi:10.1016/j.brainres.2006.02.044

Grzenda, A., Lomberk, G., Zhang, J.-S., & Urrutia, R. (2009). Sin3: master scaffold and transcriptional corepressor. Biochimica et Biophysica Acta, 1789(6-8), 443–50. doi:10.1016/j.bbagrm.2009.05.007

Gu, Z., Jiang, Q., Fu, A. K. Y., Ip, N. Y., & Yan, Z. (2005). Regulation of NMDA receptors by neuregulin signaling in prefrontal cortex. The Journal of Neuroscience: The Official Journal of the Society for Neuroscience, 25(20), 4974–84. doi:10.1523/JNEUROSCI.1086-05.2005

Guan, J.-S., Haggarty, S. J., Giacometti, E., Dannenberg, J.-H., Joseph, N., Gao, J., Tsai, L.-H. (2009a). HDAC2 negatively regulates memory formation and synaptic plasticity. Nature, 459(7243), 55–60. doi:10.1038/nature07925

Gunaydin, L.A., Grosenick, L., Finkelstein, J.C., Kauvar, I.V., Fenno, L.E., Adhikari, A., Lammel, S., Mirzabekov, J.J., Airan, R.D.,…Deisseroth, K. (2014) Natural neural projection dynamics underlying social behavior. Cell 157(7):1535-51

Gupta, S., Kim, S. Y., Artis, S., Molfese, D. L., Schumacher, A., Sweatt, J. D., Lubin, F. D. (2010). Histone methylation regulates memory formation. The Journal of Neuroscience: The Official Journal of the Society for Neuroscience, 30(10), 3589–99. doi:10.1523/JNEUROSCI.3732-09.2010

Guy, J., Cheval, H., Selfridge, J., & Bird, A. (2011). The role of MeCP2 in the brain. Annual Review of Cell and Developmental Biology, 27, 631–52. doi:10.1146/annurev-cellbio-092910-154121

Hakimi, M.-A., Bochar, D. a, Chenoweth, J., Lane, W. S., Mandel, G., & Shiekhattar, R. (2002). A core-BRAF35 complex containing histone deacetylase mediates repression of neuronal-specific genes. Proceedings of the National Academy of Sciences of the United States of America, 99(11), 7420–5. doi:10.1073/pnas.112008599

Hallahan, B. P., Craig, M. C., Toal, F., Daly, E. M., Moore, C. J., Ambikapathy, A., Murphy, D. G. M. (2011). In vivo brain anatomy of adult males with Fragile X syndrome: an MRI study. NeuroImage, 54(1), 16–24. doi:10.1016/j.neuroimage.2010.08.015

Han, J., Mark, M. D., Li, X., Xie, M., Waka, S., Rettig, J., & Herlitze, S. (2006). RGS2 determines short-term synaptic plasticity in hippocampal neurons by regulating Gi/o-mediated inhibition of presynaptic Ca2+ channels. Neuron, 51(5), 575–86. doi:10.1016/j.neuron.2006.07.012

Hanahan, D., Wagner, E. F., & Palmiter, R. D. (2007). The origins of oncomice: a history of the first transgenic mice genetically engineered to develop cancer. Genes & Development, 21(18), 2258–70. doi:10.1101/gad.1583307

Havekes, R., Canton, D. a, Park, A. J., Huang, T., Nie, T., Day, J. P., … Abel, T. (2012). Gravin orchestrates protein kinase A and β2-adrenergic receptor signaling critical for synaptic plasticity and memory. The Journal of Neuroscience: The Official Journal of the Society for Neuroscience, 32(50), 18137–49. doi:10.1523/JNEUROSCI.3612-12.2012

Hawk, J., Bookout, A., Poplawski, S., Bridi, M., Rao, A., Sulewski, M., … Abel, T. (2012). NR4A nuclear receptors support memory enhancement by histone deacetylase inhibitors. The Journal of Clinical Investigation 122(10). doi:10.1172/JCI64145.a

Hawk, J. D., & Abel, T. (2011). The role of NR4A transcription factors in memory formation. Brain Research Bulletin, 85(1-2), 21–9. doi:10.1016/j.brainresbull.2011.02.001

Hendrich, B., Guy, J., Ramsahoye, B., Wilson, V. a, & Bird, a. (2001). Closely related proteins MBD2 and MBD3 play distinctive but interacting roles in mouse development. Genes & Development, 15(6), 710–23. doi:10.1101/gad.194101

Hessl, D., Rivera, S., Koldewyn, K., Cordeiro, L., Adams, J., Tassone, F., … Hagerman, R. J. (2007). Amygdala dysfunction in men with the fragile X premutation. Brain□: A Journal of Neurology, 130(Pt 2), 404–16. doi:10.1093/brain/awl338

Hirano S, Yan Q, Suzuki ST (1999) Expression of a novel protocadherin, OL-protocadherin, in a subset of functional system of the developing mouse brain. The Journal of Neuroscience 19:995-1005.

Hite, K. C., Adams, V. H., & Hansen, J. C. (2010). Recent advances in MeCP2 structure and function. Biochem Cell Biol., 87(1), 219–227. doi:10.1139/o08-115.

Hörlein, A., Näär, A., Heinzel, T., & Torchia, J. (1995). Ligand-independent repression by the thyroid hormone receptor mediated by a nuclear receptor co-repressor. Nature. Retrieved from http://www.nature.com/nature/journal/v377/n6548/abs/377397a0.html

Huber, K. (2002). Altered synaptic plasticity in a mouse model of fragile X mental retardation. Proceedings of the National Academy of Science. Retrieved from http://www.pnas.org/content/99/11/7746.short

Humphrey, G. W., Wang, Y., Russanova, V. R., Hirai, T., Qin, J., Nakatani, Y., & Howard, B. H. (2001). Stable histone deacetylase complexes distinguished by the presence of SANT domain proteins CoREST/kiaa0071 and Mta-L1. The Journal of Biological Chemistry, 276(9), 6817–24. doi:10.1074/jbc.M007372200

Igaz, L. M., Vianna, M. R. M., Medina, J. H., & Izquierdo, I. (2002). Two Time Periods of Hippocampal mRNA Synthesis Are Required for Memory Consolidation of Fear-Motivated Learning. J Neurosci, 22(15), 6781–6789.

Iliff, A. J., Renoux, A. J., Krans, A., Usdin, K., Sutton, M. a, & Todd, P. K. (2013). Impaired activity-dependent FMRP translation and enhanced mGluR-dependent LTD in Fragile X premutation mice. Human Molecular Genetics, 22(6), 1180–92. doi:10.1093/hmg/dds525

Ishizuka, T., & Lazar, M. a. (2005). The nuclear receptor corepressor deacetylase activating domain is essential for repression by thyroid hormone receptor. Molecular Endocrinology (Baltimore, Md.), 19(6), 1443–51. doi:10.1210/me.2005-0009

Jacquemont, S., Berry-Kravis, E., Hagerman, R., von Raison, F., Gasparini, F., Apostol, G., Gomez-Mancilla, B. (2014). The challenges of clinical trials in fragile X syndrome. Psychopharmacology, 231(6), 1237–50. doi:10.1007/s00213-013-3289-0

Janzen, D., & Nguyen, M. (2010). Beyond executive function: non-executive cognitive abilities in individuals with PKU. Molecular Genetics and Metabolism, 99 Suppl 1, S47–51. doi:10.1016/j.ymgme.2009.10.009

Jaubert, P., & Golub, M. (2007). Complex, multimodal behavioral profile of the Homer1 knockout mouse. Genes, Brain and …, 141–154. doi:10.1111/j.1601-183X.2006.00240.x

Jia, Z., Lu, Y., Henderson, J., Taverna, F., Romano, C., Abramow-Newerly, W., Roder, J. (1998). Selective Abolition of the NMDA Component of Long-Term Potentiation in Mice Lacking mGluR5. Learning & Memory, 5(4), 331–343.

Jiang, Y., Jakovcevski, M., Bharadwaj, R., Connor, C., Schroeder, F. a, Lin, C. L., Akbarian, S. (2010). Setdb1 histone methyltransferase regulates mood-related behaviors and expression of the NMDA receptor subunit NR2B. The Journal of Neuroscience: The Official Journal of the Society for Neuroscience, 30(21), 7152–67. doi:10.1523/JNEUROSCI.1314-10.2010

Jiang, Y., Matevossian, A., Guo, Y., & Akbarian, S. (2011). Setdb1-mediated histone H3K9 hypermethylation in neurons worsens the neurological phenotype of Mecp2-deficient mice. Neuropharmacology, 60(7-8), 1088–97. doi:10.1016/j.neuropharm.2010.09.020

Jiang, Z., & Zhou, M. (2010). Neuregulin signaling and heart failure. Current Heart Failure Reports, 7(1), 42–7. doi:10.1007/s11897-010-0003-y

Jones, P. (1997). The early origins of schizophrenia. British Medical Bulletin, 53(1), 135–155.

Jones W, Carr K, Klin A (2008) Absence of preferential looking to the eyes of approaching adults predicts level of social disability in 2-year-old toddlers with autism spectrum disorders. Archives of General Psychiatry 65:946-954.

Jourdain, P., Fukunaga, K., & Muller, D. (2003). Calcium/calmodulin-dependent protein kinase II contributes to activity-dependent filopodia growth and spine formation. The Journal of Neuroscience, 23(33), 10645–10649.

Kammermeier, P. J., & Worley, P. F. (2007). Homer 1a uncouples metabotropic glutamate receptor 5 from postsynaptic effectors. Proceedings of the National Academy of Sciences of the United States of America, 104(14), 6055–60. doi:10.1073/pnas.0608991104

Kato, S., Yokoyama, A., & Fujiki, R. (2011). Nuclear receptor coregulators merge transcriptional coregulation with epigenetic regulation. Trends in Biochemical Sciences, 36(5), 272–81. doi:10.1016/j.tibs.2011.01.001

Kavalali, E. T., Nelson, E. D., & Monteggia, L. M. (2011). Role of MeCP2, DNA methylation, and HDACs in regulating synapse function. Journal of Neurodevelopmental Disorders, 3(3), 250–6. doi:10.1007/s11689-011-9078-3

Kelly, M. P., Stein, J. M., Vecsey, C. G., Favilla, C., Yang, X., Bizily, S. F., … Abel, T. (2009). Developmental etiology for neuroanatomical and cognitive deficits in mice overexpressing Galphas, a G-protein subunit genetically linked to schizophrenia. Molecular Psychiatry, 14(4), 398–415, 347. doi:10.1038/mp.2008.124

Khidekel, N., Ficarro, S. B., Clark, P. M., Bryan, M. C., Swaney, D. L., Rexach, J. E., … Hsieh-Wilson, L. C. (2007). Probing the dynamics of O-GlcNAc glycosylation in the brain using quantitative proteomics. Nature Chemical Biology, 3(6), 339–48. doi:10.1038/nchembio881

Kidd, S. a, Lachiewicz, A., Barbouth, D., Blitz, R. K., Delahunty, C., McBrien, D., … Berry-Kravis, E. (2014). Fragile X Syndrome: A Review of Associated Medical Problems. Pediatrics. doi:10.1542/peds.2013-4301

Kim S-Y, Yasuda S, Tanaka H, Yamagata K, Kim H (2011) Non-clustered protocadherins. Cell Adhesion & Migration 5:1-9.

King, J.A., Barkley, R.A., Delville, Y., Ferris, C.F. (2000) Early androgen treatment decreases cognitive function and catecholamine innervations in an animal model of ADHD. Behavioral Brain Research 107:35-43

Kircher, T., Krug, A., Markov, V., Whitney, C., Krach, S., Zerres, K., … Rietschel, M. (2009). Genetic variation in the schizophrenia-risk gene neuregulin 1 correlates with brain activation and impaired speech production in a verbal fluency task in healthy individuals. Human Brain Mapping, 30(10), 3406–16. doi:10.1002/hbm.20761

Klugmann, M., Symes, C. W., Leichtlein, C. B., Klaussner, B. K., Dunning, J., Fong, D., … During, M. J. (2005). AAV-mediated hippocampal expression of short and long Homer 1 proteins differentially affect cognition and seizure activity in adult rats, 28, 347–360. doi:10.1016/j.mcn.2004.10.002

Ko, T., & Evenden, J. (2009). The effects of psychotomimetic and putative cognitive-enhancing drugs on the performance of a n-back working memory task in rats. Psychopharmacology, 202(1-3), 67–78. doi:10.1007/s00213-008-1314-5

Kotecha, S. a, Jackson, M. F., Al-Mahrouki, A., Roder, J. C., Orser, B. a, & MacDonald, J. F. (2003). Co-stimulation of mGluR5 and N-methyl-D-aspartate receptors is required for potentiation of excitatory synaptic transmission in hippocampal neurons. The Journal of Biological Chemistry, 278(30), 27742–9. doi:10.1074/jbc.M301946200

Kouzarides, T. (2007). Chromatin modifications and their function. Cell, 128(4), 693–705. doi:10.1016/j.cell.2007.02.005

Krug, A., Markov, V., Krach, S., Jansen, A., Zerres, K., Eggermann, T., … Kircher, T. (2010). The effect of Neuregulin 1 on neural correlates of episodic memory encoding and retrieval. NeuroImage, 53(3), 985–91. doi:10.1016/j.neuroimage.2009.12.062

Kundaje, A., Kyriazopoulou-Panagiotopoulou, S., Libbrecht, M., Smith, C. L., Raha, D., Winters, E. E., … Sidow, A. (2012). Ubiquitous heterogeneity and asymmetry of the chromatin environment at regulatory elements. Genome Research, 22(9), 1735–47. doi:10.1101/gr.136366.111

Lakowski, B., Roelens, I., & Jacob, S. (2006). CoREST-like complexes regulate chromatin modification and neuronal gene expression. Journal of Molecular Neuroscience, 29. doi:10.1385/JMN/29

Landa, R. (2007). Social and communication development in toddlers with early and later diagnosis of autism spectrum disorders. Archives of General 64(7), 853–864.

Lanphear, B. P., Hornung, R., Khoury, J., Yolton, K., Baghurst, P., Bellinger, D. C., … Roberts, R. (2005). Low-Level Environmental Lead Exposure and Children's Intellectual Function: An International Pooled Analysis. Environmental Health Perspectives, 113(7), 894–899. doi:10.1289/ehp.7688

Law, A. J., Kleinman, J. E., Weinberger, D. R., & Weickert, C. S. (2007). Disease-associated intronic variants in the ErbB4 gene are related to altered ErbB4 splice-variant expression in the brain in schizophrenia. Human Molecular Genetics, 16(2), 129–41. doi:10.1093/hmg/ddl449

Lee, M. G., Wynder, C., Cooch, N., & Shiekhattar, R. (2005). An essential role for CoREST in nucleosomal histone 3 lysine 4 demethylation. Nature, 437(7057), 432–5. doi:10.1038/nature04021

Levenga, J., Hayashi, S., de Vrij, F. M. S., Koekkoek, S. K., van der Linde, H. C., Nieuwenhuizen, I., … Oostra, B. a. (2011). AFQ056, a new mGluR5 antagonist for treatment of fragile X syndrome. Neurobiology of Disease, 42(3), 311–7. doi:10.1016/j.nbd.2011.01.022

Levenson, J. M., O'Riordan, K. J., Brown, K. D., Trinh, M. A., Molfese, D. L., & Sweatt, J. D. (2004). Regulation of histone acetylation during memory formation in the hippocampus. J Biol Chem, 279(39), 40545–59. doi:10.1074/jbc.M402229200

Li, D., Collier, D. a, & He, L. (2006). Meta-analysis shows strong positive association of the neuregulin 1 (NRG1) gene with schizophrenia. Human Molecular Genetics, 15(12), 1995–2002. doi:10.1093/hmg/ddl122

Li, H., Zhong, X., Chau, K. F., Williams, E. C., & Chang, Q. (2011). Loss of activity-induced phosphorylation of MeCP2 enhances synaptogenesis, LTP and spatial memory. Nature Neuroscience, 14(8), 1001–8. doi:10.1038/nn.2866

Linggi, B., & Carpenter, G. (2006). ErbB receptors: new insights on mechanisms and biology. Trends in Cell Biology, 16(12), 649–56. doi:10.1016/j.tcb.2006.10.008

Lombardo, M.V., Ashwin, E., Auyeung, B., Chakrabarti, B., Taylor, K., Hackett, G., Bullmore, E.T., Baron-Cohen, S. (2012) Fetal testosterone influences sexually dimorphic gray matter in the human brain. The Journal of Neuroscience 32(2): 674-80

Loonstra, A., & Vooijs, M. (2001). Growth inhibition and DNA damage induced by Cre recombinase in mammalian cells. Proceedings of the …, 98(16), 9209–9214. Retrieved from http://www.pnas.org/content/98/16/9209.short

Luscher, C., Nicoll, R., Malenka, R., & Muller, D. (2000). Synaptic plasticity and dynamic modulation of the postsynaptic membrane. Nature Neuroscience, 545–550. Retrieved from http://www.wellwave.net/resources/Grundlagen/Luescher_2000_synaptic_plasticity.pdf

Lyst, M. J., Ekiert, R., Ebert, D. H., Merusi, C., Nowak, J., Selfridge, J., … Bird, A. (2013). Rett syndrome mutations abolish the interaction of MeCP2 with the NCoR/SMRT co-repressor. Nature Neuroscience, 16(7), 898–902. doi:10.1038/nn.3434

MacLusky, N.J., Bowlby, D.A., Brown, T.J., Peterson, R.E., Hochberg, R.B. (1997) Sex and the developing brain: Suppression of neuronal estrogen sensitivity by developmental androgen exposure. Neurochemical Research 22(11):1395-1414

Mahan, A. L., Mou, L., Shah, N., Hu, J.-H., Worley, P. F., & Ressler, K. J. (2012). Epigenetic modulation of Homer1a transcription regulation in amygdala and hippocampus with Pavlovian fear conditioning. J Neurosci, 32(13), 4651–4659. doi:10.1523/JNEUROSCI.3308-11.2012

Manahan-Vaughan, D., & Braunewell, K.-H. (2005). The metabotropic glutamate receptor, mGluR5, is a key determinant of good and bad spatial learning performance and hippocampal synaptic plasticity. Cerebral Cortex (New York, N.Y.: 1991), 15(11), 1703–13. doi:10.1093/cercor/bhi047

Mao, L., Yang, L., Tang, Q., Samdani, S., Zhang, G., & Wang, J. Q. (2005). The scaffold protein Homer1b/c links metabotropic glutamate receptor 5 to extracellular signal-regulated protein kinase cascades in neurons. The Journal of Neuroscience: The Official Journal of the Society for Neuroscience, 25(10), 2741–52. doi:10.1523/JNEUROSCI.4360-04.2005

Maren, S. (2005). Synaptic mechanisms of associative memory in the amygdala. Neuron, 47(6), 783–6. doi:10.1016/j.neuron.2005.08.009

Maren, S., & Fanselow, M. S. (1997). Electrolytic lesions of the fimbria/fornix, dorsal hippocampus, or entorhinal cortex produce anterograde deficits in contextual fear conditioning in rats. Neurobiology of Learning and Memory, 67(2), 142–9. doi:10.1006/nlme.1996.3752

Marshall CR et al. (2008) Structural variation of chromosomes in autism spectrum disorder. The American Journal of Human Genetics 82:477-488.

Martinowich, K., Hattori, D., Wu, H., Fouse, S., He, F., Hu, Y., … Sun, Y. E. (2003). DNA methylation-related chromatin remodeling in activity-dependent BDNF gene regulation. Science (New York, N.Y.), 302(5646), 890–3. doi:10.1126/science.1090842

Maze, I., Noh, K.-M., & Allis, C. D. (2013). Histone regulation in the CNS: basic principles of epigenetic plasticity. Neuropsychopharmacology: Official Publication of the American College of Neuropsychopharmacology, 38(1), 3–22. doi:10.1038/npp.2012.124

McClellan, J. M., Susser, E., & King, M.-C. (2007). Schizophrenia: a common disease caused by multiple rare alleles. The British Journal of Psychiatry: The Journal of Mental Science, 190, 194–9. doi:10.1192/bjp.bp.106.025585

McQuown, S. C., Barrett, R. M., Matheos, D. P., Post, R. J., Rogge, G. a, Alenghat, T., … Wood, M. a. (2011). HDAC3 is a critical negative regulator of long-term memory formation. The Journal of Neuroscience: The Official Journal of the Society for Neuroscience, 31(2), 764–74. doi:10.1523/JNEUROSCI.5052-10.2011

Ménard, C., & Quirion, R. (2012). Successful cognitive aging in rats: a role for mGluR5 glutamate receptors, homer 1 proteins and downstream signaling pathways. PloS One, 7(1), e28666. doi:10.1371/journal.pone.0028666

Michaelson, J. J., Shi, Y., Gujral, M., Zheng, H., Malhotra, D., Jin, X., … Sebat, J. (2012). Whole-genome sequencing in autism identifies hot spots for de novo germline mutation. Cell, 151(7), 1431–42. doi:10.1016/j.cell.2012.11.019

Mizuno, K., Antunes-Martins, a, Ris, L., Peters, M., Godaux, E., & Giese, K. P. (2007). Calcium/calmodulin kinase kinase beta has a male-specific role in memory formation. Neuroscience, 145(2), 393–402. doi:10.1016/j.neuroscience.2006.11.056

Mizuno, K., & Giese, K. P. (2010). Towards a molecular understanding of sex differences in memory formation. Trends in Neurosciences, 33(6), 285–91. doi:10.1016/j.tins.2010.03.001

Mizuno, K., Ris, L., Sánchez-Capelo, A., Godaux, E., & Giese, K. P. (2006). Ca2+/calmodulin kinase kinase alpha is dispensable for brain development but is required for distinct memories in male, though not in female, mice. Molecular and Cellular Biology, 26(23), 9094–104. doi:10.1128/MCB.01221-06

Moretti, P., Levenson, J. M., Battaglia, F., Atkinson, R., Teague, R., Antalffy, B., … Zoghbi, H. Y. (2006). Learning and memory and synaptic plasticity are impaired in a mouse model of Rett syndrome. The Journal of Neuroscience: The Official Journal of the Society for Neuroscience, 26(1), 319–27. doi:10.1523/JNEUROSCI.2623-05.2006

Morrow EM et al. (2008) Identifying autism loci and genes by tracing recent shared ancestry. Science 321:218-223.

Moy SS, Nadler JJ, Perez A, Barbaro RP, Johns JM, Magnuson TR, Piven J, Crawley JN (2004) Sociability and preference for social novelty in five inbred strains: an approach to assess autistic-like behavior in mice. Genes, Brain, and Behavior 3:287-302.

Murgatroyd, C., & Spengler, D. (2012). Genetic variation in the epigenetic machinery and mental health. Current Psychiatry Reports, 14(2), 138–49. doi:10.1007/s11920-012-0255-1

Nacewicz, B. (2006). Amygdala volume and nonverbal social impairment in adolescent and adult males with autism. Archives of Neuropsychiatry. 63. Retrieved from http://archneur.jamanetwork.com/article.aspx?articleid=209946

Nagy, A. (2000). Cre recombinase: the universal reagent for genome tailoring. Genesis, 109, 99–109.

Nagy, L., Kao, H., Chakravarti, D., Lin, R., Hassig, C., Ayer, D., … Evans, R. (1997). Nuclear receptor repression mediated by a complex containing SMRT, mSin3A, and histone deacetylase. Cell, 89, 373–380.

Nasmyth, K., Stillman, D., & Kipling, D. (1987). Both positive and negative regulators of HO transcription are required for mother-cell-specific mating-type switching in yeast. Cell, 48(4), 579–87.

Neyman, S., & Manahan-Vaughan, D. (2008). Metabotropic glutamate receptor 1 (mGluR1) and 5 (mGluR5) regulate late phases of LTP and LTD in the hippocampal CA1 region in vitro. The European Journal of Neuroscience, 27(6), 1345–52. doi:10.1111/j.1460-9568.2008.06109.x

Ng, S. B., Bigham, A. W., Buckingham, K. J., Hannibal, M. C., McMillin, M. J., Gildersleeve, H. I., … Shendure, J. (2010). Exome sequencing identifies MLL2 mutations as a cause of Kabuki syndrome. Nature Genetics, 42(9), 790–3. doi:10.1038/ng.646

Nica, A. C., Montgomery, S. B., Dimas, A. S., Stranger, B. E., Beazley, C., Barroso, I., & Dermitzakis, E. T. (2010). Candidate causal regulatory effects by integration of expression QTLs with complex trait genetic associations. PLoS Genetics, 6(4), e1000895. doi:10.1371/journal.pgen.1000895

Nicoletti, F., Bockaert, J., & Collingridge, G. (2011). Metabotropic glutamate receptors: from the workbench to the bedside. …, 60(7-8), 1017–41. doi:10.1016/j.neuropharm.2010.10.022

Nishioka, K., Rice, J. C., Sarma, K., Erdjument-bromage, H., Werner, J., Wang, Y., … Hall, B. J. (2002). PR-Set7 Is a Nucleosome-Specific Methyltransferase that Modifies Lysine 20 of Histone H4 and Is Associated with Silent Chromatin, 9, 1201–1213.

Nosyreva, E. D., & Huber, K. M. (2006). Metabotropic receptor-dependent long-term depression persists in the absence of protein synthesis in the mouse model of fragile X syndrome. Journal of Neurophysiology, 95(5), 3291–5. doi:10.1152/jn.01316.2005

O'Riordan, K., Gerstein, H., Hullinger, R., & Burger, C. (2014). The role of Homer1c in metabotropic glutamate receptor-dependent long-term potentiation. Hippocampus, 24(1), 1–6. doi:10.1002/hipo.22222

Oberdoerffer, P. (2003). Unidirectional Cre-mediated genetic inversion in mice using the mutant loxP pair lox66/lox71. Nucleic Acids Research, 31(22), 140e–140. doi:10.1093/nar/gng140

Oliveira, A. M. M., Wood, M. A., McDonough, C. B., & Abel, T. (2007). Transgenic mice expressing an inhibitory truncated form of p300 exhibit long-term memory deficits. Learn Mem, 14(9), 564–72. doi:10.1101/lm.656907

Orlando, L. R., Ayala, R., Kett, L. R., Curley, A. a., Duffner, J., Bragg, D. C., … Young, A. B. (2009). Phosphorylation of the homer-binding domain of group I metabotropic glutamate receptors by cyclin-dependent kinase 5. Journal of Neurochemistry, 110(2), 557–569. doi:10.1111/j.1471-4159.2009.06139.x

Osterweil, E. K., Chuang, S.-C., Chubykin, A. a, Sidorov, M., Bianchi, R., Wong, R. K. S., & Bear, M. F. (2013). Lovastatin corrects excess protein synthesis and prevents epileptogenesis in a mouse model of fragile X syndrome. Neuron, 77(2), 243–50. doi:10.1016/j.neuron.2012.01.034

Pagnamenta AT, Khan H, Walker S, Gerrelli D, Wing K, Bonaglia MC, Giorda R, Berney T, Mani E, Molteni M, Pinto D, Le Couteur A, Hallmayer J, Sutcliffe JS, Szatmari P, Paterson AD, Scherer SW, Vieland VJ, Monaco AP (2011) Rare familiail 16q21 microdeletions under a linkage peak implicate cadherin 8 (CDH8) in susceptibility to autism and learning disability. Journal of Medical Genetics 48:48-54.

Palm, K., Belluardo, N., Metsis, M., & Timmusk, T. (1998). Neuronal expression of zinc finger transcription factor REST/NRSF/XBR gene. The Journal of Neuroscience: The Official Journal of the Society for Neuroscience, 18(4), 1280–96. Retrieved from http://www.ncbi.nlm.nih.gov/pubmed/9454838

Peça, J., Feliciano, C., Ting, J. T., Wang, W., Wells, M. F., Venkatraman, T. N., … Feng, G. (2011). Shank3 mutant mice display autistic-like behaviours and striatal dysfunction. Nature, 472(7344), 437–42. doi:10.1038/nature09965

Peixoto, L., & Abel, T. (2013). The role of histone acetylation in memory formation and cognitive impairments. Neuropsychopharmacology: Official Publication of the American College of Neuropsychopharmacology, 38(1), 62–76. doi:10.1038/npp.2012.86

Peñagarikano, O., Abrahams, B. S., Herman, E. I., Winden, K. D., Gdalyahu, A., Dong, H., Geschwind, D. H. (2011). Absence of CNTNAP2 leads to epilepsy, neuronal migration abnormalities, and core autism-related deficits. Cell, 147(1), 235–46. doi:10.1016/j.cell.2011.08.040

Penagarikano O, Geschwind DH (2012) What does CNTNAP2 reveal about autism spectrum disorder? Trends Mol Med 18:156-163.

Phillips, R., & LeDoux, J. (1992). Differential contribution of amygdala and hippocampus to cued and contextual fear conditioning. Behavioral Neuroscience, 106(2), 274–85. Retrieved from http://psycnet.apa.org/journals/bne/106/2/274/

Piers, T. M., Kim, D. H., Kim, B. C., Regan, P., Whitcomb, D. J., & Cho, K. (2012). Translational Concepts of mGluR5 in Synaptic Diseases of the Brain. Frontiers in Pharmacology, 3(November), 199. doi:10.3389/fphar.2012.00199

Potts, R. C., Zhang, P., Wurster, A. L., Precht, P., Mughal, M. R., Wood, W. H., … Pazin, M. J. (2011). CHD5, a brain-specific paralog of Mi2 chromatin remodeling enzymes, regulates expression of neuronal genes. PloS One, 6(9), e24515. doi:10.1371/journal.pone.0024515

Price, T. J., Rashid, M. H., Millecamps, M., Sanoja, R., Entrena, J. M., & Cervero, F. (2007). Decreased nociceptive sensitization in mice lacking the fragile X mental retardation protein: role of mGluR1/5 and mTOR. The Journal of Neuroscience: The Official Journal of the Society for Neuroscience, 27(51), 13958–67. doi:10.1523/JNEUROSCI.4383-07.2007

Ranuncolo, S. M., Ghosh, S., Hanover, J. a, Hart, G. W., & Lewis, B. a. (2012). Evidence of the involvement of O-GlcNAc-modified human RNA polymerase II CTD in transcription in vitro and in vivo. The Journal of Biological Chemistry, 287(28), 23549–61. doi:10.1074/jbc.M111.330910

Rexach, J. E., Clark, P. M., Mason, D. E., Neve, R. L., Peters, E. C., & Hsieh-Wilson, L. C. (2012). Dynamic O-GlcNAc modification regulates CREB-mediated gene expression and memory formation. Nature Chemical Biology, 8(3), 253–61. doi:10.1038/nchembio.770

Rosnera, W., Hryb, D., Khan, M., Nakhla, A., & Romas, N. (1999). Androgen and estrogen signaling at the cell membrane via G-proteins and cyclic adenosine monophosphate. Steroids, 64, 100–106. Retrieved from http://www.sciencedirect.com/science/article/pii/S0039128X98001081

Rutte, C., & Taborsky, M. (2007). Generalized reciprocity in rats. PLoS Biology, 5(7), e196. doi:10.1371/journal.pbio.0050196

Ryu, H., Lee, J., Hagerty, S. W., Soh, B. Y., McAlpin, S. E., Cormier, K. A., … Ferrante, R. J. (2006). ESET/SETDB1 gene expression and histone H3 (K9) trimethylation in Huntington's disease. Proceedings of the National Academy of Sciences of the United States of America, 103(50), 19176–19181. Retrieved from http://www.ncbi.nlm.nih.gov/pubmed/17142323

Sah, P., Faber, E., De Armentia, M.L., Power, J. (2003). The amygdaloid complex: anatomy and physiology. Physiological Reveiw, 803–834. Retrieved from http://physrev.physiology.org/content/83/3/803?rss=1&ssource=mfr

Sanders, S. J., Murtha, M. T., Gupta, A. R., Murdoch, J. D., Raubeson, M. J., Willsey, a J., State, M. W. (2012). De novo mutations revealed by whole-exome sequencing are strongly associated with autism. Nature, 485(7397), 237–41. doi:10.1038/nature10945

Sanders SJ, Ercan-Sencicek AG, Hus V, Luo R, Murtha MT, Moreno-De-Luca D, Chu SH, Moreau MP, Gupta AR, Thomson SA, Mason CE, Bilguvar K, Celestino-Soper PBS, Choi M, Crawford EL, al. e (2011) Multiple recurrent de novo CNVs, including duplications of the 7q11.23 Williams syndrome region, are strongly associated with autism. Neuron 70:863-885.

Saxe, M., & Battaglia, F. (2006). Ablation of hippocampal neurogenesis impairs contextual fear conditioning and synaptic plasticity in the dentate gyrus. Proceedings of the National Academy of Sciences of the United States of America, 103(46), 17501–17506. Retrieved from http://www.pnas.org/content/103/46/17501.short

Schmidt, E., & Taylor, D. (2000). Illegitimate Cre-dependent chromosome rearrangements in transgenic mouse spermatids. Proceedings of the National Academy of Sciences of the United States of America

Schoch, H., & Abel, T. (2014). Transcriptional co-repressors and memory storage. Neuropharmacology, 80C, 53–60. doi:10.1016/j.neuropharm.2014.01.003

Schoch, H., Florian, C., Poplawski, S., Hawk, J. D., & Abel, T. (2012). Conditional Sin3a mutant mice exhibit enhanced hippocampus-dependent long-term memory. Program No. 807.14. 2012 Neuroscience Meeting Planner. New Orleans, LA: Society for Neuroscience.

Schulz, B., Fendt, M., Gasparini, F., Lingenho, K., & Kuhn, R. (2001). The metabotropic glutamate receptor antagonist 2-methyl-6- (phenylethynyl) -pyridine (MPEP) blocks fear conditioning in rats. Neuropharmacology, 41, 1–7.

Seyfarth, R. M., & Cheney, D. L. (2013). Affiliation, empathy, and the origins of theory of mind. Proceedings of the National Academy of Sciences of the United States of America, 110 Suppl 2, 10349–56. doi:10.1073/pnas.1301223110

Shiraishi-Yamaguchi, Y., & Furuichi, T. (2007). The Homer family proteins. Genome Biology, 8(2), 206. doi:10.1186/gb-2007-8-2-206

Siegal, M., & Hartl, D. (1996). Transgene coplacement and high efficiency site-specific recombination with the Cre/loxP system in Drosophila. Genetics. Retrieved from http://www.ncbi.nlm.nih.gov/pmc/articles/PMC1207562/

Silver, D., & Livingston, D. (2001). Self-excising retroviral vectors encoding the Cre recombinase overcome Cre-mediated cellular toxicity. Molecular Cell, 8, 233–243. Retrieved from http://www.sciencedirect.com/science/article/pii/S1097276501002957

Silverstein, R. a, & Ekwall, K. (2005). Sin3: a flexible regulator of global gene expression and genome stability. Current Genetics, 47(1), 1–17. doi:10.1007/s00294-004-0541-5

Sims, R. J., Millhouse, S., Chen, C.-F., Lewis, B. a, Erdjument-Bromage, H., Tempst, P., … Reinberg, D. (2007). Recognition of trimethylated histone H3 lysine 4 facilitates the recruitment of transcription postinitiation factors and pre-mRNA splicing. Molecular Cell, 28(4), 665–76. doi:10.1016/j.molcel.2007.11.010

Sims, R. J., & Reinberg, D. (2006). Histone H3 Lys 4 methylation: caught in a bind? Genes & Development, 20(20), 2779–86. doi:10.1101/gad.1468206

Skaletsky, H., Kuroda-Kawaguchi, T., Minx, P.J….Page, D.C. (2003) The male-specific region of the human Y chromosome is a mosaic of discrete sequence classes. Nature 423:825-837

St. Pourcain B, Wang K, Glessner JT, Golding J, Steer C, Ring SM, Skuse DH, Grant SFA, Hakonarson H, Smith GD (2010) Association between a high-risk autism locus on 5p14 and social communication spectrum phenotypes in the general population. American Journal of Psychiatry 167:1364-1372.

Stefansson, H., & Petursson, H. (2002). Neuregulin 1 and Susceptibility to Schizophrenia. The American Journal of …, 877–892. Retrieved from http://www.sciencedirect.com/science/article/pii/S0002929707603723

Szumlinski, K. K., Kalivas, P. W., & Worley, P. F. (2006). Homer proteins: implications for neuropsychiatric disorders. Current Opinion in Neurobiology, 16(3), 251–7. doi:10.1016/j.conb.2006.05.002

Tabuchi K, Blundell J, Etherton MR, Hammer RE, Liu X, Powell CM, Sudhof TC (2007) A neuroligin-3 mutation implicated in autism increases inhibitory synaptic transmission in mice. Science 318:71-76.

Talebizadeh, Z., Lam, D. Y., Theodoro, M. F., Bittel, D. C., Lushington, G. H., & Butler, M. G. (2006). Novel splice isoforms for NLGN3 and NLGN4 with possible implications in autism. Journal of Medical Genetics, 43(5), e21. doi:10.1136/jmg.2005.036897

Talkowski, M. E., Rosenfeld, J. a, Blumenthal, I., Pillalamarri, V., Chiang, C., Heilbut, A., … Gusella, J. F. (2012). Sequencing chromosomal abnormalities reveals neurodevelopmental loci that confer risk across diagnostic boundaries. Cell, 149(3), 525–37. doi:10.1016/j.cell.2012.03.028

Tang, L., Nogales, E., & Ciferri, C. (2010). Structure and function of SWI/SNF chromatin remodeling complexes and mechanistic implications for transcription. Progress in

Biophysics and Molecular Biology, 102(2-3), 122–8. doi:10.1016/j.pbiomolbio.2010.05.001

Tao, J., Hu, K., Chang, Q., Wu, H., Sherman, N. E., Martinowich, K., … Sun, Y. E. (2009). Phosphorylation of MeCP2 at Serine 80 regulates its chromatin association and neurological function. Proceedings of the National Academy of Sciences of the United States of America, 106(12), 4882–7. doi:10.1073/pnas.0811648106

Tarantino LM, Gould TJ, Druhan JP, Bucan M (2000) Behavior and mutagenesis screens: the importance of baseline analysis of inbred strains. Mammalian Genome 11:555-564.

Tesson, L., Usal, C., Ménoret, S., Leung, E., Niles, B. J., Remy, S., … Cost, G. J. (2011). Knockout rats generated by embryo microinjection of TALENs. Nature Biotechnology, 29(8), 695–6. doi:10.1038/nbt.1940

Thomas, G. M., & Huganir, R. L. (2004). MAPK cascade signalling and synaptic plasticity. Nature Reviews. Neuroscience, 5(3), 173–83. doi:10.1038/nrn1346

Thummel, R., Burket, C. T., Brewer, J. L., Sarras, M. P., Li, L., Perry, M., … Godwin, A. R. (2005). Cre-mediated site-specific recombination in zebrafish embryos. Developmental Dynamics : An Official Publication of the American Association of Anatomists, 233(4), 1366–77. doi:10.1002/dvdy.20475

Thyagarajan, B., Guimaraes, M., Groth, A., & Calos, M. (2000). Mammalian genomes contain active recombinase recognition sites. Gene, 244, 47–54. Retrieved from http://www.sciencedirect.com/science/article/pii/S0378111900000081

Tian, F., Marini, A. M., & Lipsky, R. H. (2010). Effects of histone deacetylase inhibitor Trichostatin A on epigenetic changes and transcriptional activation of Bdnf promoter 1 by rat hippocampal neurons. Annals of the New York Academy of Sciences, 1199, 186–93. doi:10.1111/j.1749-6632.2009.05175.x

Trifilieff, P., Herry, C., Vanhoutte, P., Caboche, J., Desmedt, A., Riedel, G., … Micheau, J. (2006). Foreground contextual fear memory consolidation requires two independent phases of hippocampal ERK / CREB activation, 349–358. doi:10.1101/lm.80206.1

Tsamis, K., & Mytilinaios, D. (2013). Glutamate Receptors in Human Caudate Nucleus in Normal Aging and Alzheimer's Disease. Current Alzheimer …, 1, 1–7. Retrieved from http://www.ingentaconnect.com/content/ben/car/2013/00000010/00000005/art00002

Tsai N-P, Wilkerson JR, Guo W, Maksimova MA, DeMartino GA, Cowan CW, Huber KM (2012) Multiple autism-linked genes mediate synapse elimination via proteasomal degradation of a synpatic scaffold PSD-95. Cell 151:1581-1594.

Tu, J. C., Xiao, B., Naisbitt, S., Yuan, J. P., Petralia, R. S., Brakeman, P., … Worley, P. F. (1999). Coupling of mGluR/Homer and PSD-95 complexes by the Shank family of postsynaptic density proteins. Neuron, 23(3), 583–92. Retrieved from http://www.ncbi.nlm.nih.gov/pubmed/10433269

Uemura M, Nakao S, Suzuki ST, Takeichi M, Hirano S (2007) OL-protocadherin is essential for growth of striatal axons and thalamocortical projections. Nature Neuroscience 10:1151-1159.

Ultanir, S., & Kim, J. (2007). Regulation of spine morphology and spine density by NMDA receptor signaling in vivo. Proceedings of the …, 104(49). Retrieved from http://www.pnas.org/content/104/49/19553.short

Uslaner, J. M., Parmentier-Batteur, S., Flick, R. B., Surles, N. O., Lam, J. S. H., McNaughton, C. H., … Hutson, P. H. (2009). Dose-dependent effect of CDPPB, the mGluR5 positive allosteric modulator, on recognition memory is associated with GluR1 and CREB phosphorylation in the prefrontal cortex and hippocampus. Neuropharmacology, 57(5-6), 531–8. doi:10.1016/j.neuropharm.2009.07.022

Van Oevelen, C., Bowman, C., Pellegrino, J., Asp, P., Cheng, J., Parisi, F., … Dynlacht, B. D. (2010). The mammalian Sin3 proteins are required for muscle development and sarcomere specification. Molecular and Cellular Biology, 30(24), 5686–97. doi:10.1128/MCB.00975-10

Vecsey, C. G., Hawk, J. D., Lattal, K. M., Stein, J. M., Fabian, S. a, Attner, M. a, … Wood, M. a. (2007). Histone deacetylase inhibitors enhance memory and synaptic plasticity via CREB:CBP-dependent transcriptional activation. The Journal of Neuroscience: The Official Journal of the Society for Neuroscience, 27(23), 6128–40. doi:10.1523/JNEUROSCI.0296-07.2007

Vo, N., & Goodman, R. H. (2001). CREB-binding protein and p300 in transcriptional regulation. The Journal of Biological Chemistry, 276(17), 13505–8. doi:10.1074/jbc.R000025200

Vogel-Ciernia, A., Matheos, D. P., Barrett, R. M., Kramár, E. a, Azzawi, S., Chen, Y., … Wood, M. a. (2013). The neuron-specific chromatin regulatory subunit BAF53b is necessary for synaptic plasticity and memory. Nature Neuroscience, 16(5), 552–61. doi:10.1038/nn.3359

Walsh, T., McClellan, J. M., McCarthy, S. E., Addington, A. M., Pierce, S. B., Cooper, G. M., … Sebat, J. (2008). Rare structural variants disrupt multiple genes in neurodevelopmental pathways in schizophrenia. Science (New York, N.Y.), 320(5875), 539–43. doi:10.1126/science.1155174

Walss-Bass, C., Liu, W., Lew, D. F., Villegas, R., Montero, P., Dassori, A., … Raventos, H. (2006). A novel missense mutation in the transmembrane domain of neuregulin 1 is associated with schizophrenia. Biological Psychiatry, 60(6), 548–53. doi:10.1016/j.biopsych.2006.03.017

Wang K, Zhang H, Ma D, Bucan M, Glessner JT, Abrahams BS, al. e (2009) Common genetic variants on 5p14.1 associate with autism spectrum disorders. Nature 459:528-533.

Wang, X., Snape, M., Klann, E., Stone, J. G., Singh, A., Petersen, R. B., … Zhu, X. (2012). Activation of the extracellular signal-regulated kinase pathway contributes to the

behavioral deficit of fragile x-syndrome. Journal of Neurochemistry, 121(4), 672–9. doi:10.1111/j.1471-4159.2012.07722.x

Warren, Z., McPheeters, M.L., Sathe, N., Foss-Feig, J.H., Glasser, A., Veenstra-VanderWeele, J. (2011) A systematic review of early intensive intervention for autism spectrum disorders. Pediatrics 127:1303-11

Wells, L., Whelan, S. a, & Hart, G. W. (2003). O-GlcNAc: a regulatory post-translational modification. Biochemical and Biophysical Research Communications, 302(3), 435–441. doi:10.1016/S0006-291X(03)00175-X

Williams, K., Christensen, J., & Pedersen, M. (2011). TET1 and hydroxymethylcytosine in transcription and DNA methylation fidelity. Nature, 473(7347), 343–348. doi:10.1038/nature10066.Tet1

Winocur, G., Wojtowicz, J. M., Sekeres, M., Snyder, J. S., & Wang, S. (2006). Inhibition of neurogenesis interferes with hippocampus-dependent memory function. Hippocampus, 16(3), 296–304. doi:10.1002/hipo.20163

Won H, Lee H-R, Gee HY, Mah W, Kim J-I, Lee J, Ha S, Chung C, Jung ES, Cho YS, Park S-G, Lee J-S, Lee K, Kim D, Bae YC, Kaang B-K, Lee MG, Kim E (2012) Autistic-like social behaviour in Shank2-mutant mice improved by restoring NMDA receptor function. Nature 486:261-265.

Wysocka, J., Myers, M. P., Laherty, C. D., Eisenman, R. N., & Herr, W. (2003). Human Sin3 deacetylase and H3-K4 methyltransferase are tethered together selectively by the cell-proliferation factor HCF-1. Genes & Development, 896–911. doi:10.1101/gad.252103.conserved

Xiao, B., Tu, J. C., Petralia, R. S., Yuan, J. P., Doan, a, Breder, C. D., … Worley, P. F. (1998). Homer regulates the association of group 1 metabotropic glutamate receptors with multivalent complexes of homer-related, synaptic proteins. Neuron, 21(4), 707–16. Retrieved from http://www.ncbi.nlm.nih.gov/pubmed/9808458

Xie, F., Raetzman, L. T., & Siegel, R. E. (2004). Neuregulin induces GABAA receptor beta2 subunit expression in cultured rat cerebellar granule neurons by activating multiple signaling pathways. Journal of Neurochemistry, 90(6), 1521–9. doi:10.1111/j.1471-4159.2004.02685.x

Xing, G., Zhang, L., Russell, S., & Post, R. (2006). Reduction of dopamine-related transcription factors Nurr1 and NGFI-B in the prefrontal cortex in schizophrenia and bipolar disorders. Schizophrenia Research, 84(1), 36–56. doi:10.1016/j.schres.2005.11.006

Yan, J., Noltner, K., Feng, J., Li, W., Schroer, R., Skinner, C., … Sommer, S. S. (2008). Neurexin 1alpha structural variants associated with autism. Neuroscience Letters, 438(3), 368–70. doi:10.1016/j.neulet.2008.04.074

Yan, Y.-G., Zhang, J., Xu, S.-J., Luo, J.-H., Qiu, S., & Wang, W. (2014). Clustering of surface NMDA receptors is mainly mediated by the C-terminus of GluN2A in cultured rat

hippocampal neurons. Neuroscience Bulletin, 30(4), 655–66. doi:10.1007/s12264-014-1450-8

Yang, L., Mei, Q., Zielinska-Kwiatkowska, A., Matsui, Y., Blackburn, M., Benedetti, D., … Chansky, H. (2003). An ERG (ets-related gene)-associated histone methyltransferase interacts with histone deacetylases 1/2 and transcription co-repressors mSin3A/B. Biochem. J, 657, 651–657.

Yang M, Crawley JN (2009) Simple behavioral assessment of mouse olfaction. Current Protocols in Neuroscience Supplement 48:8.24.21-28.24.12.

Yasui, D., & Peddada, S. (2007). Integrated epigenomic analyses of neuronal MeCP2 reveal a role for long-range interaction with active genes. Proceedings of the National Academy of Science, 1–6.

Yildirim, O., Li, R., Hung, J.-H., Chen, P. B., Dong, X., Ee, L.-S., Fazzio, T. G. (2011). Mbd3/NURD complex regulates expression of 5-hydroxymethylcytosine marked genes in embryonic stem cells. Cell, 147(7), 1498–510. doi:10.1016/j.cell.2011.11.054

Yokoyama, A., & Wang, Z. (2004). Leukemia proto-oncoprotein MLL forms a SET1-like histone methyltransferase complex with menin to regulate Hox gene expression. … and Cellular Biology, 24(13), 5639–5649. doi:10.1128/MCB.24.13.5639

Youn, H. D., & Liu, J. O. (2000). Cabin1 represses MEF2-dependent Nur77 expression and T cell apoptosis by controlling association of histone deacetylases and acetylases with MEF2. Immunity, 13(1), 85–94.

Zeng, H., Chattarji, S., Barbarosie, M., Rondi-Reig, L., Philpot, B., Miyakawa, T., … Tonegawa, S. (2001). Forebrain-specific calcineurin knockout selectively impairs bidirectional synaptic plasticity and working/episodic-like memory. *Cell*, *107*, 617–629.

Zhang, D., Yoon, H., & Wong, J. (2005). JMJD2A is a novel N-CoR-interacting protein and is involved in repression of the human transcription factor achaete scute-like homologue 2 (ASCL2/Hash2). Molecular and Cellular Biology, 25(15), 6404–6414. doi:10.1128/MCB.25.15.6404

Zhang, H., Zhang, X., Clark, E., Mulcahey, M., Huang, S., & Shi, Y. G. (2010). TET1 is a DNA-binding protein that modulates DNA methylation and gene transcription via hydroxylation of 5-methylcytosine. Cell Research, 20(12), 1390–3. doi:10.1038/cr.2010.156

Zhao, C., Gao, H., Liu, Y., Papoutsi, Z., Jaffrey, S., Gustafsson, J.-A., & Dahlman-Wright, K. (2010). Genome-wide mapping of estrogen receptor-beta-binding regions reveals extensive cross-talk with transcription factor activator protein-1. Cancer Research, 70(12), 5174–83. doi:10.1158/0008-5472.CAN-09-4407

Zhao, M.-G., Toyoda, H., Ko, S. W., Ding, H.-K., Wu, L.-J., & Zhuo, M. (2005). Deficits in trace fear memory and long-term potentiation in a mouse model for fragile X syndrome. The Journal of Neuroscience: The Official Journal of the Society for Neuroscience, 25(32), 7385–92. doi:10.1523/JNEUROSCI.1520-05.2005

Zhou, Y., Lu, Y., & Tian, W. (2012). Epigenetic features are significantly associated with alternative splicing. BMC Genomics, 13(1), 123. doi:10.1186/1471-2164-13-123

This was a triumph!
I'm making a note here:
Huge success!

It's hard to overstate
my satisfaction.

Aperture Science:
We do what we must
because we can
For the good of all of us.
Except the ones who are dead.

But there's no sense crying
over every mistake.
You just keep on trying
'til you run out of cake.
And the science gets done.
And you make a neat gun
for the people who are
still alive…

-GlaDOS

Aperture Science Laboratories